638

The EFFECTS of LOADINGS on BRIDGE LIFE

MICHIGAN DEPARTMENT OF STATE HIGHWAYS

THE EFFECTS OF LOADINGS ON BRIDGE LIFE

G. R. Cudney

Final Report on a Highway Planning and Research Investigation
Conducted in Cooperation with the U. S. Department of Transportation
Bureau of Public Roads

Research Laboratory Section
Testing and Research Division
Research Project 62 F-71
Research Report No. R-638

State of Michigan
Department of State Highways
Charles H. Hewitt, Chairman; Wallace D. Nunn, Vice-Chairman;
Ardale W. Ferguson; Richard VanderVeen; Henrik E. Stafseth, Director
Lansing, January 1968

INFORMATION RETRIEVAL DATA

REFERENCE: Cudney, G. R. The Effects of Loadings on Bridge Life. Michigan Department of State Highways Research Report No. R-638. Research Project 62 F-71.

ABSTRACT: This study estimates the effects of traffic loadings on the fatigue life of longitudinal stringers of bridges, based on stress histories acquired at crucial points. A limited lateral stress distribution study with a special test vehicle was conducted for various speeds and lateral vehicle positions. Eight spans of 8 composite longitudinal stringer-slab type bridges were used (2 welded plate girders, 5 rolled beam with tapered end cover plates, and 1 prestressed concrete I-beam). The report includes frequency distributions of maximum live load stress, rebound stress, live load stress range, and vehicle type; bridge dynamic characteristics (natural frequency, damping factors, and decay time); dynamic amplification factors and dynamic stress increments for the various test vehicle speeds; and miscellaneous frequency distributions of gross vehicle load on 2 bridges and gross vehicle load according to truck type. This study indicates that the effect of current traffic loading on bridge life is insignificant, limited, of course, by the particular characteristics of the test structures, truck volumes, types and load distributions encountered, and interpretation and applicability of the fatigue strength data (Munse-Stallmeyer) and failure criteria (Miner's Hypothesis).

KEY WORDS: bridge dynamics, fatigue life, loading tests, stringers, stress analysis, stress distribution, lateral stress.

CONTENTS

THE EFFECTS OF LOADINGS ON BRIDGE LIFE

The Michigan study of bridge strain histories began in July 1963 as a cooperative study with the U. S. Department of Transportation--Bureau of Public Roads under the Highway Planning and Research Program. The study arose as a result of a memorandum to the Highway Research Board Committee on Bridges from the Advisory Panel on Bridges of the AASHO Road Test. It was the opinion of this panel that a high priority should be given to application of repeated load fatigue life data from the AASHO Road Test bridge studies to highway structures subjected to actual highway traffic.

Results of the AASHO bridge tests revealed significant agreement between the predicted fatigue life of the bridge structure, based on fatigue characteristics of the bridge materials as determined by laboratory tests, and the structure's actual fatigue life. It should be pointed out, however, that the longitudinal stringers of the test bridges utilized in the AASHO study were specially designed for stress levels commensurate with the objective concerned, i.e., to induce fatigue fractures. In the tests, the load applications were relatively uniform and continuous having been confined to a few specific vehicle types and loadings. The laboratory fatigue testing involved constant amplitude cycling utilizing limited combinations of minimum stress levels and stress ranges. It is also significant that the majority of today's highway bridges are of the slab and steel stringer variety, in which the stringers contain welded partial-length cover plates, or are welded plate girders with a flange width or thickness transition. This study is primarily concerned with the fatigue life of these two types of longitudinal steel stringer bridge components as effected by their geometry, fatigue strength, and load application characteristics.

Michigan was in a unique position to perform this study since it is the only state without a maximum gross weight limit. Axle load limits are 18 kips for single axles and 32 kips for tandem axles, except that a given truck is permitted only one 32-kip tandem and the remaining tandem axle loads are limited to 26 kips. With these axle load requirements, however, and a 55-ft overall length limit for tractor-semi-trailer or tractor-semi-trailer-trailer combinations, total vehicle-axle configurations in Michigan have been such as to carry as great a legal load as possible. One innovation is the use of triple axles which legally can carry 39 kips. Thirteen-axle vehicles legally carrying 169 kips are possible and seen occasionally, and 11-axle units for hauling gravel, steel, and other heavy items are not uncommon.

Objectives

The specific objectives of this study as outlined in the Project Proposal were as follows:

"1. To establish a statistical sampling procedure to insure that representative traffic selection is being obtained.

"2. To determine the maximum live load dynamic strains imposed on each representative bridge type.

"3. To determine the live load stress range to which the bridge is subjected.

"4. To determine the changing dynamic characteristics of the representative bridges with time.

"5. To establish a systematic procedure for obtaining strain histories of a sufficient number and type of bridges to warrant basic conclusions.

"6. To correlate and predict life of structure with respect to established (fatigue strength) properties."

In connection with accumulation of maximum stringer stress and stress range frequency distributions, histograms of truck type and typical stringer stress response from the most common truck types are also presented.

In addition, a series of tests were conducted with a special Highway Department load-test vehicle for evaluating, to a limited degree, the lateral stress distribution and dynamic characteristics of four sample bridges. Also, for two of the test bridges, limited supplementary data were gathered on gross load-truck type distributions and corresponding maximum induced stringer stresses for vehicles with known axle loads.

Selection of Bridges

All test bridges were composite and designed for H 20-S16-44 loading. They were selected on the basis of span type, length, traffic volume, and ease of instrumentation. Eight spans of eight bridges were chosen: two welded plate girder spans with a flange thickness transition, five rolled beam with tapered end cover plates welded all the way around, and one prestressed precast concrete I-beam span which was included in the lateral stress distribution phase of the study. The eight test bridges included two end anchor spans, two center suspended spans, three simple spans, and one semi-suspended span. The angle of skew for six of these bridges was less than 5°, one was 14°, and one was 30°. Elevation views of the eight test

spans are shown in Figure 1, and plan and elevation views are given in Figures 2 through 9. The sample bridge number, location, type, span length, and degree of skewness were as follows:

Bridge	Location	Bridge Type	Span Length, ft	Angle of Skew
1	I 96 WB over Grand River	End Anchor span, welded plate girder with flange thickness transition	95.0	0° 00'
2	I 96 SB over Saginaw St.	Suspended center span, rolled beam with welded tapered end cover plate	79.5	4° 37'
3	I 94 WB over Telegraph Rd.	Semi-suspended span, rolled beam with welded tapered end cover plate	66.0	4° 28'
4	I 96 EB over NYC RR	Simple span; prestressed, precast concrete I-beam	45.5	4° 02'
5	US 23 NB over M 59	Simple span, rolled beam with welded tapered end cover plate	71.9	3° 18'
6	I 94 EB over US 131 NB	Suspended span, rolled beam with welded tapered end cover plate	58.7	5° 01'
7	US 23 SB over Huron River and NYC RR	Simple span, rolled beam with welded tapered end cover plate	78.5	14° 00'
8	I 96 EB over Grand River	End anchor span, welded plate girder with flange thickness transition	128.7	30° 00'

Instrumentation

Strain gage locations were selected at mid-span and at the stress concentration point of the two most highly stressed stringers in the traffic lane on the seven steel stringer test bridges. Strain gages were placed at the mid-point of all stringers on Bridges 1, 2, 4, and 5, and at points 1 ft from the stress concentration point on Bridges 1, 2, 3, 6, 7, and 8.

All paint and scale were removed from the beams with a disc sander at these locations, and the area wiped clean with acetone prior to gage

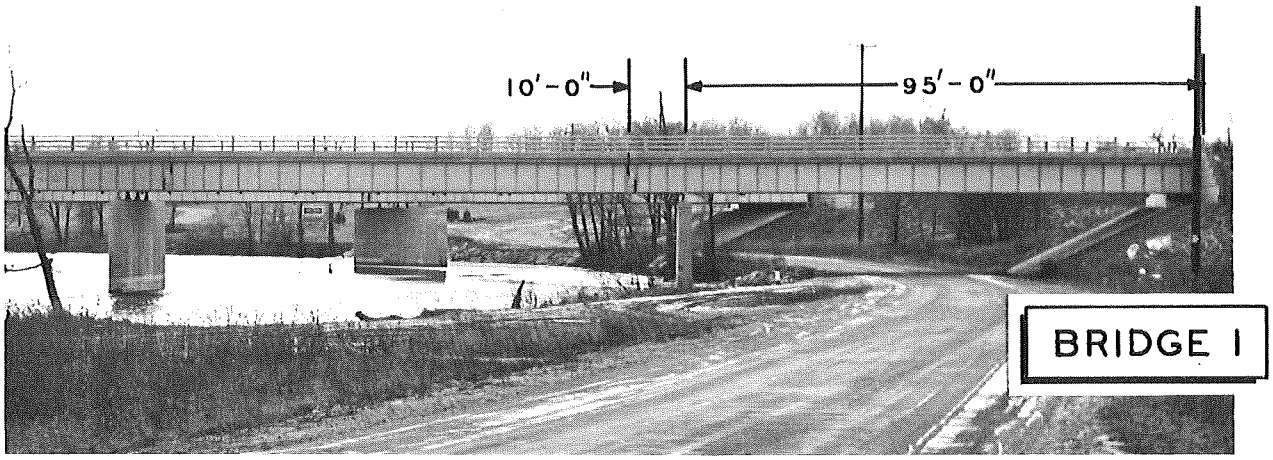

Bridge 1: End anchor span, welded plate girder with flange thickness transition

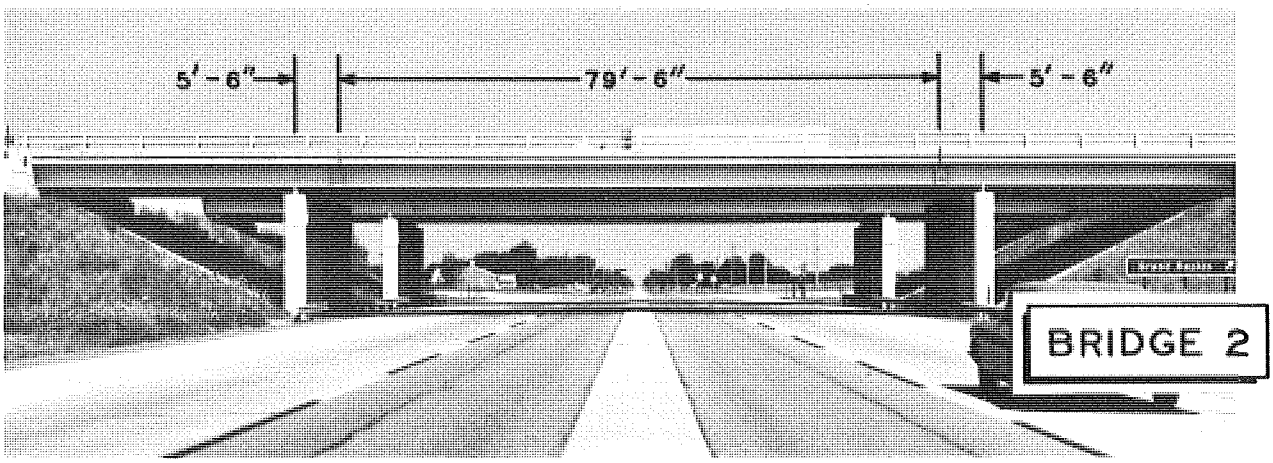

Bridge 2: Suspended center span, rolled beam with tapered end cover plate

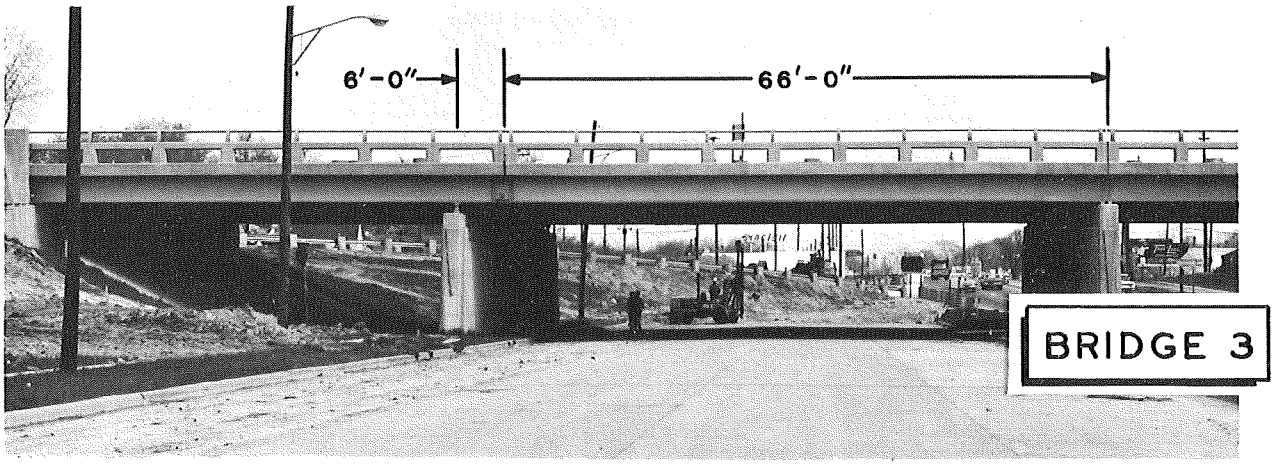

Bridge 3: Semi-suspended span, rolled beam with tapered end cover plate

Figure 1. Elevation views of the test spans.

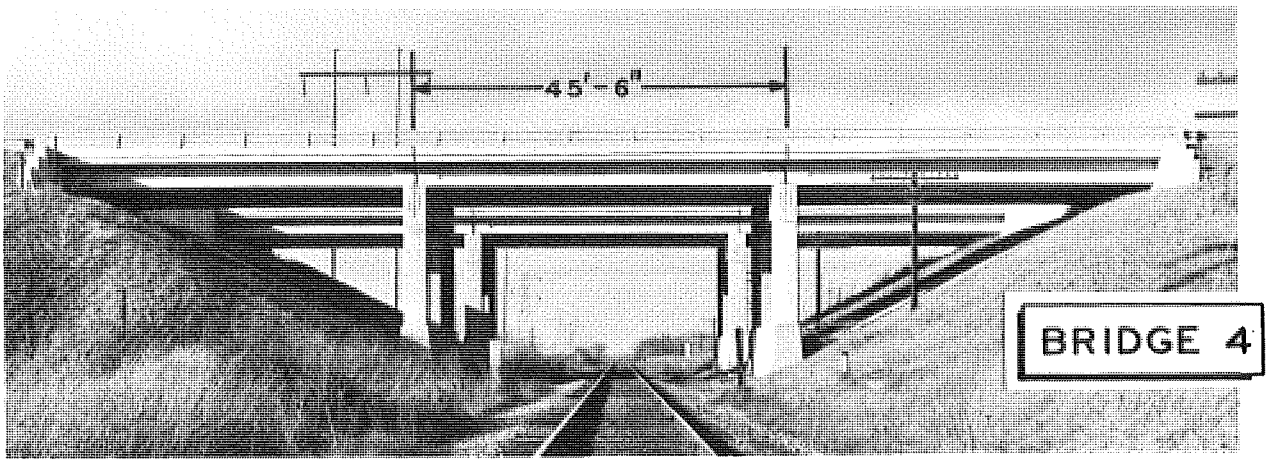

Bridge 4: Simple span; prestressed, precast I-beam

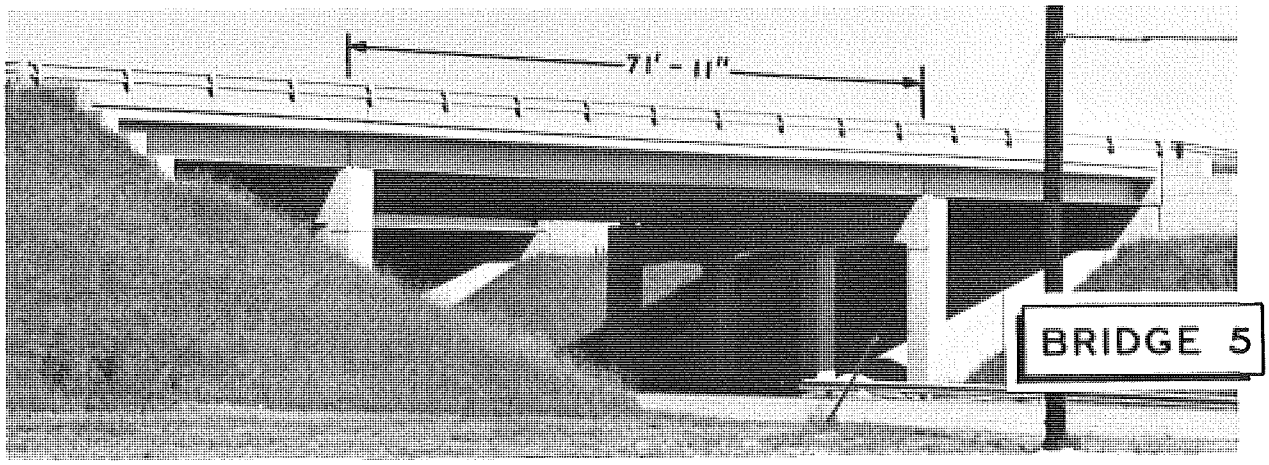

Bridge 5: Simple span, rolled beam with tapered end cover plate

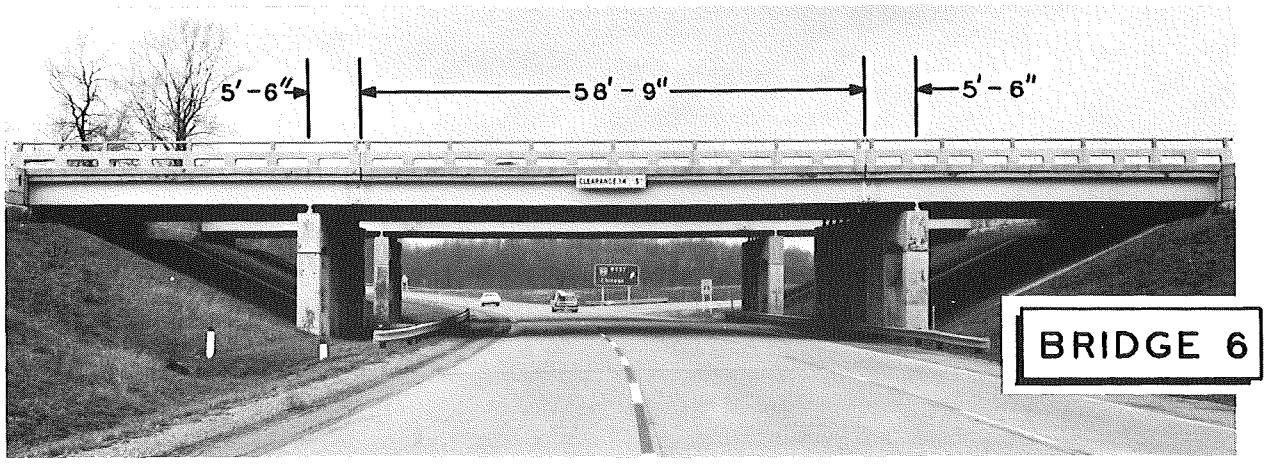

Bridge 6: Suspended span, rolled beam with tapered end cover plate

Figure 1 (cont.). Elevation views of the test spans.

Bridge 7: Simple span, rolled beam with tapered end cover plate

Bridge 8: End anchor span, welded plate girder with flange thickness transition

Figure 1 (cont.). Elevation views of the test spans.

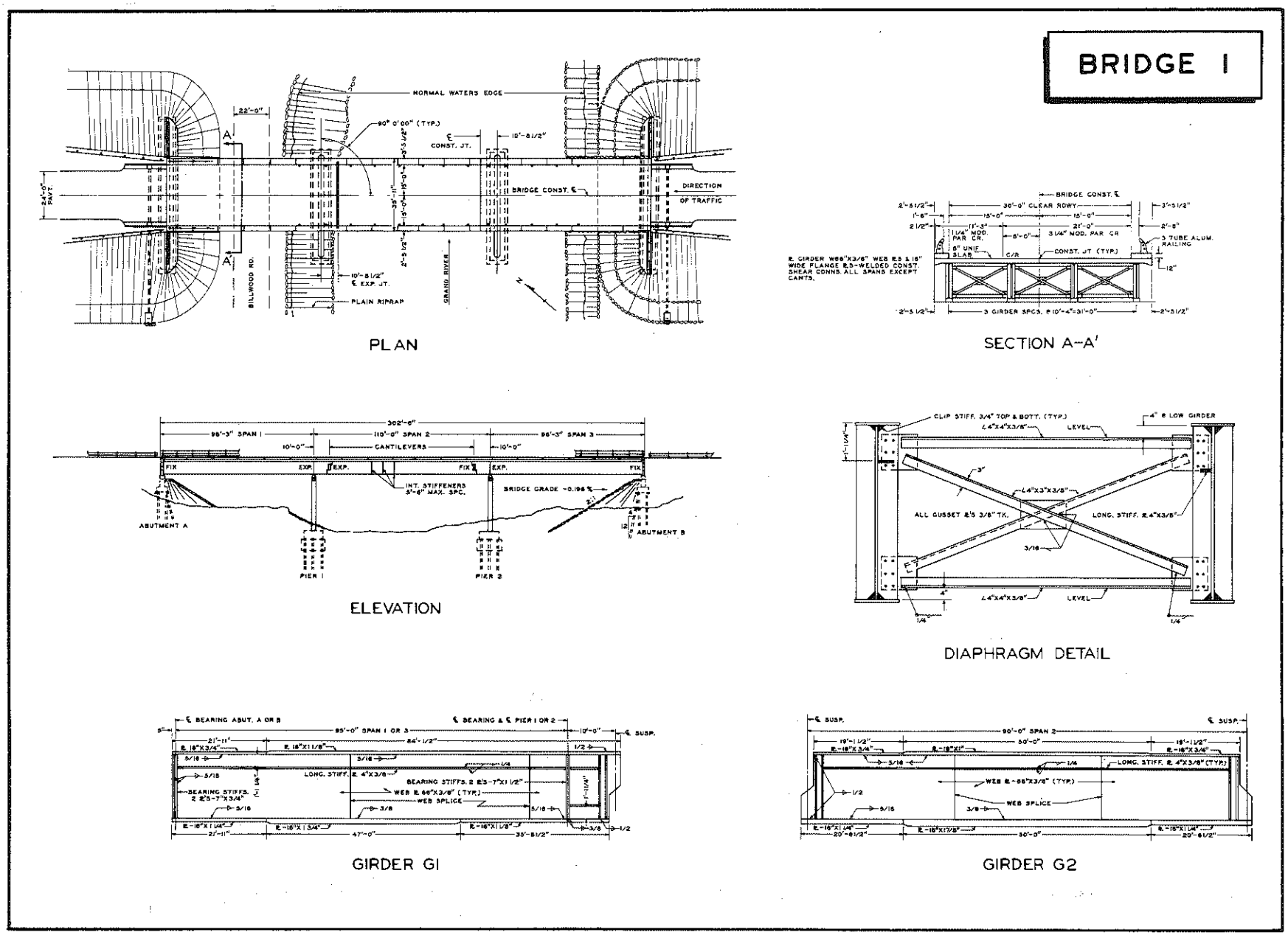

Figure 2. Plan and elevation views, with details.

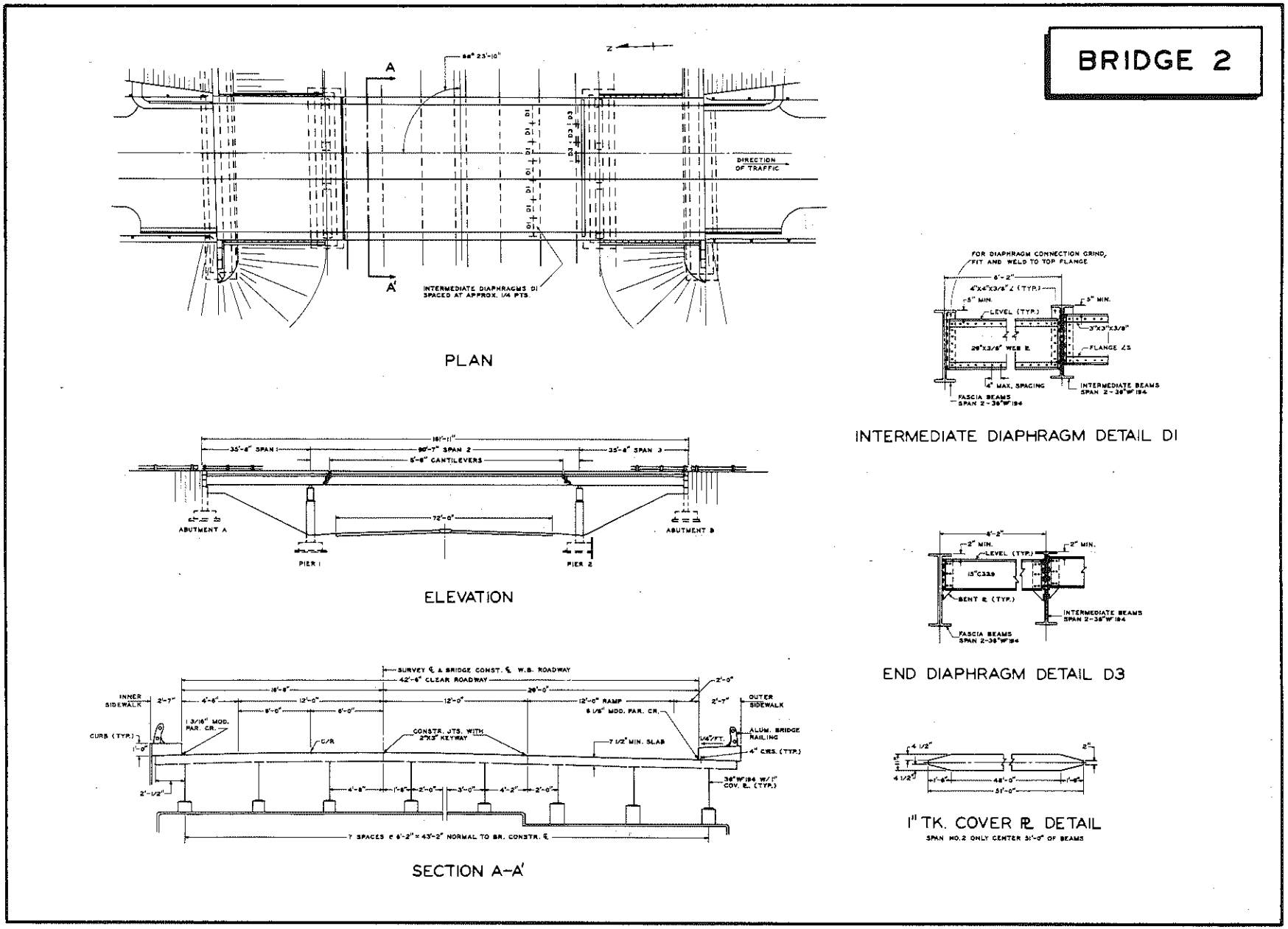

Figure 3. Plan and elevation views, with details.

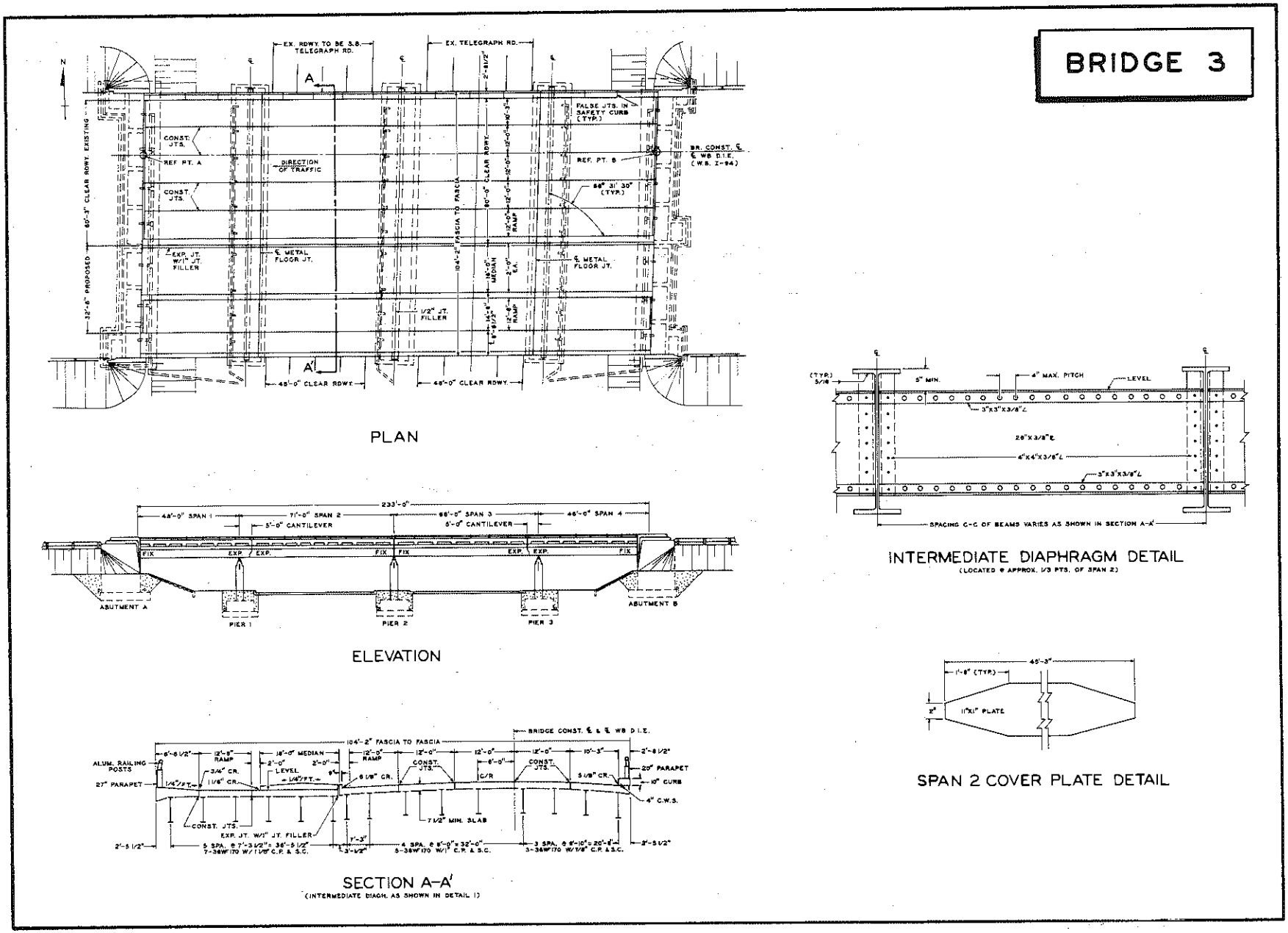

Figure 4. Plan and elevation views, with details.

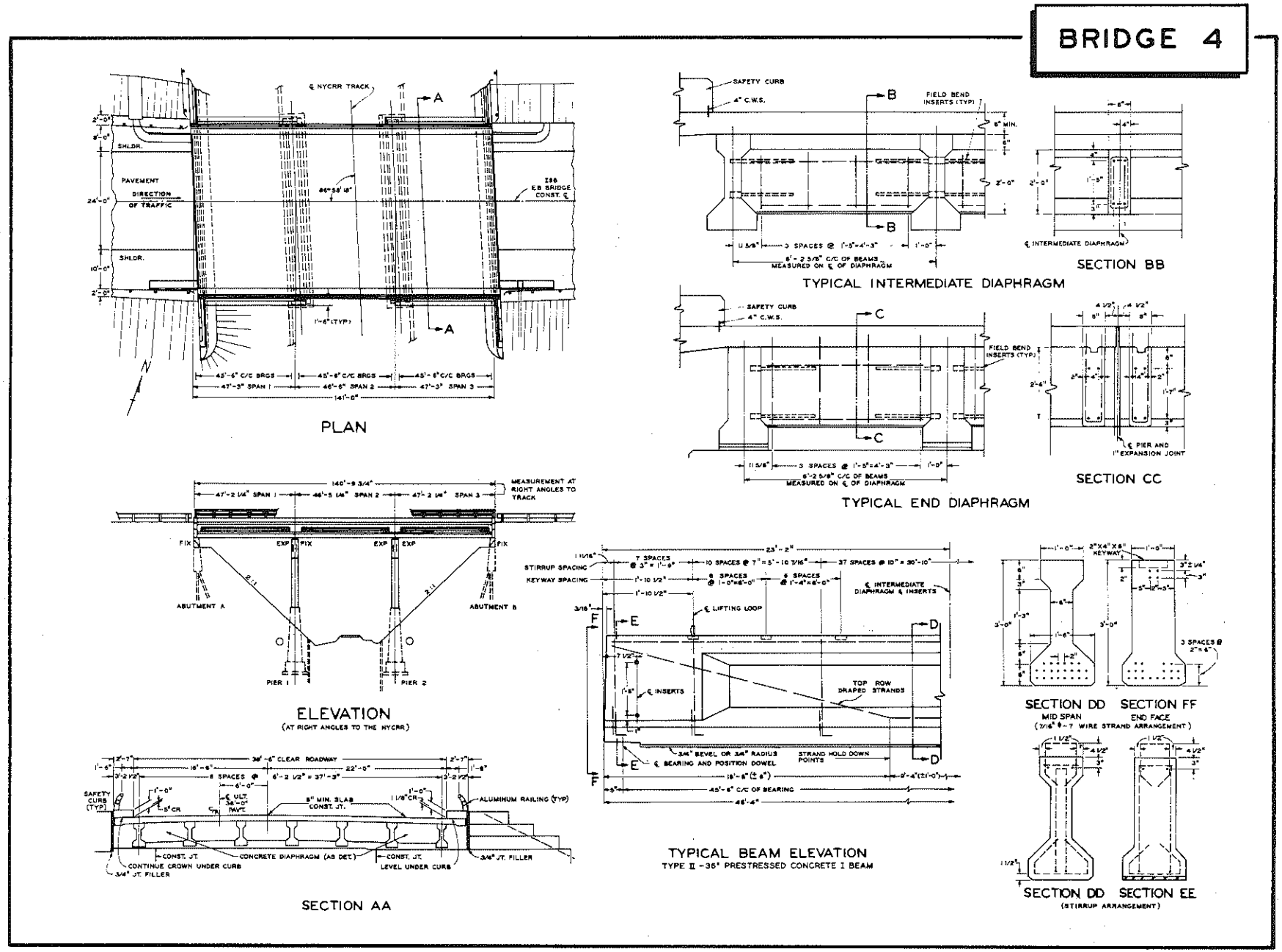

Figure 5. Plan and elevation views, with details.

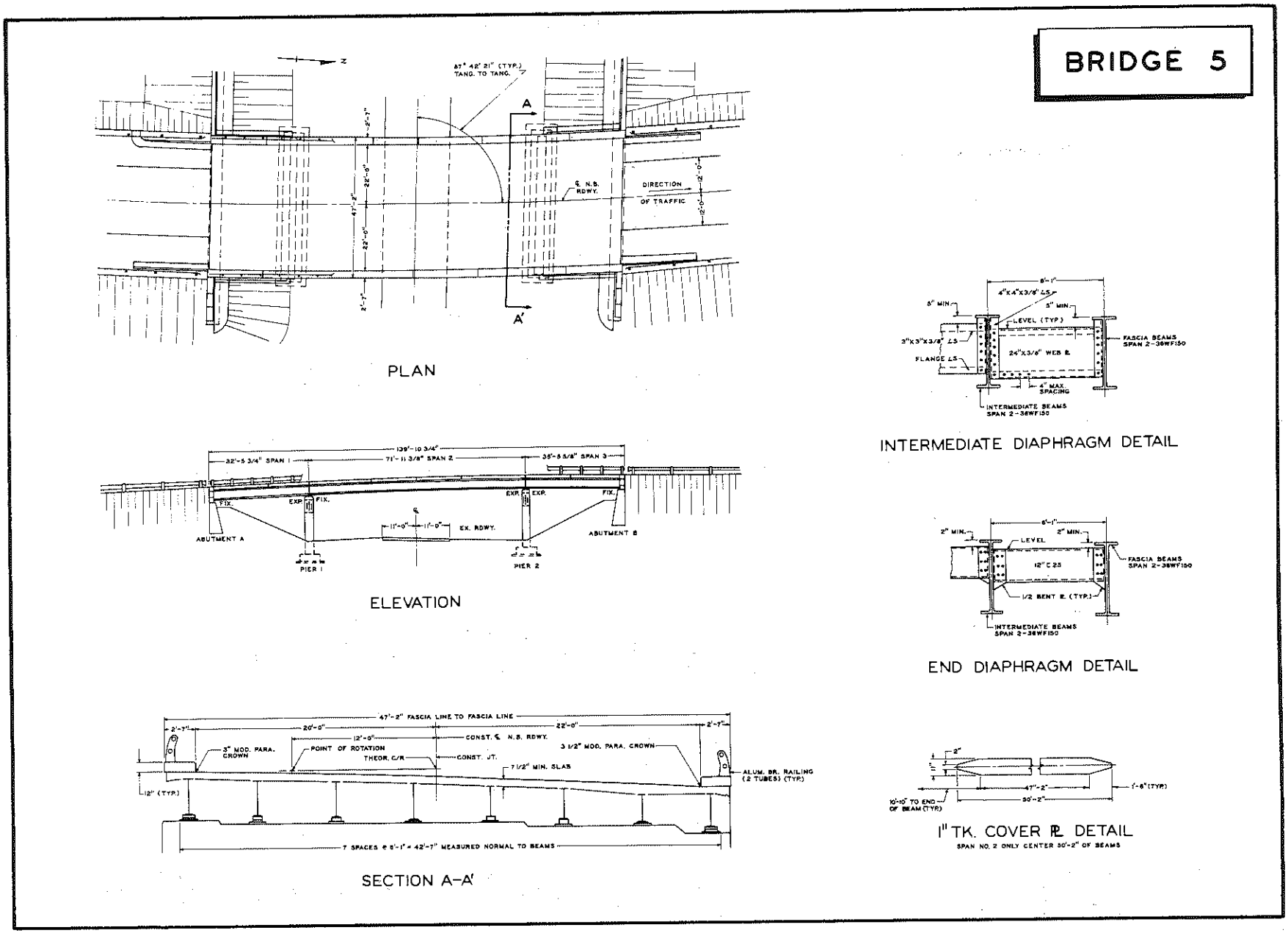

Figure 6. Plan and elevation views, with details.

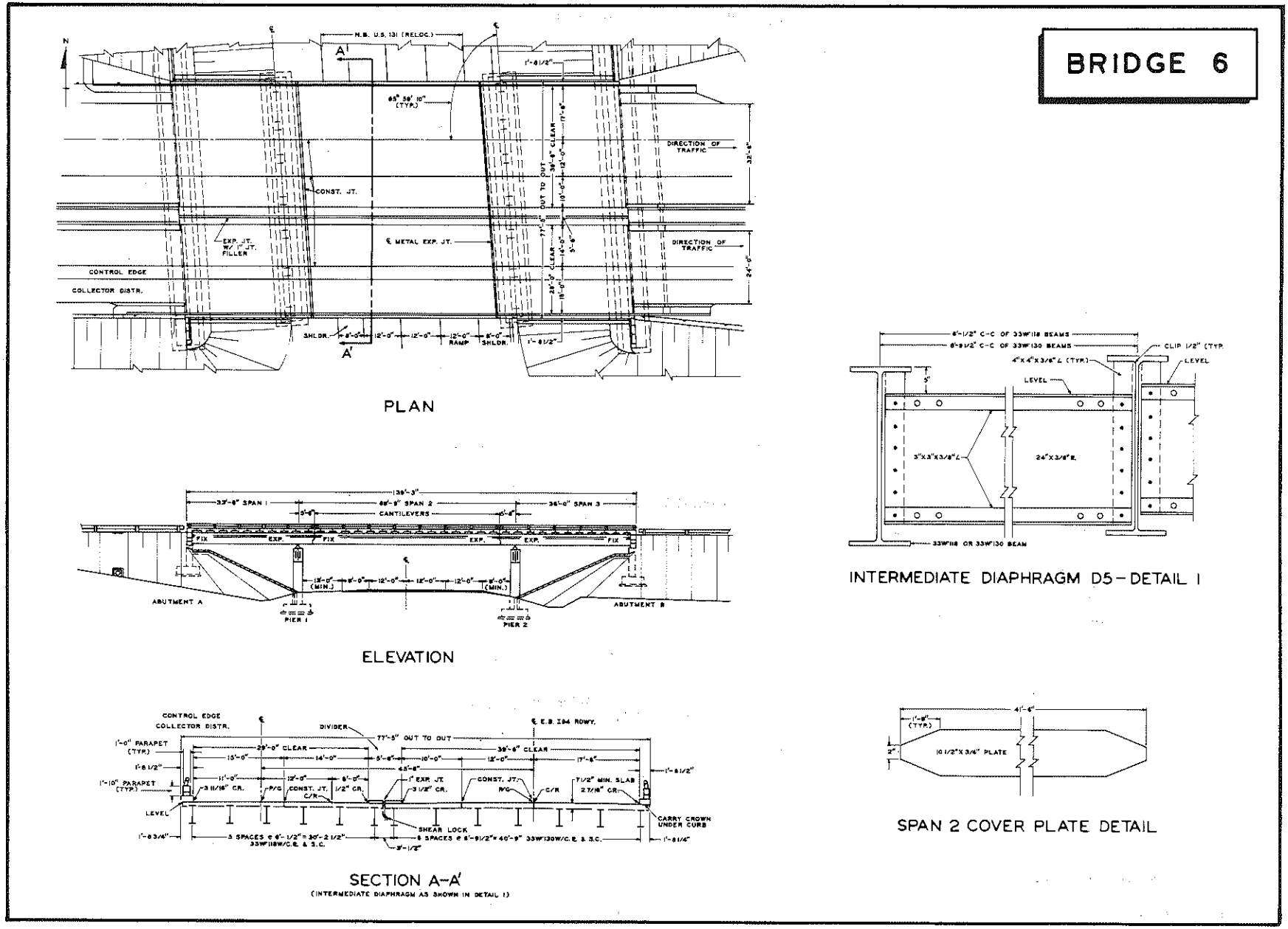

Figure 7. Plan and elevation views, with details.

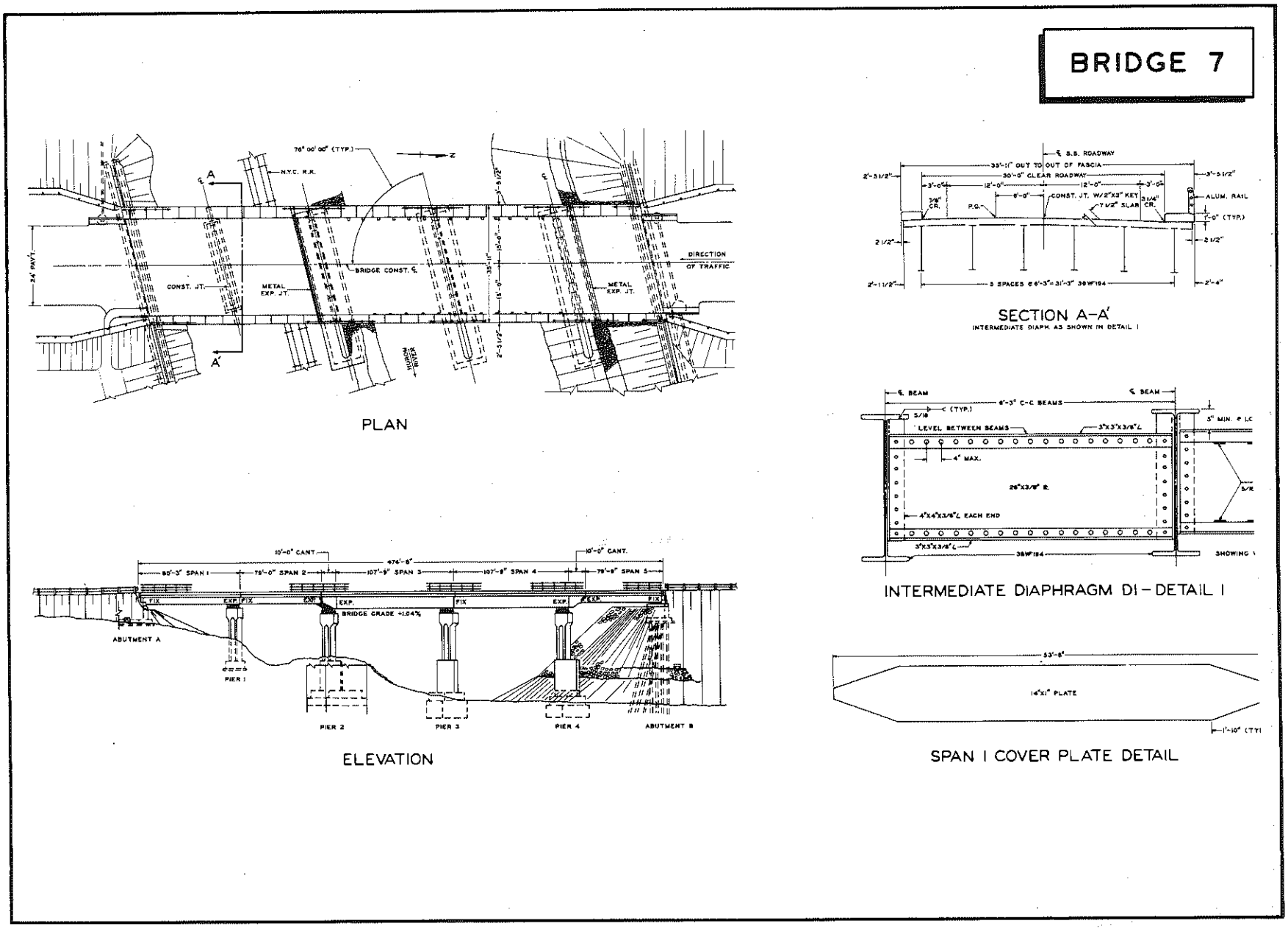

Figure 8. Plan and elevation views, with details.

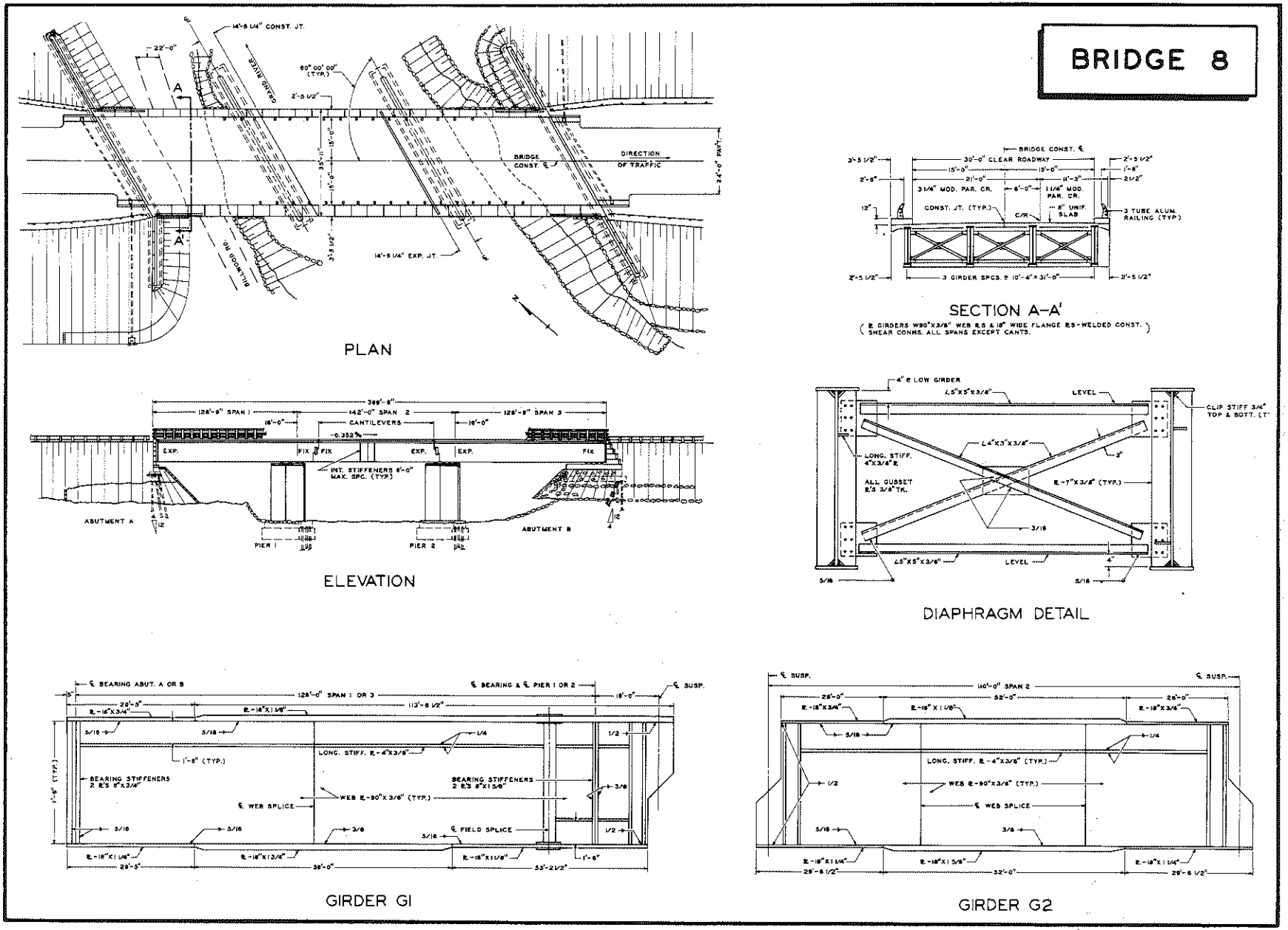

Figure 9. Plan and elevation views, with details.

attachment. Two gages were placed in each area using Eastman 910 adhesive. No traffic was allowed on the bridge for 4 min after gage placement, which was sufficient time for proper adhesion and bonding. Epoxy resin blocks with lead-out wires were attached to the beam adjacent to the gages with Armstrong A-1 adhesive. Connections were made and the entire gage installation covered with either two coats of Armstrong A-1 adhesive plus two coats of Fuller's Resiweld 7200, or Bill Bean's Gage Coat Nos. 1, 2, and 5.

Temperature compensating gages were applied to steel blocks 3/4 by 4 by 4 in. using the same cementing and waterproofing procedure just outlined. A terminal strip was cemented to the steel blocks and the entire assembly was clamped to the lower beam flange in the vicinity of the beam gage installation.

Lead-out wires from the active beam gages were attached to the terminal strips, completing a four-arm external bridge circuit at each strain gage location with the two active arms connected for double output. Belden No. 8404 four-conductor shielded leads were secured by C-clamps to the stringers and terminated in five-pin AN connectors at convenient locations, so that extension leads could be easily attached to complete the connection to the instruments in the mobile laboratory when strain sampling was in progress.

Instrumentation used for the traffic sampling periods consisted of a four-channel Sanborn system with master oscillator power supply (Model 150-1900). Each channel included a preamplifier (Model 150-1100) with driver amplifier (Model 150-200B/400). Recording was done on a Sanborn four-channel oscillograph (Model 154).

In the lateral stress distribution tests, strains were recorded at all mid-span stringer gages. For these tests, a Honeywell 12-channel system was used with a direct-writing light-beam oscillograph (Model 1108 Visicorder).

All gages at the mid-point and end of cover plate locations for the steel rolled beam bridges were SR-4 Type AB-3. All gages at the fillet in the steel plate girder flange thickness transitions were SR-4 Type ABD-7. All gages at the mid-point of the prestressed concrete I-beam bridge were SR-4 Type A-9.

At the mid-point strain gage locations, two active gages were symmetrically placed on the bottom of the lower beam flange 4 to 6 in. from each edge. At the stress concentration point locations in the rolled beam spans,

gages were placed with the gage centerline 1 in. from the end and in line with the terminal edges of the tapered cover plate. In the plate girder bridges, gages were placed 1/4 in. from the point of tangency of the weld and the smaller flange and 5 in. from the flange edge. All of the mid-span gages were placed at the mid-point of the span, with the exception of the two plate girder structures in which the mid-span gages were offset about 1 ft to avoid being directly in line with a vertical web stiffener. The number, configuration, and type of gages for points 1 ft from the stress concentration point locations on Bridges 1, 2, 3, 6, 7, and 8 were identical with gages used at the mid-span gage point locations. Numerous balance and calibration checks were made during each sample period to insure accurate operation of the strain measuring system. The instrumentation systems are shown in Figure 10.

Data Acquisition

After the bridges had been selected and instrumented, sample 6-hr periods were chosen so that each period would be equally represented, i.e., 12 p.m.-6 a.m., 6 a.m.-12 noon, 12 noon-6 p.m., and 6 p.m.-12 p.m. Sampling began August 1963, was completed November 1965, and was confined to the months between June and January.

Traffic data collected over a 3-yr period from 1962 through 1964, with regard to commercial traffic volume variation have been analyzed in conjunction with another Highway Planning and Research study, "Determination of Highway Loadings and Conversion to 18-Kip Single-Axle Load Equivalents," carried on by the Michigan Department of State Highways. It was concluded from that study that the two most significant commercial traffic volume variables were the time of the day and month of the year. Factors based on the study were developed for each weigh station in the Michigan highway system on a 3-hr time period basis. Commercial traffic volume variation for six weigh stations showing the 3-hr time period-to-week, and week-to-year conversion factors are shown in Figure 11. These factors were used for determination of yearly commercial traffic volume for each of the test bridges, utilizing corresponding factors for the weigh station nearest to each bridge. Dashed lines on either side of the shaded area represent one standard deviation. For example, if a test sample were taken from 12 noon to 3 p.m. on westbound I 94 near the Grass Lake north scale in August, this volume would be multiplied by 40 to obtain the weekly volume. Since the conversion factor from week-to-year depends on the month in which samples were taken, weekly volume would have to be multiplied by approximately 56 to get yearly volume.

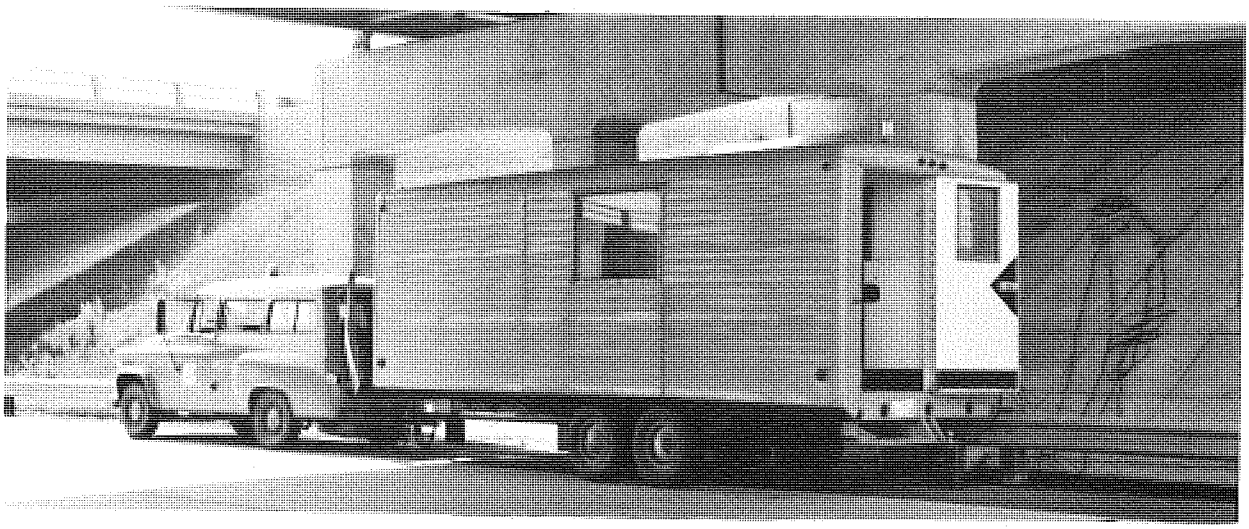

Mobile Laboratory Trailer

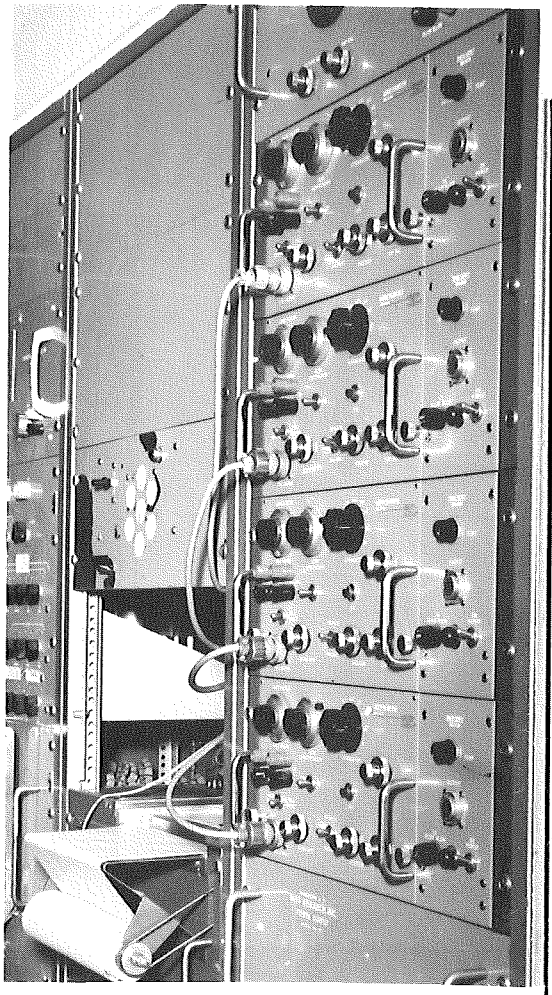

Four-Channel Sanborn Instrumentation in Mobile Laboratory

Minneapolis-Honeywell 12-Channel "Visicorder" Recording Oscillograph

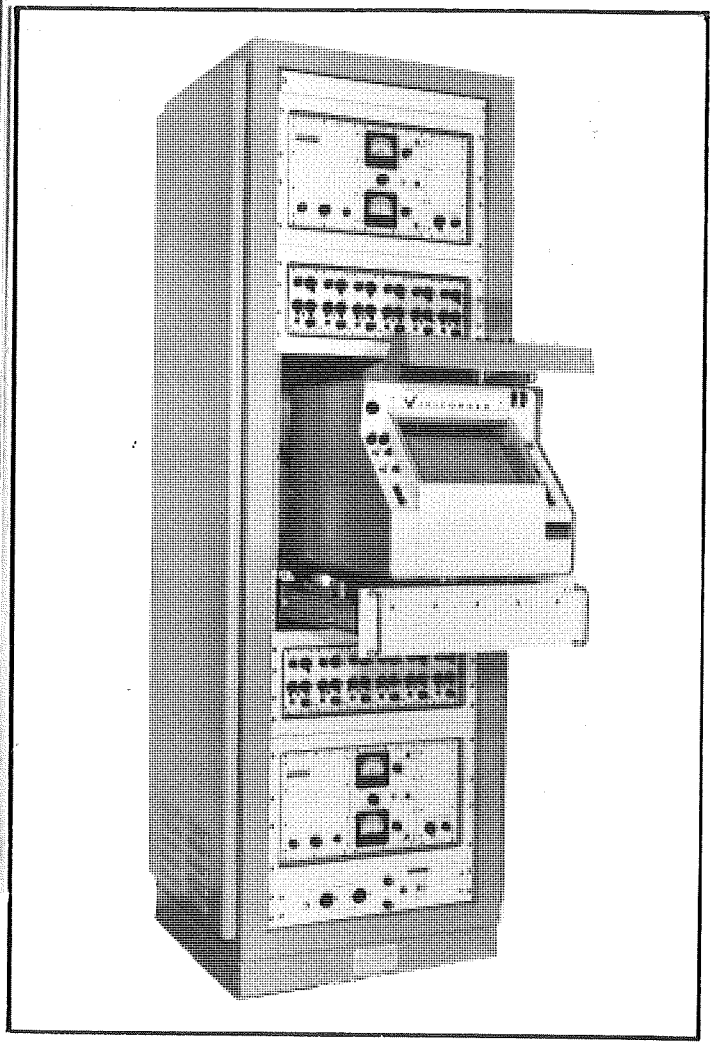

Figure 10. Instrumentation Systems.

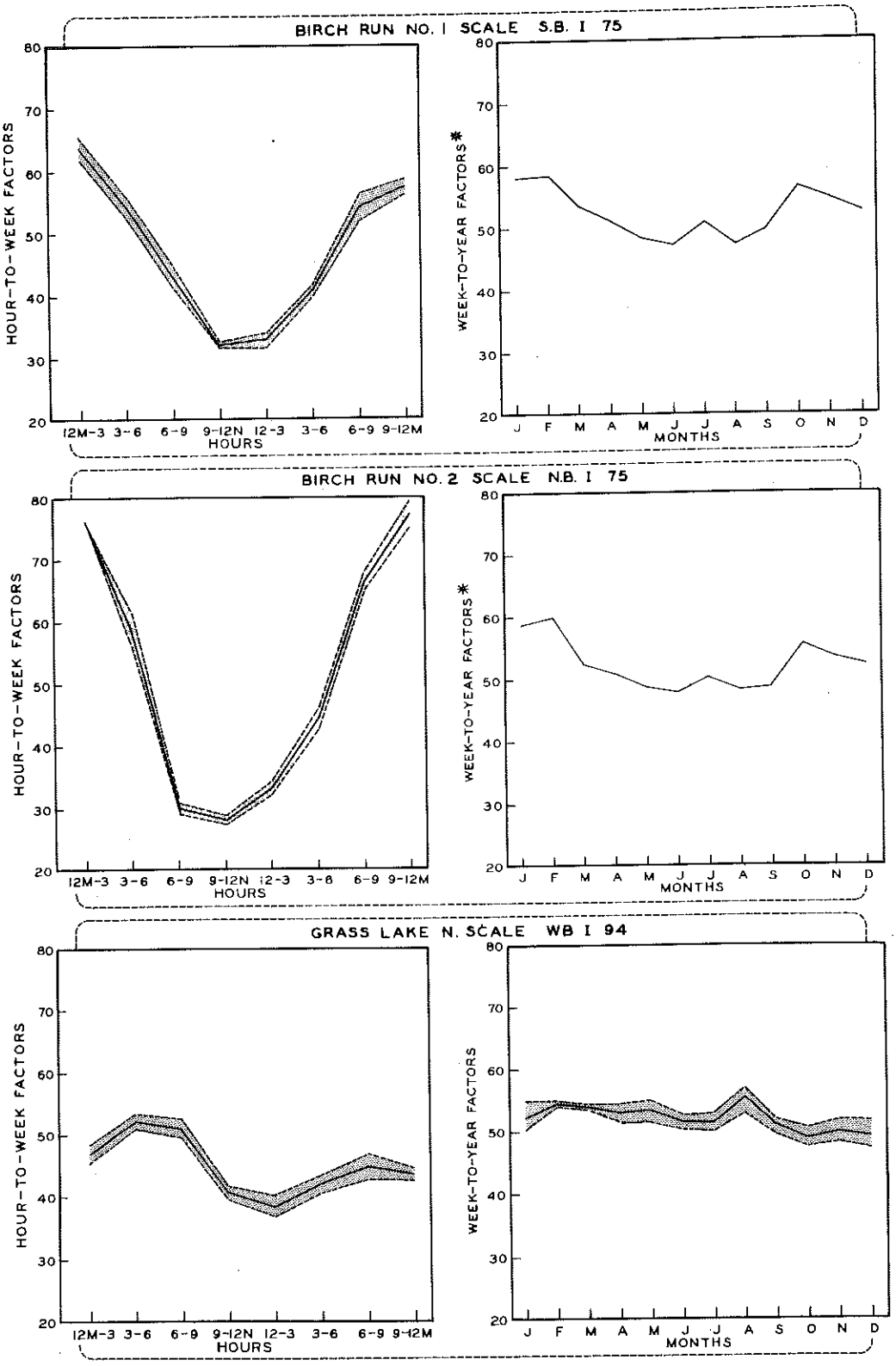

* TRAFFIC DATA WAS COLLECTED ONLY IN 1964 WHEN SCALES WERE FIRST OPERATIONAL AND WAS INSUFFICIENT TO DETERMINE THE FACTOR VARIANCE.

Figure 11. Commercial traffic volume conversion factors.

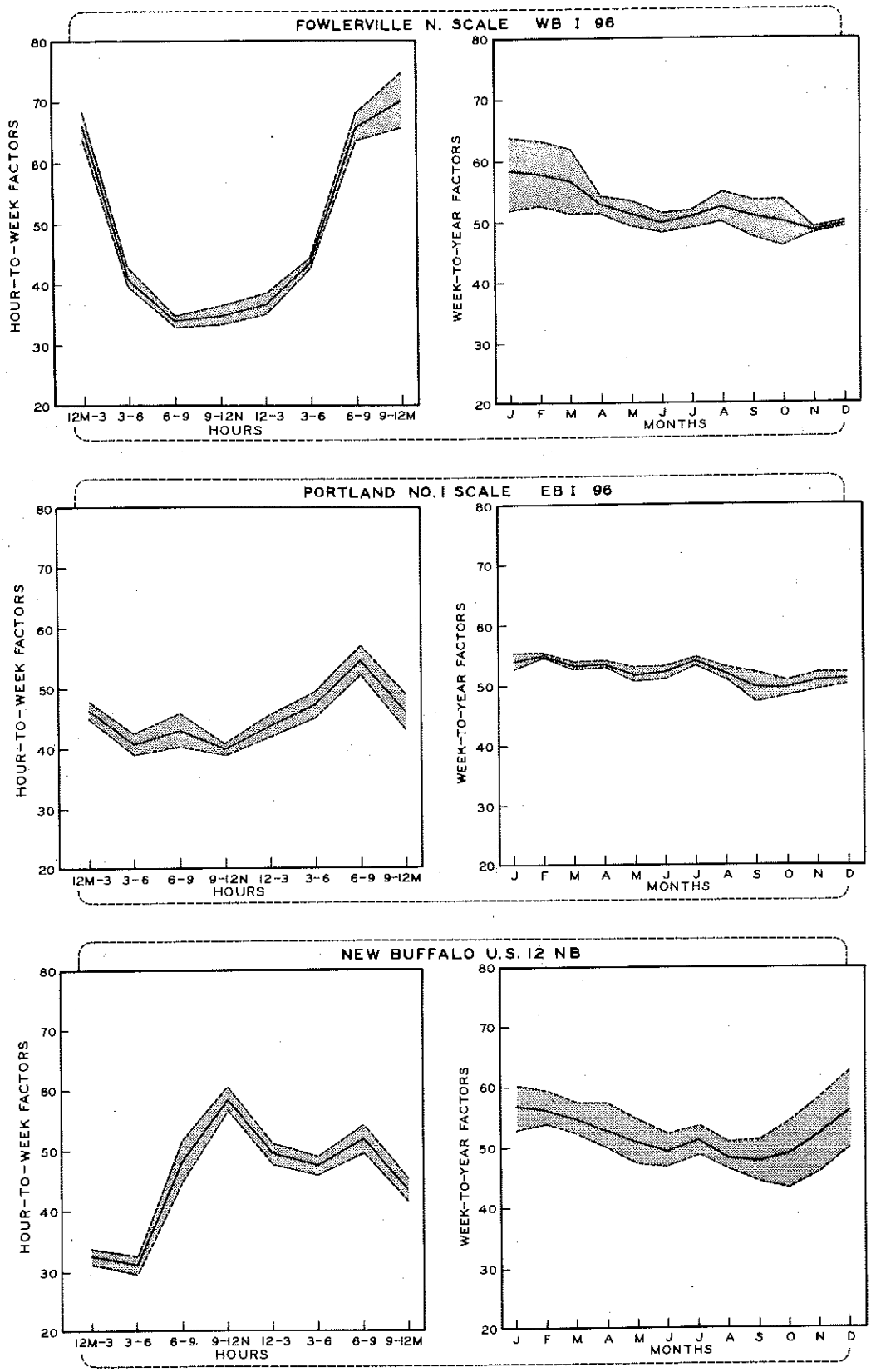

Figure 11 (cont.). Commercial traffic volume conversion factors.

A total of sixty-eight 6-hr sampling periods were taken on the seven steel bridges and four 6-hr periods on the prestressed concrete I-beam bridge. During each 6-hr sample period, the type of each commercial vehicle that passed over the test span was noted, and strains were recorded at mid-span and the stress concentration point of the two most highly stressed stringers in the traffic lane. For Bridges 1, 2, 3, 6, 7, and 8, strains were also recorded at a point 1 ft away from the stress concentration point. In those cases where more than one vehicle was on the span at a time, the number and type were noted; however, no attempt was made to determine relative position of these vehicles. Commercial vehicles as defined herein were all vehicles with the exception of passenger cars and two axle trucks containing single wheels. With the exception of the prestressed concrete structure, (Bridge 4) at which, the mobile laboratory trailer had to be placed in the median, all of the instrumentation equipment and operating personnel were positioned below the structures. The observer noting the number and type of vehicles crossing the individual spans was stationed on the opposite roadway and as much out of sight as possible. In all of the sixty eight, six hour sampling periods, there was no discernable indication that the field test set up had any influence on the normal traffic flow or vehicle placement on the test bridges.

The number of commercial vehicles that passed over the test span with respect to time was also recorded and these data were used in conjunction with the traffic volume factors for estimating average yearly commercial volume. Each 6-hr strain sample yielded two 3-hr sample volumes. The mean yearly value based on the individual 3-hr sample periods was used for determining the average annual commercial traffic volume for each test bridge.

The resulting oscillograph traces were processed through a Benson-Lehner Strip Chart Reader and values of the maximum live load stress and rebound stress were punched on IBM cards. A program was prepared for a Control Data 3600 digital computer located at Michigan State University, for processing these data into stress range, rebound stress and maximum live load stress frequency distributions.

In this study, stress range is defined as the algebraic difference between the peak maximum stress and the maximum peak half-cycle of negative or rebound stress for any vehicle or combination of vehicles producing this stress. Stress parameter definitions used in this report are the same used in reporting AASHO Road Test results (1).

Resulting histograms of stress range, maximum live load stress, and rebound stress for the most highly stressed stringer for each steel test bridge for all 6-hr sampling periods are given in Appendix A. Frequency distributions of the eleven most common truck types plus all remaining types for each sample period on each test bridge are given in Appendix B. The truck type coding system utilized in this study is shown in Figure 12.

Lateral Stress Distribution

An original objective of this study was to observe any significant changes in load-induced stringer stresses with respect to time. A special load test vehicle, built previously for use in rigid pavement research studies, was used for control purposes. This vehicle is a 2S2 type with a 42-ft spacing between the tractor drive axle and the tandem trailer axle. This vehicle, its axle loads, and axle spacings are shown in Figure 13.

On three separate occasions throughout the 2-yr testing period, test runs were made on Bridges 1, 2, 4, and 5. The test vehicle was positioned in the traffic lane, along the center of the bridge, and in the passing lane. Strains were recorded at the mid-point of all stringers for creep speed, 30-, 40-, and 50-mph test runs. Three trials were run in each position on each of three consecutive days.

Although there was no significant variation in the stringer stresses during this short time interval, accumulated data were analyzed, and lateral stress distribution due to this test vehicle was determined at mid-span for the different vehicle speeds and positions. Internal and external moments as determined from the measured strains, were compared with each other as well as with the H 20-S16 design moments. Dynamic stress increments and amplification factors caused by the test vehicle were also determined at various speeds. This testing phase of the study also presented an opportunity to check the reliability of the strain measuring system throughout the 2-yr test period.

Supplementary Tests on Bridges 1 and 2.

In addition to the regular 6-hr sampling periods conducted on Bridges 1 and 2, two special 6-hr sampling periods were scheduled in which gross loads of vehicles crossing these two spans were known. Also, in the case of a few of the larger, heavier, multiple-axle vehicle types, individual axle spacing and axle loads were determined. These data are tabulated in Table 1.

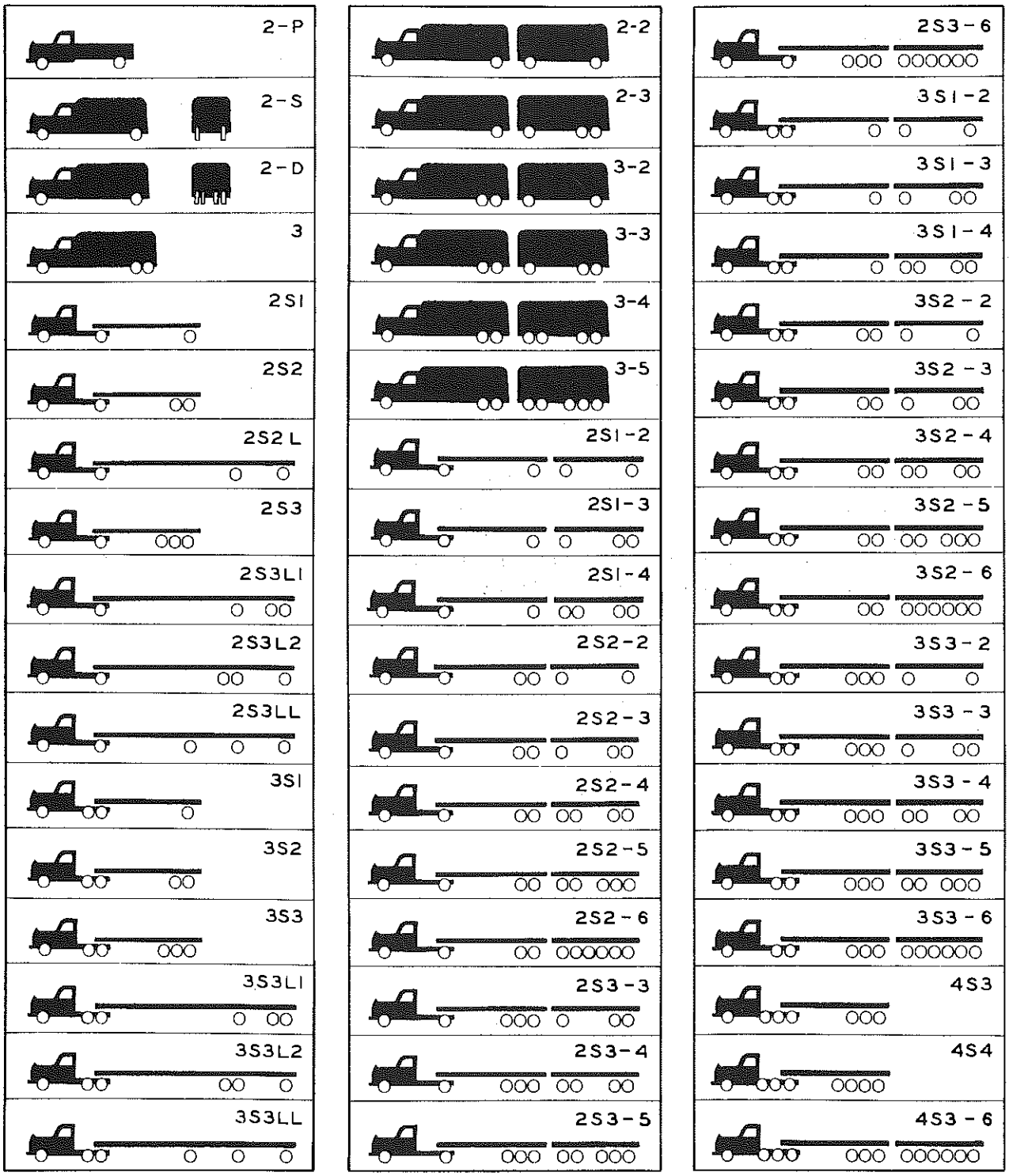

Figure 12. Truck type coding system.

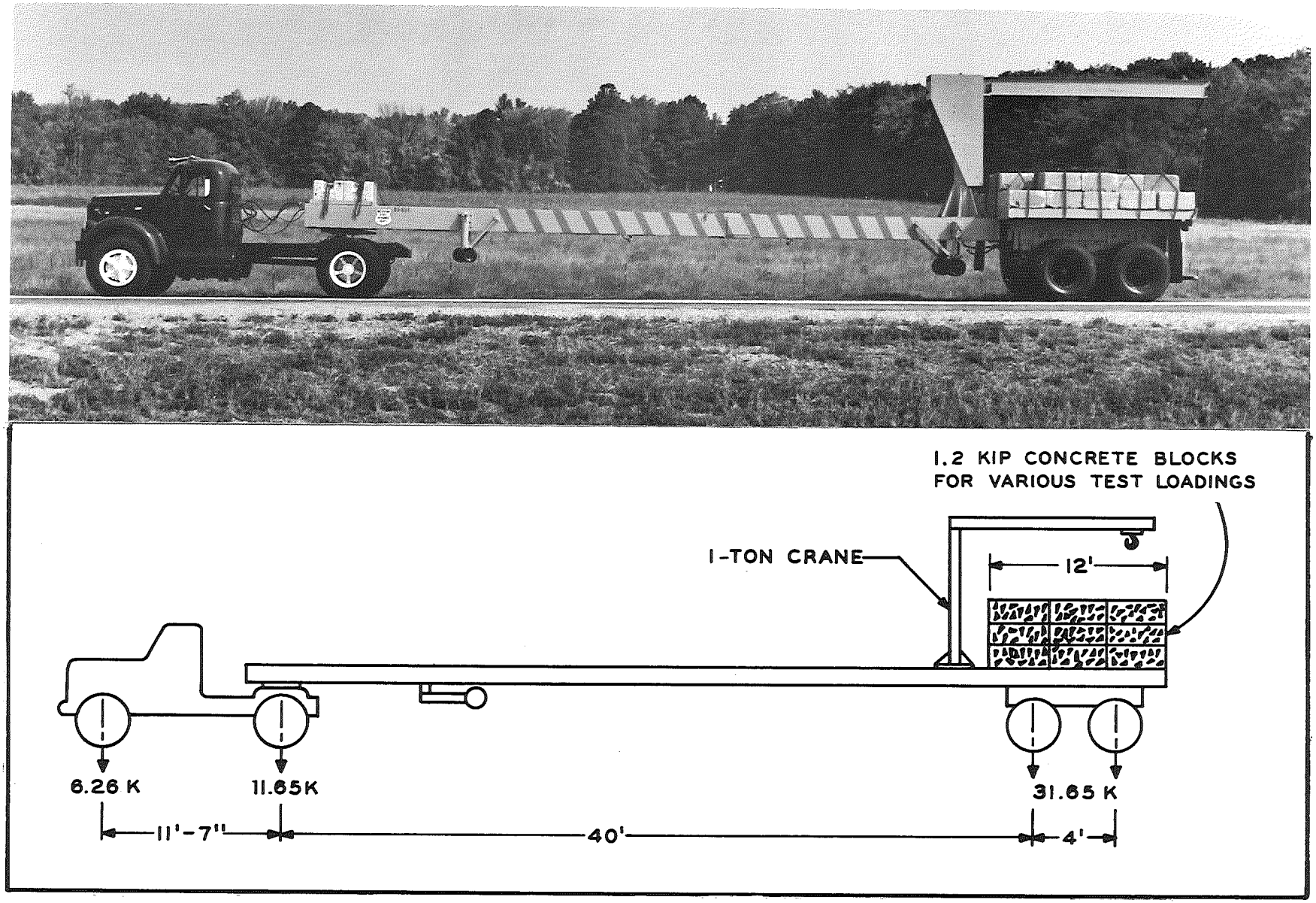

Figure 13. Michigan Department of State Highways special load-test vehicle.

TABLE 1
SUMMARY DATA ON MULTIPLE AXLE VEHICLES ON BRIDGES 1 AND 2

Bridge	Truck Type	Axle Weight, kips (and Spacing, ft)*													Total Load, kips
		Axle 1	Axle 2	Axle 3	Axle 4	Axle 5	Axle 6	Axle 7	Axle 8	Axle 9	Axle 10	Axle 11	Axle 12	Axle 13	
1	4S4-5	16 (9)	13 (3.8)	13 (4.3)	12.5 (4.5)	12.5 (4.8)	11.5 (4.8)	11.5 (4.8)	11.5 (4.8)	11.5 (4.8)	9 (4.5)	9 (3.8)	8 (3.5)	8	147
	2S3L1	11 (12.3)	18 (17.3)	18 (9)	15.5 (4.2)	15.5									78
	3S5L1	12 (10.5)	14.5 (4.3)	14.5 (11.3)	17 (9.1)	13.5 (4)	13.5 (4)	13 (4)	13						111
	3S5L1	10 (10.5)	16 (4.3)	16 (11.3)	16 (9.1)	13.5 (4)	13.5 (4)	13.5 (4)	13.5						112
	3S3-2	11 (10.8)	16.5 (4.2)	16.5 (9.5)	13 (3.8)	13 (3.8)	13 (9.1)	17 (9.1)	16						116
	2S2-2	9 (11.3)	18 (11)	15 (4.3)	15 (10.3)	17 (11.6)	17								91
	3S2L	12 (11.8)	16 (4.3)	16 (18.5)	14 (9.2)	14									72
2	3S3-2	14 (11)	15 (4.3)	15 (9)	12.6 (3.5)	12.6 (3.5)	12.6 (7.2)	14 (10)	17						112.8
	2S2-3	10 (9)	16 (9.2)	15 (4.1)	15 (10.1)	18 (11.3)	12 (4.3)	12							98
	3S3	11 (11.7)	30 (4.5)	30 (26)	18 (4.1)	18 (4.1)	18								125
	3S4-4	14 (10.2)	13 (4.3)	13 (5.6)	12 (3.7)	12.6 (3.7)	12.6 (3.7)	12.6 (5.8)	13 (3.8)	13 (5.2)	13 (3.8)	13			141.8

* First number denotes weight on axle, number in parenthesis is the spacing between axles. Axles are numbered sequentially from the steering axle (Axle 1).

The vehicle weight and measurement data were obtained at the Portland I 96 weigh station located approximately 35 mi west of Bridge 2, and the Fowlerville I 96 weigh station located about 25 mi east of Bridge 1. All vehicles that were to cross these bridges were measured, weighed, and tagged. From these two 6-hr sampling periods for each bridge, maximum stress range and gross load frequency distributions were prepared for the six most common vehicle types, as well as frequency distributions of gross vehicle load, and gross load versus maximum live load stringer stress correlation curves. Dynamic induced stresses caused by these vehicles were also compared with the H 20-S16 design stresses.

DISCUSSION OF RESULTS

Dynamic Characteristics

Table 2 summarizes pertinent dynamic characteristics of the eight test bridges, including natural frequency of vibration, damping factors, decay time of free vibration, and relative beam-to-slab stiffness.

The 128.7-ft plate girder span and the 79.5-ft suspended span structures had the lowest natural frequencies of vibration--3.2 and 3.9 cps, respectively. The remaining steel structures had natural frequencies ranging from 4.5 to 6.4 cps. The prestressed concrete I-beam structure was considerably stiffer with a natural frequency of about 8.5 cps. The relative beam-to-slab thickness ratio was about 4 for the rolled beam bridges. This was about twice the ratio of the prestressed I-beam structure, which had the lowest stiffness ratio, and about one-third of the ratio of the plate girder spans. In computing relative beam-to-slab stiffness of the steel bridges, the average weighted moment of inertia of the composite section was used, based on the average slab depth and an "n" of 6. For the prestressed concrete I-beam, the moment of inertia of the composite section was used based on the average slab depth and a modular ratio, $\frac{E_{beam}}{E_{slab}}$ of 1.3.

While there was no discernable free vibration oscillation period for Bridges 3, 4, 5, 6, and 7, with respect to stringer strain output, it took about three times longer for the longer span plate girder (Bridge 8) and the suspended rolled beam span (Bridge 2) to damp out than the shorter span plate girder (Bridge 1). This is reflected in the damping factors, in which the computed logarithmic decrement for Bridge 1 was about 2-1/2 times greater than for Bridges 2 and 8. In computing these factors and determining

TABLE 2
DYNAMIC CHARACTERISTICS OF TEST BRIDGES

Bridge	Bridge Type	Span Length, ft	Natural Frequency, cps		Logarithmic Decrement (α)	Solid Damping Factor (δ)	Decay Time, sec	Relative Stiffness, H[2]	Stringer Spacing-to-Span Length Ratio
			Computed[1]	Measured					
1	End anchor span, welded plate girder with flange thickness transition	95.0	4.27	4.54	0.111	0.035	6.2	11.4	0.109
2	Suspended center span, rolled beam with welded tapered end cover plate	79.5	4.06 (4.30)	3.87	0.043	0.014	18.3	3.8	0.078
3	Semi-suspended span, rolled beam with welded tapered end cover plate	66.0	5.46 (5.72)	--	--	--	--	4.2	0.121
4	Simple span; prestressed, precast concrete I-beam	45.5	(8.55)	--	--	--	--	2.3	0.136
5	Simple span, rolled beam with welded tapered end cover plate	72.0	5.00 (5.27)	5.71	--	--	--	3.8	0.085
6	Suspended span, rolled beam with welded tapered end cover plate	58.7	6.24 (6.54)	6.39	--	--	--	4.1	0.115
7	Simple span, rolled beam with welded tapered end cover plate	78.5	4.35 (4.60)	5.00	--	--	--	4.2	0.080
8	End anchor span, welded plate girder with flange thickness transition	128.7	3.16	3.23*	0.050	0.016	20.8	14.8	0.081

(1) Based on prismatic simply supported beam using weighted moment of inertia of variable cross-section. Parenthesized values based on moment of inertia at mid-span.

(2) $H = \frac{(EI)_{beam}}{L(EI)_{slab}}$

For steel beam bridges, the moment of inertia was based on the weighted composite cross section with an average slab depth and an "n" of 6.

For the prestressed concrete I-beam bridge, the moment of inertia was based on the midspan composite cross section with an average slab depth and a modular ratio $\frac{E\ beam}{E\ slab}$ of 1.3.

*Not the damped free vibration; includes effect of vehicle on adjacent suspended span.

decay time, the span was assumed to have stopped vibrating when the stringer strain amplitude reached 5 percent of the maximum induced stringer strain.

Strain Response

Typical oscillograph records depicting the resulting stress patterns at the mid-point and stress concentration point of the most highly stressed stringer of each of the eight test spans, for six of the most prevalent vehicle types, are shown in Figures 14 through 21. These traces were obtained from the resulting strain measurement at the described locations. As can be seen, depending on the structure and type of vehicle, a stress excursion resulting from the passage of the particular vehicle type shown ranges from a single half cycle response to a multiple cycle variable wave form. Typical oscillograph records illustrating the relatively long decay times of Bridges 1, 2, and 8 are shown in Figure 22.

Frequency Distributions

Individual histograms of stress range, maximum live load stress, and rebound stress at the mid-point and stress concentration point for the sixty-eight 6-hr sampling periods conducted on the seven steel test bridges are given in Appendix A. Frequency distributions of the eleven most common vehicle types plus all remaining types on each test span for each sample period are given in Appendix B. Also included in Appendix B are frequency distributions of truck type with respect to the four 6-hr sample time periods. These latter histograms show the variability in distribution of vehicle type as a function of daily time period.

Extra Oscillations

In determining frequency distributions of stress range, and maximum live load stress, the maximum peak strain was utilized regardless of the number of distinct strain cycles immediately preceding or following the peak value. Since a stress event was defined in terms of this absolute peak strain, certain vehicles and vehicle combinations, in addition to the resulting cycles of free vibration in those spans with a high vibration susceptibility, produce additional stress cycles of significant magnitude with respect to the absolute maximum stress range excursion. In other words, certain vehicles or vehicle combinations produced complementary stress cycles with greater amplitudes than the absolute maximum induced stress

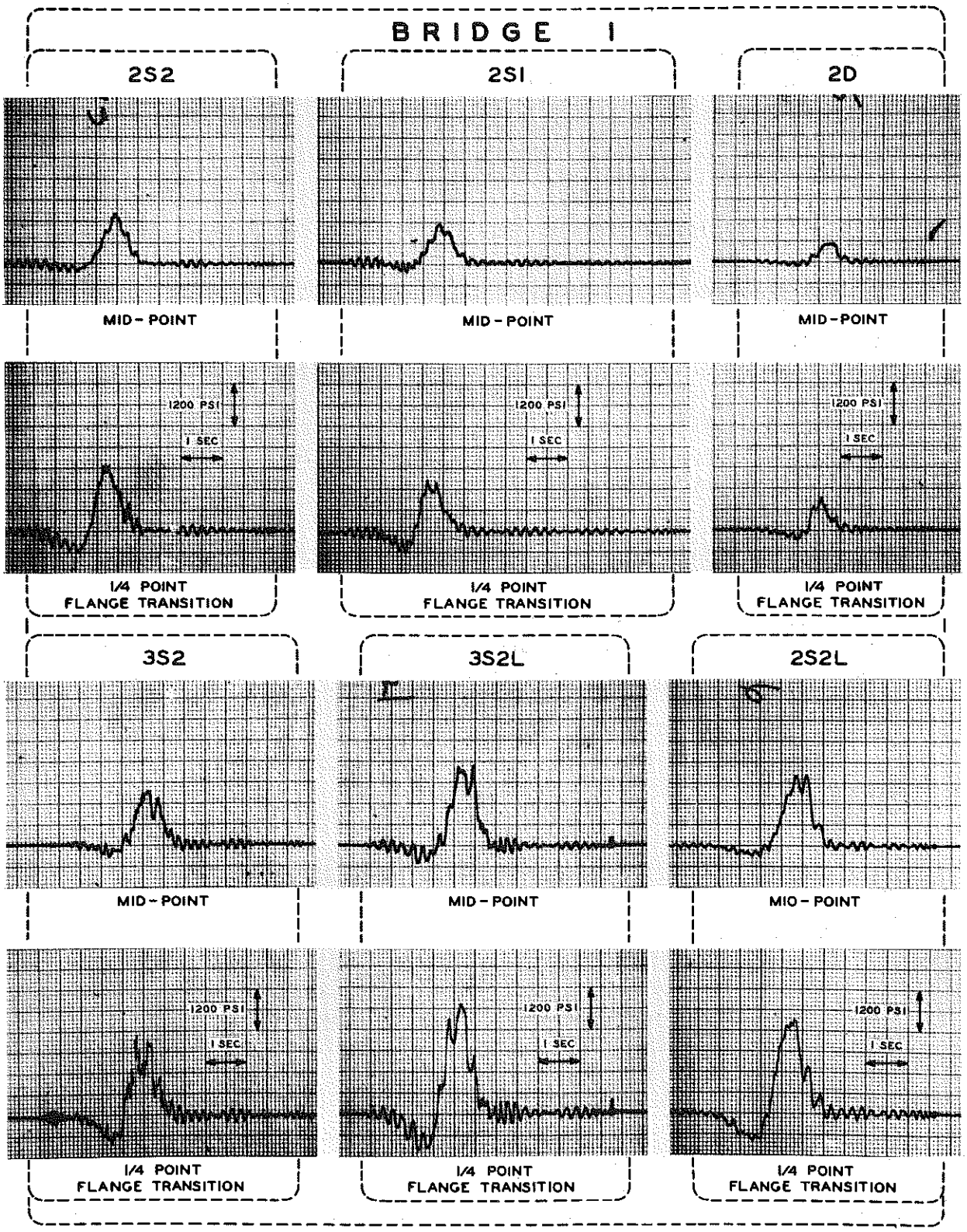

Figure 14. Typical stress patterns at mid-point and stress concentration point for most common vehicle types.

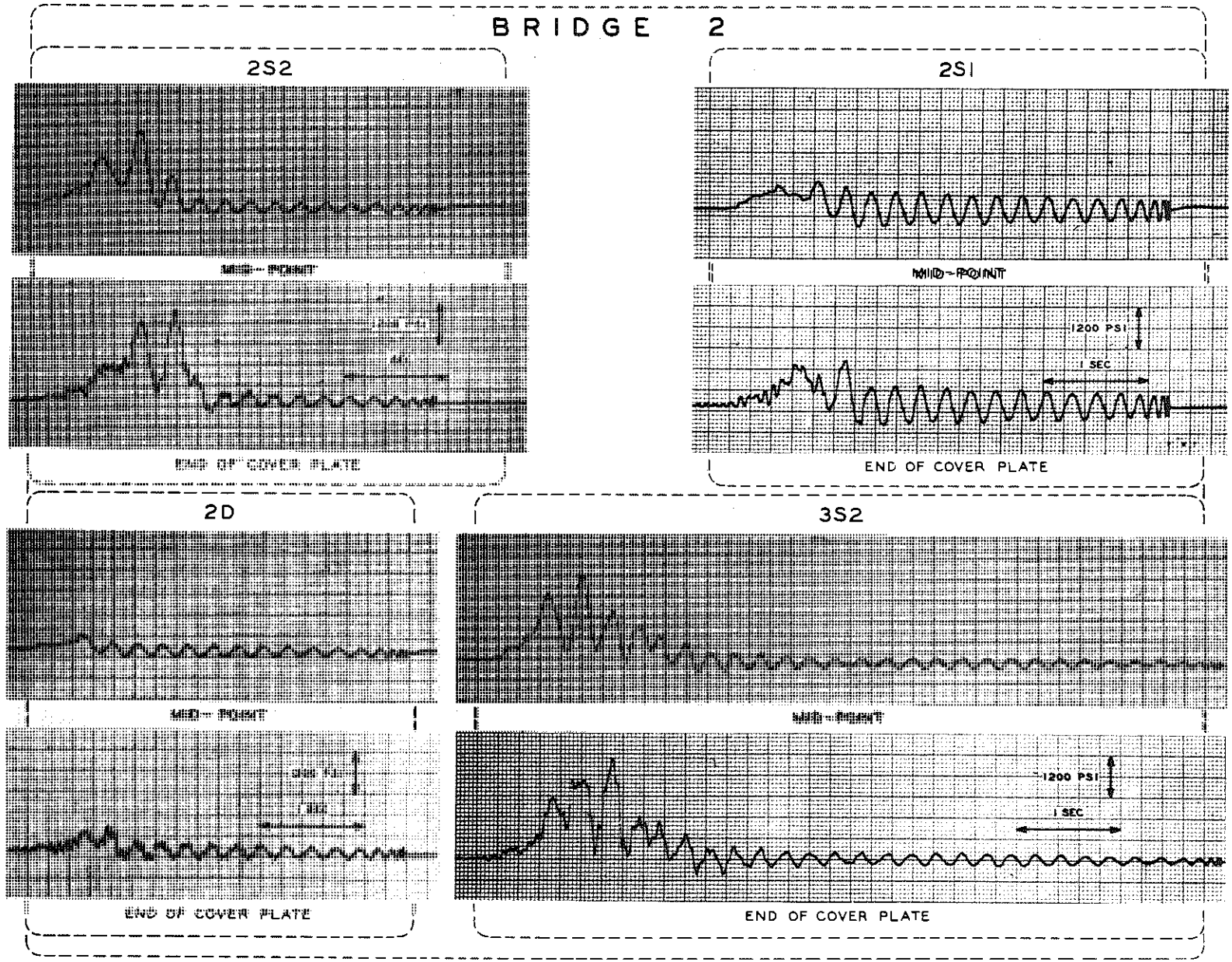

Figure 15. Typical stress patterns at mid-point and stress concentration point for most common vehicle types.

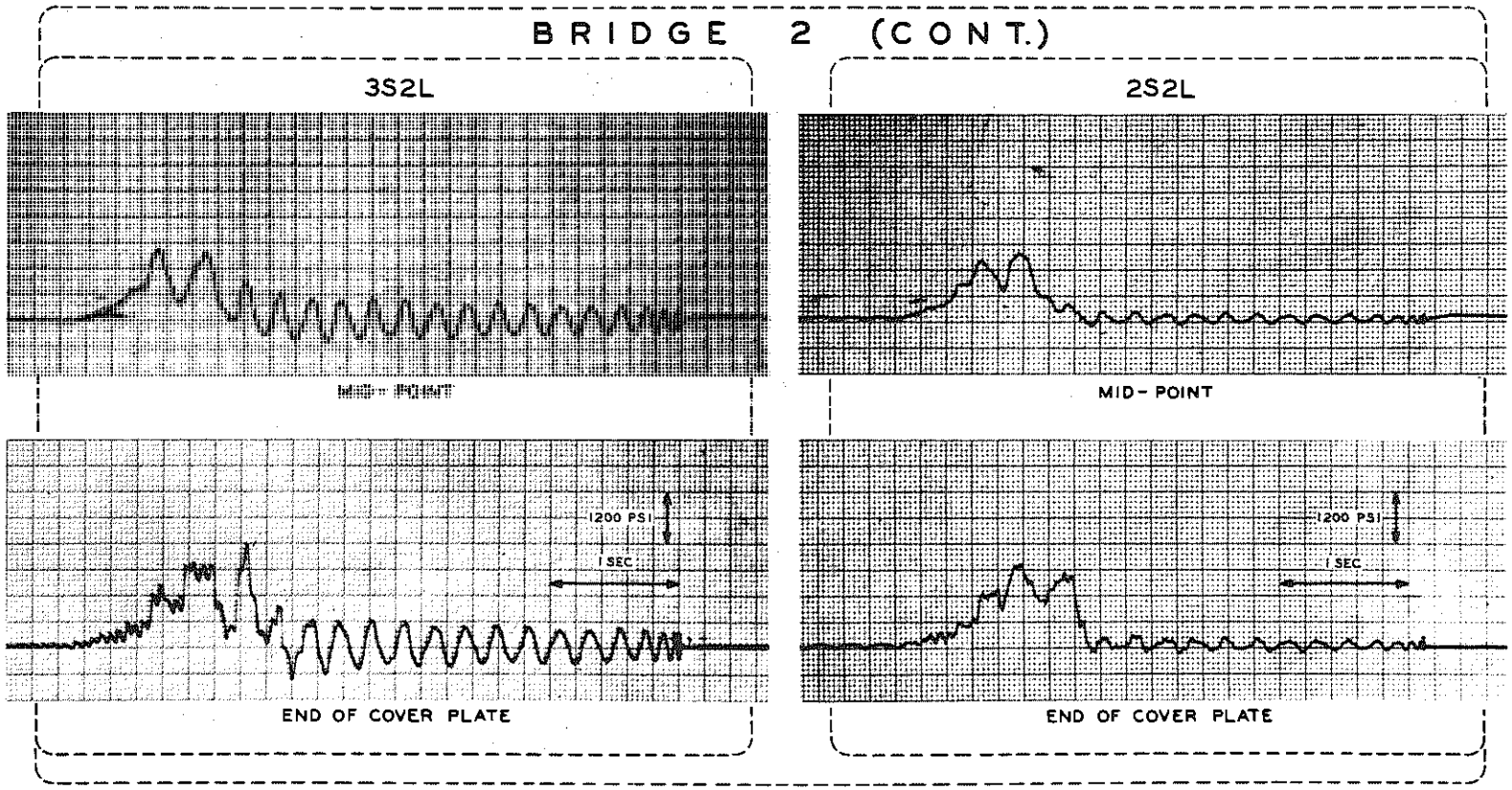

Figure 15 (cont.). Typical stress patterns at mid-point and stress concentration point for most common vehicle types.

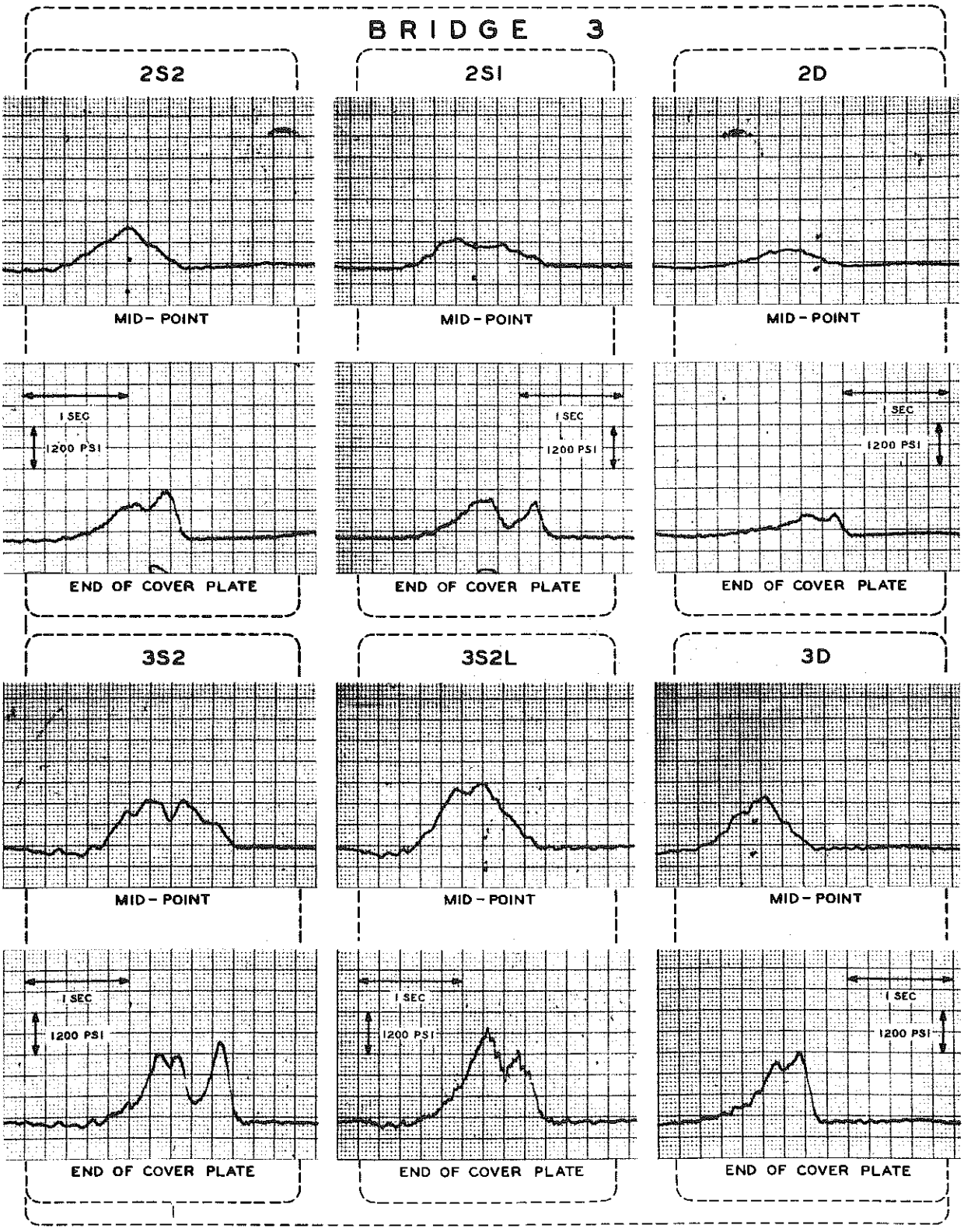

Figure 16. Typical stress patterns at mid-point and stress concentration point for most common vehicle types.

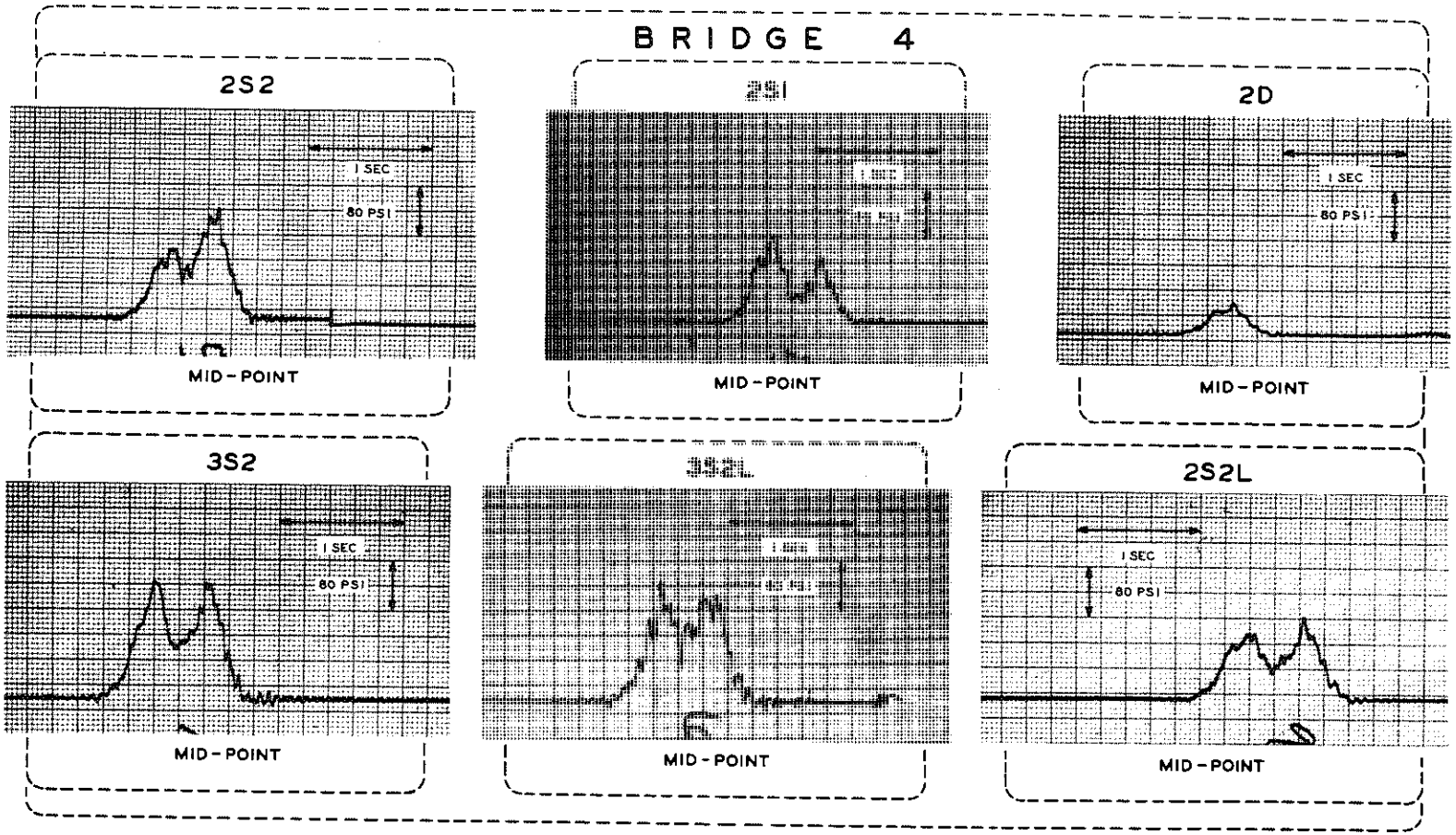

Figure 17. Typical stress patterns at mid-point and stress concentration point for most common vehicle types.

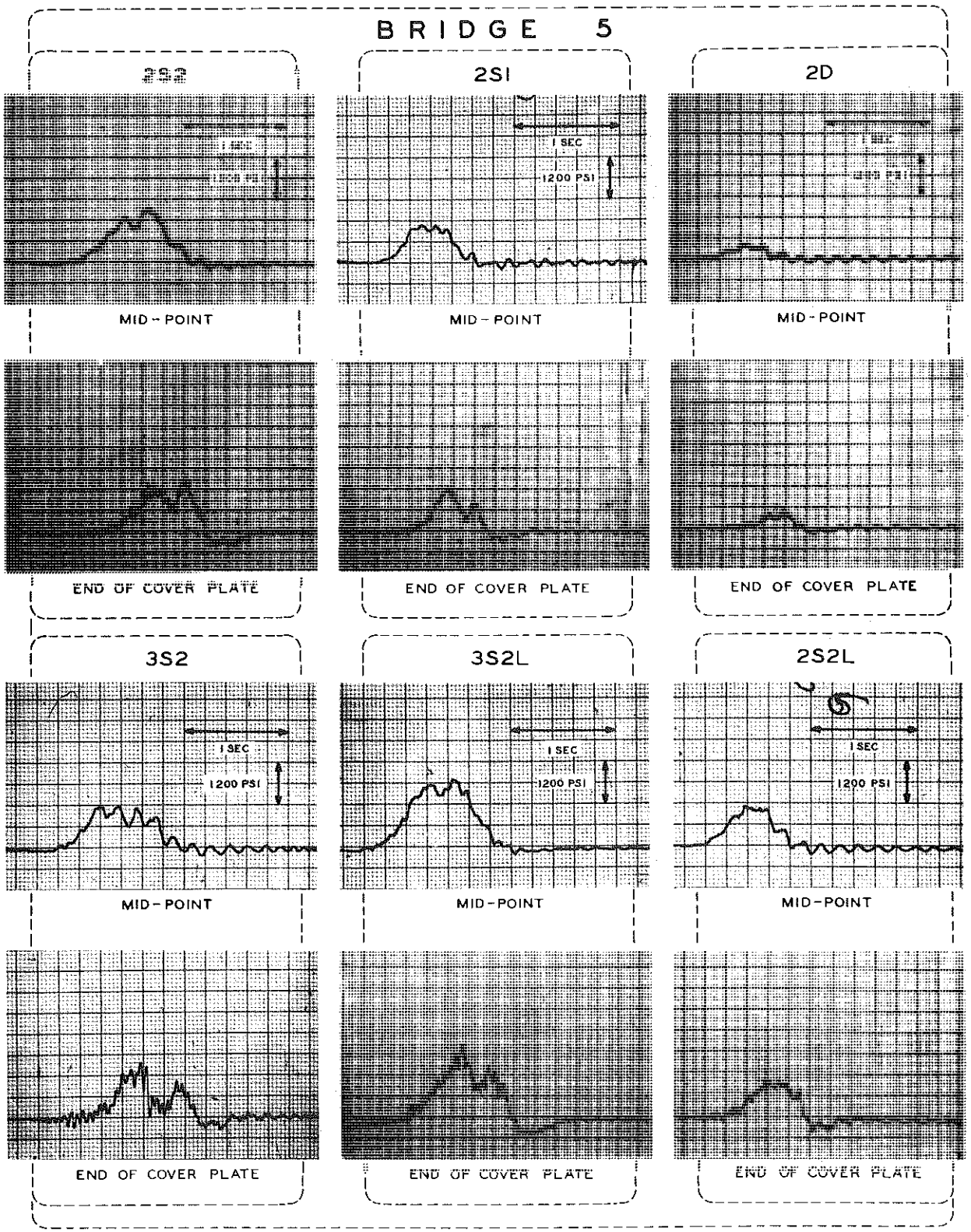

Figure 18. Typical stress patterns at mid-point and stress concentration point for most common vehicle types.

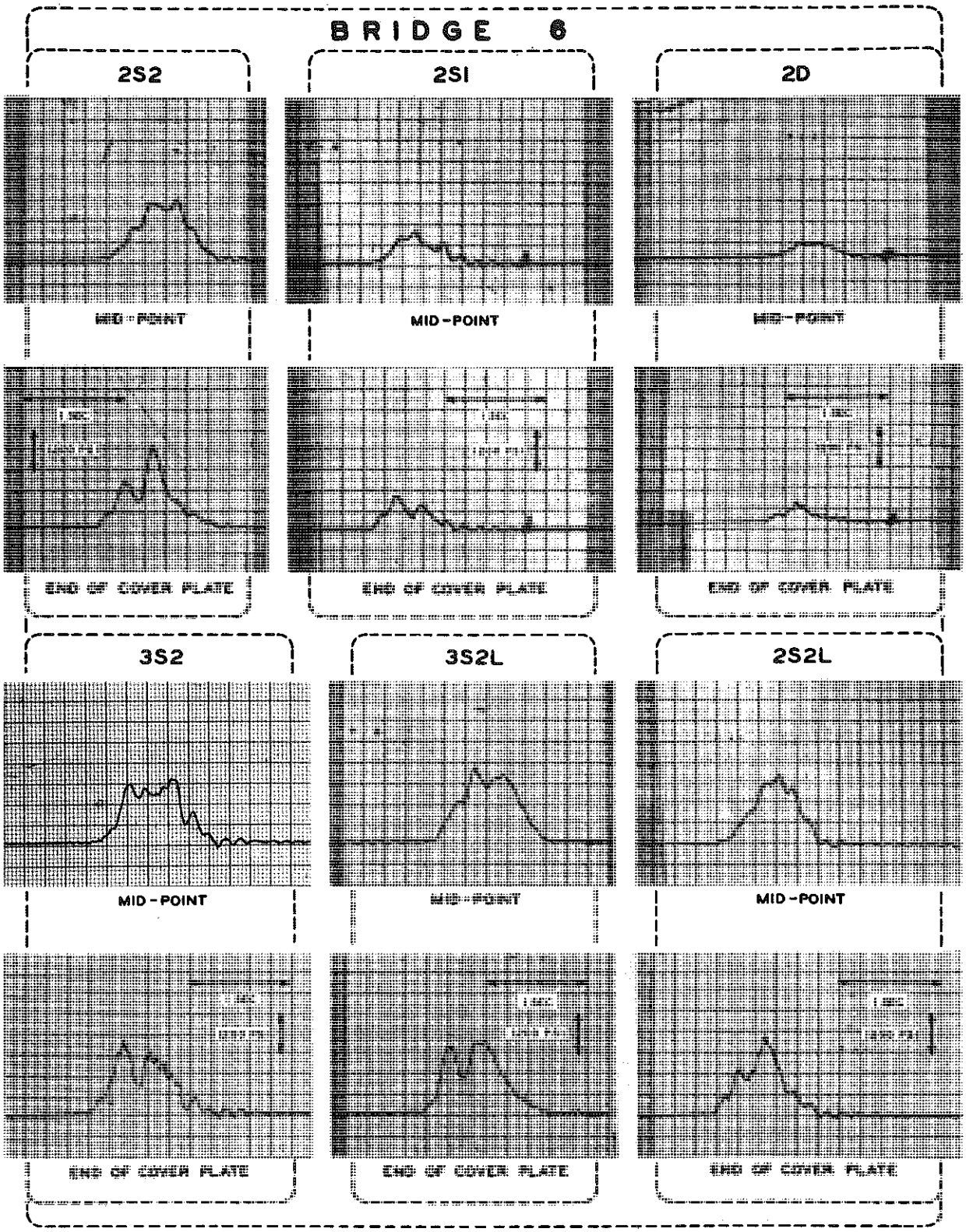

Figure 19. Typical stress patterns at mid-point and stress concentration point for most common vehicle types.

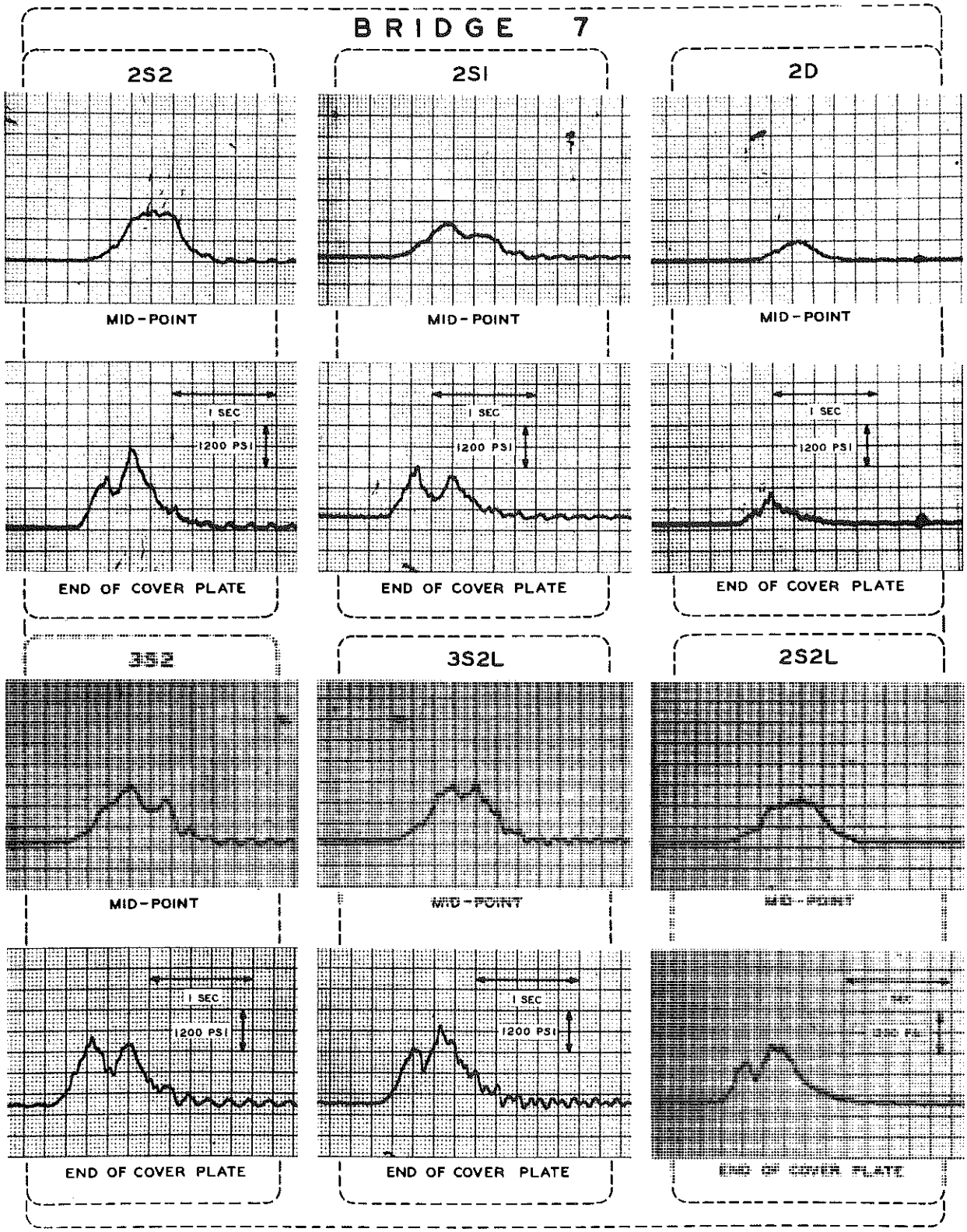

Figure 20. Typical stress patterns at mid-point and stress concentration point for most common vehicle types.

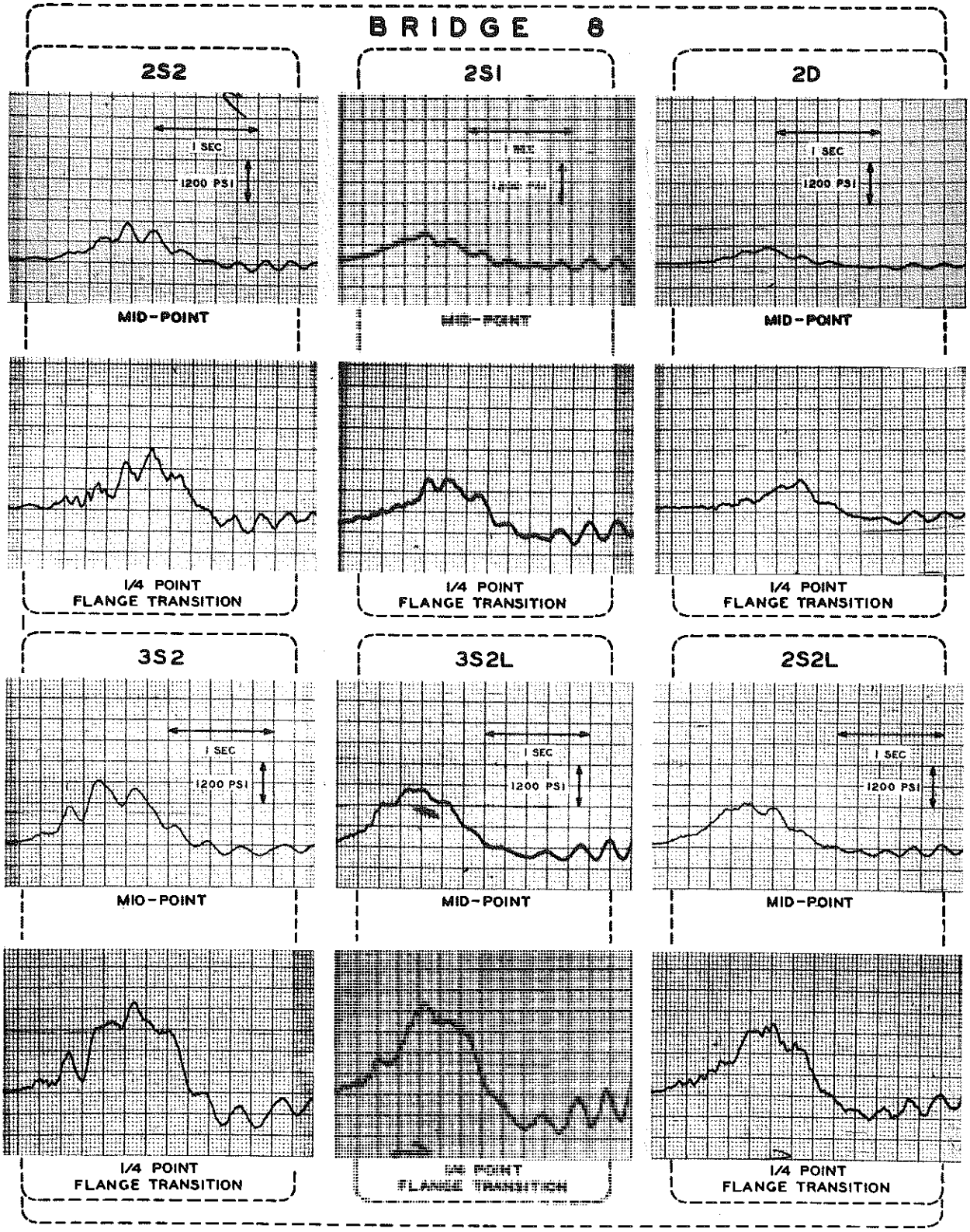

Figure 21. Typical stress patterns at mid-point and stress concentration point for most common vehicle types.

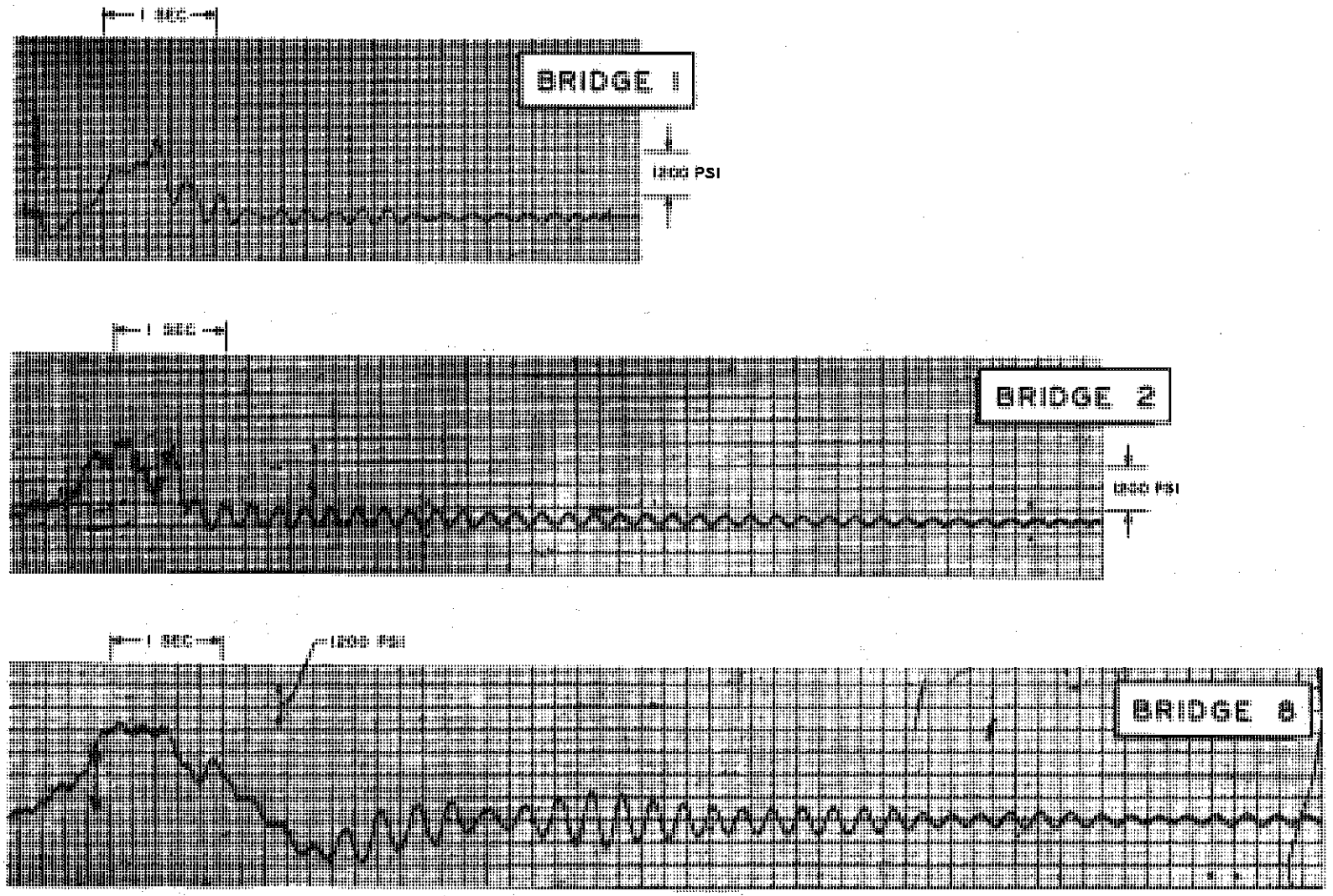

Figure 22. Oscillograph records illustrating decay time on Bridges 1, 2, and 8.

amplitude caused by other vehicle types. Frequency distributions of these additional peak-to-peak cycles of stress range at the stress concentration points of the affected test spans for stress ranges greater than 600 psi are shown in Figure 23. For Bridges 1, 6, 7, and 8, the percentage of additional stress range cycles which exceeded 600 psi varied from approximately 20 to 50 percent of the number of vehicle events. In the case of Bridge 2, the 79.5-ft suspended span, the number of additional stress range cycles exceeding 600 psi was about 360 percent of the number of vehicle events. Approximately 62 percent of these, however, were in the 600 to 900 psi range and were primarily the result of the free vibration mode of this structure.

Based on the fatigue analysis utilized in this study, these additional strain range cycles were adjudged to be insignificant with respect to their effect on the stringer fatigue life. It is interesting to note however, that under the various prevailing vehicle types, speeds, and dynamic characteristics, a stress event simplified into a one-cycle peak-to-peak excursion cannot be ascribed to the cyclic strain variation that actually takes place.

Rebound Factors

Rebound factors, $\frac{\sigma_{LL}\,max + \sigma\ rebound}{\sigma_{LL}\,max}$, as determined for the most highly stressed stringer at the mid-point and stress concentration point for the eight sample spans, are given in Table 3. With the exception of the 79.5-ft suspended span (Bridge 2), the rolled beam bridges had a rebound factor varying from 1.07 to 1.12 at mid-span. Rebound factors for these bridges at the stress concentration points were in the same range with the exception of the 72-ft simple span (Bridge 5) in which there was an 11.5-percent increase over the mid point value. The 79.5-ft suspended span had a rebound factor of 1.25 at the mid-point and 1.26 at the stress concentration point. In the case of the prestressed I-beam structure (Bridge 4), rebound stress was essentially non-existent and the resulting rebound factor was reduced to unity. In the case of the two welded plate girder spans (Bridges 1 and 8), the effect of loadings on the center suspended spans produced negative moments in the test anchor spans. The maximum "negative" strain caused by these moments was used in determining the maximum rebound stress, and the corresponding factors in Table 3 for these two spans were based on these values. The large induced "negative" stress due to the center suspended span loading is reflected in the larger rebound factors presented.

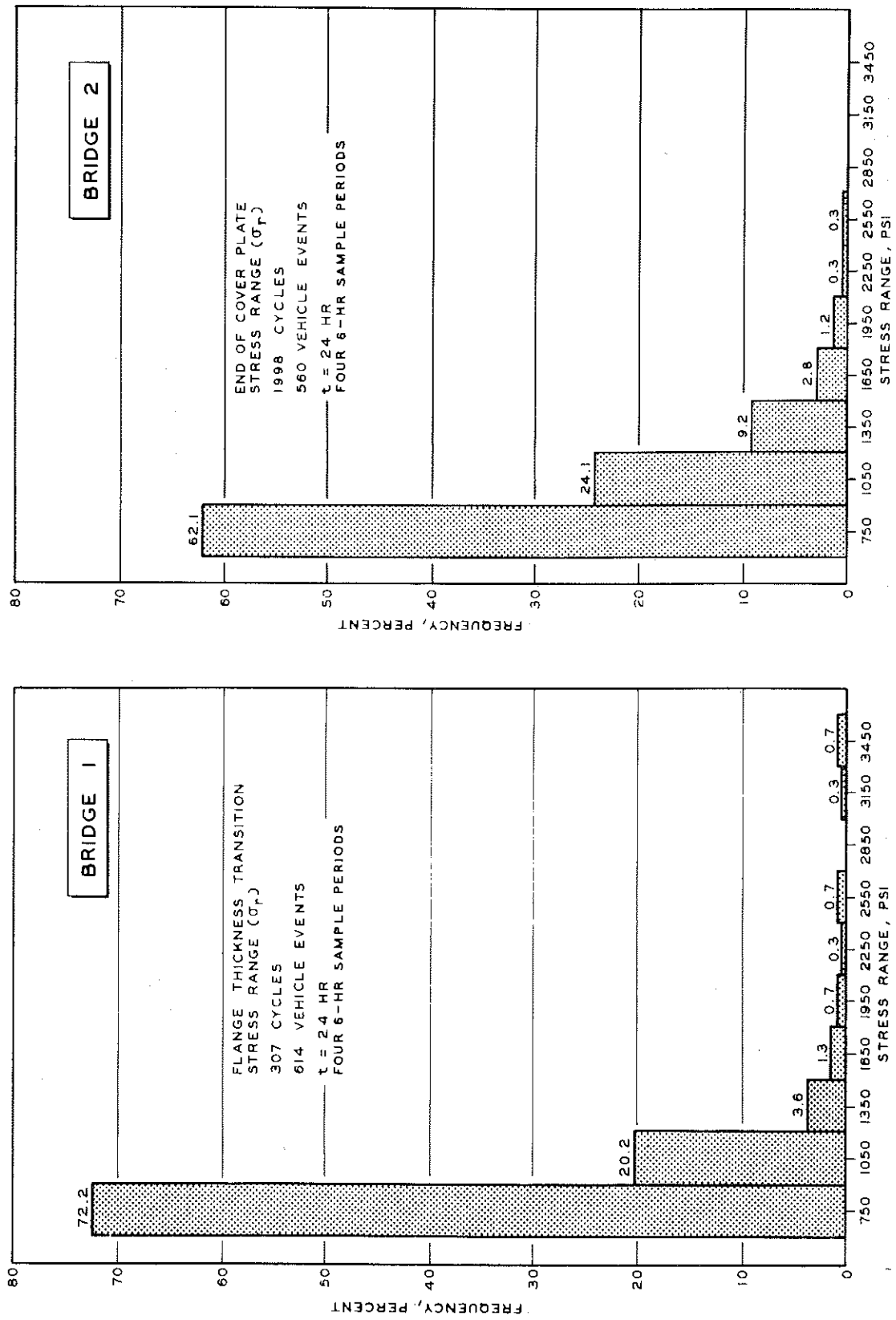

Figure 23. Distributions of extra oscillations of stress range at the stress concentration point.

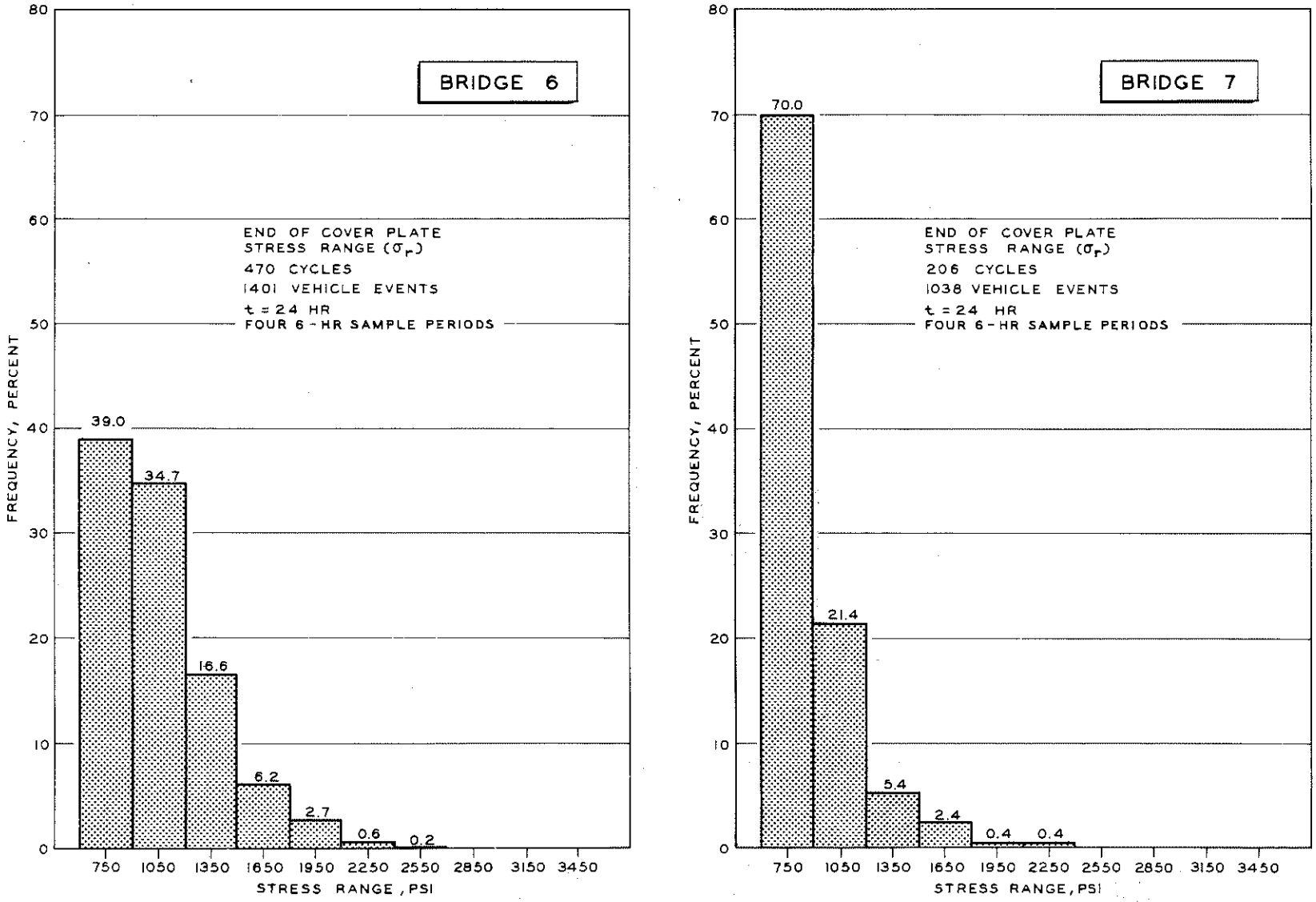

Figure 23 (cont.). Distributions of extra oscillations of stress range at the stress concentration point.

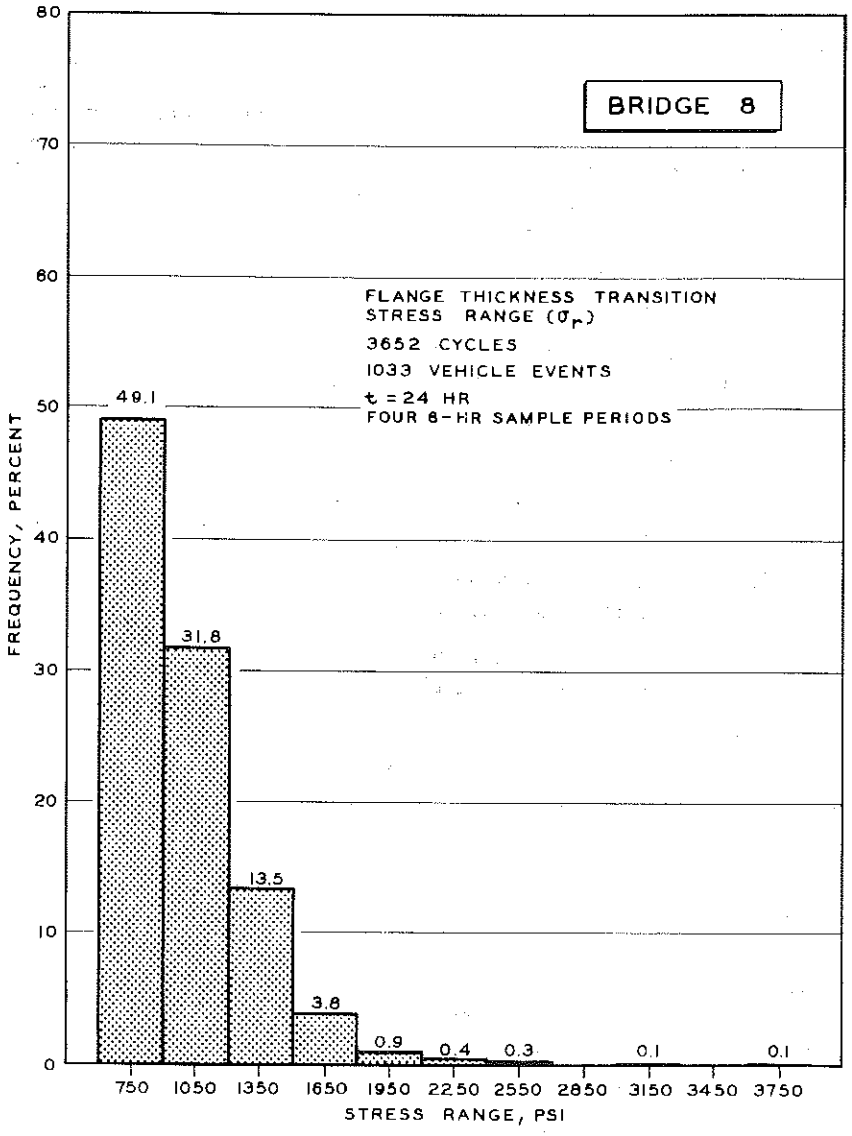

Figure 23 (cont.). Distributions of extra oscillations of stress range at the stress concentration point.

TABLE 3
REBOUND FACTORS FOR MAXIMUM STRESSED BEAM

Bridge	Bridge Type	Rebound Factor $\left(\frac{\sigma_{LL}\ max + \sigma\ rebound}{\sigma_{LL}\ max}\right)$	
		Mid-Point	Stress Concentration Point
1	End anchor span, welded plate girder with flange thickness transition	1.22	1.37
2	Suspended center span, rolled beam with welded tapered end cover plate	1.26	1.25
3	Semi-suspended span, rolled beam with welded tapered end cover plate	1.12	1.09
4	Simple span; prestressed, precast concrete I-beam	1.00	
5	Simple span, rolled beam with welded tapered end cover plate	1.12	1.25
6	Suspended span, rolled beam with welded tapered end cover plate	1.07	1.07
7	Simple span, rolled beam with welded tapered end cover plate	1.10	1.11
8	End anchor span, welded plate girder with flange thickness transition	1.30	1.41

Fatigue Curves

The fatigue curves utilized in this study were developed from the Munse-Stallmeyer data (2), and are designated Methods 1 and 2. The Munse-Stallmeyer data represents a number of tests demonstrating the effect of details such as splices, stiffeners, cover plates and attachments on the fatigue behavior of welded flexural members. These tests were conducted on A373 steel utilizing E 7016 electrodes and manual arc welding, and with a few exceptions represent constant cycle zero to tension loadings. Fatigue strengths at 100,000 and 2,000,000 cycles are given for the various types of splice geometry as well as the various cover plate details represented. The respective nominal zero to tension fatigue strengths at two million cycles for partial length tapered end cover plates welded all the way around, and for butt-welded flange thickness transitions were reported as 11,400 psi and 18,500 psi, respectively.

The Method 1 fatigue curve (Fig. 24) was obtained as follows: using the 0-to-tension cycle Munse-Stallmeyer data for butt-welded flange thickness transition and partial-length tapered end cover plates welded all the way around, the Modified Goodman Law was used to establish corresponding stress range values at 2×10^6 cycles for dead load tension-to-tension stress range cycles. In this determination, the ultimate tensile strength of the stringer material was assumed to be 60,000 psi and the minimum stress value corresponding to the dead load stress represented the average nominal dead load stress at the stress concentration points of the respective bridge types, i.e., 7,660 psi for the welded plate girders and 6,970 psi for the rolled beams with cover plates. Based on the assumption that the stress range value at 200×10^6 cycles is equal to one-third the stress range value at 2×10^6 cycles, as assumed in House Document 354 (3), and assuming that the stress range and cycles to failure have a linear log-log relation, the following equations were derived.

For butt-welded flange thickness transition	$\log N = 11.38 - 4.18 \log \sigma_r$ for $2 \times 10^6 \leq N \leq 200 \times 10^6$	(1a)
For tapered end cover plates welded all the way around	$\log N = 10.45 - 4.18 \log \sigma_r$ for $2 \times 10^6 \leq N \leq 200 \times 10^6$	(1b)

The Method 2 fatigue curve (Fig. 24) is based on the same basic data and the assumption of House Document 354 (3). In this method, however, the minimum or dead load stress is ignored as being inconsequential, and the stress range is assumed to be a linear function of the log of the number of cycles to failure. The resulting equations for this method are given as follows:

For butt-welded flange thickness transition	$\log N = 9.30 - 0.162\ \sigma_r$ for $2 \times 10^6 \leq N \leq 200 \times 10^6$	(2a)
For tapered end cover plates welded all the way around	$\log N = 9.30 - 0.263\ \sigma_r$ for $2 \times 10^6 \leq N \leq 200 \times 10^6$	(2b)

Both of these methods and corresponding fatigue curves were used in conjunction with Miner's cumulative damage hypothesis of fatigue failure, i.e., failure occurs when $\sum \frac{n_i}{N_i} = 1$, where n_i = number of cycles at stress range level σ_i, and N_i = number of cycles at stress range level σ_i which would cause a fatigue failure.

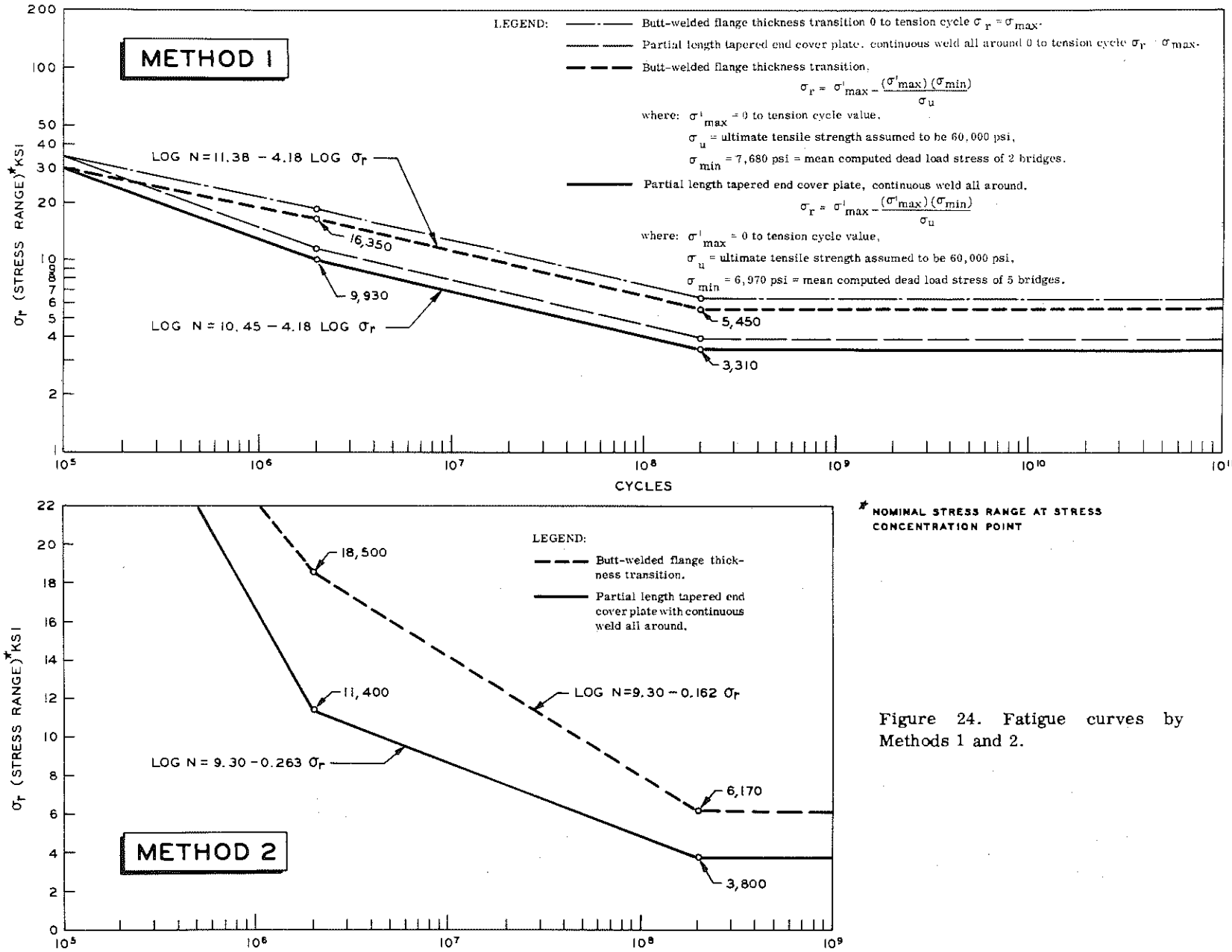

Figure 24. Fatigue curves by Methods 1 and 2.

All strains and subsequent stresses used in determining test span fatigue life were measured at, or very near, the particular stress concentration points. The Munse-Stallmeyer fatigue data (2) are based on the nominal stress at the stress concentration point section. As previously described, additonal strain gages were placed 1 ft from stress concentration points on Bridges 1, 2, 3, 6, 7, and 8. It was assumed that output from these gages would be representative of the nominal stress at the stress concentration point section. Based on a random sample of 30 events for each bridge, regression lines relating the strain output at the stress concentration point and 1 ft away are shown in Figure 25 for the six sample bridges. The average ratio of strain 1 ft away from the stress concentration point, to strain at the stress concentration point for these six bridges was about 70 percent.

All steel test structures were fabricated from ASTM A 373 steel.

Stress Range Frequency Distributions

Frequency distributions of stress range at the stress concentration point for the seven steel test bridges, based on total accumulated vehicle events for each bridge, are shown in Figure 26. Histograms of stress range at the mid-point for the eight sample test spans are shown in Figure 27. In addition, each frequency distribution contains a range for each stress range interval equal to $\pm$ 2 standard deviations. These standard deviations were computed as the standard error of a proportion which is equal to $\sigma_p = \frac{\sigma}{\sqrt{n}}$ where σ is the standard deviation of the population from which the sample size n is drawn, and is given by $\sigma = \sqrt{P\,(1-P)}$ where P is the population proportion or population mean. Thus, $\sigma_p = \sqrt{\frac{P\,(1-P)}{n}}$. For $np > 5$, the normal distribution can be substituted for the binominal distribution and the range of $\pm$ 2 standard errors ($\pm 2\,\sigma_p$) gives a confidence interval probability of 0.95. The upper limit of the confidence interval range was used in determining cumulative fatigue damage and fatigue life of the respective test spans.

As can be seen from Figure 26, the highest ratio of the maximum stress range histogram interval to the nominal design live load plus impact stress at the stress concentration point was approximately 82 percent, occurring in Bridges 2, 3, 7, and 8. The maximum occurrence frequency was 0.7 percent in Bridge 8. The smallest ratio was about 55 percent with an occurrence frequency of 0.1 percent in Bridge 6.

With reference to Figure 27, it can be seen that the maximum stress range histogram interval at mid-span did not exceed the corresponding design live load plus impact stress for any of the sample bridges. The highest ratio of the maximum stress range interval (6300 $\pm$ 300 psi) to the design live load plus impact stress occurred in Bridge 8. This ratio was about 90 per-

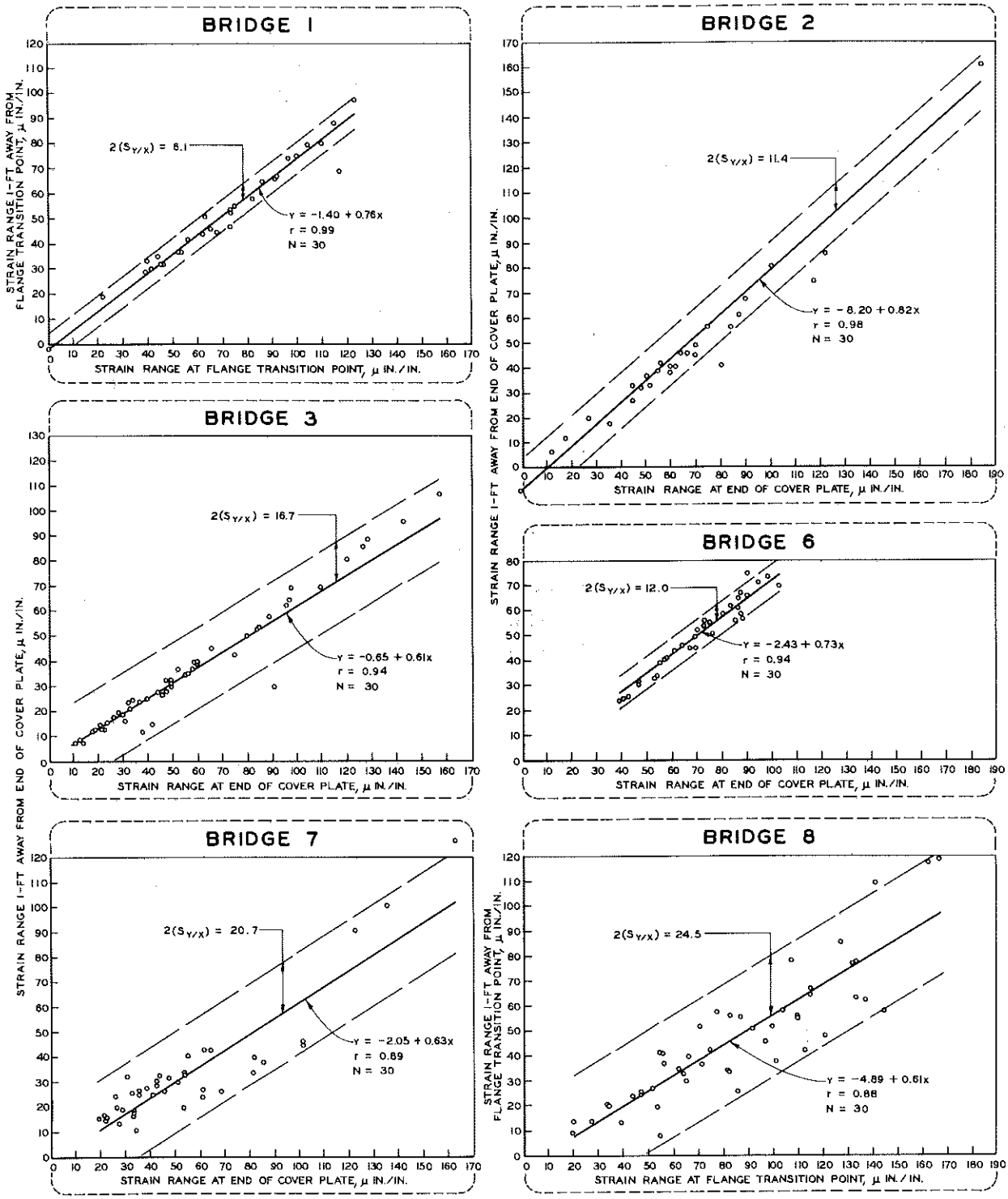

Figure 25. Correlation between strain at the stress concentration points and at a point 1-ft away.

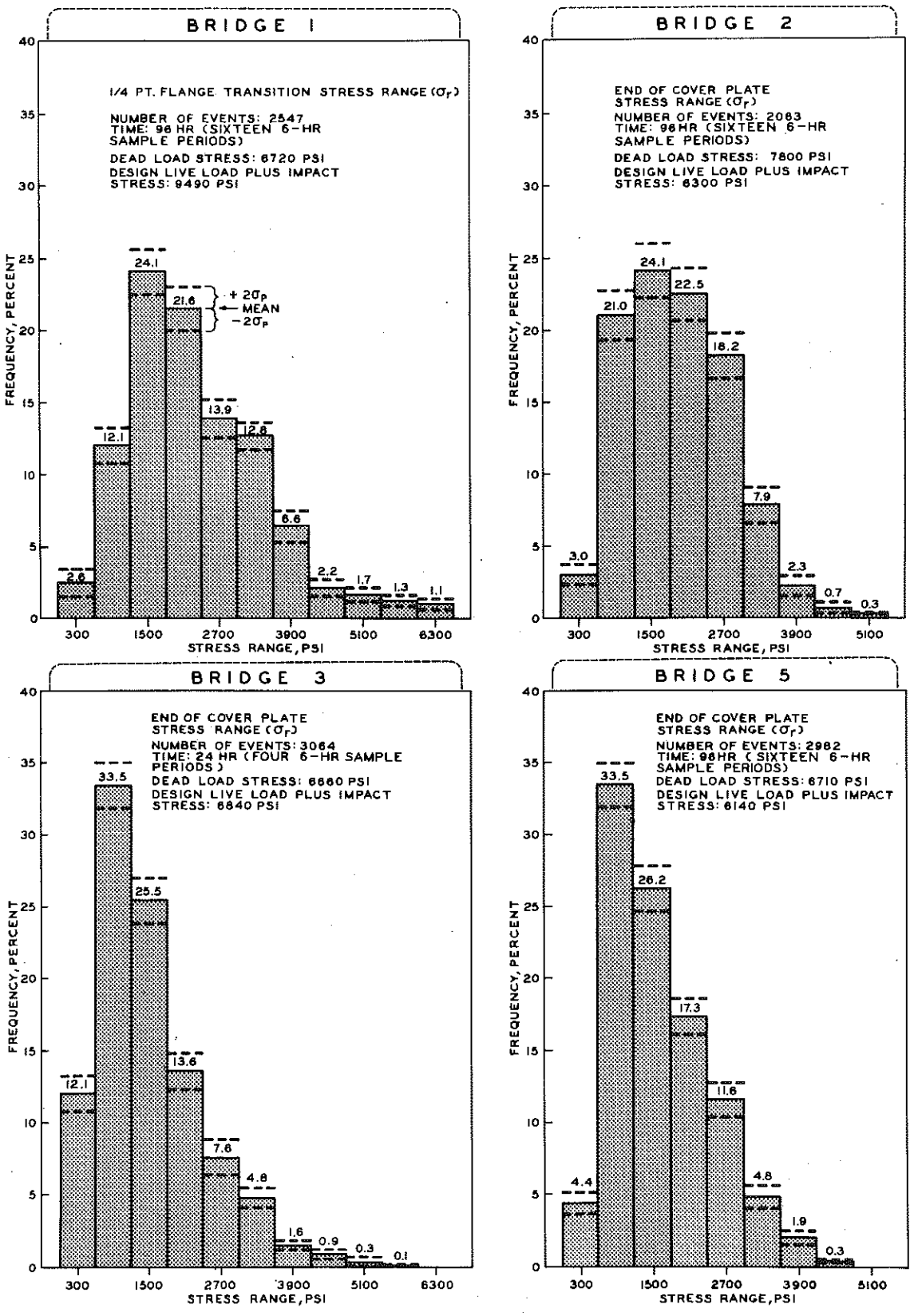

Figure 26. Frequency distribution of stress range at the stress concentration point.

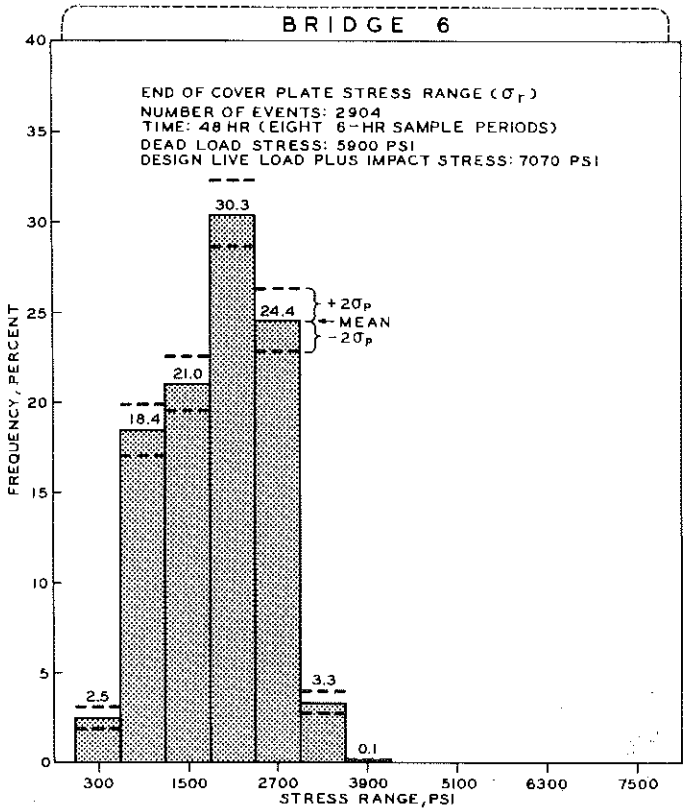

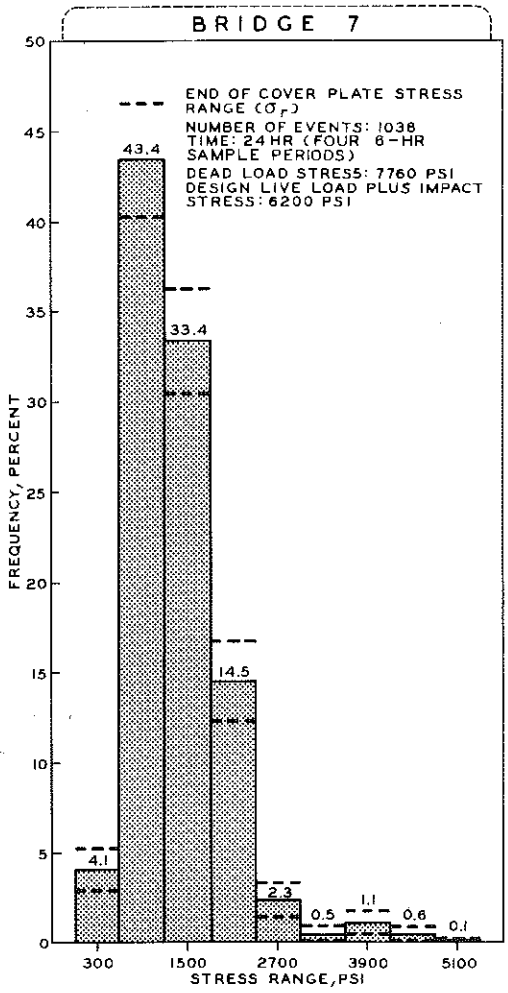

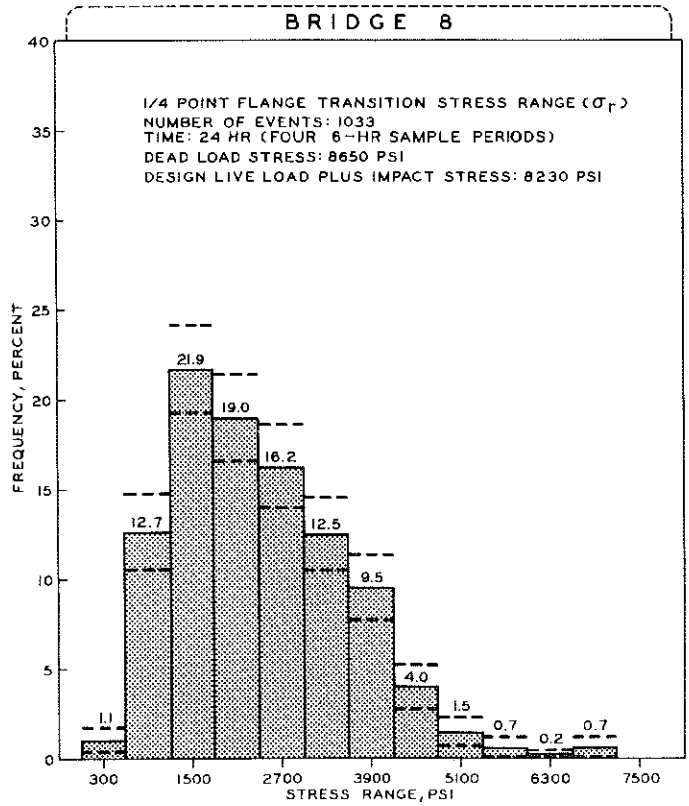

Figure 26 (cont.). Frequency distribution of stress range at the stress concentration point.

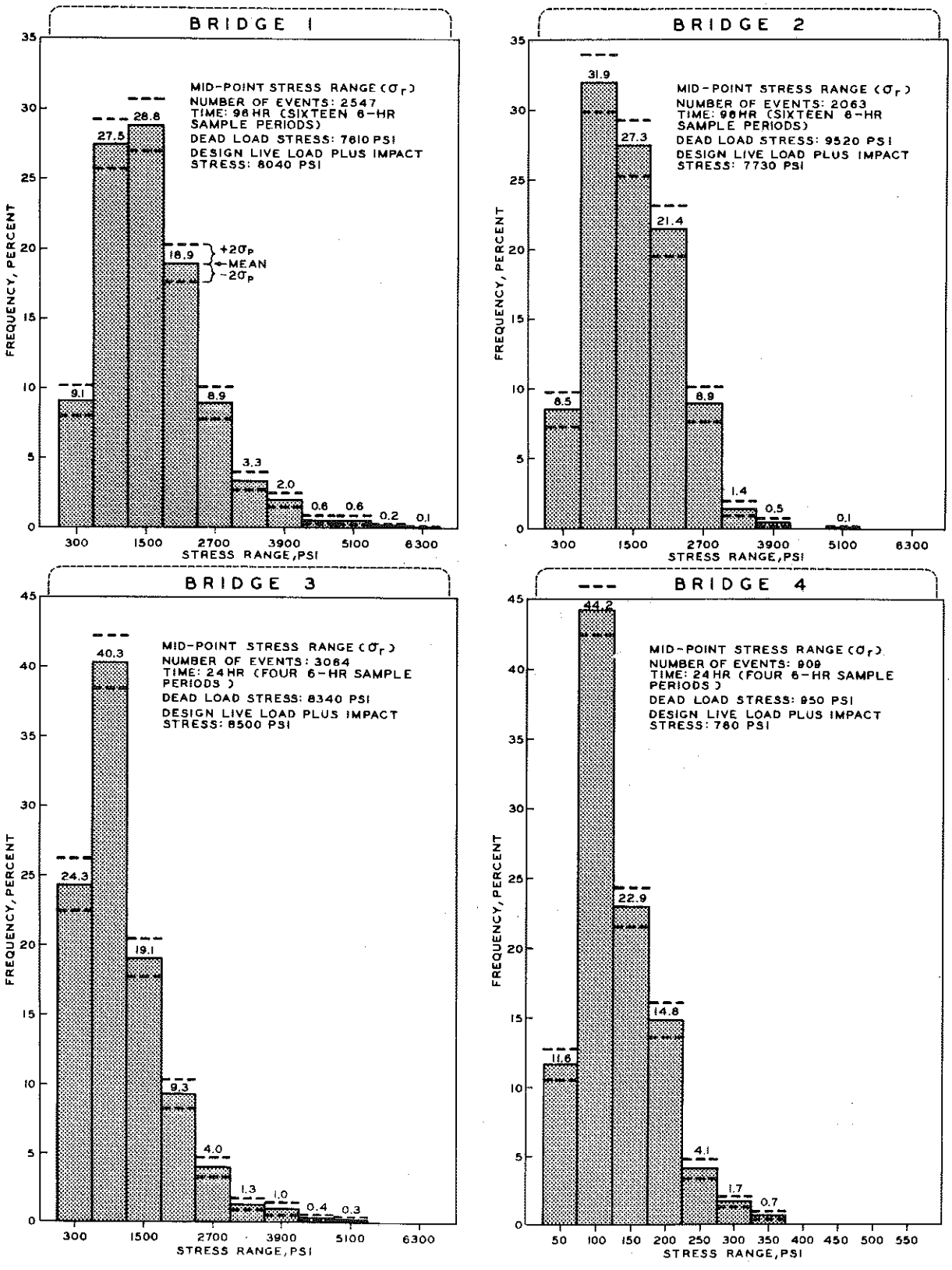

Figure 27. Frequency distribution of stress range at the mid-point.

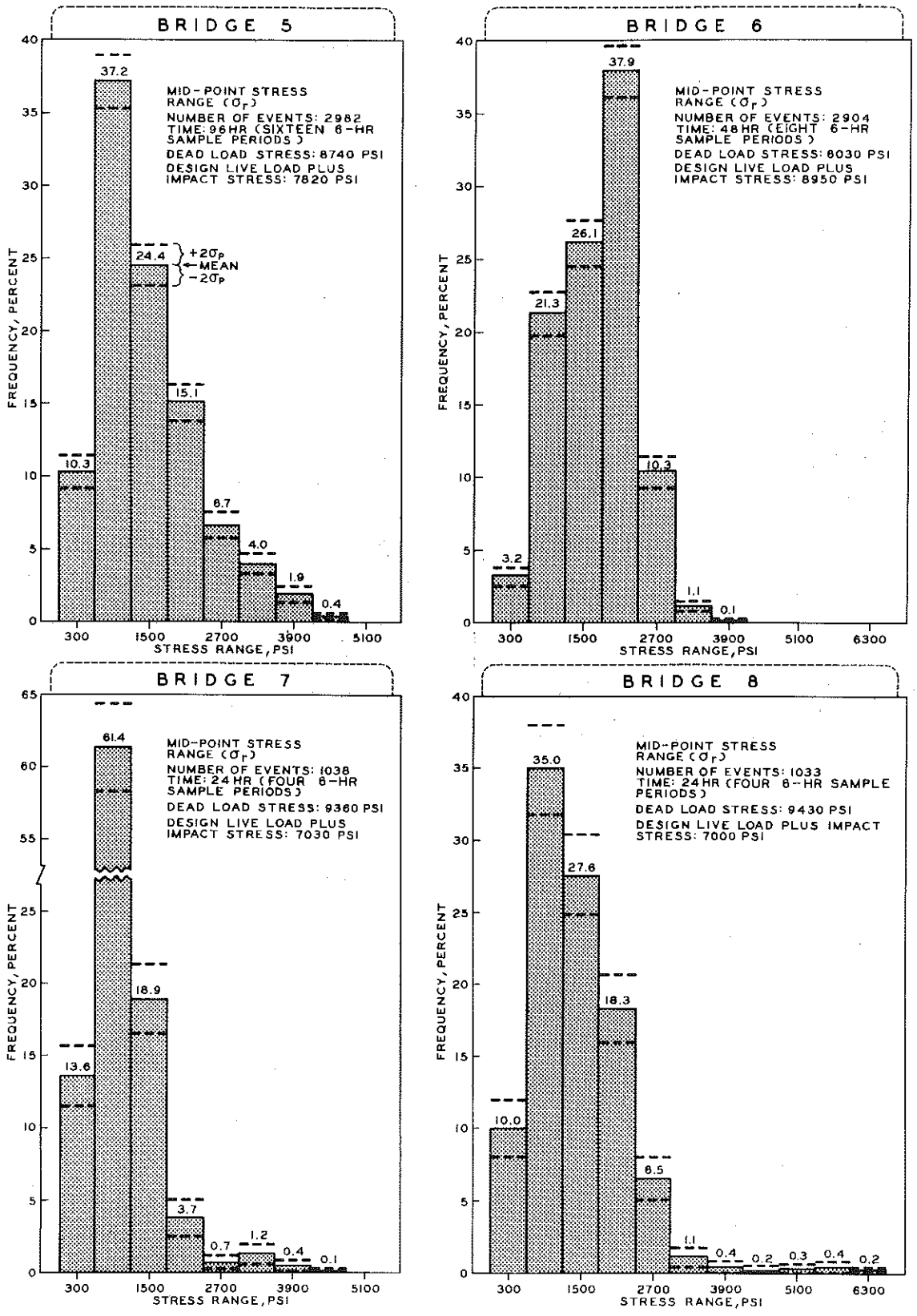

Figure 27 (cont.). Frequency distribution of stress range at the mid-point.

cent, with a corresponding frequency of occurrence of 0.2 percent. The lowest ratio was about 43.5 percent, representing an occurrence frequency of 0.1 percent for Bridge 6.

The dead load stress values given in Figures 26 and 27 do not include the effect of the future wearing surface.

Sample Precision

To ascertain the degree of precision or reliability in determining sample bridge commercial traffic volume, a yearly estimate of traffic volume for each bridge was made, utilizing the corresponding 3-hr time period-to-week and month-to-year volume factors. Based on these estimates, the standard deviation was determined and assumed to be equal to the standard deviation of the entire population. The sample number of 3-hr periods used varied from a minimum of 8 to a maximum of 32.

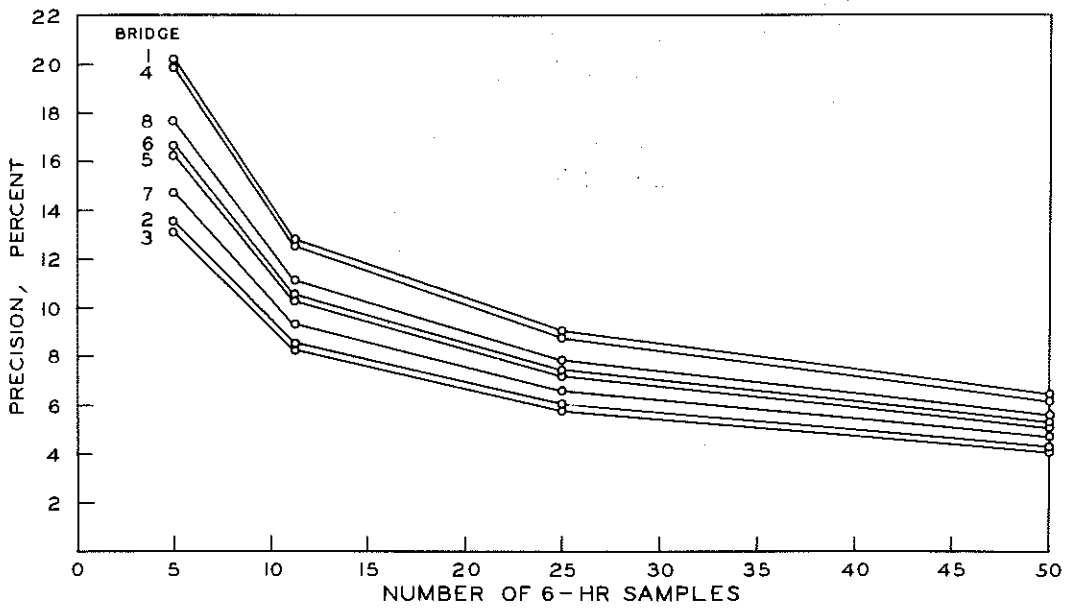

Figure 28. Number of sample periods and corresponding precision for 0.95-percent confidence level.

The resulting precision percentage, or coefficient of variation, for a 95-percent confidence level, i.e., $\pm$ 2 standard errors from the grand mean $\left(p = \pm \frac{2\sigma}{\bar{x}\sqrt{n}} \quad 100 \right)$, in terms of the number of 6-hr sample periods is given in Figure 28 for each of the eight test bridges. It can be seen that based on an average of the eight bridges, about fifteen 6-hr sample periods should

yield annual commercial volume estimates of within ± 10 percent of the true value, with a probability of 0.95. The maximum percentage error for this confidence level varied from about ± 13 to ± 20, corresponding to five 6-hr sample periods for the eight test bridges. It is assumed that two consecutive 3-hr sample periods comprising one 6-hr sample period would give the same results as two randomly selected 3-hr time periods in every case.

Fatigue Life

Table 4 summarizes various factors based on the two fatigue curves (Method 1 and Method 2, respectively) for determining the cumulative fatigue damage and life for each of the seven steel test spans. A frequency interval of ± 2 standard deviations for each of the significant stress range levels is given in Column 2. Annual commercial traffic volume shown was determined as the average value of all 3-hr sample period estimates for each bridge, utilizing appropriate traffic volume factors for the weigh station nearest to each bridge. The number of contributing cycles of damage for each of the significant stress range intervals is given in Column 3. The endurance lives for each of these stress range intervals are computed from the appropriate equations (Method 1 and Method 2) and are given in Column 5. The damage factor or ratio of the number of damage cycles at a given stress range interval to the endurance life at that stress range interval is shown in Column 6. The accumulated total damage factor which is the sum of the damage factors for the individual stress range intervals in Column 6 is given in Column 7. The fatigue life or reciprocal of the total accumulated damage factors and the total number of contributing damage cycles are shown in Columns 8 and 9.

As can be seen from Table 4, test span fatigue lives as controlled by the longitudinal stringer strength were less when minimum stress was considered (Method 1) than when it was ignored (Method 2). The average Method 1-to-Method 2 ratio of the fatigue lives of test spans was approximately 42 percent. Fatigue lives as determined by Method 1 varied from 1,610 years for Bridge 3 to 105,000 years for Bridge 6. These results are based on a constant annual commercial traffic volume. No attempt was made to introduce a growth rate or vehicle distribution changes into the analysis, since these factors would not contribute a significant reduction in the extremely large values that were obtained assuming a constant traffic volume and vehicle distribution.

The joint ASCE-AASHO Committee on Flexural Members (4) recently concluded that the minimum stress, as well as the end-of-cover plate geometry is relatively insignificant with respect to fatigue fracture of rolled beams

TABLE 4
TABULATION OF FATIGUE LIFE FACTORS

Bridge	Annual Commercial Traffic Volume	Method 1									Method 2								
		Stress Range (σ_r), ksi	Frequency Range ($\pm$ 2S), percent	Damage Cycle Range	Log N*	N	Damage Factor Range: Damage Cycles / N	Annual Damage Range: $\sum$ Damage Factor	Fatigue Life Range, yr: 1 / Annual Damage	Total Damage Cycle Range	Stress Range (σ_r), ksi	Frequency Range ($\pm$ 2S), percent	Damage Cycle Range	Log N*	N	Damage Factor Range: Damage Cycles / N	Annual Damage Range: $\sum$ Damage Factor	Fatigue Life Range, yr: 1 / Annual Damage	Total Damage Cycle Range
		1	2	3	4	5	6	7	8	9	1	2	3	4	5	6	7	8	9
1	192,000	6.3	0.89 1.51	1,325 2,900	8.04	10.96×10^7	1.21×10^{-5} 2.64	2.19×10^{-5} 4.66	45,700 21,600	2,955 6,260	6.3	0.89 1.51	1,325 2,900	8.28	19.10×10^7	6.92×10^{-6} 15.15	6.92×10^6 15.15	144,000 66,000	1,325 2,900
		5.7	0.85 1.75	1,630 3,360	8.22	16.60	0.98 2.02												
2	150,000	5.1	0.06 0.54	90 810	7.49	3.09	0.29 2.62	3.80 10.31	26,300 9,700	3,045 6,855	5.1	0.06 0.54	90 810	7.96	9.94	0.91 8.13	17.67 43.81	56,600 22,800	3,045 6,855
		4.5	0.33 1.07	495 1,605	7.72	5.25	0.94 3.05				4.5	0.33 1.07	495 1,605	8.12	13.12	3.76 12.21			
		3.9	1.64 2.96	2,460 4,440	7.98	9.55	2.57 4.64				3.9	1.64 2.96	2,460 4,440	8.28	18.88	13.00 23.48			
3	860,000	5.7	0.00 0.21	0 1,805	7.29	1.95	0.00 9.26	22.32 61.95	4,480 1,610	15,570 34,365	5.7	0.00 0.21	0 1,805	7.80	6.35	0.00 28.43	97.74 246.35	10,200 4,060	15,570 34,365
		5.1	0.10 0.50	860 4,300	7.49	3.09	2.78 13.92				5.1	0.10 0.50	860 4,300	7.96	9.94	8.65 43.26			
		4.5	0.56 1.24	4,820 10,660	7.72	5.25	9.18 20.31				4.5	0.56 1.24	4,820 10,660	8.12	13.12	36.71 81.28			
		3.9	1.15 2.05	9,890 17,600	7.98	9.55	10.36 18.46				3.9	1.15 2.05	9,890 17,600	8.28	18.88	52.38 93.38			
5	222,000	4.5	0.10 0.50	220 1,110	7.72	5.25	0.42 2.11	3.67 7.68	27,200 13,000	3,330 6,440	4.5	0.10 0.50	220 1,110	8.12	13.12	1.69 8.45	18.12 36.64	55,200 27,300	3,330 6,440
		3.9	1.40 2.40	3,110 5,330	7.98	9.55	3.25 5.57				3.9	1.40 2.40	3,110 5,330	8.28	18.88	16.44 28.19			
6	413,000	3.9	0.00 0.22	0 910	7.98	9.55	0.00 0.95	0.00 0.95	∞ 105,000	0 910	3.9	0.00 0.22	0 910	8.28	18.88	0.00 4.82	0.00 4.82	∞ 208,000	0 910
7	291,000	5.1	0.00 0.30	0 875	7.49	3.09	0.00 2.83	2.03 14.15	49,100 7,070	1,660 9,120	5.1	0.00 0.30	0 875	7.96	9.94	0.00 8.78	9.59 59.71	104,000 16,800	1,660 9,120
		4.5	0.12 1.08	350 3,145	7.72	5.25	0.66 5.99				4.5	0.12 1.08	350 3,145	8.12	13.12	2.68 23.96			
		3.9	0.45 1.75	1,310 5,100	7.98	9.55	1.37 5.33				3.9	0.45 1.75	1,310 5,100	8.28	18.88	6.93 26.97			
8	293,000	6.9	0.18 1.22	530 3,575	7.87	7.41	0.71 4.82	1.03 8.25	97,400 12,100	1,060 8,555	6.9	0.18 1.22	530 3,575	8.18	15.28	3.45 23.37	3.45 30.73	290,000 32,600	530 4,980
		6.3	0.00 0.48	0 1,405	8.04	10.96	0.00 1.28				6.3	0.00 0.48	0 1,405	8.28	19.10	0.00 7.36			
		5.7	0.18 1.22	530 3,575	8.22	16.60	0.32 2.15												

* Method 1

Log N = 10.45 -4.18 log σ_r (Bridges 2, 3, 5, 6, and 7)
Log N = 11.38 -4.18 log σ_r (Bridges 1 and 8)

Method 2

Log N = 9.30 -0.263 σ_r (Bridges 2, 3, 5, 6, and 7)
Log N = 9.30 -0.162 σ_r (Bridges 1 and 8)

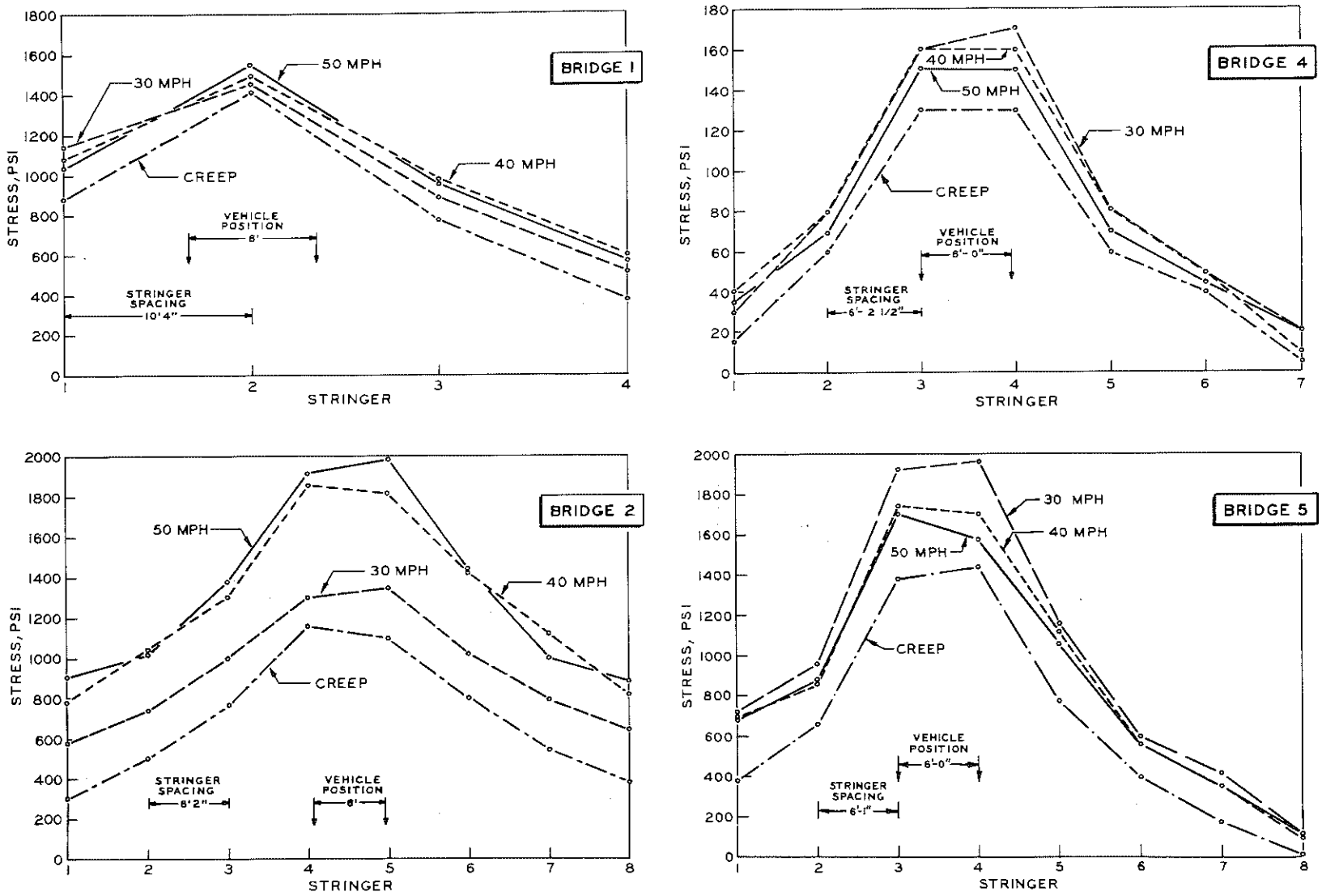

Figure 29. Stringer stress distribution at various test vehicle speeds.

with welded cover plates. They also recommend a stress range value of 9,000 psi for fracture at 2×10^6 cycles for rolled beams with cover plates of ASTM A 36 or A 441 steel. The corresponding stress range values at 2×10^6 cycles used in developing this study's fatigue curves, as noted previously, were 11,400 psi for the welded tapered end cover plates and 18,500 psi for the welded flange thickness transitions.

Based on a linear-logarithmic stress range-cycle relation, and the suggested stress range value of 9,000 psi at 2×10^6 cycles, neglecting the minimum stress, and assuming that the limiting stress range at 200×10^6 cycles would be 3,000 psi, the resulting fatigue life of Bridge 3, for example, would be 1,580 years. This corresponds to a reduction of about 61 percent of the value obtained in this study, utilizing the stress range value of 11,400 psi at 2×10^6 cycles and the Method 2 fatigue curve.

The highest stress range at the stress concentration point which occurred for any of the sample bridges was $5,700 \pm 300$ psi for the rolled beam with cover plate stringers, and $6,900 \pm 300$ psi for the welded plate girders. The occurrence frequencies for these stress range intervals were 0.1 percent and 0.7 percent, respectively. If it is assumed that the Laboratory determined nominal stress range values at 2×10^6 cycles represent a fatigue or endurance limit, then the maximum recorded stress ranges would fall considerably below these respective values for both beam types for the bridges tested. The two fatigue curves utilized in this study are not intended as a quantitative attempt to estimate the actual fatigue life of these types of beams for applications of loading between two million and two hundred million cycles, but were utilized in conjunction with Miner's cumulative damage hypothesis to illustrate the relative fatigue effect of the sample test bridges. The use of these curves in the cycle range indicated is questionable and the practicability of the finite fatigue life values given are dubious.

Lateral Stress Distribution

Lateral stringer stress distribution at mid-span of Bridges 1, 2, 4, and 5 with the special Michigan load-test vehicle at creep speed, 30, 40, and 50 mph is shown in Figure 29. In general, the shape of the static and dynamic stringer stress distributions was essentially the same in each of the four test bridges. In the maximum stressed stringer, stress increased with increasing speed on Bridges 1 and 2, and increased with decreasing speed on Bridge 4 and 5. In Bridges 1, 2, and 4, both the forced and free vibration of all stringers at mid-span were in phase for any of the three test velocities and lateral vehicle positions. In Bridges 1 and 2, the absolute maximum peak strains for each stringer did not occur simultaneously,

TABLE 5
DYNAMIC STRESS INCREMENT AND AMPLIFICATION FACTORS AT MID-SPAN WITH SPECIAL TEST VEHICLE IN TRAFFIC LANE*

Bridge	Speed, mph	Dynamic Stress Increment ($\sigma_D - \sigma_S$), psi	Dynamic Amplification Factor (σ_D / σ_S)
1	30	40	1.03
	40	80	1.06
	50	140	1.10
2	30	80	1.07
	40	700	1.60
	50	760	1.66
4	30	40	1.31
	40	30	1.23
	50	20	1.15
5	30	520	1.36
	40	260	1.19
	50	140	1.10

*Most highly stressed stringer; average of three trials each on three consecutive days.

TABLE 6
COMPARISON OF EXPERIMENTALLY DETERMINED INTERNAL AND EXTERNAL MOMENTS WITH SPECIAL TEST VEHICLE AT MID-SPAN(1)

Bridge	Static External Moment at Mid-Point (Special Test Vehicle), ft-lb	Experimentally Determined Internal Moment, (2) ft-lb	Ratio of Internal to External Moments, percent
1	749,100	722,000	96.3
2	601,600	577,000	96.0
4	328,600	242,000	73.7
5	531,600	464,000	87.5

(1) Based on average strain of three trials each on three consecutive days for three lateral positions of the special load vehicle.

(2) Bridges 1, 2, and 5, based on n = 10 and minimum design slab thickness neglecting sidewalk.

Bridge 4 based on $\frac{E_{beam}}{E_{slab}} = 1.3$, $E_{beam} = 5 \times 10^6$ psi, and minimum design slab thickness neglecting sidewalk.

but were all within one to two cycles of one another. In Bridge 4, all stringers reached their peak strain simultaneously. In Bridge 5, the forced vibration was in phase, but the free vibration oscillation was such that the fascia and first interior beam on each side were vibrating 180° out of phase with the remaining interior stringers.

The dynamic stress increments ($\sigma_D - \sigma_S$) and dynamic amplification factors (σ_D / σ_S) for the four test bridges with the special test vehicle are shown in Table 5. The dynamic amplification factors for the maximum stressed stringer at mid-span were 1.10 and 1.66 for Bridges 1 and 2, respectively, with the test vehicle run at 50 mph, and 1.31 and 1.36 for Bridges 4 and 5, respectively, with the test vehicle at 30 mph. Based on total stringer stresses at mid-span, the amplification factors for Bridges 1, 2, 4, and 5 were 1.20, 1.90, 1.34, and 1.50, respectively, illustrating the high susceptibility of the suspended span-type bridge to dynamic response.

The external and experimentally determined mid-span moment with the special test vehicle may be compared for Bridges 1, 2, 4, and 5 in Table 6. Based on measured stringer strain, using the design slab thickness and an "n" of 10, for computing the section modulus, and neglecting sidewalk and rail effects on the fascia beam section modulus, the average internal moment for Bridges 1, 2, and 5 was 93 percent of the external moment with the test vehicle at mid-span. For the prestressed I-beam span (Bridge 4), using the design slab thickness, an $\frac{E_{beam}}{E_{slab}}$ ratio of 1.3, and a modulus of elasticity, E_{beam}, of 5×10^6 psi, the resulting internal mid-span moment was 74 percent of the external moment. The discrepancy in comparing the total internal and external moments at the mid-span cross-section most probably results from lack of uniformity of slab thickness, the larger actual slab thickness, and the effect of the sidewalk and rail on the computed section modulus. Further, in the case of the concrete structure, applying a spurious value for the modulus of elasticity and corresponding modulus ratio between the slab and beam would also contribute to this discrepancy.

Mid-point stringer stresses of Bridges 1, 2, 4, and 5 with the special test vehicle at three lateral positions are given in Table 7 and shown in Figure 30. Each stress value tabulated represents the average of three trials on each of three consecutive days. The variation in the total mid-point stringer stress was less than $\pm$ 2 percent from the mean for Bridges 1 and 2, $\pm$ 3 percent from the mean for Bridge 5, and $\pm$ 5 percent from the mean for Bridge 4. The relative invariability of total stringer strain at the mid-span section with respect to lateral placement of the test vehicle at mid-span, implies that either the composite section modulus of each stringer

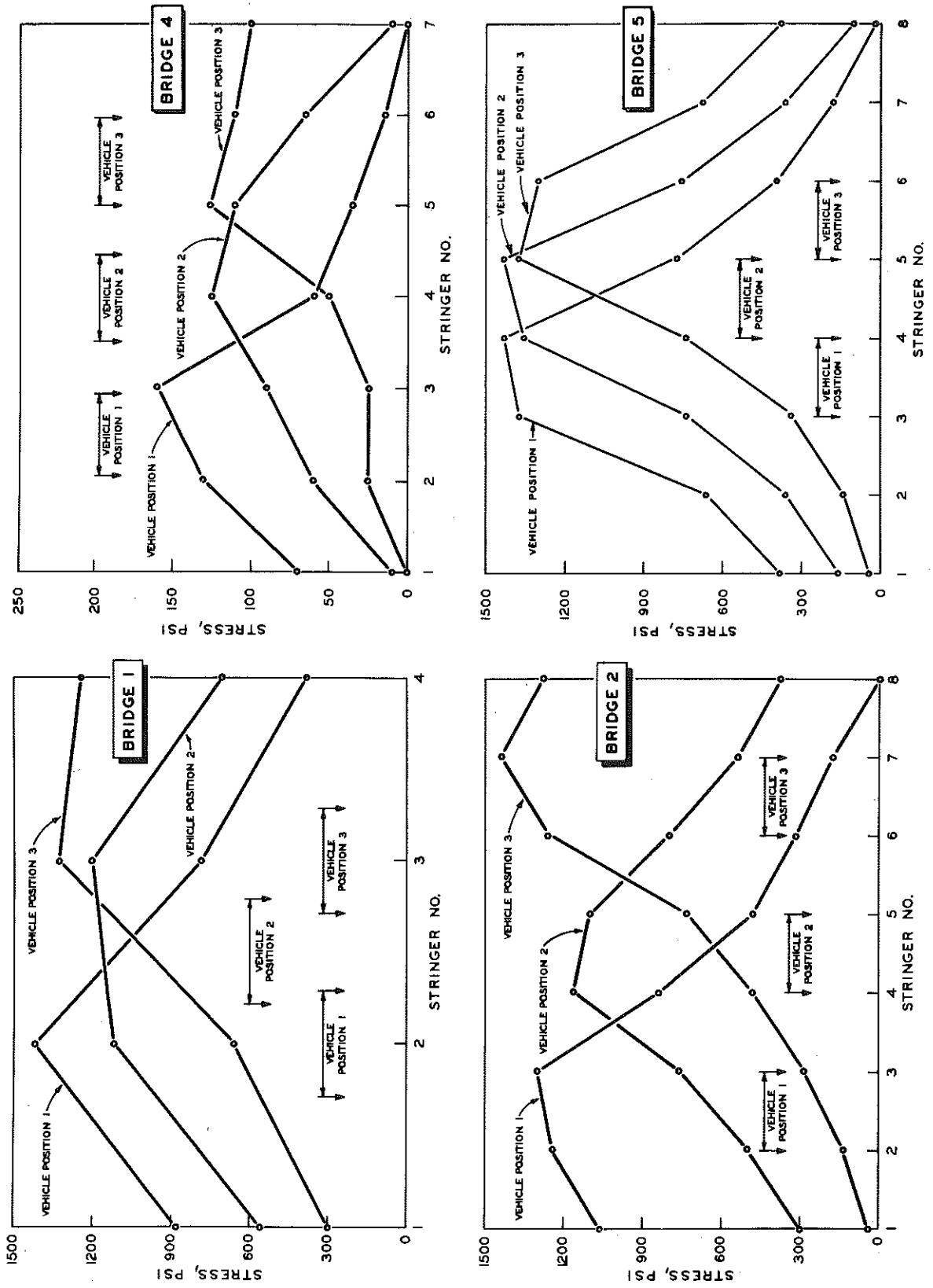

Figure 30. Lateral stress distribution at mid-span with special test vehicle at mid-span.

TABLE 7
LATERAL LOAD DISTRIBUTION STRESSES AT MID-SPAN
WITH SPECIAL TEST VEHICLE AT MID-SPAN[1] (psi)

	Vehicle Position	Stress, psi, for Indicated Stringers							
		1	2	3	4	5	6	7	8
Bridge 1	Traffic lane	880	1,420	780	380				
	Center of bridge	560	1,120	1,200	700				
	Passing lane	300	660	1,320	1,240				
Bridge 2	Traffic lane	1,060	1,240	1,300	840	480	320	180	0
	Center of bridge	300	500	760	1,160	1,100	800	540	380
	Passing lane	40	140	280	480	740	1,260	1,420	1,280
Bridge 4	Traffic lane	70	130	160	60	35	15	0	
	Center of bridge	10	60	90	125	110	65	10	
	Passing lane	0	25	25	50	125	110	100	
Bridge 5	Traffic lane	380	660	1,380	1,440	780	760	180	20
	Center of bridge	160	360	740	1,360	1,440	1,440	360	100
	Passing lane	40	140	360	740	1,380	1,320	680	380

[1] Each stress entry represents the average of three trials each on three consecutive days.

remains constant, or that the section modulus and stringer moment distributions vary in such a manner that $\sum M/Z$ is constant.

Moment and stress comparisons between the maximum static mid-span stringer stress based on the H 20-S16 AASHO design criteria and the experimentally determined maximum stringer stress due to the load test vehicle are given in Table 8. The ratio of the maximum experimentally determined stringer stress to the H 20-S16 design live load stress (no impact) is given in Item 2. This ratio was about 21 percent for Bridges 1, 2, and 5, and 22 percent for Bridge 4. By superposition, the maximum stringer stress ratio with adjacent lanes loaded by the test vehicle, to that with the test vehicle in the traffic lane only is given in Item 3. This ratio was about 66 percent for Bridges 1 and 5, and 60 percent for Bridges 2 and 4. In these tests, lateral positioning of the test vehicle was such that the center-to-center transverse vehicle spacing with two adjacent lanes loaded was 10 ft 4 in., 12 ft 4 in., 9 ft 4 in., and 12 ft 2 in. for Bridges 1, 2, 4, and 5, respectively. AASHO design criteria presume this spacing to be 10 ft. Item 6 gives average maximum stringer stress due to two test vehicles in adjacent lanes as 64 percent of the design value for Bridges 1, 2, and 5, and 76 percent for Bridge 4.

TABLE 8

STATIC MOMENT AND STRESS COMPARISON OF SPECIAL TEST VEHICLE WITH H 20-S16-44 DESIGN LIVE LOAD (NO IMPACT) AT MID-SPAN

Item	Moment and Stress Ratios	Bridge			
		1	2	4	5
1	Ratio of Total Moment of Special Test Vehicle to H 20-S16-44 Design Vehicle $\left(R_M = \frac{M_H}{M_{LL}}\right)$	$\frac{749.1}{1,433.2} = 0.52$	$\frac{601.6}{1,157.6} = 0.52$	$\frac{328.6}{547.6} = 0.60$	$\frac{531.6}{1,007.1} = 0.53$
2	Ratio of Maximum Stringer Stress with Special Vehicle in Traffic Lane to H 20-S16-44 Design Live Load Stress $\left(R_\sigma = \frac{\sigma_H}{\sigma_{LL}}\right)$	$\frac{1,420}{6,560} = 0.22$	$\frac{1,300}{6,200} = 0.21$	$\frac{160}{585} = 0.27$	$\frac{1,280}{6,220} = 0.21$
3	Ratio of Stress in Maximum Stressed Stringer Due to Special Vehicle in Traffic Lane to Stress with Special Vehicle in Traffic Lane Plus Adjacent Lane[1].	0.66	0.61	0.59	0.65
4	Ratio of Maximum Stringer Stress with Special Vehicle in Traffic Lane Plus Adjacent Lane to H 20-S16-44 Design Live Load Stress (R'_σ)	$\frac{0.22}{0.66} = 0.33$	$\frac{0.21}{0.61} = 0.34$	$\frac{0.27}{0.59} = 0.46$	$\frac{0.21}{0.65} = 0.32$
5	R_σ/R_M	0.42	0.40	0.45	0.40
6	R'_σ/R_M	0.64	0.66	0.76	0.62

(1) By superposition. (Center to center vehicle spacings with two adjacent lanes loaded were 10 ft 4 in., 12 ft 4 in., 9 ft 4 in., and 12 ft 2 in. for Bridges 1, 2, 4, and 5 respectively.)

Supplementary Test on Bridges 1 and 2

Frequency distributions of gross vehicle load on Bridges 1 and 2 for a 6-hr time period on each of two days are shown in Figure 31. Average gross vehicle weight for the two sample periods on Bridge 1 was about 42 kips, and on Bridge 2 about 38 kips. For the four sample periods on the two bridges, more than 90 percent of the gross vehicle loads were less than 72 kips. The maximum gross vehicle load for Bridge 1 was 145 ± 5.5 kips, with an occurrence frequency of 1.8 percent. On Bridge 2, the maximum vehicle load was 155 kips ± 5.5 kips occurring at a frequency of 1.6 percent.

TABLE 9
MAXIMUM STRESS RANGE(1), GROSS LOADS, AND FREQUENCIES WITH RESPECT TO VEHICLE TYPE

	Vehicle Type	Maximum Stress Range, psi	Maximum Stress Range Frequency, percent	Maximum Gross Load, kips	Maximum Gross Load Frequency, percent
Bridge 1	2D	1,650 ± 150	16.7	22.5 ± 2.5	16.7
	2S2L	1,950 ± 150	25.0	37.0 ± 3.0	25.0
	2S1	2,250 ± 150	38.2	45.0 ± 4.0	44.1
	2S2	3,750 ± 150	1.8	69.0 ± 3.0	1.8
	3S2	4,050 ± 150	11.5	70.5 ± 2.5	3.9
	3S2L	4,350 ± 150	7.1	77.5 ± 2.5	7.1
	Others	6,300 ± 300	12.5	142.0 ± 6.0	12.5
Bridge 2	2D	1,350 ± 150	9.5	19.5 ± 2.0	9.5
	2S1	1,950 ± 150	11.8	32.5 ± 3.0	23.5
	2S2L	2,250 ± 150	20.0	43.5 ± 3.0	20.0
	2S2	2,850 ± 150	4.9	52.0 ± 2.5	9.8
	3S2L	2,850 ± 150	5.9	73.0 ± 4.5	5.9
	3S2	3,450 ± 150	11.1	74.5 ± 3.0	11.1
	Others	5,700 ± 300	7.1	154.0 ± 8.5	10.7

(1) At the stress concentration point.

Histograms are shown in Figure 32 of maximum stress range at the stress concentration points and gross load frequency distributions according to truck type, based on the two 6-hr sample periods for each of the two test bridges. Maximum gross load, stress ranges, and corresponding frequencies with respect to vehicle type are shown in Table 9. With the exception of the 2S2 vehicle type on Bridge 2, the maximum stress range

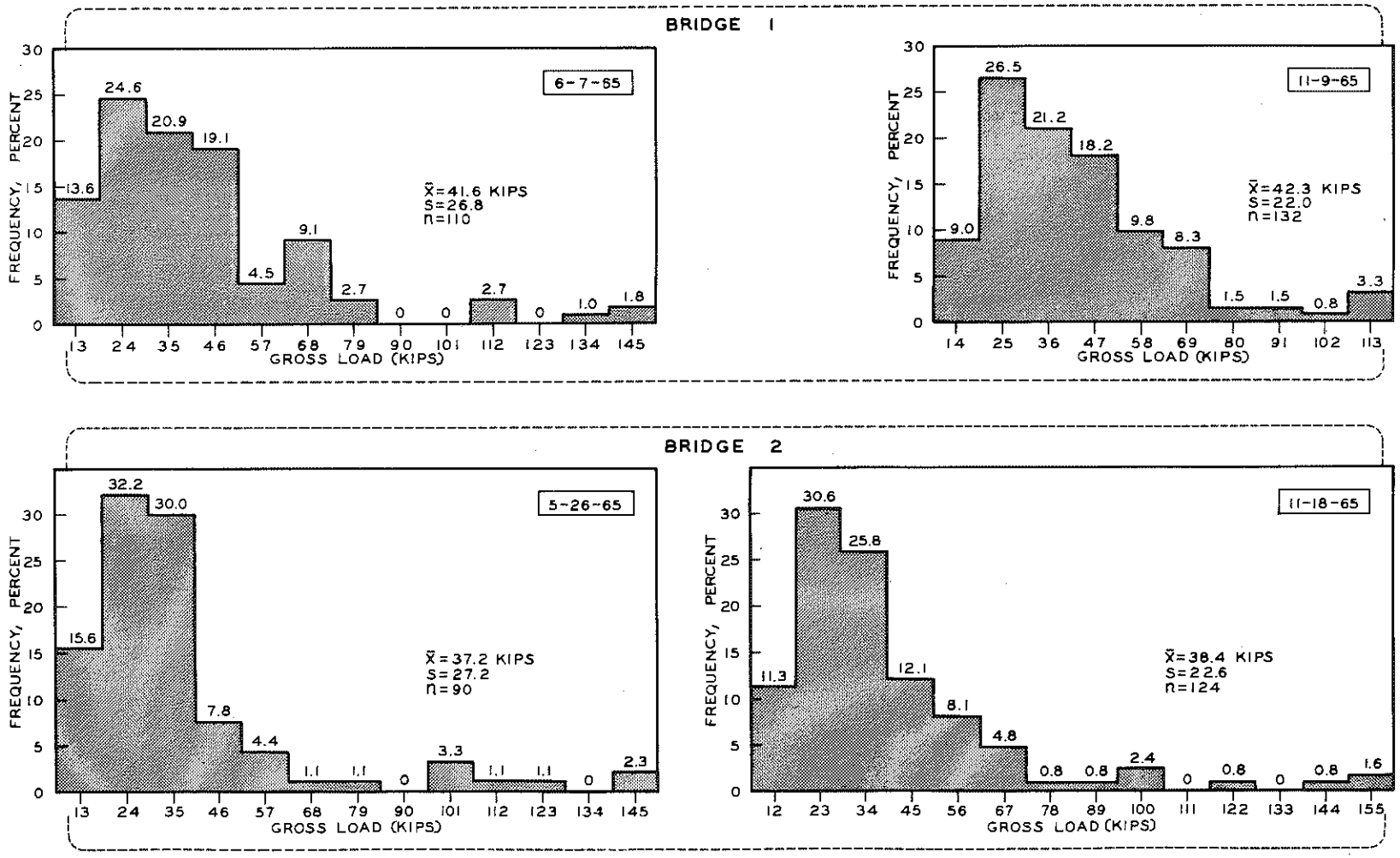

Figure 31. Gross load frequency distributions.

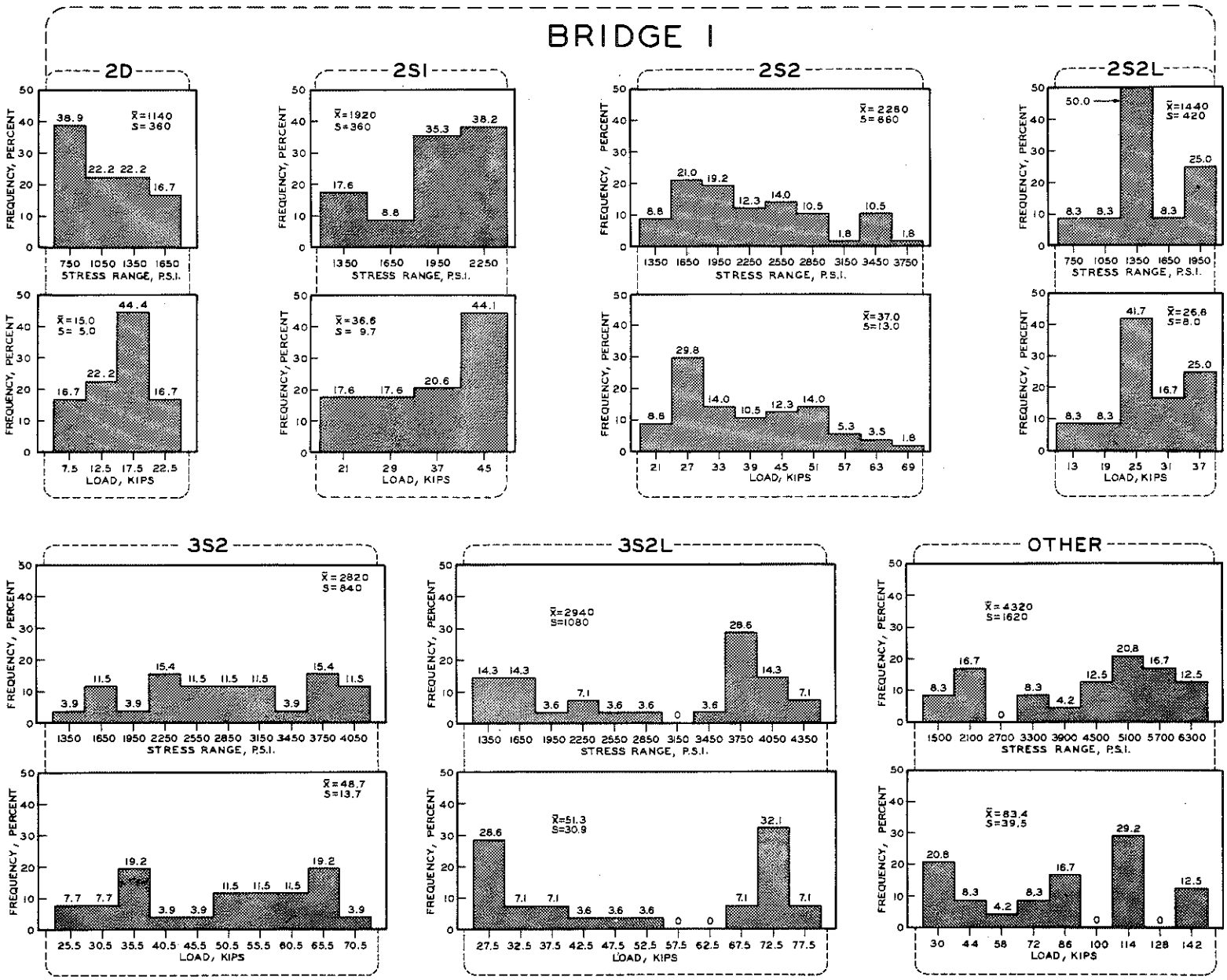

Figure 32. Gross load and maximum stress range frequency distributions at the stress concentration point with respect to truck type.

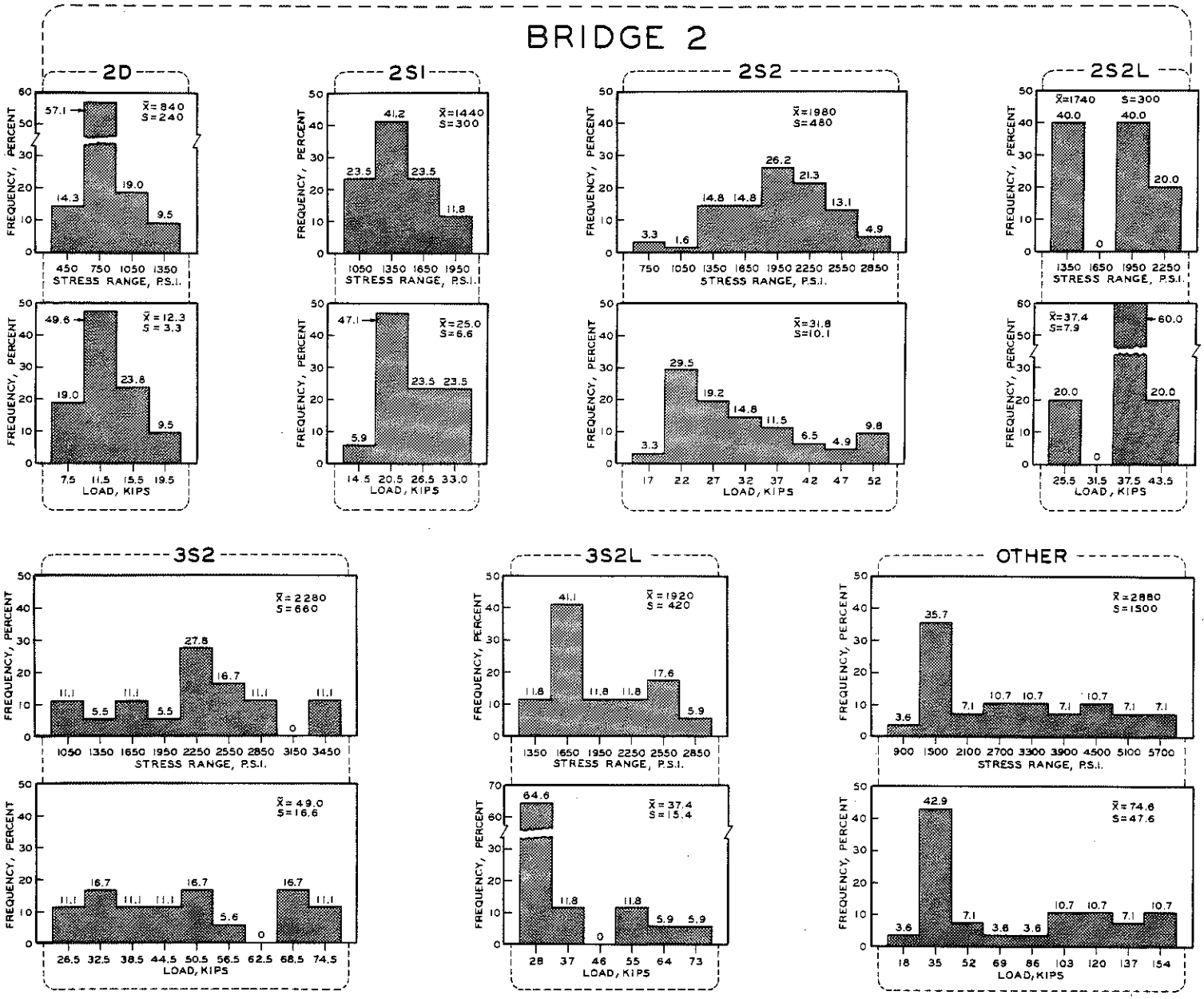

Figure 32 (cont.). Gross load and maximum stress range frequency distributions at the stress concentration point with respect to truck type.

interval increased with increasing gross vehicle load. The dynamic effect of the 2S2 vehicle type on Bridge 2 caused a maximum stress range interval equal to that of the 3S2L-type vehicle, which had a maximum gross load of 73 kips $\pm$ 4.5 kips as compared to 52 kips $\pm$ 2.5 kips for the 2S2 type. Appendix B indicates that of the total 2,575 commercial vehicles crossing Bridge 1 and 2,090 crossing Bridge 2, approximately 85 percent were of the six vehicle types represented here. Nominal design live load plus impact stress at the stress concentration points was 9,490 psi for Bridge 1 and 6,300 psi for Bridge 2. Maximum stress range produced by any of these six vehicle types was 4,500 psi for Bridge 1, and 3,600 psi for Bridge 2. The maximum recorded stress range for these four 6-hr periods was 6,300 $\pm$ 300 psi for Bridge 1, and 5,700 $\pm$ 300 psi for Bridge 2. This represents approximately 67 percent and 91 percent respectively, of the nominal design live load plus impact stress at the stress concentration points for these two bridges.

Linear regression lines for maximum live load stress at the mid-point and stress concentration point versus gross vehicle load for the two test spans are shown in Figure 33. These curves were drawn from the data for 50 randomly selected vehicles from the two 6-hr sampling periods. Based on these data, the linear correlation coefficients were very high for the mid-point stress versus gross vehicle load for both bridges. Two standard deviations corresponding to maximum live load stresses of 480 psi for Bridges 1 and 2 represent a relatively inconsequential stress magnitude for maximum live load stringer stress prediction, based on gross load, when considered from a design point of view. As can be seen from Figure 33, however, about 74 percent of the data for Bridge 1 and 82 percent for Bridge 2 represent gross vehicle loads less than 50 kips. For a 40-kip vehicle load on Bridge 2, for example, the predicted maximum stringer stress for a 95-percent confidence level would be about 1,200 $\pm$ 480 psi. This would represent a maximum error of 40 percent. If the data representing gross vehicle loads of 60 kips or less are used, the linear correlation coefficients for the maximum mid-span stringer stress would be 0.82 for Bridge 1 and 0.75 for Bridge 2. Two standard errors (2 $S_{y/x}$) based on the regression analysis of these data were 540 psi for Bridge 1 and 480 psi for Bridge 2. Although the data presented in Figure 33 were primarily concentrated in the less than 50-kip gross load range, the relatively low values of the standard errors of estimate suggest that the gross vehicle load, without regard to axle load distribution for the types of vehicles and span lengths represented here at least, could be used for determining maximum stringer stress.

In Table 10, dynamic maximum stringer stresses for a few of the heavier multiple axle vehicles are compared with the H 20-S16 design live load

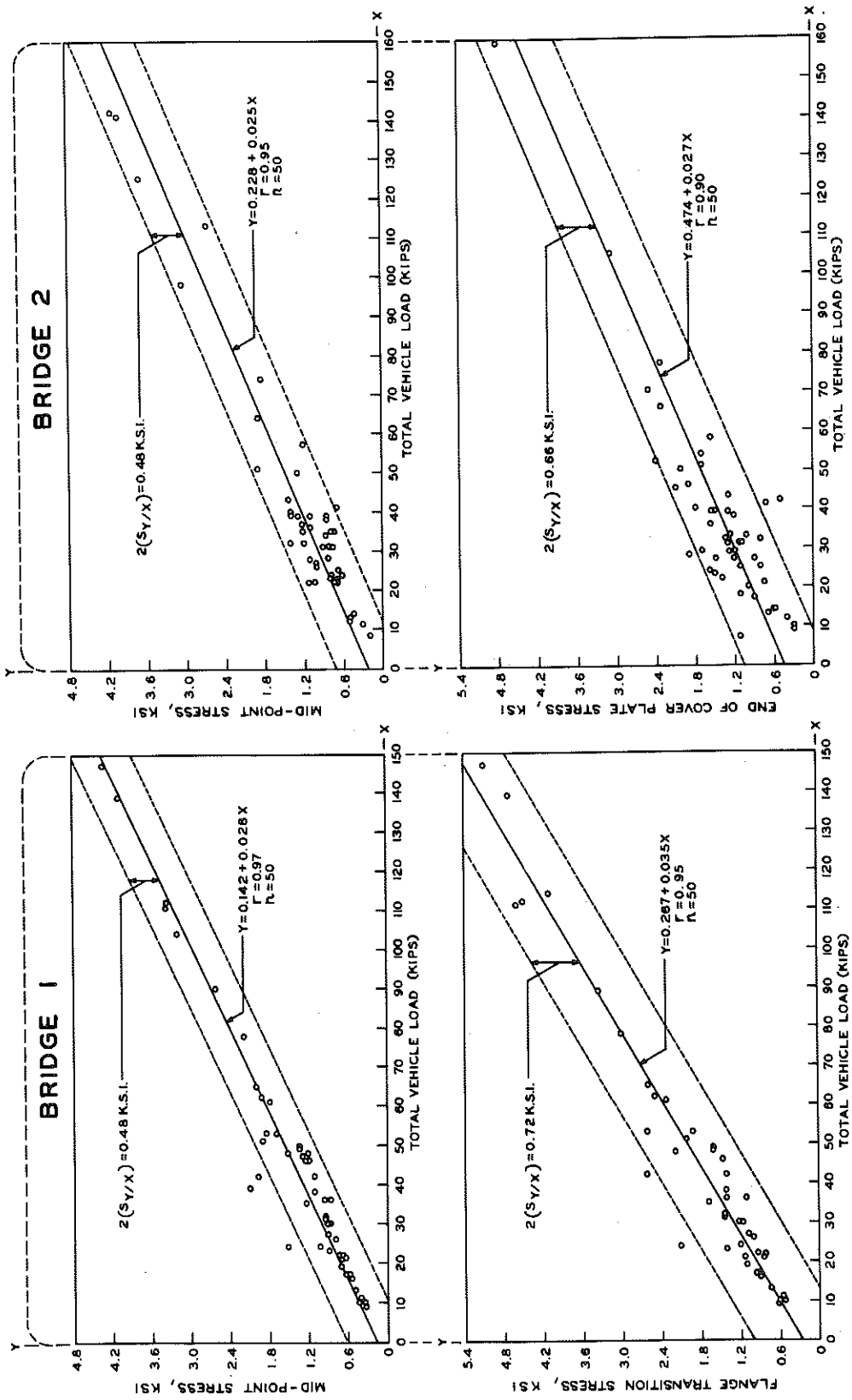

Figure 33. Regression lines for maximum live load stringer stress - gross vehicle load.

TABLE 10
COMPARISON OF MOMENTS AND DYNAMIC STRESSES
AT MID-SPAN FOR TYPICAL HEAVIER LOADED VEHICLES

	Truck Type	Gross Vehicle Load, kips	Maximum Live Load Stringer Stress, psi(1)	Static Moment (M_S), ft-kip(2)	Ratio of Static Moment to H 20-S16-44 Design Moment ($R_M = M_S/M_{LL}$)	Ratio of Maximum Live Load Stress to Design Live Load Plus Impact Stress ($R_\sigma = \sigma_D/\sigma_{LL+I}$)	R_σ/R_M
Bridge 1	4S4-5	147	4,320	2,399.3	1.67	0.54	0.31
	2S3L1	78	2,280	1,362.7	0.95	0.28	0.29
	2S5L1	111	3,480	1,885.5	1.32	0.43	0.33
	3S5L1	112	3,360	1,906.8	1.33	0.42	0.32
	3S3-2	116	3,540	2,009.6	1.40	0.44	0.31
	2S2-2	91	2,580	1,596.2	1.11	0.32	0.29
	3S2L	72	2,400	1,253.2	0.87	0.30	0.34
Bridge 2	3S3-2	112.8	2,820	1,534.2	1.32	0.36	0.27
	2S2-3	98	2,880	1,329.5	1.15	0.37	0.32
	3S3	125	2,760	1,517.6	1.31	0.36	0.27
	3S4-4	141.8	4,080	1,927.4	1.66	0.53	0.32

(1) Computed from strain measurement.
(2) Computed external moment.

plus impact stress for the two test bridges. The average ratio of induced stringer stress to design live load plus impact stress, considering relative external moments, was 0.31 for Bridge 1 and 0.30 for Bridge 2. In the lateral stress distribution tests with the special load-test vehicle, the average ratio of induced static stringer stress to design live load stress (no impact) was 0.42 for Bridge 1 and 0.40 for Bridge 2. In these limited tests involving the heavier multiple axle vehicles, the speed and lateral position of the vehicle as it passed over the span were unknown. The data however, represent only those vehicles in the traffic lane, and of course the only vehicle on the span at the time. The smaller dynamic stress ratios due to these vehicles with respect to the design stresses, as compared to the static stress ratios utilizing the special test vehicle, indicate a smaller actual dynamic effect than the design impact factor prescribes, or a greater lateral distribution of stringer stress due to longitudinal spreading of the load through the multiple axles, or both.

Although these supplementary data, involving the determination of gross vehicle loads and related stringer stresses on the two selected test bridges, are of interest, their quantity and scope are insufficient to warrant any basic conclusions.

CONCLUSIONS AND LIMITATIONS

Fatigue Life

Results of this study of specific test bridges indicate that the effect of current traffic loading on bridge life is insignificant with respect to fatigue failure of longitudinal stringers consisting of rolled beams with welded tapered end cover plates or welded plate girders with flange thickness transitions. This conclusion, however, should not be taken as a sweeping generalization for all highway bridges. This study and these conclusions are necessarily limited to the particular characteristics of the structures tested, the truck volumes, types, and load distributions encountered, and the interpretation and applicability of the fatigue strength data and failure criteria. The study was confined to fatigue life of welded longitudinal steel stringers incorporating some form of stress concentration geometry, and does not relate to possible fatigue failure of any other structural bridge components.

All sample bridges were designed for H 20-S16-44 loading and were of composite construction. None contained haunched slabs over the stringers, and the average slab thickness which was estimated at about 1-1/2 in. greater than the minimum design slab depth, included encasement of the top flange. In addition, all bridges had 2-1/2- to 3-1/2-ft wide by 10-in. thick concrete sidewalks tied into the deck slab. Previous studies have shown that sidewalks materially stiffen the bridge and improve lateral load distribution.

The test bridges were selected by type, but no attempt was made to obtain situations where traffic volume, truck type, or load distributions would be maximum. The maximum daily truck volume observed in this study was 2,400 trucks on Bridge 3. While this is fairly high, it does not represent the maximum volume existing on some other structures.

All commercial vehicle types on Michigan highways are subject to regulation of width, length, and axle load distribution. It was not known whether any "special permit" trucks with loads over the legal limits passed over any of the bridges during testing. In general, the frequency and prevailing policy with respect to operation of trucks exceeding the legal limit should also be considered.

All stress range intervals for all sample bridges correspond to the portion of the fatigue curves for application cycles greater than 2 million. This portion of the fatigue curves represents an extrapolation beyond actual fatigue test values and was based on the assumption that the stress range at 200×10^6 cycles is one-third the value at 2×10^6 cycles.

The tests were confined to the effect of live load induced stress applications only, and the cyclic stress effect due to environmentally induced forces including differential temperature changes, and the initial stringer stresses caused by concrete shrinkage of the slab in composite construction were not considered.

Significant effects of the sequence of stress amplitudes and the effect of low stress amplitude levels on fatigue life have been observed. (5, 6, 7) The application of empirical fatigue data as determined from constant amplitude fatigue tests to actual structural components subjected to a random amplitude and sequence of stress cycles for prediction of fatigue life is questionable. The prediction of service life is further impeded by the deficiencies of present cumulative damage hypotheses.

All strains and resulting stresses used in determining fatigue life were measured at or very near the actual stress concentration points. The Munse-Stallmeyer fatigue data are based on nominal stress at the stress concentration point section and not actual stress. If nominal stresses were used in the analysis, the resulting stringer fatigue life values of these test bridges would have been even greater.

Lateral Stress Distribution

As previously stated, the lateral stress distribution phase of this study arose as an outgrowth of the primary project objective of obtaining stringer strain histories and determining their effect on the life of the structure. For this reason, this part of the study presents only limited data pertaining to physical characteristics of the particular structures tested and the special test vehicle utilized. A comprehensive lateral stress distribution study should include a thorough strain instrumentation program to locate the neutral axis of each stringer. This would have involved more time and money than were originally intended or allotted.

The specific point of interest resulting from this limited study is the apparent conservatism of the AASHO design criteria with respect to determination of maximum stringer stress. For the structures tested, it appears that there is a much greater distribution of wheel load through the slab to the stringers, especially since in these tests the maximum external moment applied to the structures was essentially the result of a pair of concentrated wheel loads at the center of the span. For any given total static moment, the moment causing least lateral distribution and thus maximum stringer stress would be that due to a single concentrated load.

The maximum mid-point external moments due to the test vehicle were approximately 52 percent of the moments that would be caused by an H 20-S16 design vehicle for Bridges 1, 2, and 5, and about 60 percent for Bridge 4. Maximum stresses in the most highly stressed stringer due to location of the test vehicle in the traffic lane were approximately 66 percent of the maximum stress with two adjacent lanes loaded (by superposition) for Bridges 1 and 5, and 60 percent for Bridges 2 and 4. The resulting maximum stringer stresses, with the test vehicle placed in two adjacent lanes, were about 33 percent of the H 20-S16 design stress (no impact) for Bridges 1, 2, and 5, and 46 percent for Bridge 4. As a result, average maximum stringer stresses were about two-thirds of the design value for Bridges 1, 2, and 5, and about three-quarters for Bridge 4.

ACKNOWLEDGEMENTS

The research reported here was conducted by the Michigan Department of State Highways, in cooperation with the Bureau of Public Roads--U.S. Department of Transportation, under the Bureau's Highway Planning and Research Program. At the time this study was in progress, Michigan's highway research program was under the general administration of W. W. McLaughlin, Testing and Research Engineer, (retired), and immediate administration of E. A. Finney, Director, Research Laboratory Division (retired).

The author expresses his gratitude to C. J. Arnold, who was responsible for the management of the field testing program and the acquisition of all strain data, to M. J. Fongers who with Mr. Arnold was responsible for the strain gage instrumentation and installation procedures, to L. F. Holbrook and J. R. Darlington for processing the data, to M. A. Chiunti for preparation of the numerous histograms and related analytical operations, and to J. B. Alfredson and J. Perrone and their respective editorial and graphic presentation staffs for the preparation of the manuscript.

NOTE

The opinions, findings, and conclusions expressed in this publication are those of the authors and not necessarily those of the Bureau of Public Roads.

REFERENCES

1. AASHO Road Test: Report 4--Bridge Research, Highway Research Board Special Report 51D, 1962.

2. Munse, W. H., and Stallmeyer, J. E., "Fatigue in Welded Beams and Girders," Highway Research Board Bulletin 315, 1962, pp. 45-62.

3. "Maximum Desirable Dimensions and Weights of Vehicles Operated on the Federal Aid System," House Document No. 354, 88th Congress, 2nd Session, August 19, 1964, pp. 143-149.

4. ASCE-AASHO Joint Committee on Flexural Members, Subcommittee 7--Cover Plates, "Commentary on the Behavior and Design of Welded Cover Plates," July 1966.

5. Dolan, T. J., Richart, F. E., Jr., Work, C. E., "The Influence of Fluctuations in Stress Amplitude on the Fatigue of Metals," Proceedings, American Society for Testing and Materials 49, 1949, pp. 646-682.

6. Freudenthal, A. M., "Fatigue of Structural Metals Under Random Loading," Symposium on Acoustical Fatigue, STP No. 284, American Society for Testing and Materials, Philadelphia, Pa. 1961, pp. 26-44.

7. Plantema, F. J., Schijve J., eds., Full Scale Fatigue Testing of Aircraft Structures. Pergaman Press, New York, 1961.

SUGGESTED BIBLIOGRAPHY

Foster, G. M., "Tests in Rolled Beam Bridge Using H20-S16 Loading," Highway Research Board Report 14-B, 1952.

Linger, D. A. and Hulsbos, C. L., "Dynamic Load Distribution in Continuous I-Beam Highway Bridges," Highway Research Record No. 34, 1963.

Newmark, N. M., "Design of I-Beam Bridges," ASCE Proceedings, Part 1, March 1948.

Newmark, N. M. and Siess, C. P., "Moments in I-Beam Bridges," University of Illinois Bulletin No. 44, Engineering Experiment Station.

Reilly, R. J. and Looney, C. T. G., "Dynamic Behavior of Highway Bridges, Final Report," University of Maryland, Department of Civil Engineering, March 1966.

Siess, C. P. and Velestsos, A. S., "Distribution of Loads to Girders in Slab-and-Girder Bridges. Theoretical Analysis and Their Relation to Field Tests," Highway Research Board Report 14-B, 1952.

Stephenson, H. K., "Repeated Stresses in Highway Bridges," Highway Research Record No. 34, 1963.

APPENDIX A

Stress Range, Maximum Live Load Stress, and Rebound Stress Frequency Distributions For Individual Test Bridges and Sample Periods

B R I D G E 1

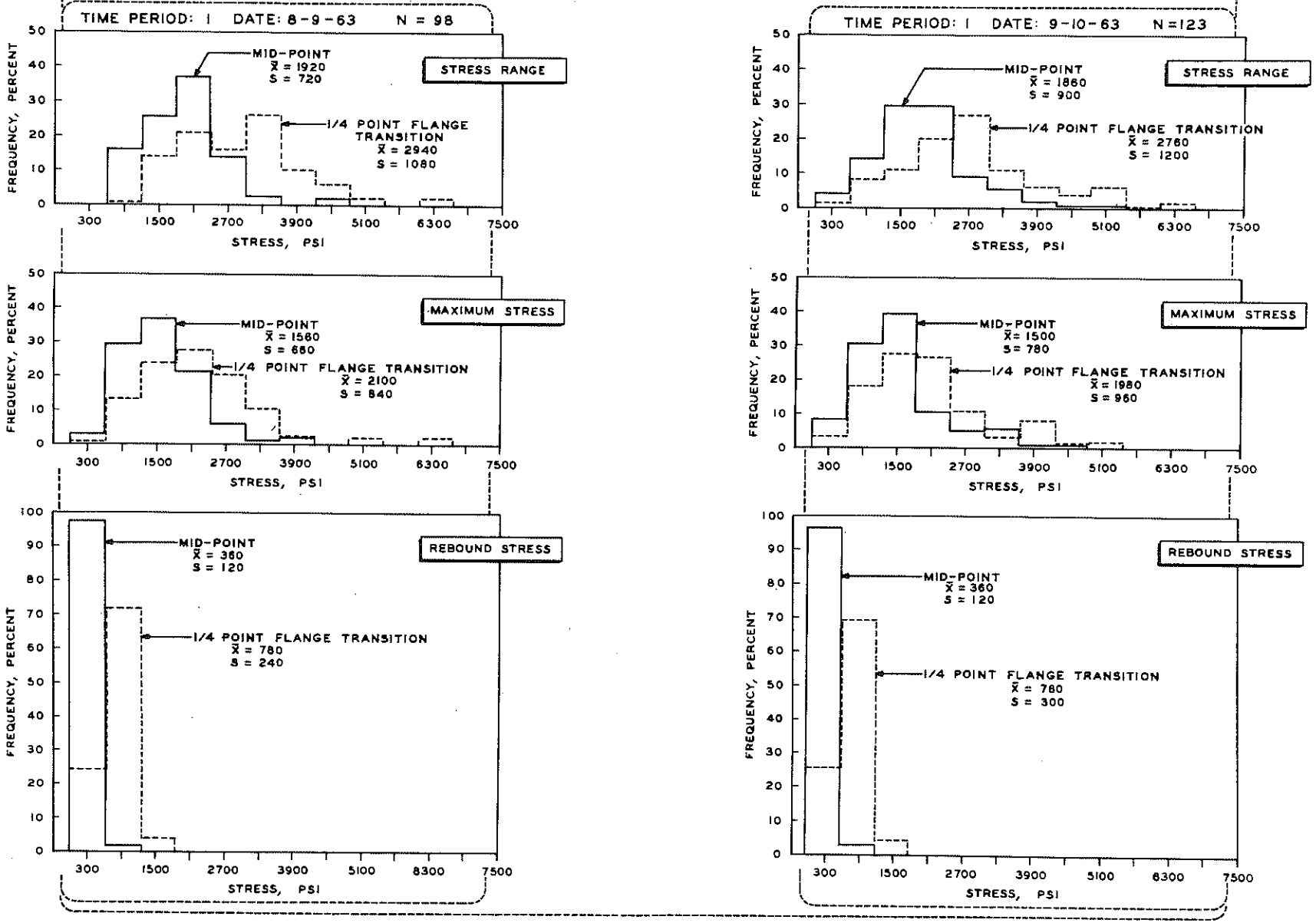
TIME PERIOD: 1 DATE: 8-9-63 N = 98
STRESS RANGE
MID-POINT
X̄ = 1920
S = 720
1/4 POINT FLANGE TRANSITION
X̄ = 2940
S = 1080
MAXIMUM STRESS
MID-POINT
X̄ = 1560
S = 660
1/4 POINT FLANGE TRANSITION
X̄ = 2100
S = 840
REBOUND STRESS
MID-POINT
X̄ = 360
S = 120
1/4 POINT FLANGE TRANSITION
X̄ = 780
S = 240
TIME PERIOD: 1 DATE: 9-10-63 N=123
STRESS RANGE
MID-POINT
X̄ = 1860
S = 900
1/4 POINT FLANGE TRANSITION
X̄ = 2760
S = 1200
MAXIMUM STRESS
MID-POINT
X̄ = 1500
S = 780
1/4 POINT FLANGE TRANSITION
X̄ = 1980
S = 960
REBOUND STRESS
MID-POINT
X̄ = 360
S = 120
1/4 POINT FLANGE TRANSITION
X̄ = 780
S = 300
FREQUENCY, PERCENT
STRESS, PSI
300 1500 2700 3900 5100 6300 7500
8300

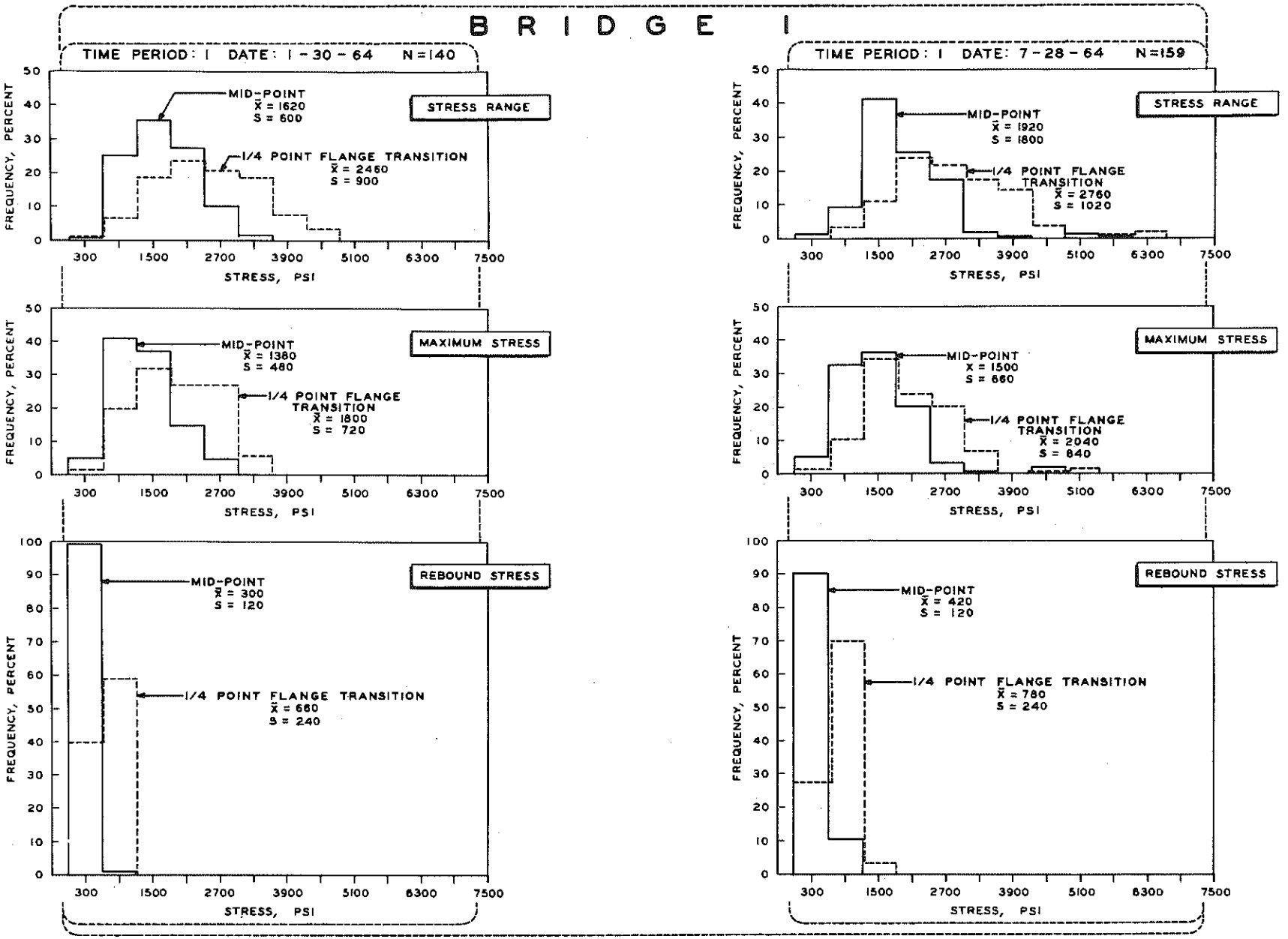
BRIDGE I
TIME PERIOD: I DATE: 1-30-64 N=140
STRESS RANGE
MID-POINT
X̄ = 1620
S = 600
1/4 POINT FLANGE TRANSITION
X̄ = 2460
S = 900
MAXIMUM STRESS
MID-POINT
X̄ = 1380
S = 480
1/4 POINT FLANGE TRANSITION
X̄ = 1800
S = 720
REBOUND STRESS
MID-POINT
X̄ = 300
S = 120
1/4 POINT FLANGE TRANSITION
X̄ = 660
S = 240
TIME PERIOD: I DATE: 7-28-64 N=159
STRESS RANGE
MID-POINT
X̄ = 1920
S = 1800
1/4 POINT FLANGE TRANSITION
X̄ = 2760
S = 1020
MAXIMUM STRESS
MID-POINT
X̄ = 1500
S = 660
1/4 POINT FLANGE TRANSITION
X̄ = 2040
S = 840
REBOUND STRESS
MID-POINT
X̄ = 420
S = 120
1/4 POINT FLANGE TRANSITION
X̄ = 780
S = 240
FREQUENCY, PERCENT
STRESS, PSI
300 1500 2700 3900 5100 6300 7500

B R I D G E I

TIME PERIOD: 2 DATE: 8-14-63 N=140

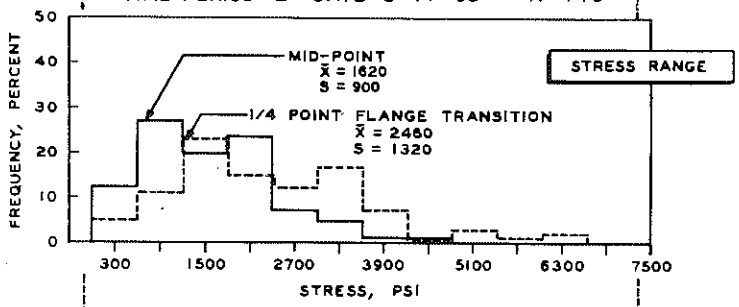

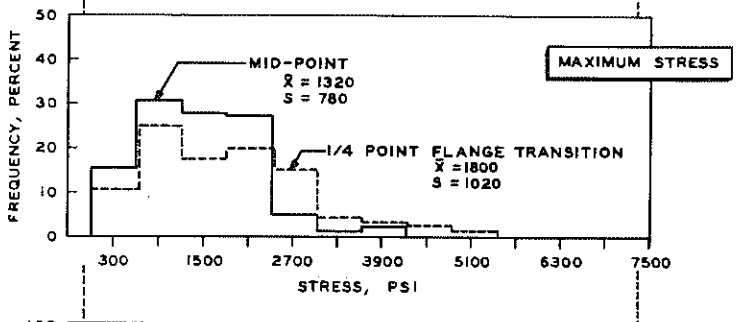

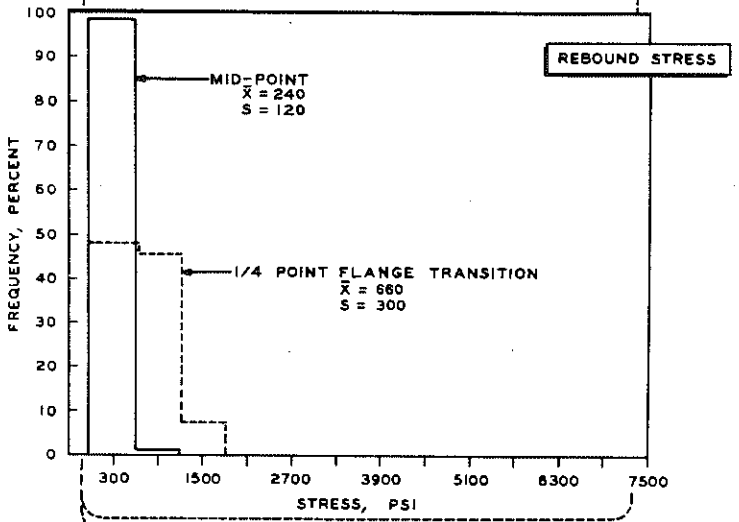

TIME PERIOD: 2 DATE: 9-10-63 N=210

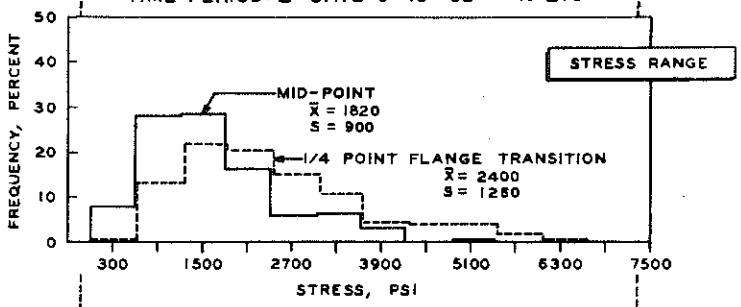

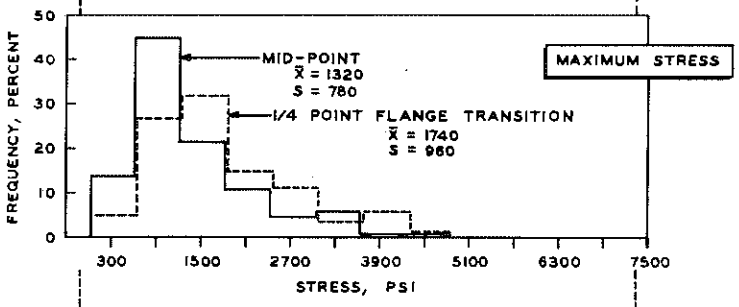

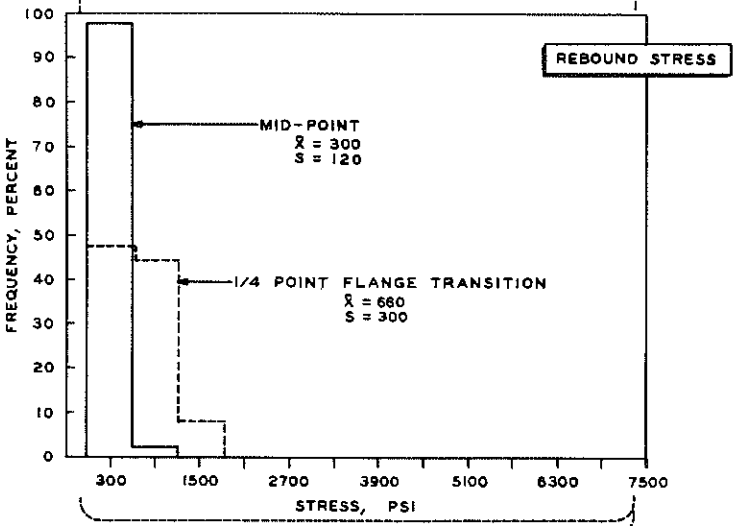

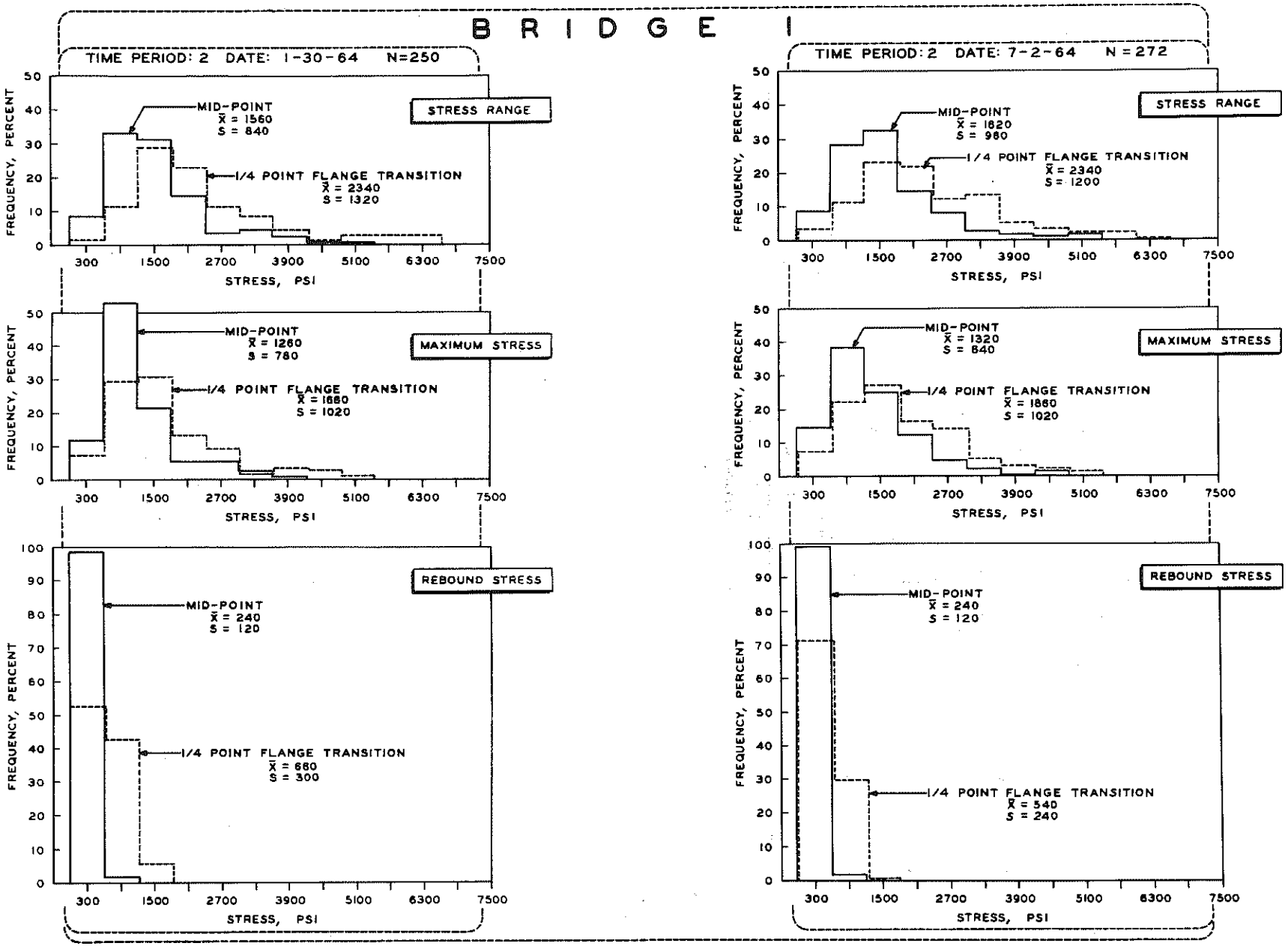
BRIDGE I
TIME PERIOD: 2 DATE: 1-30-64 N=250
STRESS RANGE
MID-POINT
X̄ = 1560
S = 840
1/4 POINT FLANGE TRANSITION
X̄ = 2340
S = 1320
MAXIMUM STRESS
MID-POINT
X̄ = 1260
S = 780
1/4 POINT FLANGE TRANSITION
X̄ = 1680
S = 1020
REBOUND STRESS
MID-POINT
X̄ = 240
S = 120
1/4 POINT FLANGE TRANSITION
X̄ = 660
S = 300
TIME PERIOD: 2 DATE: 7-2-64 N = 272
STRESS RANGE
MID-POINT
X̄ = 1820
S = 980
1/4 POINT FLANGE TRANSITION
X̄ = 2340
S = 1200
MAXIMUM STRESS
MID-POINT
X̄ = 1320
S = 840
1/4 POINT FLANGE TRANSITION
X̄ = 1860
S = 1020
REBOUND STRESS
MID-POINT
X̄ = 240
S = 120
1/4 POINT FLANGE TRANSITION
X̄ = 540
S = 240
FREQUENCY, PERCENT
STRESS, PSI
300 1500 2700 3900 5100 6300 7500

B R I D G E I

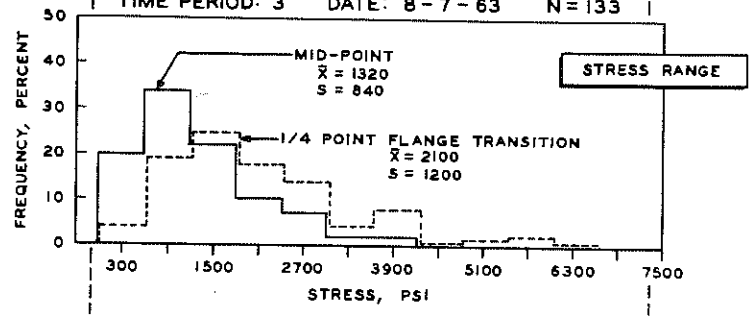
TIME PERIOD: 3 DATE: 8-7-63 N=133
STRESS RANGE
MID-POINT
X̄ = 1320
S = 840
1/4 POINT FLANGE TRANSITION
X̄ = 2100
S = 1200
FREQUENCY, PERCENT
STRESS, PSI
300 1500 2700 3900 5100 6300 7500

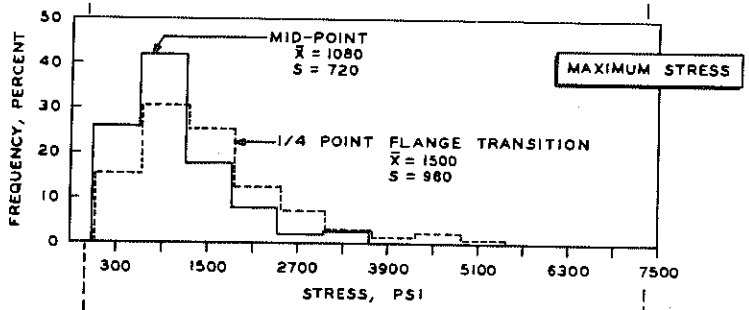
MAXIMUM STRESS
MID-POINT
X̄ = 1080
S = 720
1/4 POINT FLANGE TRANSITION
X̄ = 1500
S = 980
FREQUENCY, PERCENT
STRESS, PSI
300 1500 2700 3900 5100 6300 7500

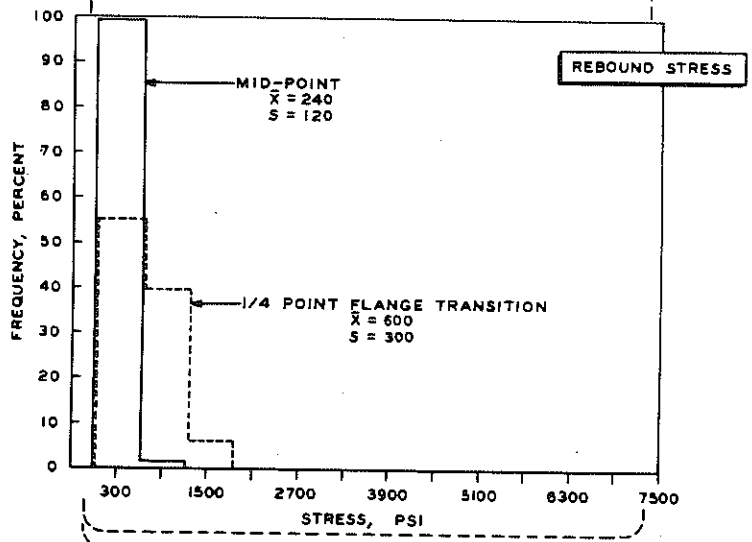
REBOUND STRESS
MID-POINT
X̄ = 240
S = 120
1/4 POINT FLANGE TRANSITION
X̄ = 600
S = 300
FREQUENCY, PERCENT
STRESS, PSI
300 1500 2700 3900 5100 6300 7500

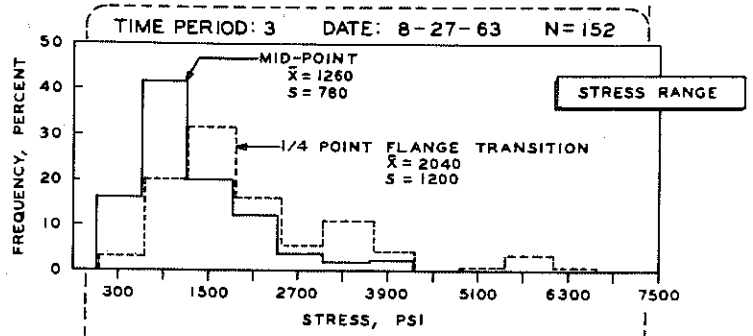
TIME PERIOD: 3 DATE: 8-27-63 N=152
STRESS RANGE
MID-POINT
X̄ = 1260
S = 780
1/4 POINT FLANGE TRANSITION
X̄ = 2040
S = 1200
FREQUENCY, PERCENT
STRESS, PSI
300 1500 2700 3900 5100 6300 7500

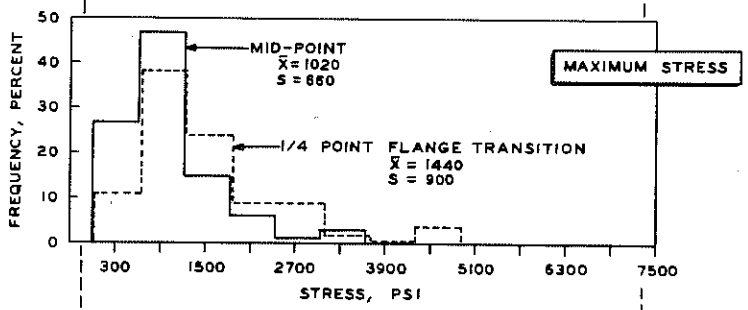
MAXIMUM STRESS
MID-POINT
X̄ = 1020
S = 660
1/4 POINT FLANGE TRANSITION
X̄ = 1440
S = 900
FREQUENCY, PERCENT
STRESS, PSI
300 1500 2700 3900 5100 6300 7500

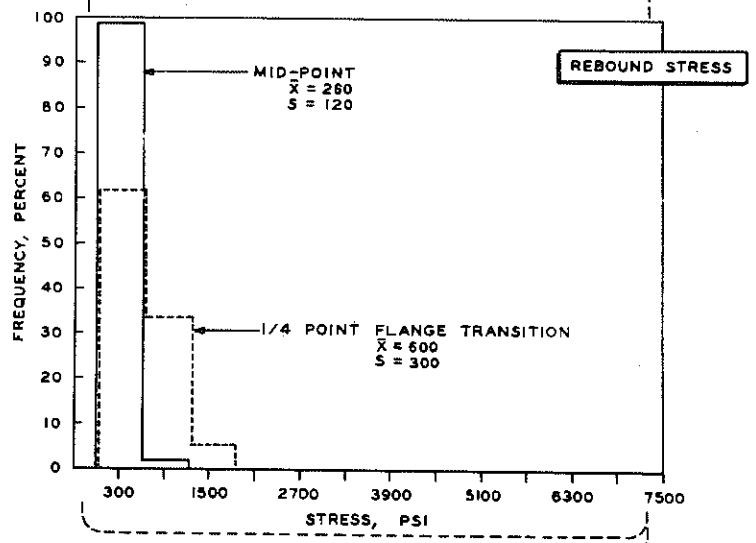
REBOUND STRESS
MID-POINT
X̄ = 260
S = 120
1/4 POINT FLANGE TRANSITION
X̄ = 600
S = 300
FREQUENCY, PERCENT
STRESS, PSI
300 1500 2700 3900 5100 6300 7500

BRIDGE 1

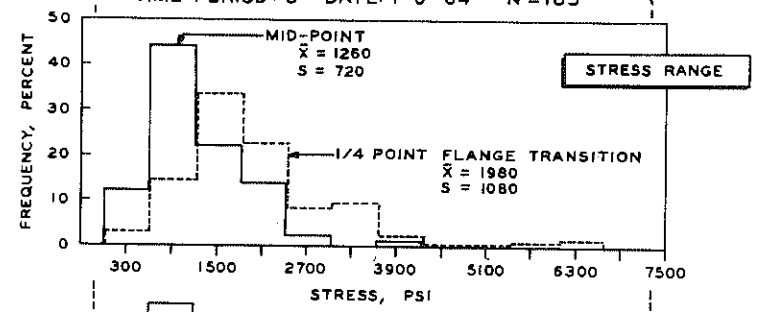
TIME PERIOD: 3 DATE: 1-6-64 N=185
STRESS RANGE
MID-POINT
X̄ = 1260
S = 720
1/4 POINT FLANGE TRANSITION
X̄ = 1980
S = 1080
FREQUENCY, PERCENT
STRESS, PSI
300 1500 2700 3900 5100 6300 7500

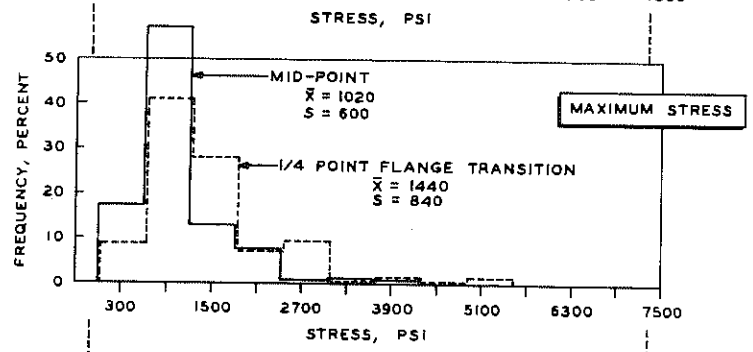
MAXIMUM STRESS
MID-POINT
X̄ = 1020
S = 600
1/4 POINT FLANGE TRANSITION
X̄ = 1440
S = 840
FREQUENCY, PERCENT
STRESS, PSI
300 1500 2700 3900 5100 6300 7500

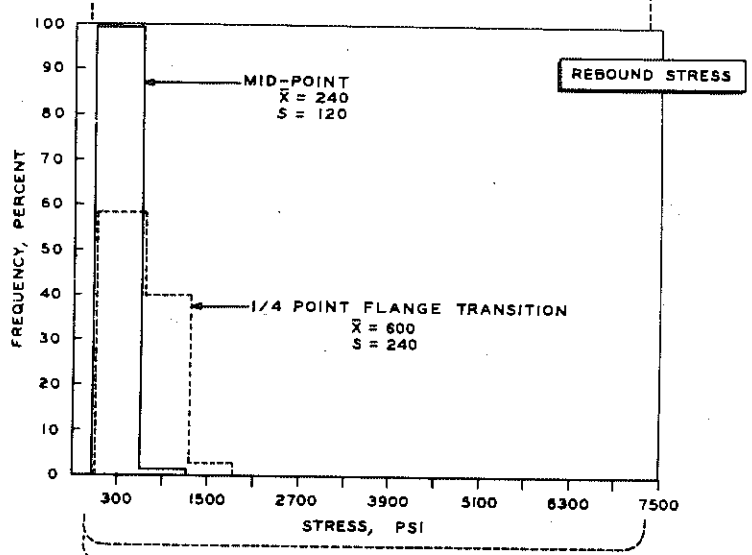
REBOUND STRESS
MID-POINT
X̄ = 240
S = 120
1/4 POINT FLANGE TRANSITION
X̄ = 600
S = 240
FREQUENCY, PERCENT
STRESS, PSI
300 1500 2700 3900 5100 6300 7500

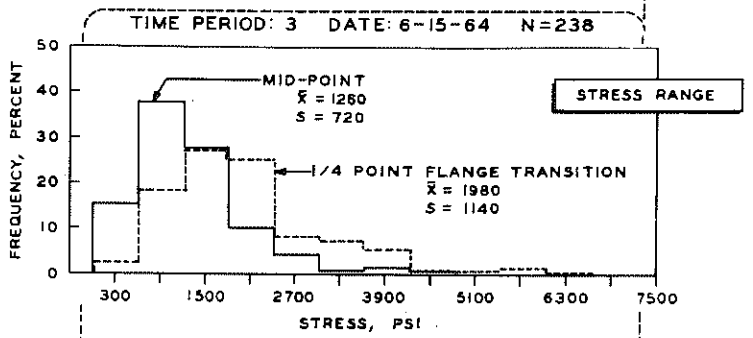
TIME PERIOD: 3 DATE: 6-15-64 N=238
STRESS RANGE
MID-POINT
X̄ = 1260
S = 720
1/4 POINT FLANGE TRANSITION
X̄ = 1980
S = 1140
FREQUENCY, PERCENT
STRESS, PSI
300 1500 2700 3900 5100 6300 7500

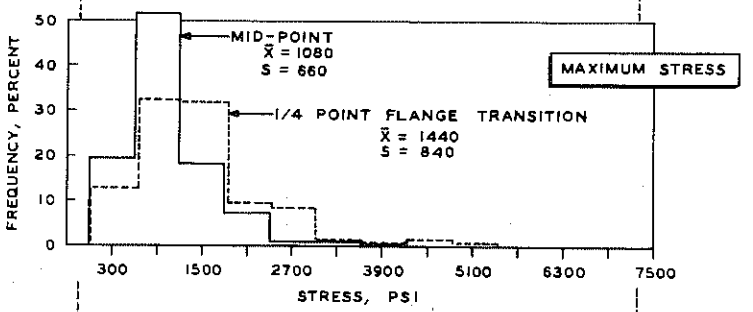
MAXIMUM STRESS
MID-POINT
X̄ = 1080
S = 660
1/4 POINT FLANGE TRANSITION
X̄ = 1440
S = 840
FREQUENCY, PERCENT
STRESS, PSI
300 1500 2700 3900 5100 6300 7500

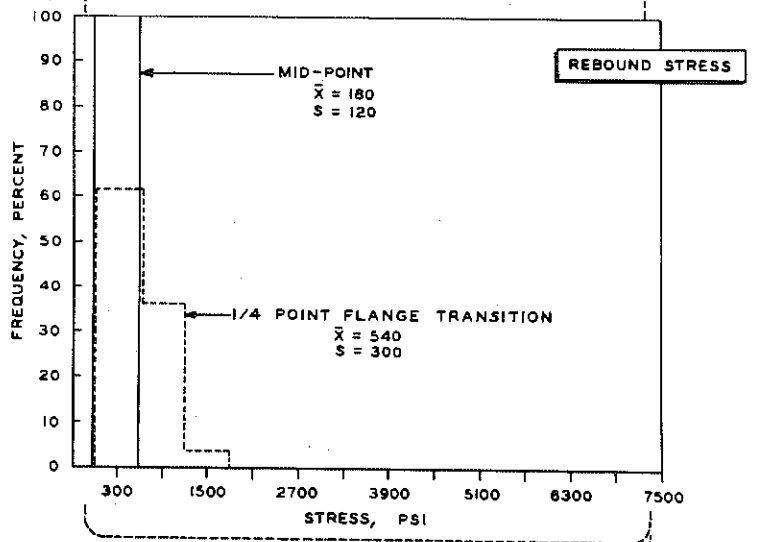
REBOUND STRESS
MID-POINT
X̄ = 180
S = 120
1/4 POINT FLANGE TRANSITION
X̄ = 540
S = 300
FREQUENCY, PERCENT
STRESS, PSI
300 1500 2700 3900 5100 6300 7500

BRIDGE I

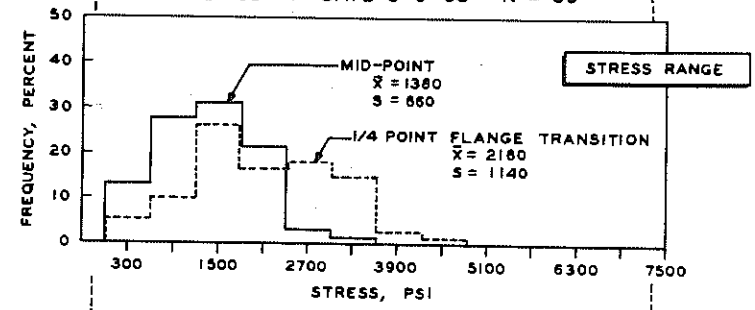
TIME PERIOD: 4 DATE: 8-6-63 N = 60
STRESS RANGE
MID-POINT
X̄ = 1380
S = 660
1/4 POINT FLANGE TRANSITION
X̄ = 2180
S = 1140
FREQUENCY, PERCENT
STRESS, PSI
300 1500 2700 3900 5100 6300 7500

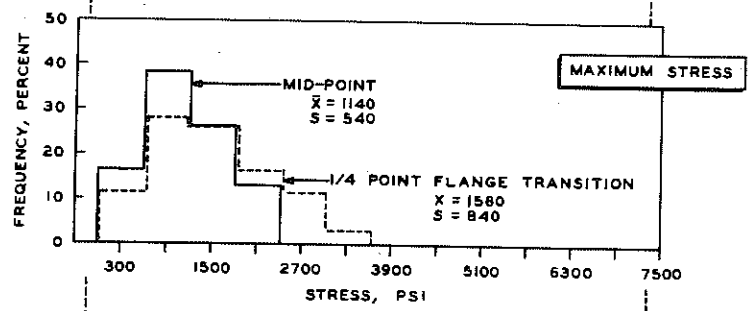
MAXIMUM STRESS
MID-POINT
X̄ = 1140
S = 540
1/4 POINT FLANGE TRANSITION
X̄ = 1580
S = 840
FREQUENCY, PERCENT
STRESS, PSI
300 1500 2700 3900 5100 6300 7500

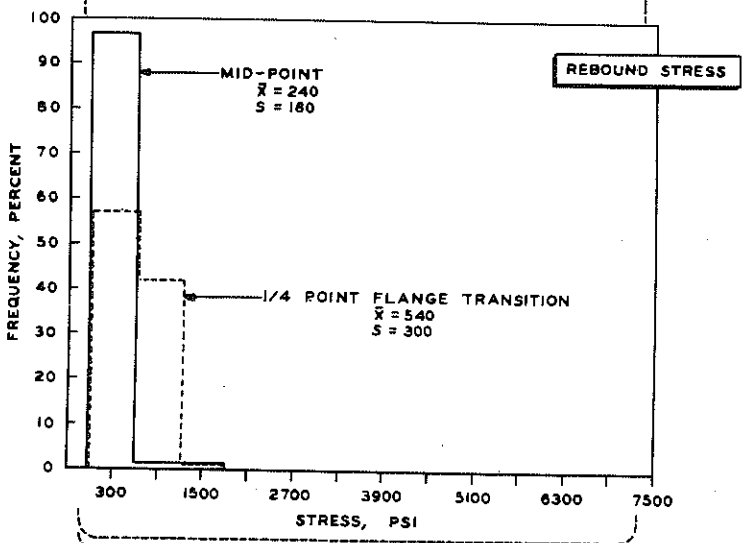
REBOUND STRESS
MID-POINT
X̄ = 240
S = 180
1/4 POINT FLANGE TRANSITION
X̄ = 540
S = 300
FREQUENCY, PERCENT
STRESS, PSI
300 1500 2700 3900 5100 6300 7500

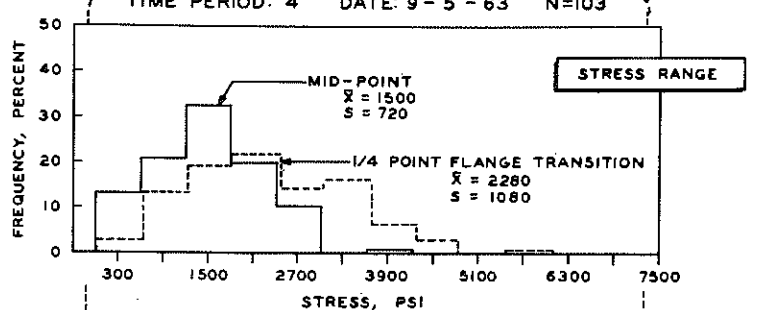
TIME PERIOD: 4 DATE: 9-5-63 N=103
STRESS RANGE
MID-POINT
X̄ = 1500
S = 720
1/4 POINT FLANGE TRANSITION
X̄ = 2280
S = 1080
FREQUENCY, PERCENT
STRESS, PSI
300 1500 2700 3900 5100 6300 7500

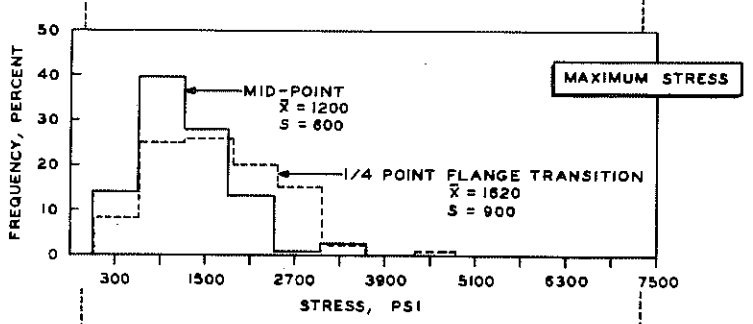
MAXIMUM STRESS
MID-POINT
X̄ = 1200
S = 600
1/4 POINT FLANGE TRANSITION
X̄ = 1620
S = 900
FREQUENCY, PERCENT
STRESS, PSI
300 1500 2700 3900 5100 6300 7500

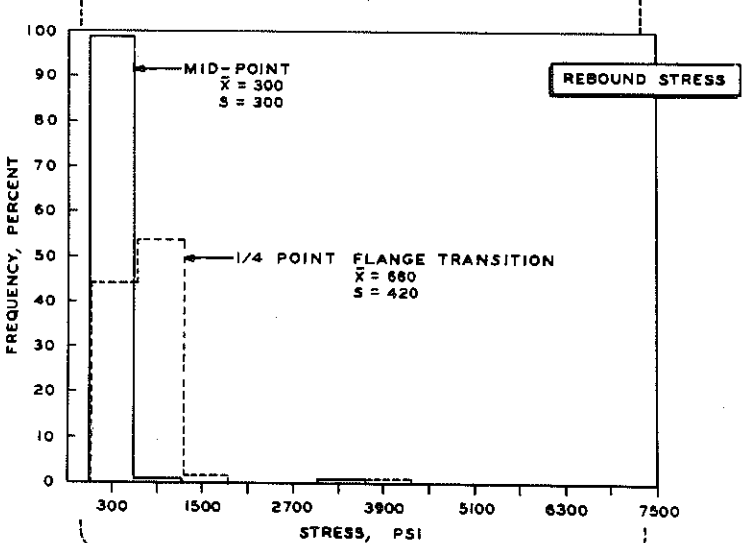
REBOUND STRESS
MID-POINT
X̄ = 300
S = 300
1/4 POINT FLANGE TRANSITION
X̄ = 660
S = 420
FREQUENCY, PERCENT
STRESS, PSI
300 1500 2700 3900 5100 6300 7500

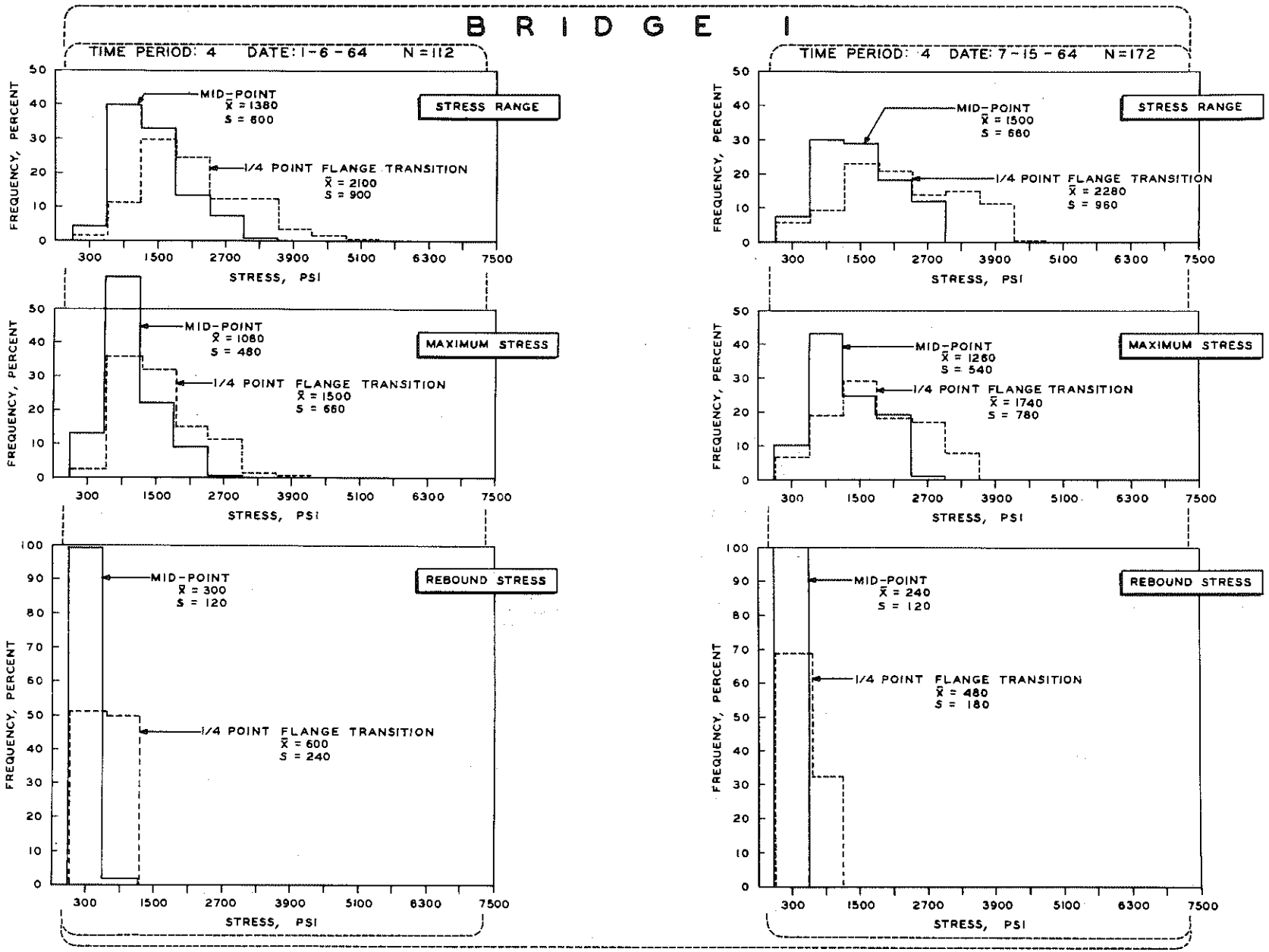
B R I D G E I
TIME PERIOD: 4 DATE: 1-6-64 N=112
STRESS RANGE
MID-POINT
X̄ = 1380
S = 800
1/4 POINT FLANGE TRANSITION
X̄ = 2100
S = 900
MAXIMUM STRESS
MID-POINT
X̄ = 1080
S = 480
1/4 POINT FLANGE TRANSITION
X̄ = 1500
S = 660
REBOUND STRESS
MID-POINT
X̄ = 300
S = 120
1/4 POINT FLANGE TRANSITION
X̄ = 600
S = 240
TIME PERIOD: 4 DATE: 7-15-64 N=172
STRESS RANGE
MID-POINT
X̄ = 1500
S = 680
1/4 POINT FLANGE TRANSITION
X̄ = 2280
S = 960
MAXIMUM STRESS
MID-POINT
X̄ = 1260
S = 540
1/4 POINT FLANGE TRANSITION
X̄ = 1740
S = 780
REBOUND STRESS
MID-POINT
X̄ = 240
S = 120
1/4 POINT FLANGE TRANSITION
X̄ = 480
S = 180
FREQUENCY, PERCENT
STRESS, PSI
300 1500 2700 3900 5100 6300 7500

BRIDGE 2

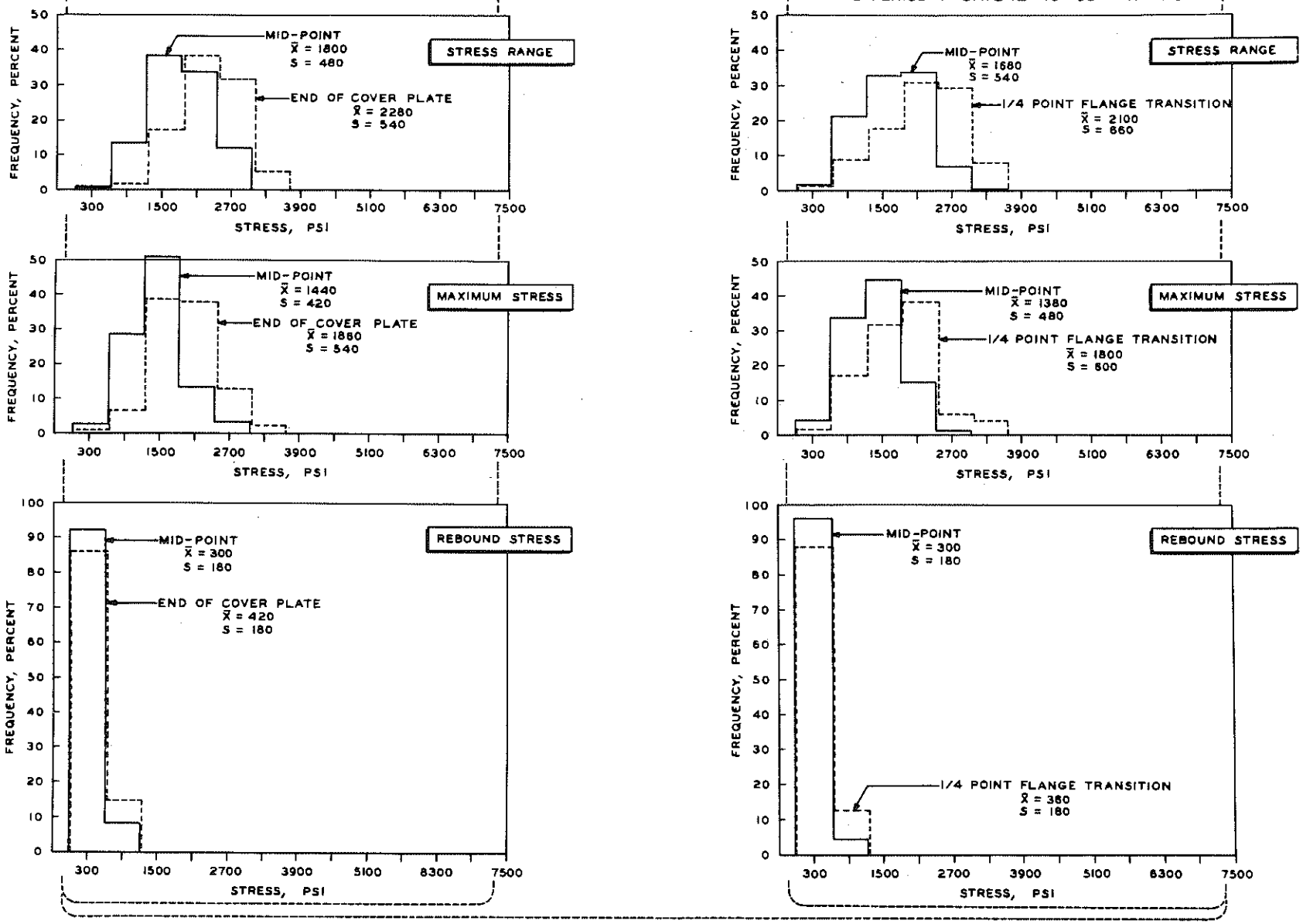
TIME PERIOD: 1 DATE: 9 - 12 - 63 N=108
STRESS RANGE
MID-POINT
X̄ = 1800
S = 480
END OF COVER PLATE
X̄ = 2280
S = 540
MAXIMUM STRESS
MID-POINT
X̄ = 1440
S = 420
END OF COVER PLATE
X̄ = 1860
S = 540
REBOUND STRESS
MID-POINT
X̄ = 300
S = 180
END OF COVER PLATE
X̄ = 420
S = 180
TIME PERIOD: 1 DATE: 12 - 10 - 63 N = 110
STRESS RANGE
MID-POINT
X̄ = 1680
S = 540
1/4 POINT FLANGE TRANSITION
X̄ = 2100
S = 660
MAXIMUM STRESS
MID-POINT
X̄ = 1380
S = 480
1/4 POINT FLANGE TRANSITION
X̄ = 1800
S = 600
REBOUND STRESS
MID-POINT
X̄ = 300
S = 180
1/4 POINT FLANGE TRANSITION
X̄ = 360
S = 180
FREQUENCY, PERCENT
STRESS, PSI
300 1500 2700 3900 5100 6300 7500
8300

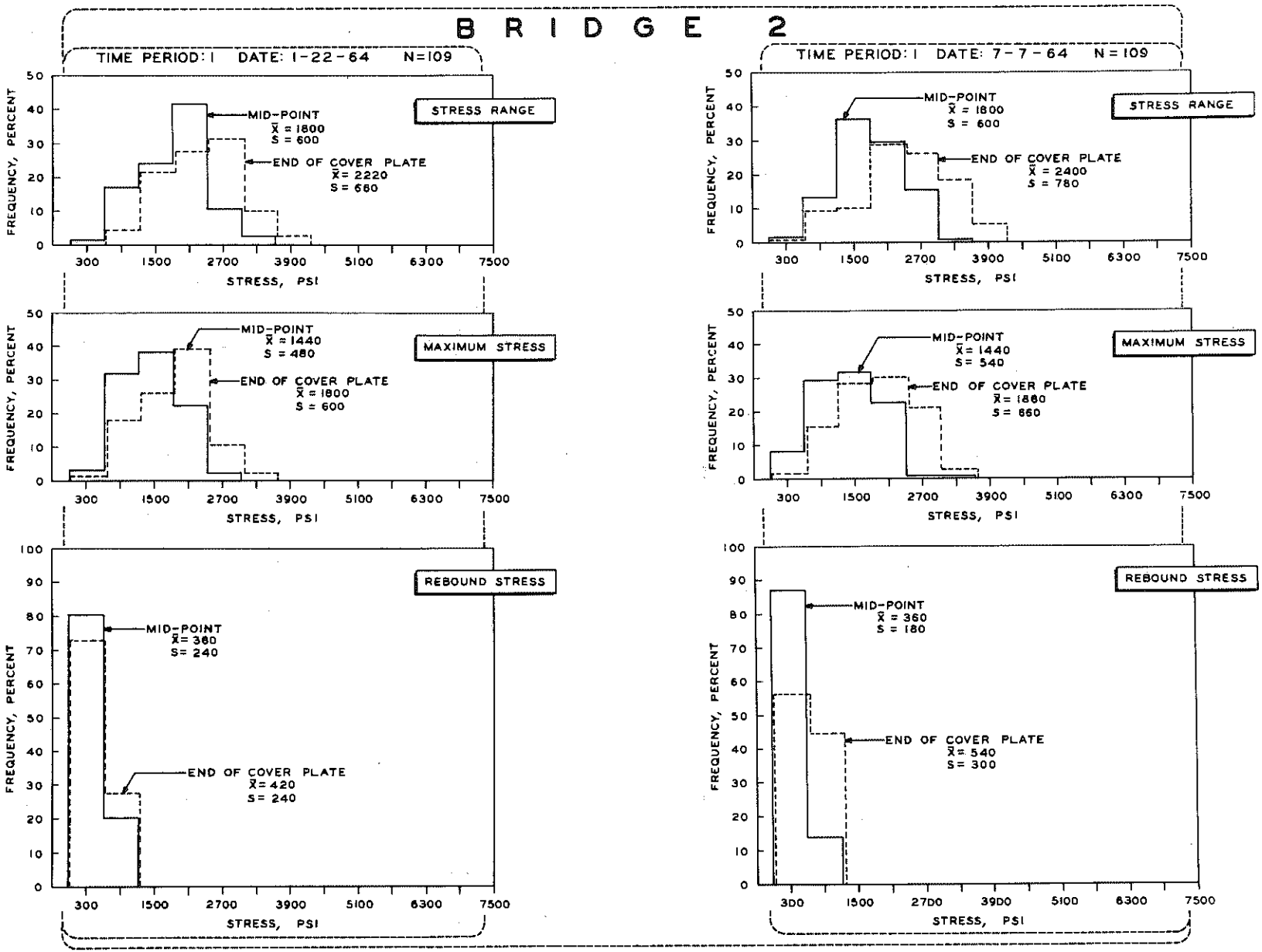
BRIDGE 2
TIME PERIOD: 1 DATE: 1-22-64 N=109
STRESS RANGE
MID-POINT
X̄ = 1800
S = 600
END OF COVER PLATE
X̄ = 2220
S = 660
MAXIMUM STRESS
MID-POINT
X̄ = 1440
S = 480
END OF COVER PLATE
X̄ = 1800
S = 600
REBOUND STRESS
MID-POINT
X̄ = 360
S = 240
END OF COVER PLATE
X̄ = 420
S = 240
TIME PERIOD: 1 DATE: 7-7-64 N=109
STRESS RANGE
MID-POINT
X̄ = 1800
S = 600
END OF COVER PLATE
X̄ = 2400
S = 780
MAXIMUM STRESS
MID-POINT
X̄ = 1440
S = 540
END OF COVER PLATE
X̄ = 1860
S = 660
REBOUND STRESS
MID-POINT
X̄ = 360
S = 180
END OF COVER PLATE
X̄ = 540
S = 300
FREQUENCY, PERCENT
STRESS, PSI
300 1500 2700 3900 5100 6300 7500

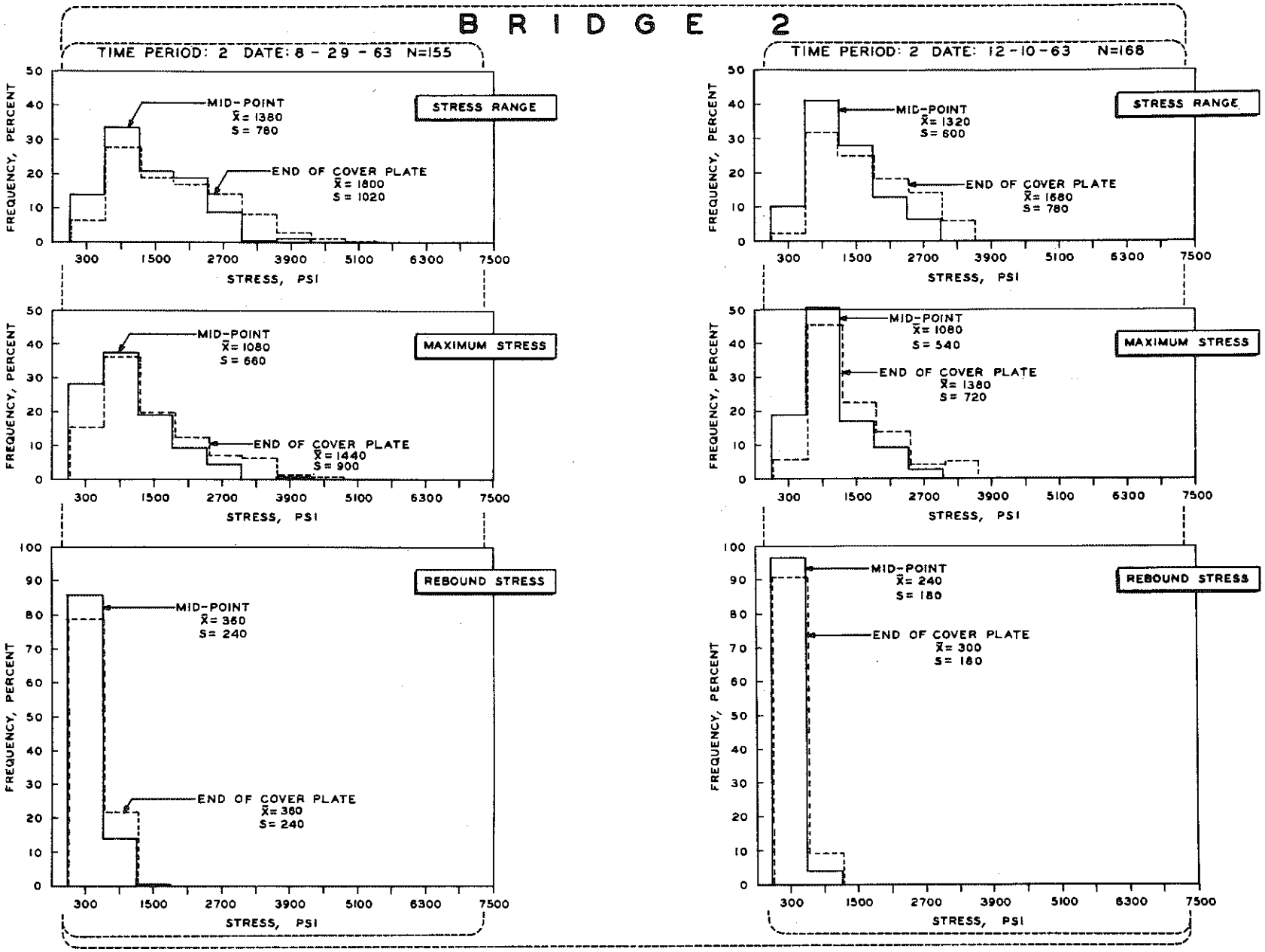
BRIDGE 2
TIME PERIOD: 2 DATE: 8 - 29 - 63 N=155
TIME PERIOD: 2 DATE: 12 - 10 - 63 N=168
STRESS RANGE
MAXIMUM STRESS
REBOUND STRESS
FREQUENCY, PERCENT
STRESS, PSI
MID-POINT
X̄= 1380
S= 780
END OF COVER PLATE
X̄= 1800
S= 1020
MID-POINT
X̄= 1320
S= 600
END OF COVER PLATE
X̄= 1680
S= 780
MID-POINT
X̄= 1080
S= 660
END OF COVER PLATE
X̄= 1440
S= 900
MID-POINT
X̄= 1080
S= 540
END OF COVER PLATE
X̄= 1380
S= 720
MID-POINT
X̄= 360
S= 240
END OF COVER PLATE
X̄= 360
S= 240
MID-POINT
X̄= 240
S= 180
END OF COVER PLATE
X̄= 300
S= 180

BRIDGE 2

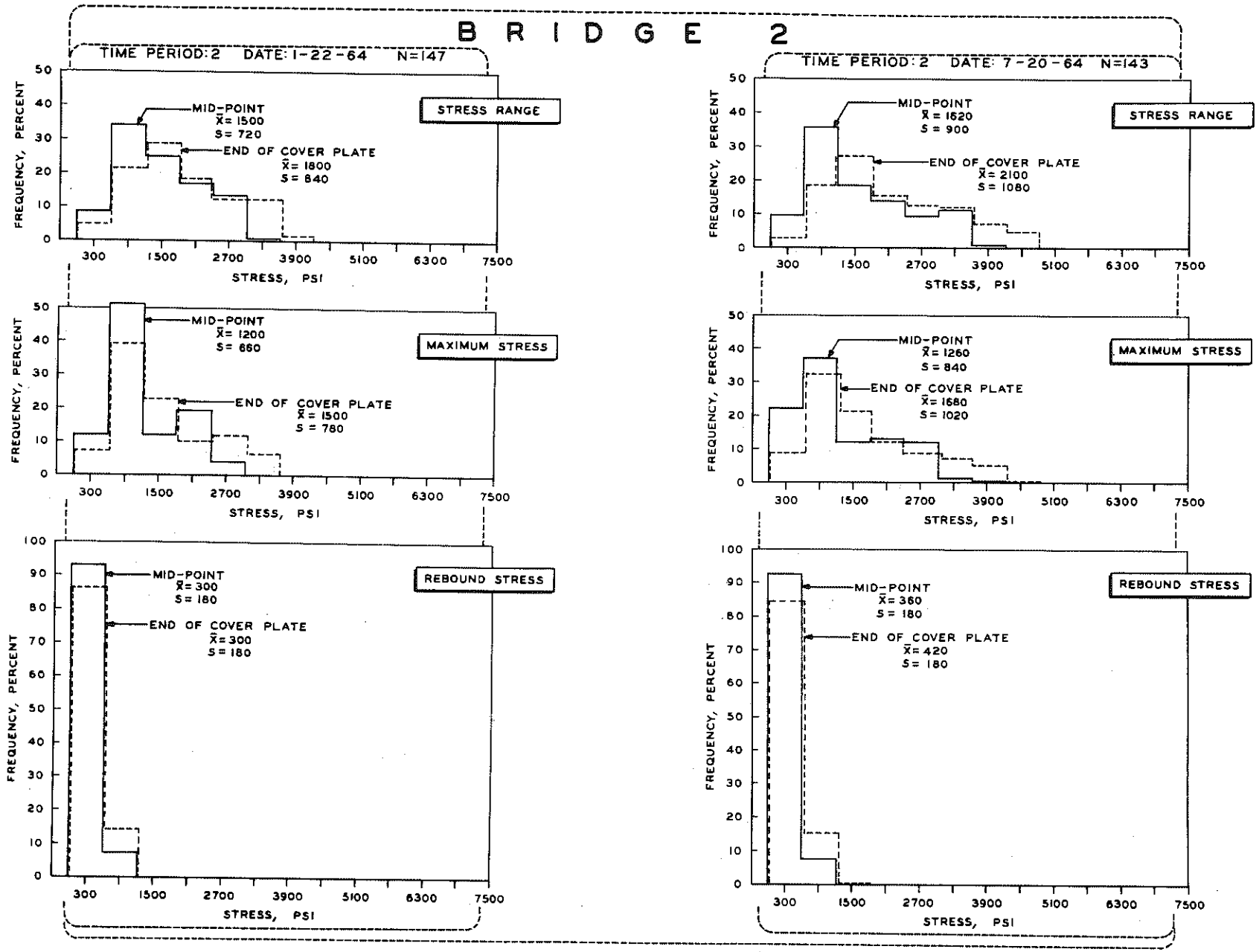
TIME PERIOD: 2 DATE: 1-22-64 N=147
STRESS RANGE
MID-POINT
X̄ = 1500
S = 720
END OF COVER PLATE
X̄ = 1800
S = 840
MAXIMUM STRESS
MID-POINT
X̄ = 1200
S = 660
END OF COVER PLATE
X̄ = 1500
S = 780
REBOUND STRESS
MID-POINT
X̄ = 300
S = 180
END OF COVER PLATE
X̄ = 300
S = 180
TIME PERIOD: 2 DATE: 7-20-64 N=143
STRESS RANGE
MID-POINT
X̄ = 1620
S = 900
END OF COVER PLATE
X̄ = 2100
S = 1080
MAXIMUM STRESS
MID-POINT
X̄ = 1260
S = 840
END OF COVER PLATE
X̄ = 1680
S = 1020
REBOUND STRESS
MID-POINT
X̄ = 360
S = 180
END OF COVER PLATE
X̄ = 420
S = 180
FREQUENCY, PERCENT
STRESS, PSI
300 1500 2700 3900 5100 6300 7500

BRIDGE 2

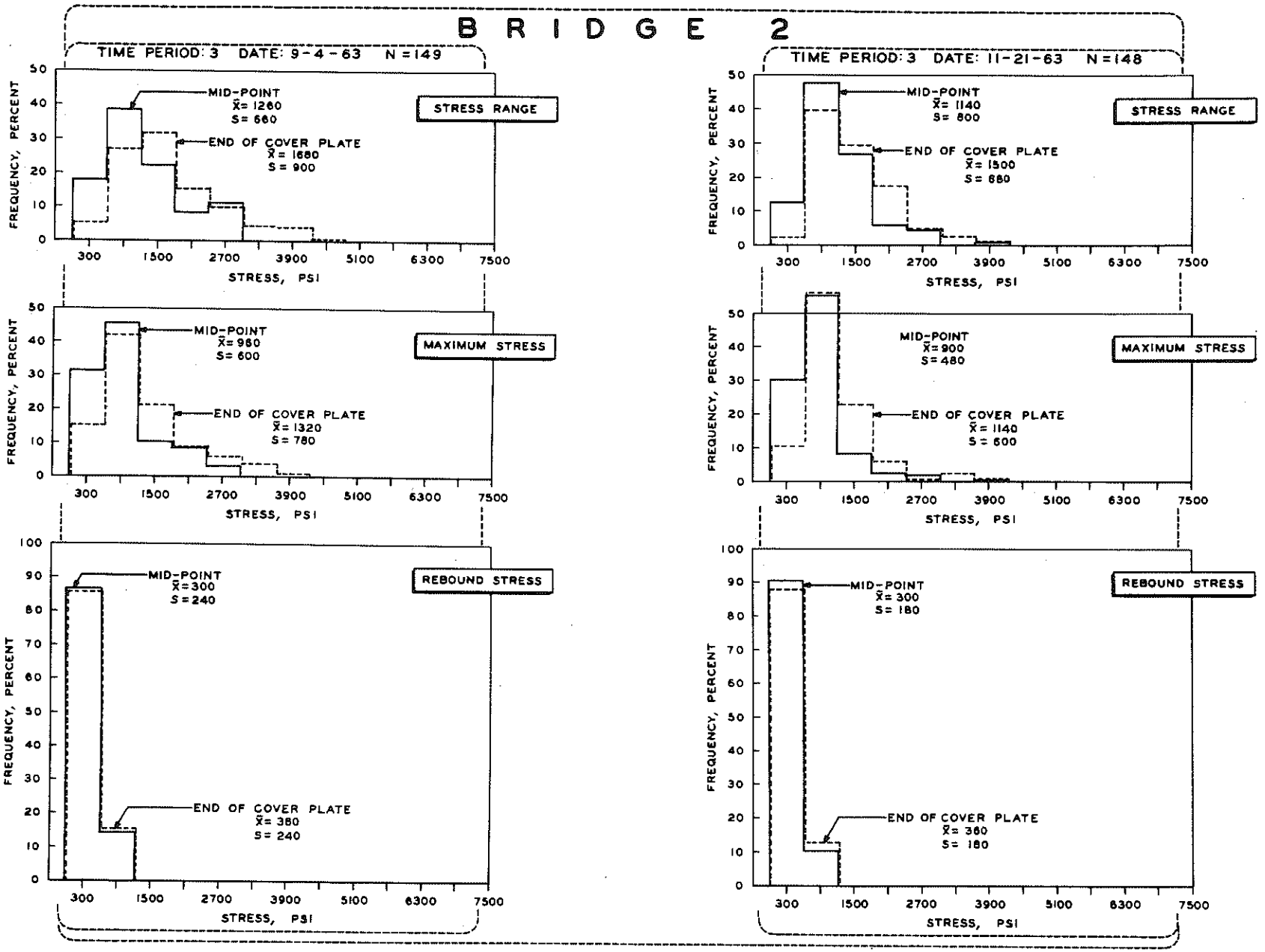
TIME PERIOD: 3 DATE: 9-4-63 N=149
STRESS RANGE
MID-POINT
X̄= 1260
S= 660
END OF COVER PLATE
X̄= 1680
S= 900
MAXIMUM STRESS
MID-POINT
X̄= 980
S= 600
END OF COVER PLATE
X̄= 1320
S= 780
REBOUND STRESS
MID-POINT
X̄= 300
S= 240
END OF COVER PLATE
X̄= 360
S= 240
TIME PERIOD: 3 DATE: 11-21-63 N=148
STRESS RANGE
MID-POINT
X̄= 1140
S= 800
END OF COVER PLATE
X̄= 1500
S= 680
MAXIMUM STRESS
MID-POINT
X̄= 900
S= 480
END OF COVER PLATE
X̄= 1140
S= 600
REBOUND STRESS
MID-POINT
X̄= 300
S= 180
END OF COVER PLATE
X̄= 360
S= 180
FREQUENCY, PERCENT
STRESS, PSI
300 1500 2700 3900 5100 6300 7500

BRIDGE 2

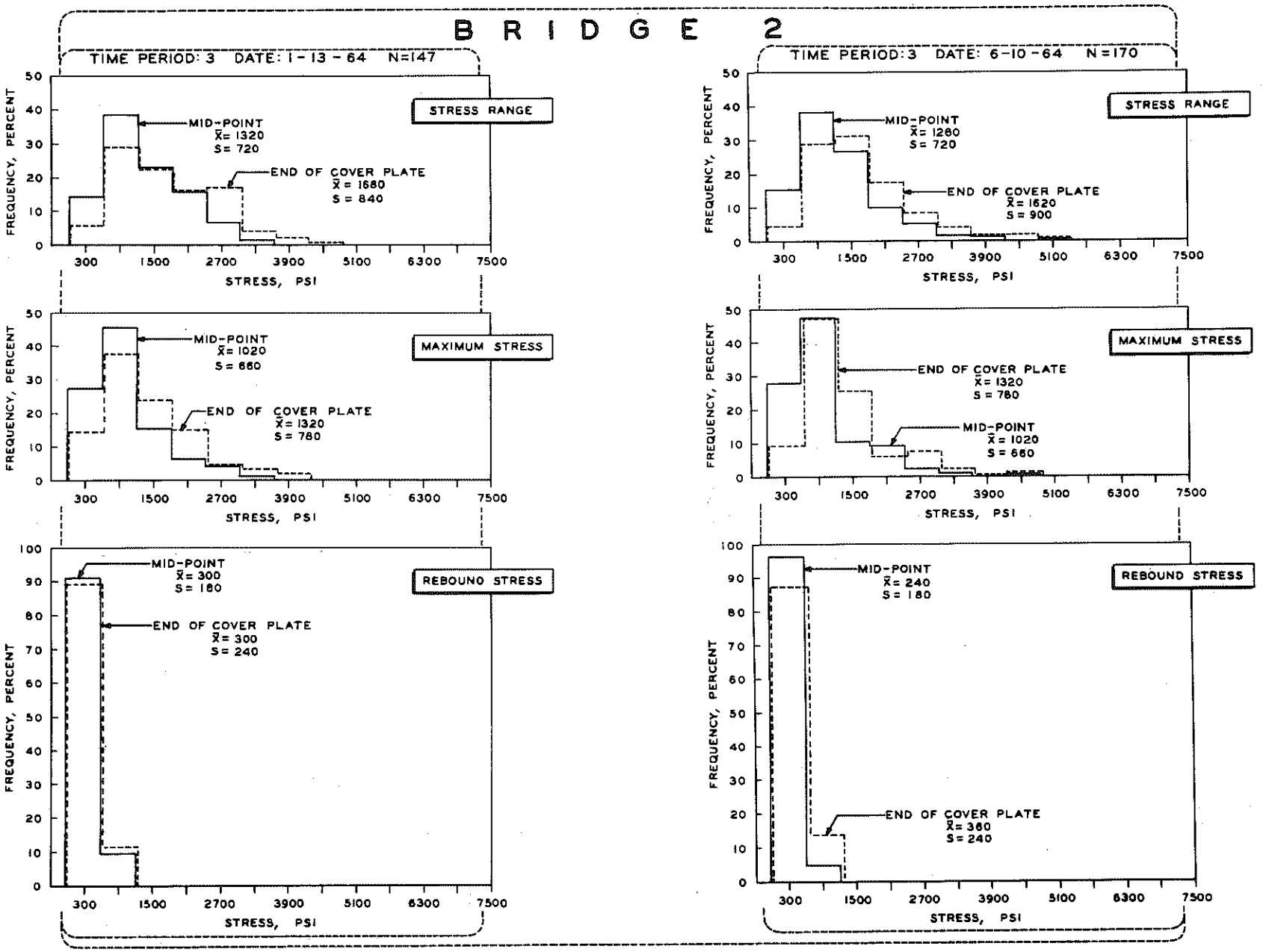
TIME PERIOD: 3 DATE: 1-13-64 N=147
STRESS RANGE
MID-POINT
X̄= 1320
S= 720
END OF COVER PLATE
X̄= 1680
S= 840
MAXIMUM STRESS
MID-POINT
X̄= 1020
S= 660
END OF COVER PLATE
X̄= 1320
S= 780
REBOUND STRESS
MID-POINT
X̄= 300
S= 180
END OF COVER PLATE
X̄= 300
S= 240
TIME PERIOD: 3 DATE: 6-10-64 N=170
STRESS RANGE
MID-POINT
X̄= 1260
S= 720
END OF COVER PLATE
X̄= 1620
S= 900
MAXIMUM STRESS
END OF COVER PLATE
X̄= 1320
S= 780
MID-POINT
X̄= 1020
S= 660
REBOUND STRESS
MID-POINT
X̄= 240
S= 180
END OF COVER PLATE
X̄= 360
S= 240
FREQUENCY, PERCENT
STRESS, PSI
300
1500
2700
3900
5100
6300
7500

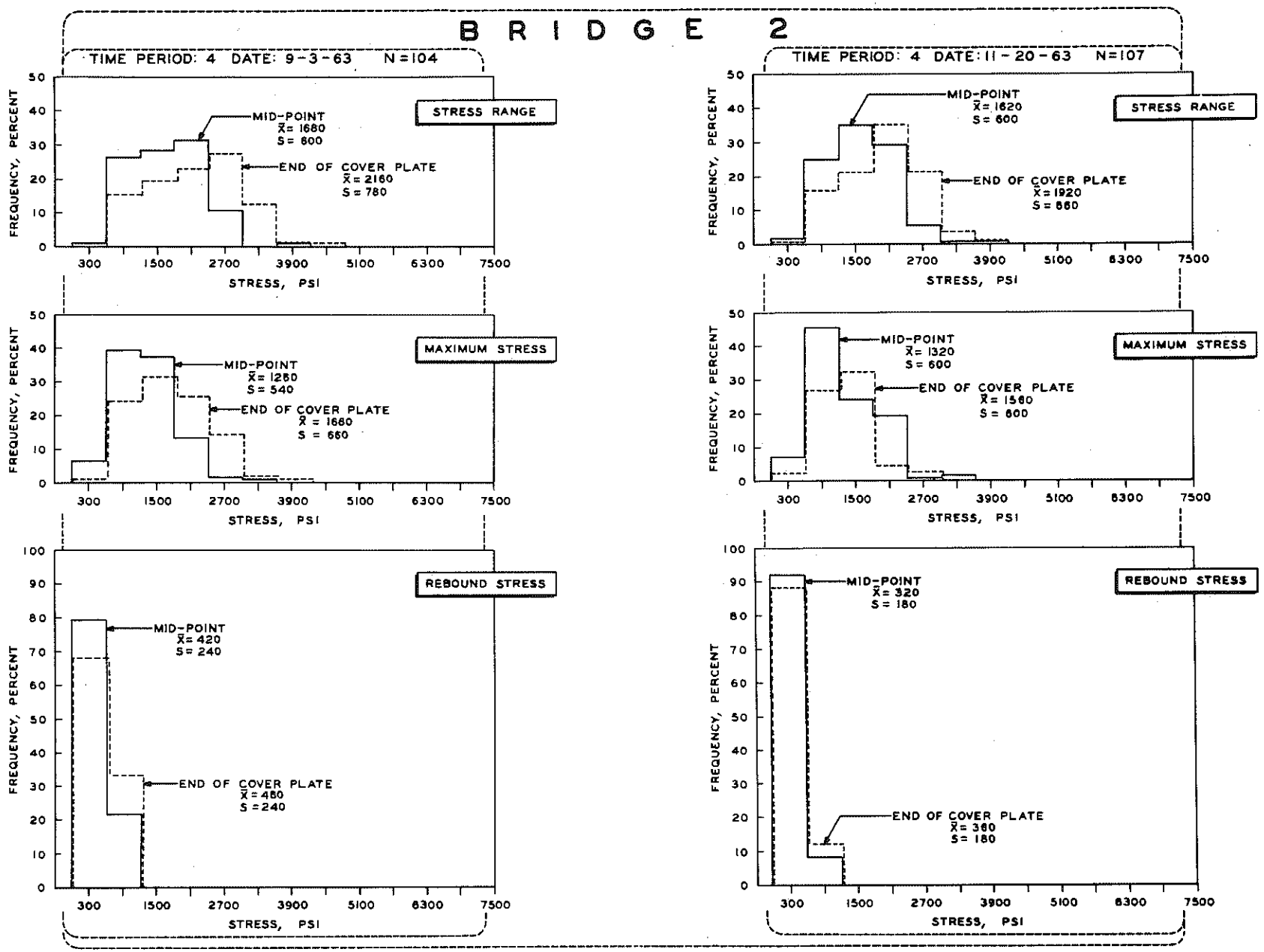
BRIDGE 2
TIME PERIOD: 4 DATE: 9-3-63 N=104
STRESS RANGE
MID-POINT
X̄= 1680
S= 800
END OF COVER PLATE
X̄= 2160
S= 780
MAXIMUM STRESS
MID-POINT
X̄= 1260
S= 540
END OF COVER PLATE
X̄= 1680
S= 660
REBOUND STRESS
MID-POINT
X̄= 420
S= 240
END OF COVER PLATE
X̄= 480
S= 240
TIME PERIOD: 4 DATE: 11-20-63 N=107
STRESS RANGE
MID-POINT
X̄= 1620
S= 600
END OF COVER PLATE
X̄= 1920
S= 860
MAXIMUM STRESS
MID-POINT
X̄= 1320
S= 600
END OF COVER PLATE
X̄= 1560
S= 600
REBOUND STRESS
MID-POINT
X̄= 320
S= 180
END OF COVER PLATE
X̄= 360
S= 180
FREQUENCY, PERCENT
STRESS, PSI
300 1500 2700 3900 5100 6300 7500

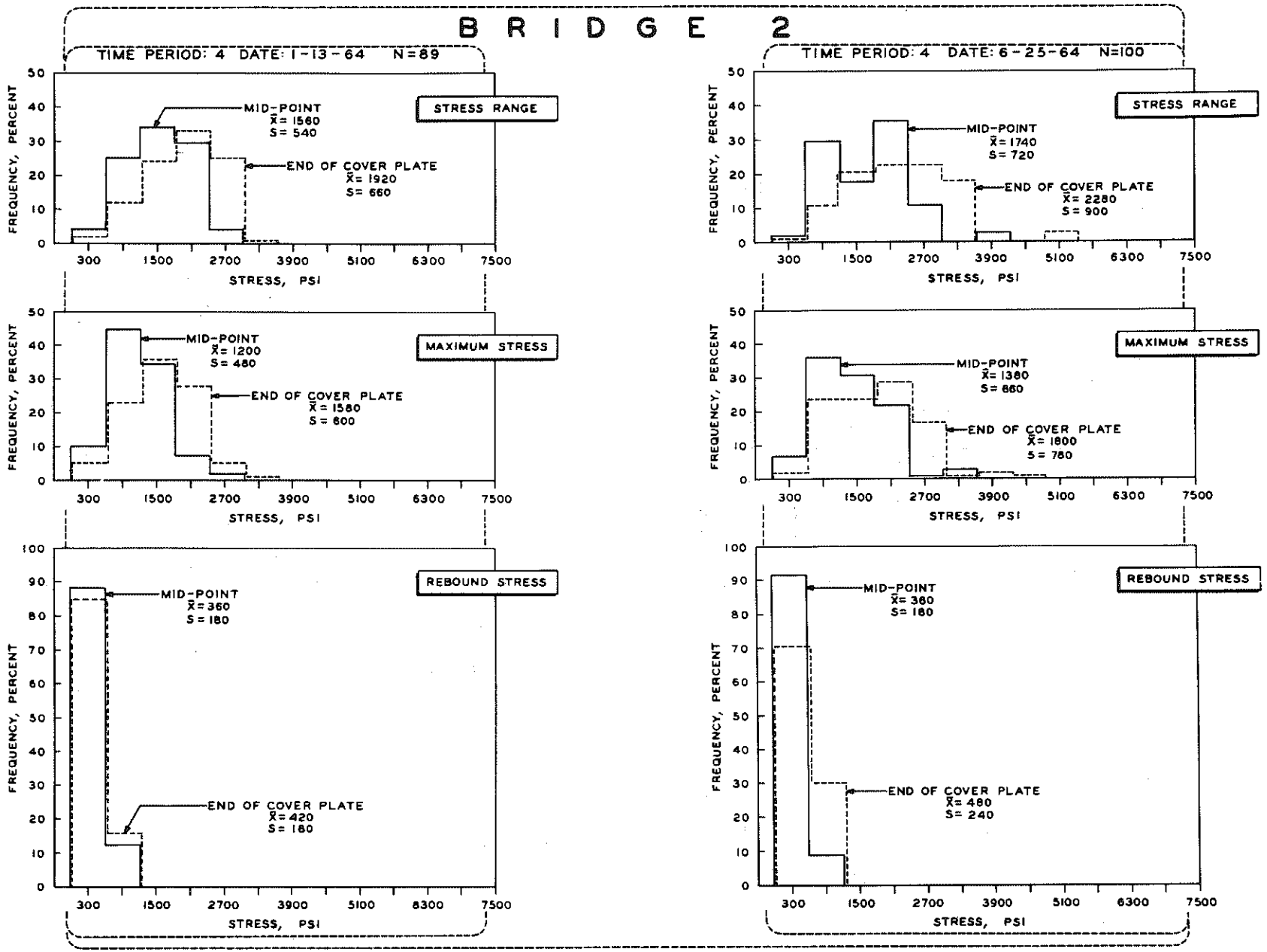
BRIDGE 2
TIME PERIOD: 4 DATE: 1-13-64 N=89
TIME PERIOD: 4 DATE: 6-25-64 N=100
STRESS RANGE
MAXIMUM STRESS
REBOUND STRESS
MID-POINT
X̄= 1560
S= 540
END OF COVER PLATE
X̄= 1920
S= 660
MID-POINT
X̄= 1740
S= 720
END OF COVER PLATE
X̄= 2280
S= 900
MID-POINT
X̄= 1200
S= 480
END OF COVER PLATE
X̄= 1580
S= 600
MID-POINT
X̄= 1380
S= 660
END OF COVER PLATE
X̄= 1800
S= 780
MID-POINT
X̄= 360
S= 180
END OF COVER PLATE
X̄= 420
S= 180
MID-POINT
X̄= 360
S= 180
END OF COVER PLATE
X̄= 480
S= 240
FREQUENCY, PERCENT
STRESS, PSI
300
1500
2700
3900
5100
6300
7500

B R I D G E 3

TIME PERIOD: I DATE: 9 - 16 - 65 N=446

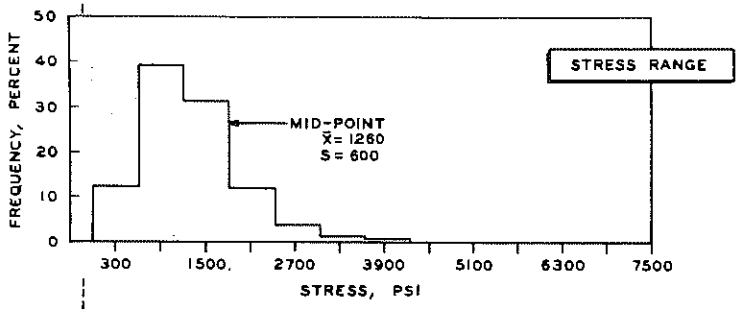

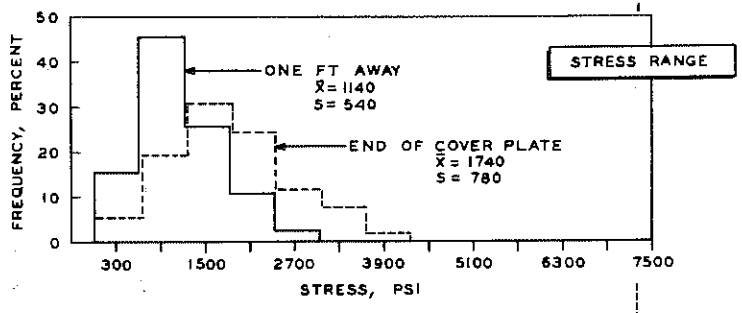

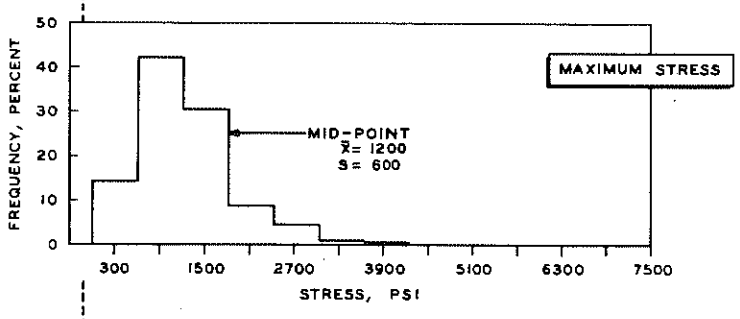

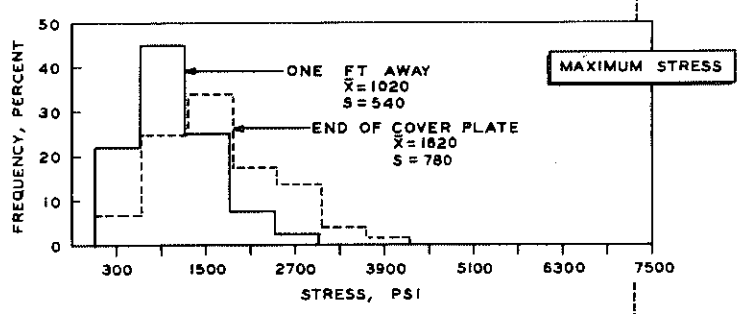

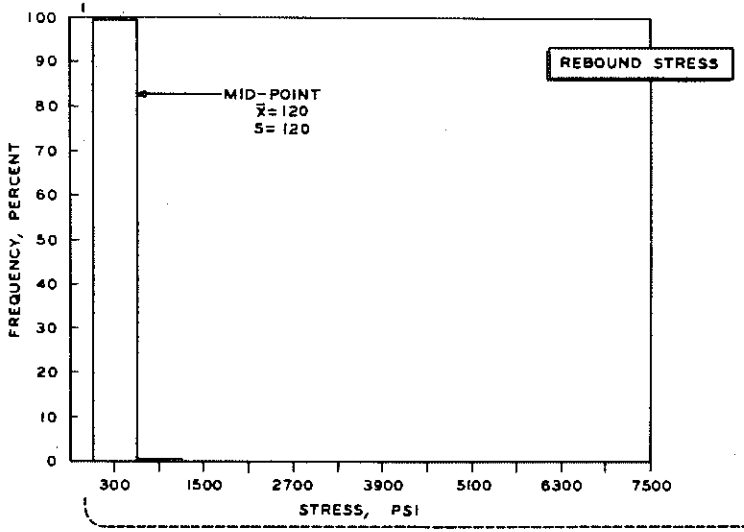

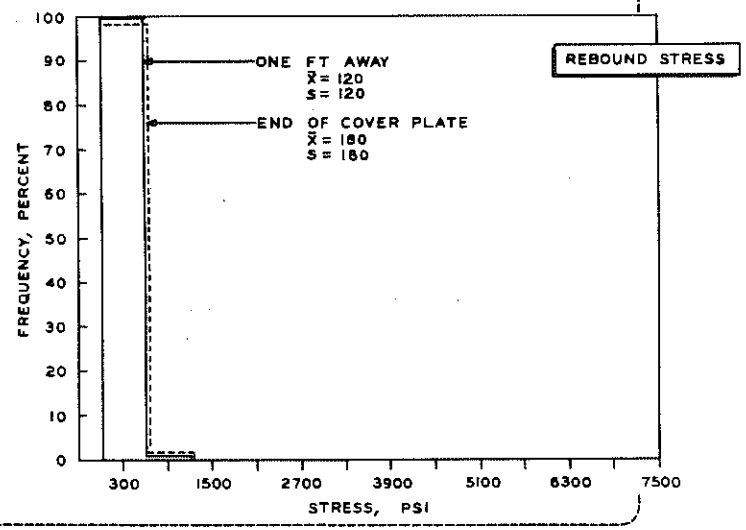

BRIDGE 3

TIME PERIOD: 2 DATE: 10-26-65 N=1117

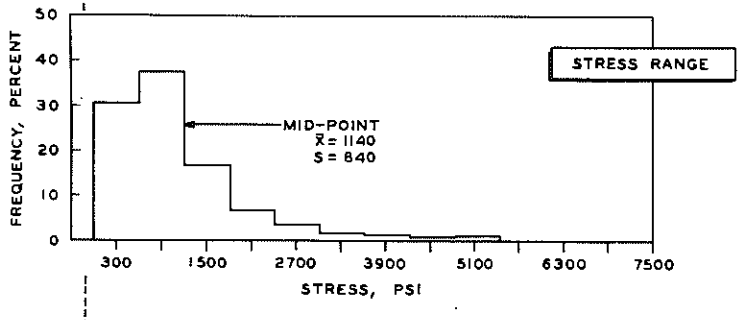

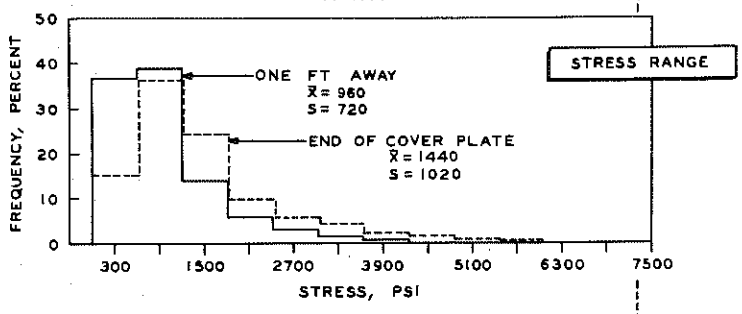

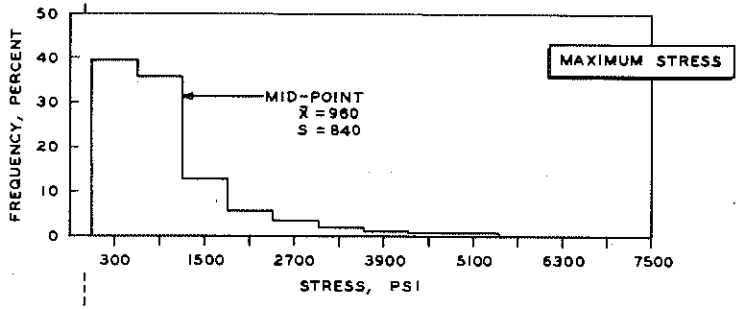

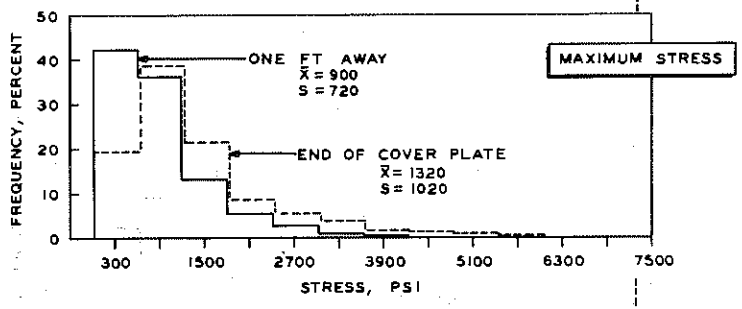

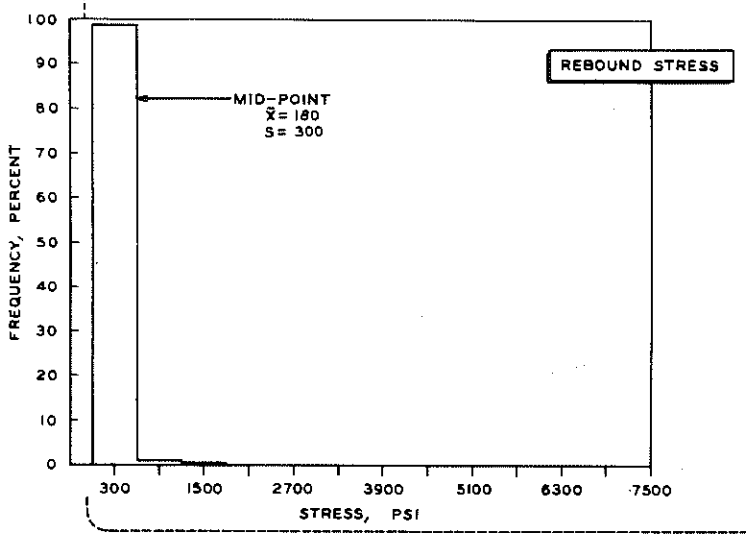

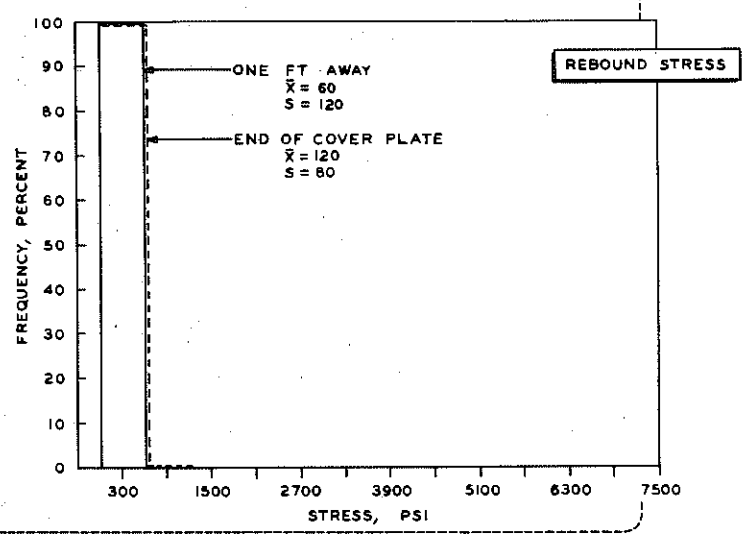

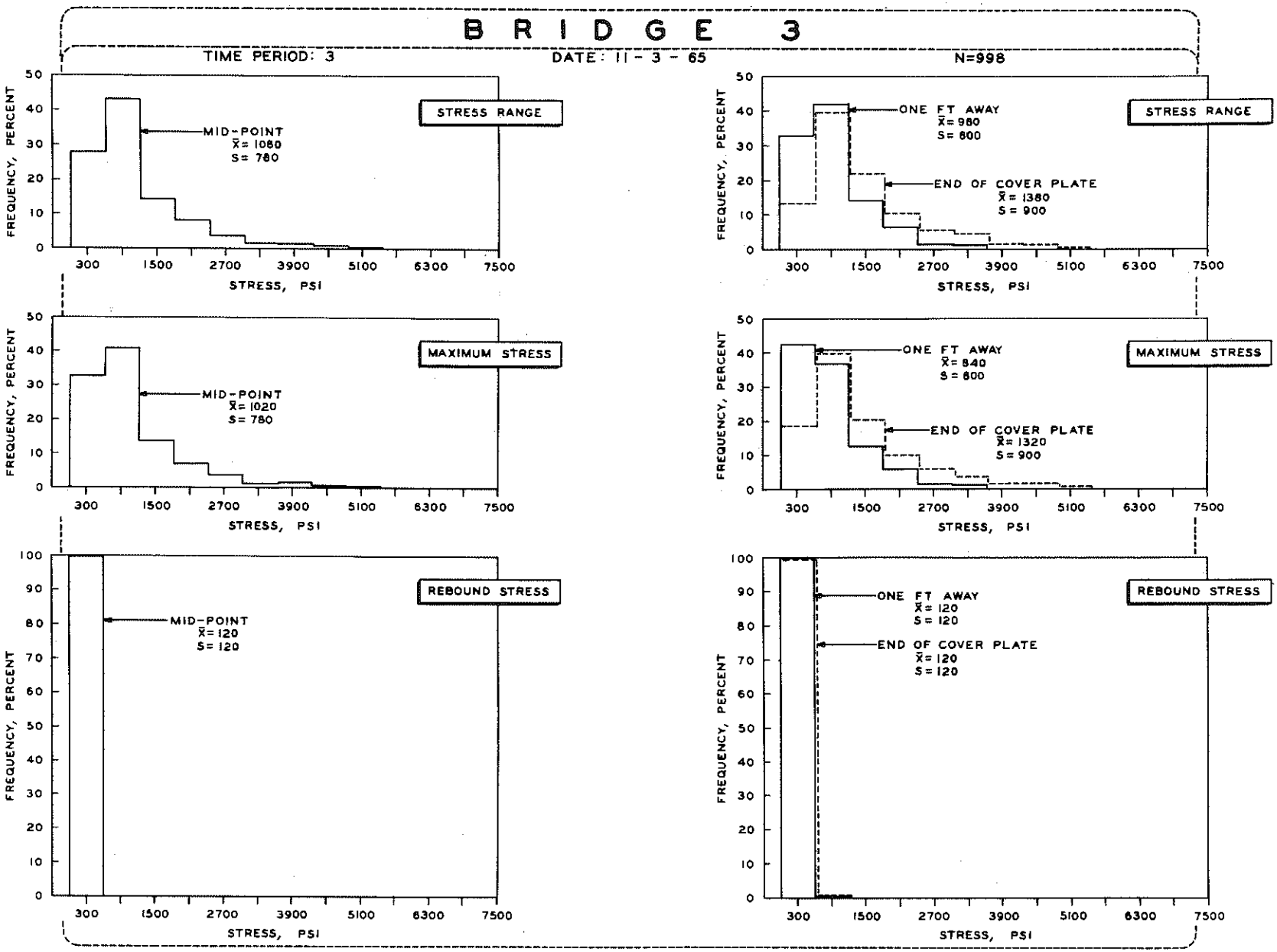
BRIDGE 3
TIME PERIOD: 3
DATE: 11 - 3 - 65
N=998
STRESS RANGE
MID-POINT
X̄ = 1080
S = 780
ONE FT AWAY
X̄ = 980
S = 800
END OF COVER PLATE
X̄ = 1380
S = 900
MAXIMUM STRESS
MID-POINT
X̄ = 1020
S = 780
ONE FT AWAY
X̄ = 840
S = 800
END OF COVER PLATE
X̄ = 1320
S = 900
REBOUND STRESS
MID-POINT
X̄ = 120
S = 120
ONE FT AWAY
X̄ = 120
S = 120
END OF COVER PLATE
X̄ = 120
S = 120
FREQUENCY, PERCENT
STRESS, PSI
300
1500
2700
3900
5100
6300
7500

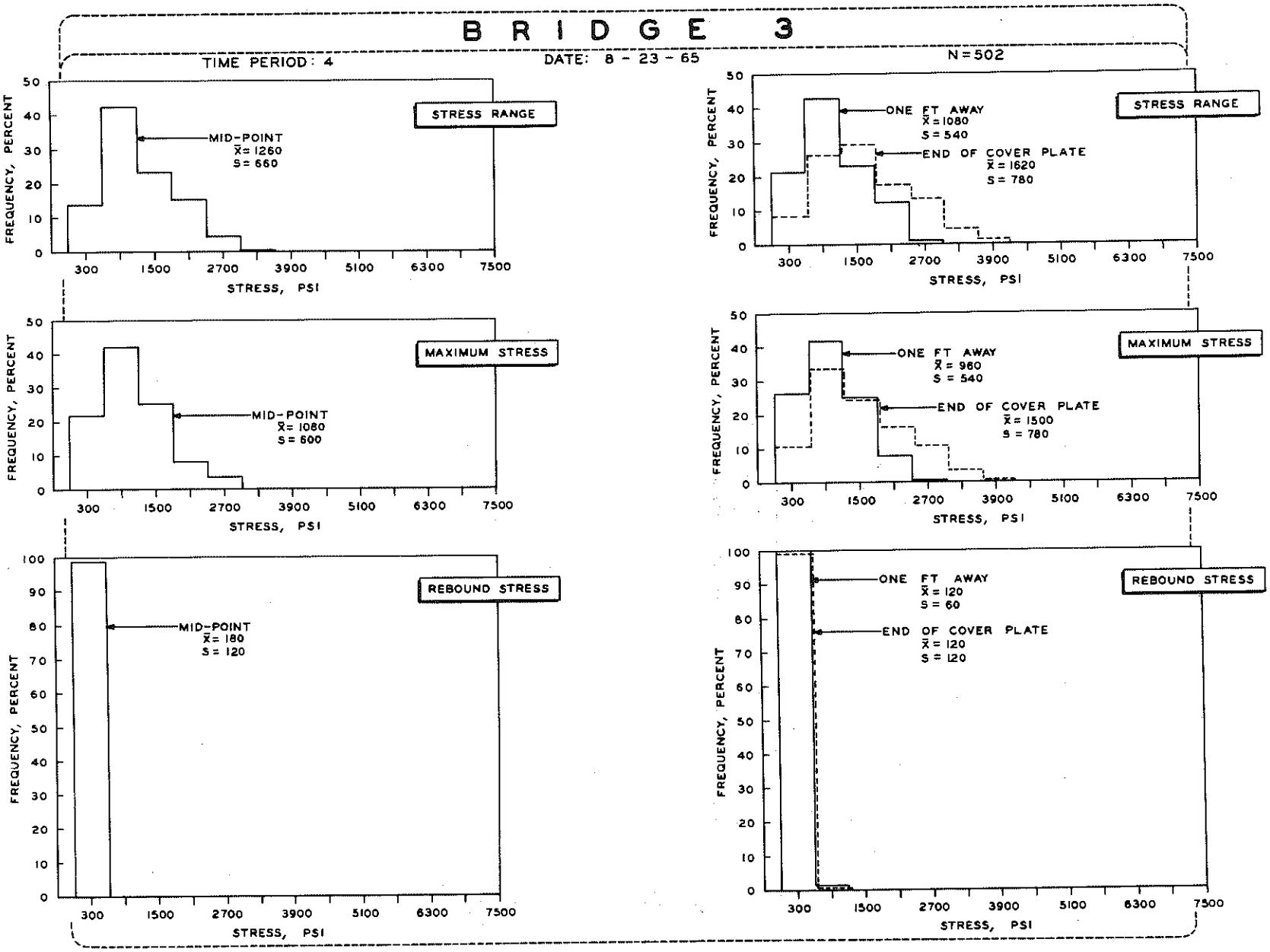
BRIDGE 3
TIME PERIOD: 4
DATE: 8 - 23 - 65
N=502
STRESS RANGE
MID-POINT
X̄= 1260
S= 660
ONE FT AWAY
X̄= 1080
S= 540
END OF COVER PLATE
X̄= 1620
S= 780
MAXIMUM STRESS
MID-POINT
X̄= 1080
S= 600
ONE FT AWAY
X̄= 960
S= 540
END OF COVER PLATE
X̄= 1500
S= 780
REBOUND STRESS
MID-POINT
X̄= 180
S= 120
ONE FT AWAY
X̄= 120
S= 60
END OF COVER PLATE
X̄= 120
S= 120
FREQUENCY, PERCENT
STRESS, PSI
300
1500
2700
3900
5100
6300
7500

BRIDGE 5

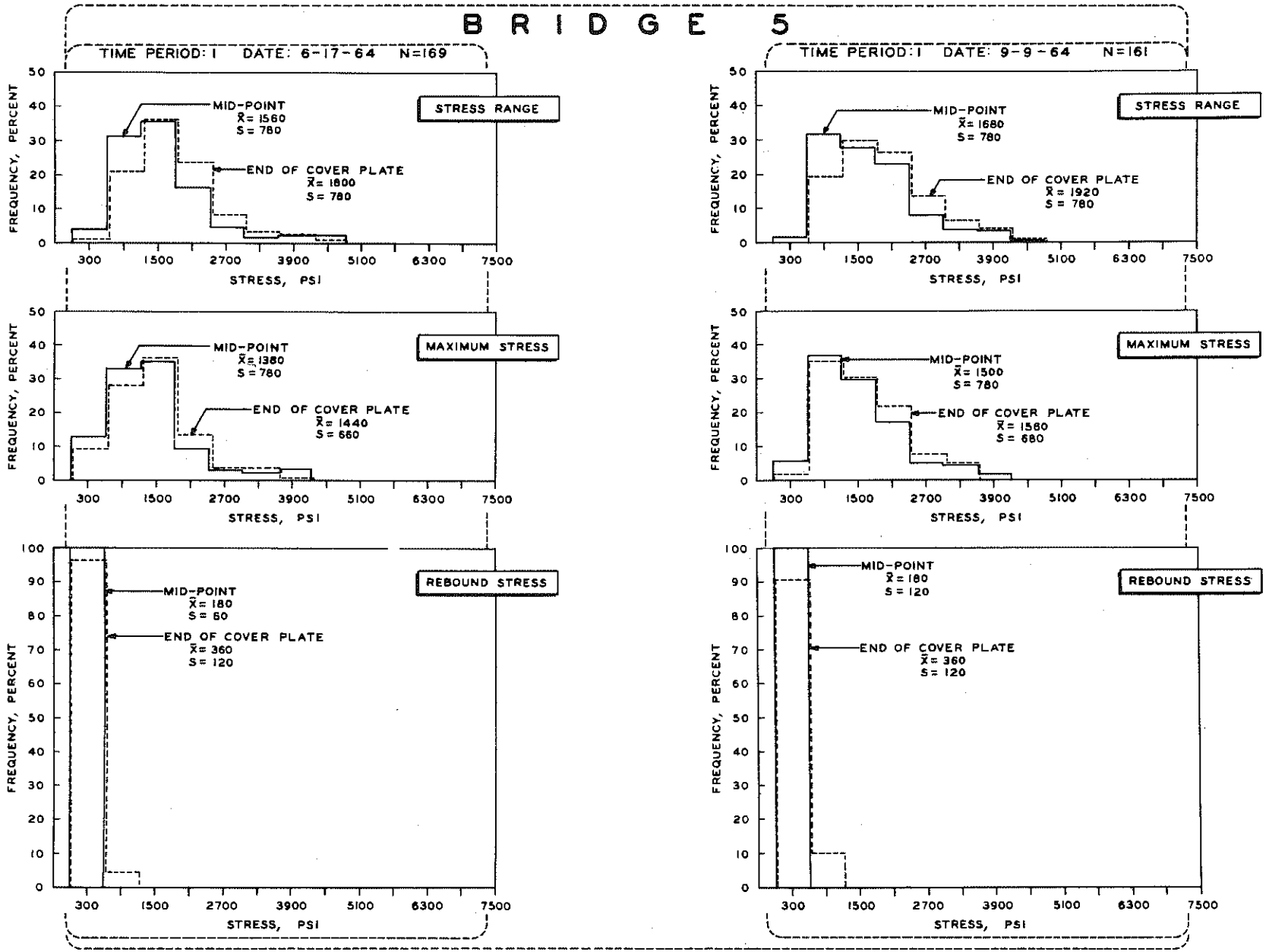
TIME PERIOD: 1 DATE: 6-17-64 N=169
STRESS RANGE
MID-POINT
X̄ = 1560
S = 780
END OF COVER PLATE
X̄ = 1800
S = 780
MAXIMUM STRESS
MID-POINT
X̄ = 1380
S = 780
END OF COVER PLATE
X̄ = 1440
S = 660
REBOUND STRESS
MID-POINT
X̄ = 180
S = 60
END OF COVER PLATE
X̄ = 360
S = 120
TIME PERIOD: 1 DATE: 9-9-64 N=161
STRESS RANGE
MID-POINT
X̄ = 1680
S = 780
END OF COVER PLATE
X̄ = 1920
S = 780
MAXIMUM STRESS
MID-POINT
X̄ = 1500
S = 780
END OF COVER PLATE
X̄ = 1560
S = 680
REBOUND STRESS
MID-POINT
X̄ = 180
S = 120
END OF COVER PLATE
X̄ = 360
S = 120
FREQUENCY, PERCENT
STRESS, PSI
300 1500 2700 3900 5100 6300 7500

BRIDGE 5

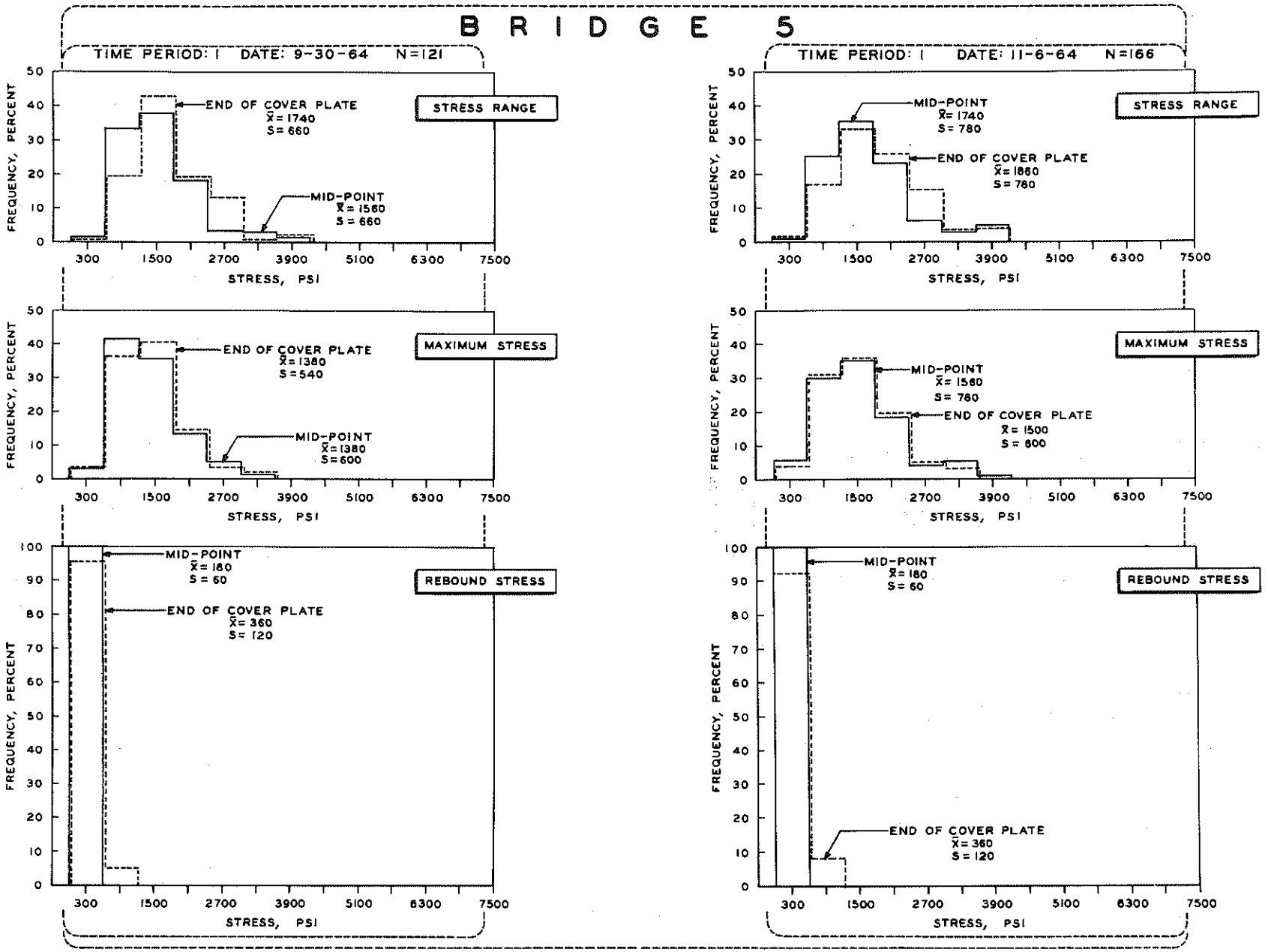
TIME PERIOD: 1 DATE: 9-30-64 N=121
STRESS RANGE
END OF COVER PLATE
X̄ = 1740
S = 660
MID-POINT
X̄ = 1560
S = 660
MAXIMUM STRESS
END OF COVER PLATE
X̄ = 1380
S = 540
MID-POINT
X̄ = 1380
S = 600
REBOUND STRESS
MID-POINT
X̄ = 180
S = 60
END OF COVER PLATE
X̄ = 360
S = 120
TIME PERIOD: 1 DATE: 11-6-64 N=166
STRESS RANGE
MID-POINT
X̄ = 1740
S = 780
END OF COVER PLATE
X̄ = 1860
S = 780
MAXIMUM STRESS
MID-POINT
X̄ = 1560
S = 780
END OF COVER PLATE
X̄ = 1500
S = 600
REBOUND STRESS
MID-POINT
X̄ = 180
S = 60
END OF COVER PLATE
X̄ = 360
S = 120
FREQUENCY, PERCENT
STRESS, PSI
300 1500 2700 3900 5100 6300 7500

BRIDGE 5

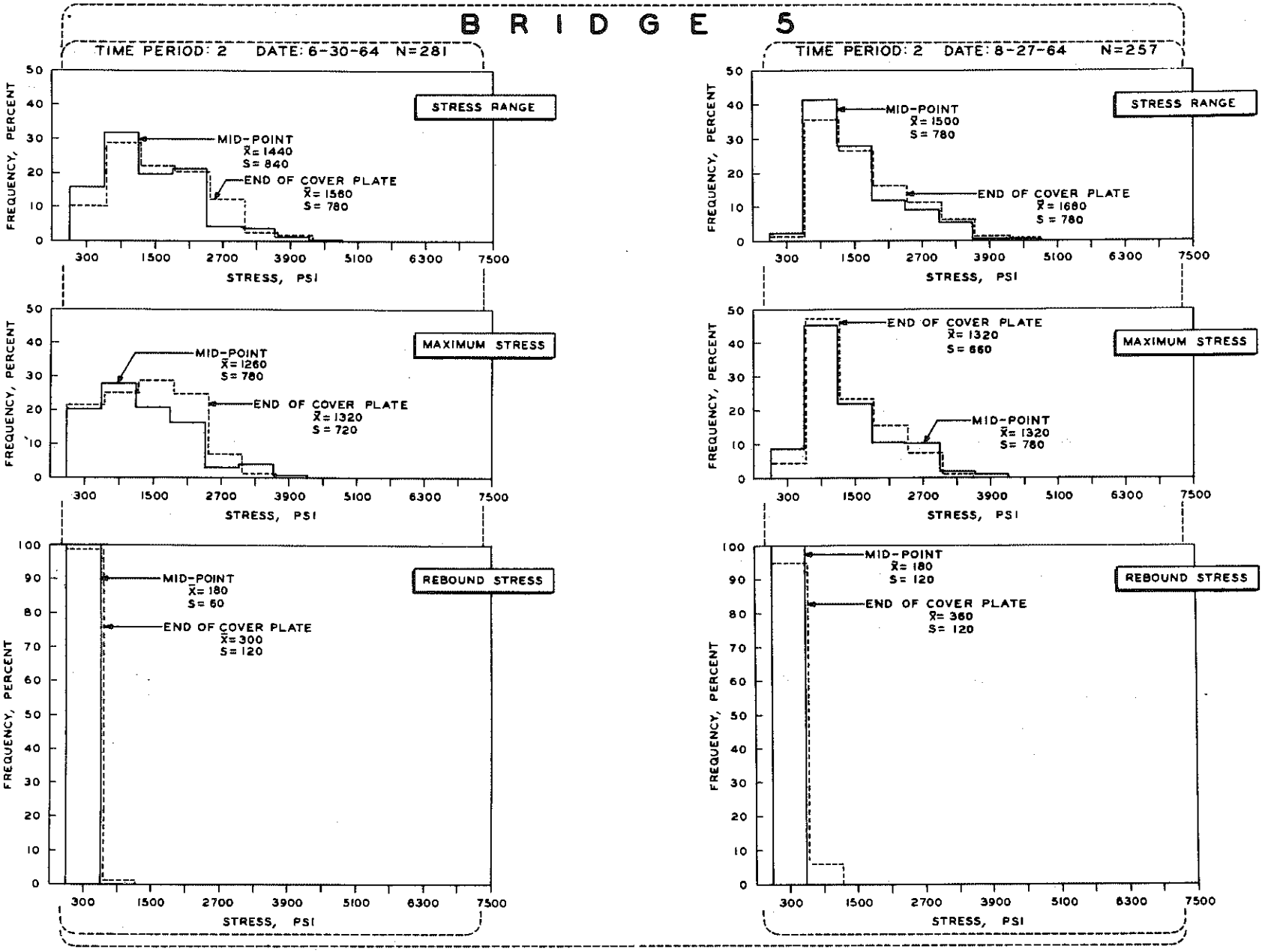
TIME PERIOD: 2 DATE: 6-30-64 N=281
STRESS RANGE
MID-POINT
X̄= 1440
S= 840
END OF COVER PLATE
X̄= 1580
S= 780
MAXIMUM STRESS
MID-POINT
X̄= 1260
S= 780
END OF COVER PLATE
X̄= 1320
S= 720
REBOUND STRESS
MID-POINT
X̄= 180
S= 60
END OF COVER PLATE
X̄= 300
S= 120
TIME PERIOD: 2 DATE: 8-27-64 N=257
STRESS RANGE
MID-POINT
X̄= 1500
S= 780
END OF COVER PLATE
X̄= 1680
S= 780
MAXIMUM STRESS
END OF COVER PLATE
X̄= 1320
S= 660
MID-POINT
X̄= 1320
S= 780
REBOUND STRESS
MID-POINT
X̄= 180
S= 120
END OF COVER PLATE
X̄= 360
S= 120
FREQUENCY, PERCENT
STRESS, PSI
300 1500 2700 3900 5100 6300 7500

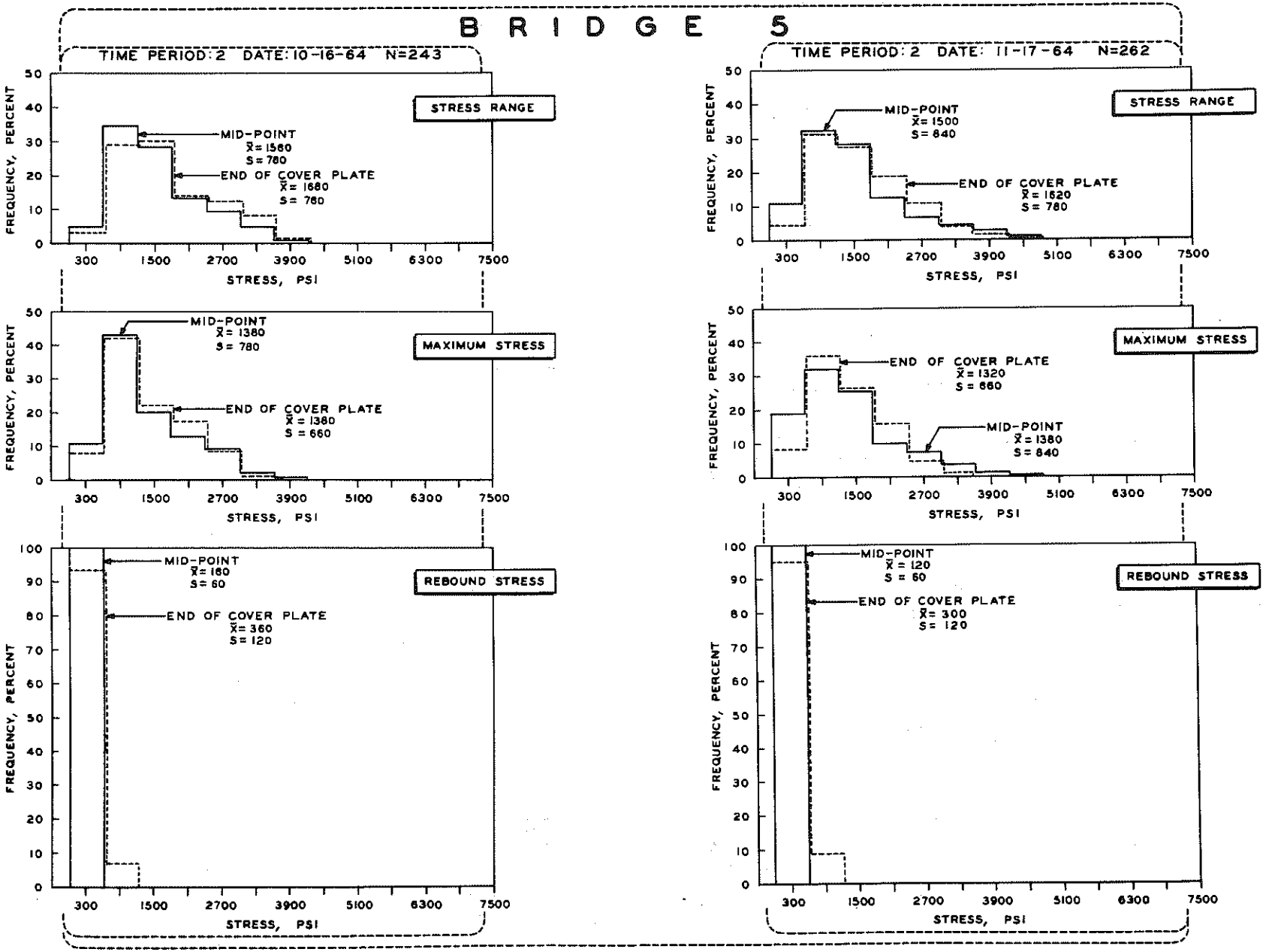
BRIDGE 5
TIME PERIOD: 2 DATE: 10-16-64 N=243
TIME PERIOD: 2 DATE: 11-17-64 N=262
STRESS RANGE
MID-POINT
X̄= 1560
S= 780
END OF COVER PLATE
X̄= 1680
S= 760
STRESS RANGE
MID-POINT
X̄= 1500
S= 840
END OF COVER PLATE
X̄= 1620
S= 780
MAXIMUM STRESS
MID-POINT
X̄= 1380
S= 780
END OF COVER PLATE
X̄= 1380
S= 660
MAXIMUM STRESS
END OF COVER PLATE
X̄= 1320
S= 660
MID-POINT
X̄= 1380
S= 840
REBOUND STRESS
MID-POINT
X̄= 160
S= 60
END OF COVER PLATE
X̄= 360
S= 120
REBOUND STRESS
MID-POINT
X̄= 120
S= 60
END OF COVER PLATE
X̄= 300
S= 120
FREQUENCY, PERCENT
STRESS, PSI
300
1500
2700
3900
5100
6300
7500

BRIDGE 5

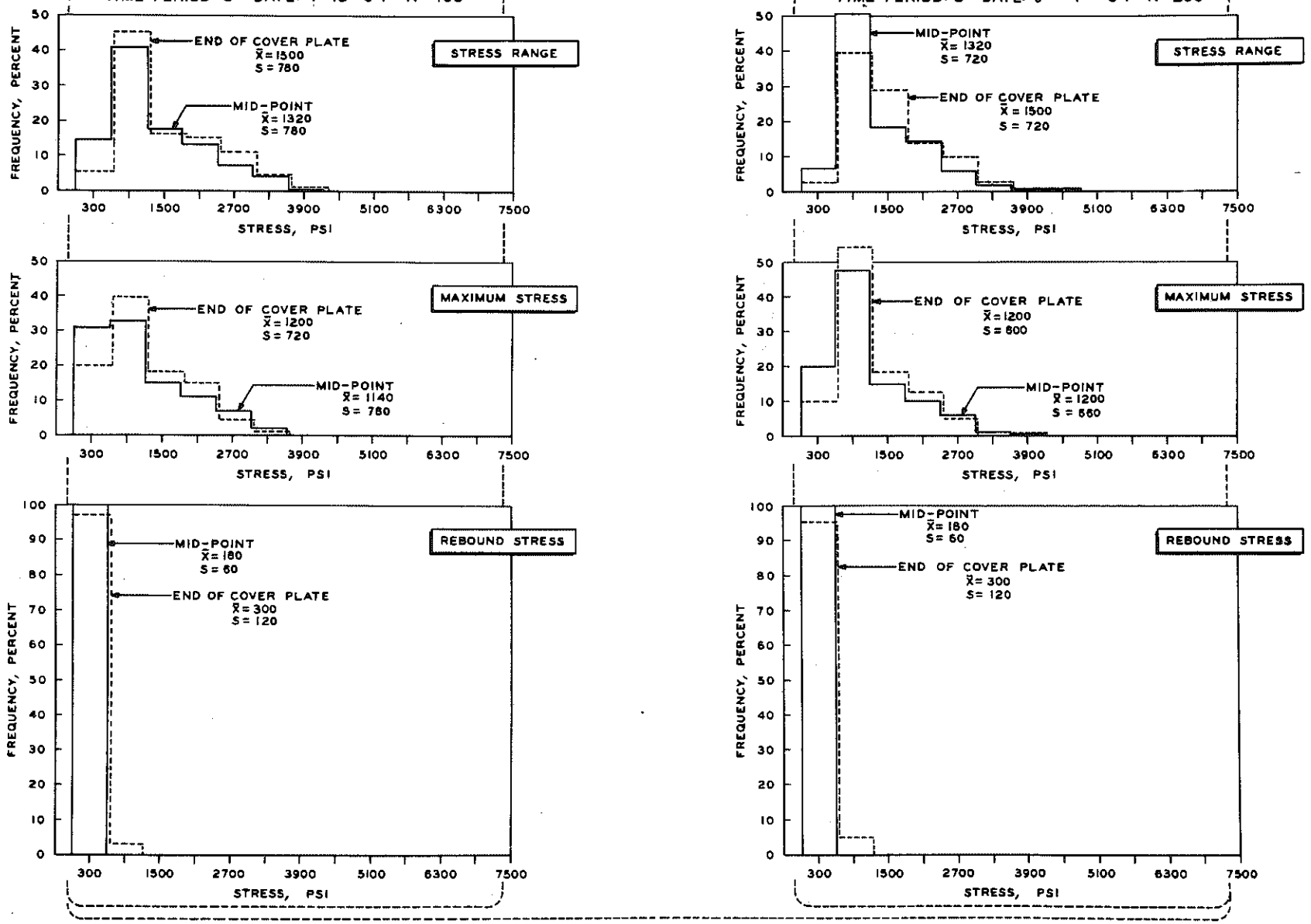
TIME PERIOD: 3 DATE: 7-13-64 N=168
STRESS RANGE
END OF COVER PLATE
X̄=1500
S=780
MID-POINT
X̄=1320
S=780
MAXIMUM STRESS
END OF COVER PLATE
X̄=1200
S=720
MID-POINT
X̄=1140
S=780
REBOUND STRESS
MID-POINT
X̄=180
S=60
END OF COVER PLATE
X̄=300
S=120
TIME PERIOD: 3 DATE: 9-1-64 N=206
STRESS RANGE
MID-POINT
X̄=1320
S=720
END OF COVER PLATE
X̄=1500
S=720
MAXIMUM STRESS
END OF COVER PLATE
X̄=1200
S=800
MID-POINT
X̄=1200
S=660
REBOUND STRESS
MID-POINT
X̄=180
S=60
END OF COVER PLATE
X̄=300
S=120
FREQUENCY, PERCENT
STRESS, PSI
300
1500
2700
3900
5100
6300
7500

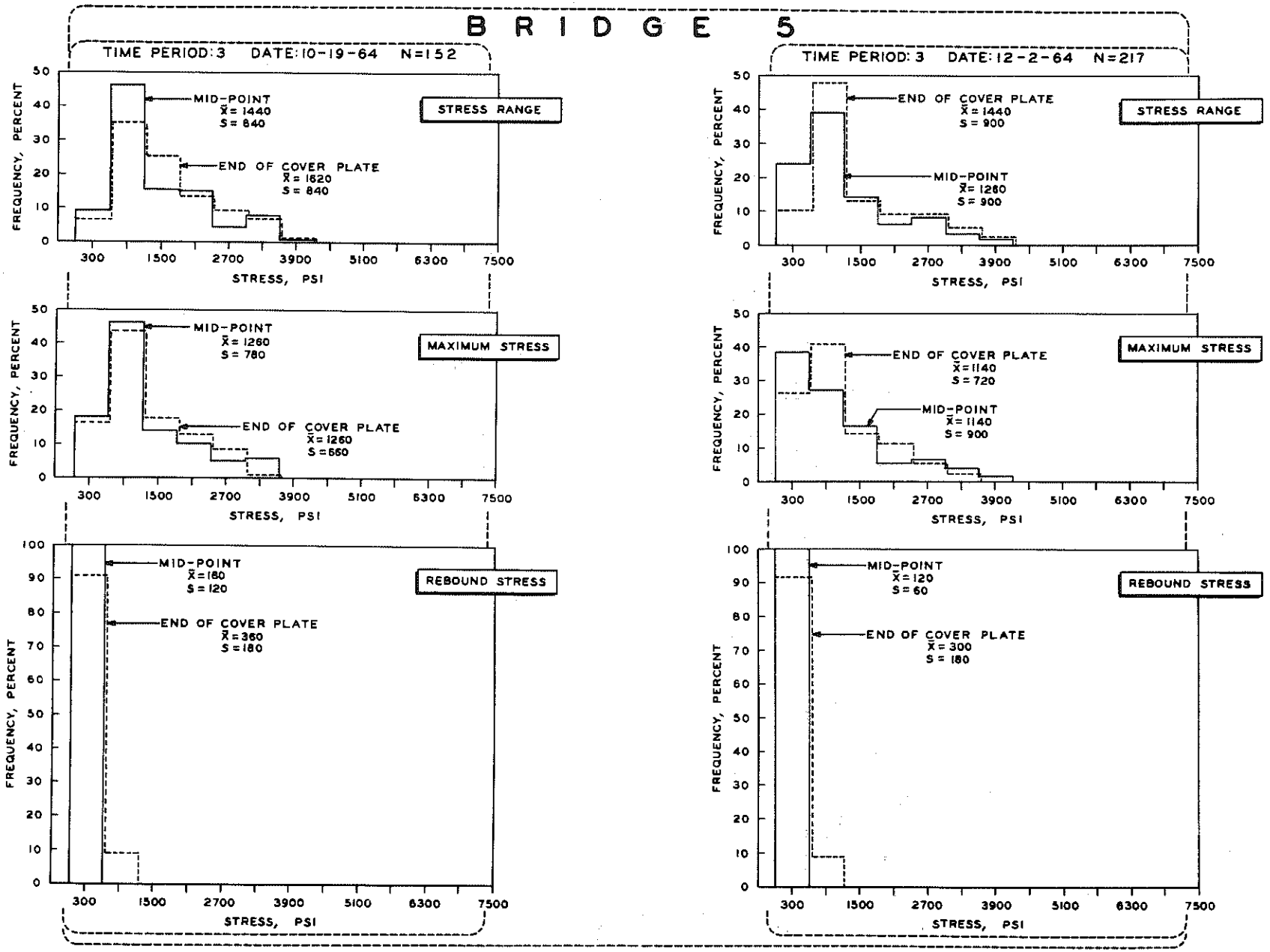
BRIDGE 5
TIME PERIOD: 3 DATE: 10-19-64 N=152
TIME PERIOD: 3 DATE: 12-2-64 N=217
STRESS RANGE
MID-POINT
X̄ = 1440
S = 840
END OF COVER PLATE
X̄ = 1620
S = 840
STRESS RANGE
END OF COVER PLATE
X̄ = 1440
S = 900
MID-POINT
X̄ = 1260
S = 900
MAXIMUM STRESS
MID-POINT
X̄ = 1260
S = 780
END OF COVER PLATE
X̄ = 1260
S = 660
MAXIMUM STRESS
END OF COVER PLATE
X̄ = 1140
S = 720
MID-POINT
X̄ = 1140
S = 900
REBOUND STRESS
MID-POINT
X̄ = 180
S = 120
END OF COVER PLATE
X̄ = 360
S = 180
REBOUND STRESS
MID-POINT
X̄ = 120
S = 60
END OF COVER PLATE
X̄ = 300
S = 180
FREQUENCY, PERCENT
STRESS, PSI
300
1500
2700
3900
5100
6300
7500

BRIDGE 5

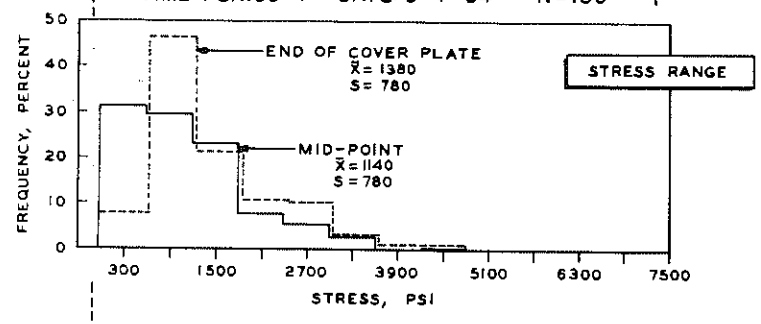
TIME PERIOD: 4 DATE: 6-4-64 N=156
STRESS RANGE
END OF COVER PLATE
X̄ = 1380
S = 780
MID-POINT
X̄ = 1140
S = 780
FREQUENCY, PERCENT
STRESS, PSI
0
10
20
30
40
50
300
1500
2700
3900
5100
6300
7500

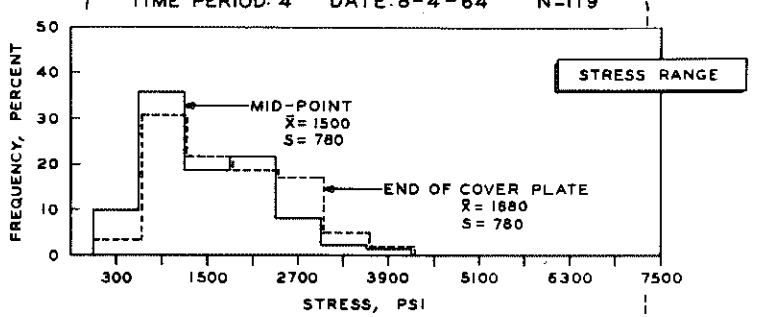
TIME PERIOD: 4 DATE: 8-4-64 N=119
STRESS RANGE
MID-POINT
X̄ = 1500
S = 780
END OF COVER PLATE
X̄ = 1680
S = 780
FREQUENCY, PERCENT
STRESS, PSI
0
10
20
30
40
50
300
1500
2700
3900
5100
6300
7500

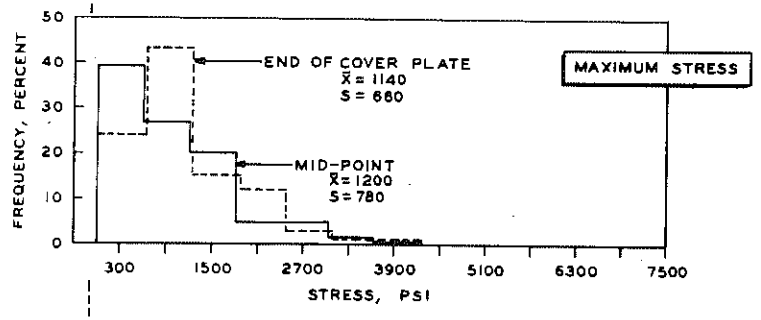
MAXIMUM STRESS
END OF COVER PLATE
X̄ = 1140
S = 660
MID-POINT
X̄ = 1200
S = 780
FREQUENCY, PERCENT
STRESS, PSI
0
10
20
30
40
50
300
1500
2700
3900
5100
6300
7500

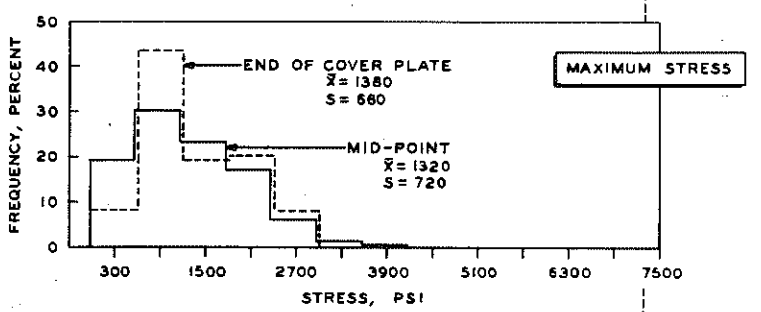
MAXIMUM STRESS
END OF COVER PLATE
X̄ = 1380
S = 660
MID-POINT
X̄ = 1320
S = 720
FREQUENCY, PERCENT
STRESS, PSI
0
10
20
30
40
50
300
1500
2700
3900
5100
6300
7500

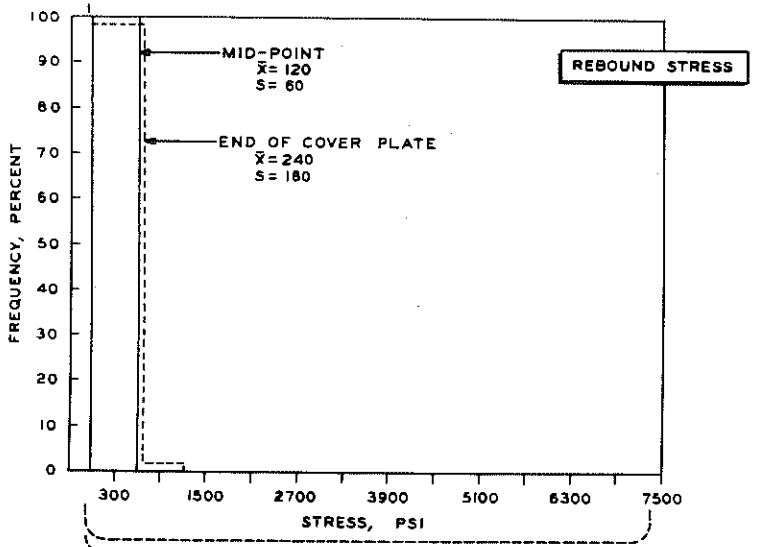
REBOUND STRESS
MID-POINT
X̄ = 120
S = 60
END OF COVER PLATE
X̄ = 240
S = 180
FREQUENCY, PERCENT
STRESS, PSI
0
10
20
30
40
50
60
70
80
90
100
300
1500
2700
3900
5100
6300
7500

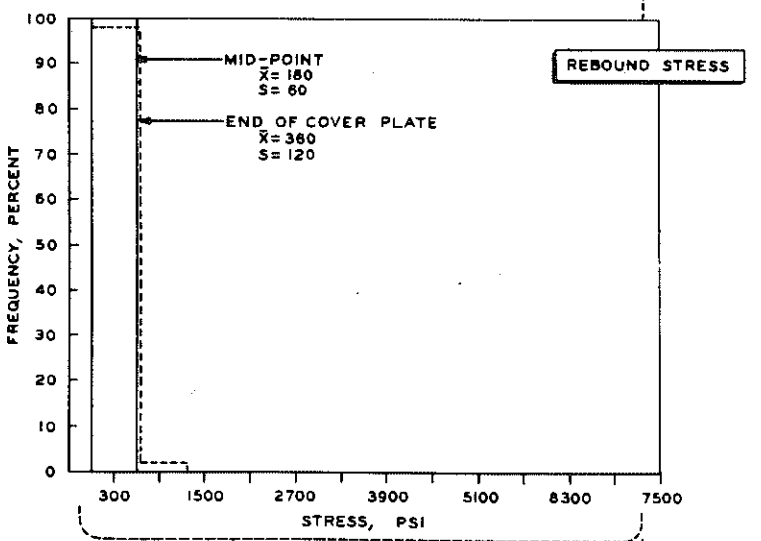
REBOUND STRESS
MID-POINT
X̄ = 180
S = 60
END OF COVER PLATE
X̄ = 360
S = 120
FREQUENCY, PERCENT
STRESS, PSI
0
10
20
30
40
50
60
70
80
90
100
300
1500
2700
3900
5100
8300
7500

BRIDGE 5

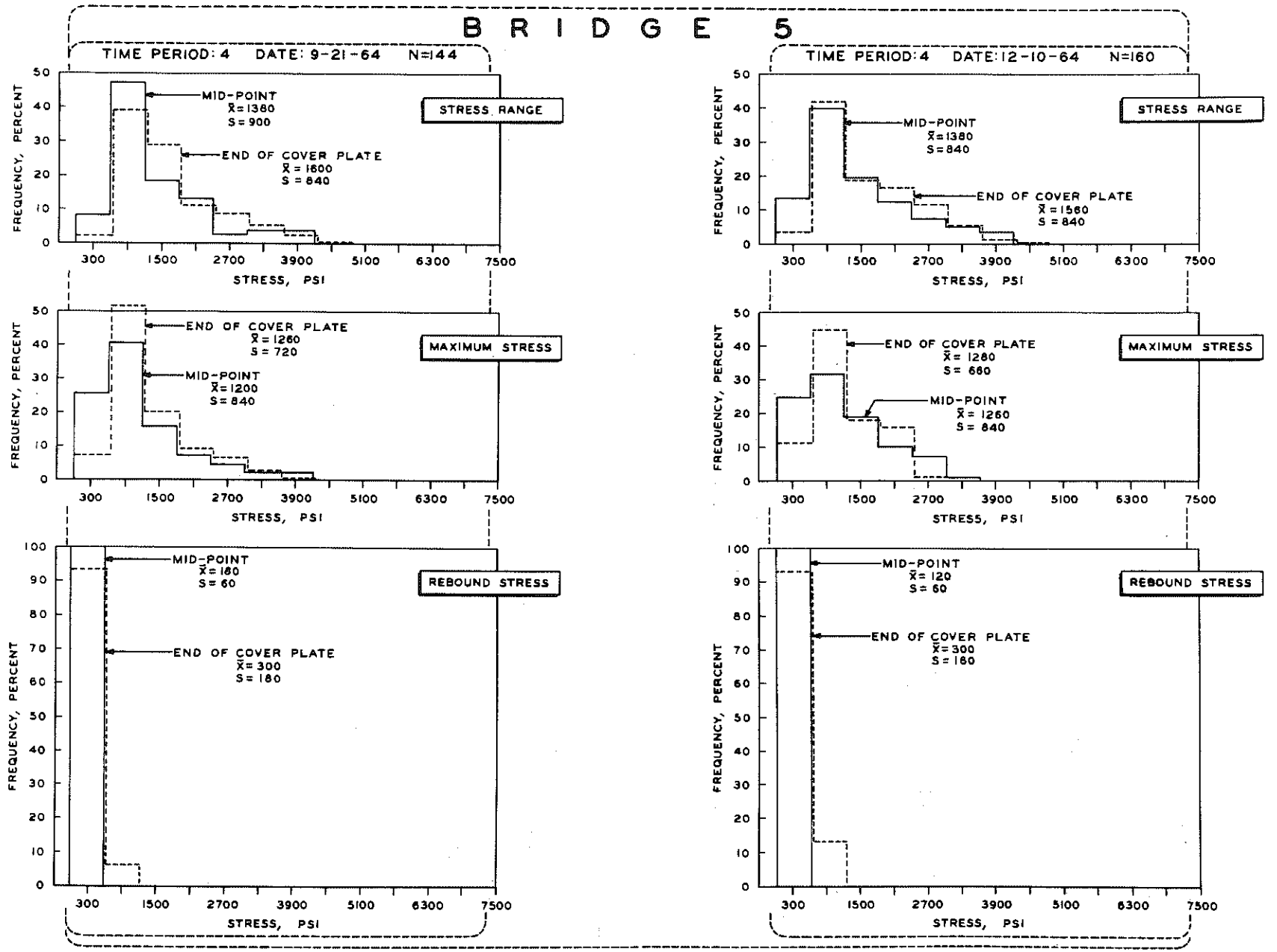
TIME PERIOD: 4 DATE: 9-21-64 N=144
STRESS RANGE
MID-POINT
X̄=1380
S=900
END OF COVER PLATE
X̄=1600
S=840
MAXIMUM STRESS
END OF COVER PLATE
X̄=1260
S=720
MID-POINT
X̄=1200
S=840
REBOUND STRESS
MID-POINT
X̄=180
S=60
END OF COVER PLATE
X̄=300
S=180
TIME PERIOD: 4 DATE: 12-10-64 N=160
STRESS RANGE
MID-POINT
X̄=1380
S=840
END OF COVER PLATE
X̄=1560
S=840
MAXIMUM STRESS
END OF COVER PLATE
X̄=1280
S=660
MID-POINT
X̄=1260
S=840
REBOUND STRESS
MID-POINT
X̄=120
S=60
END OF COVER PLATE
X̄=300
S=180
FREQUENCY, PERCENT
STRESS, PSI
300
1500
2700
3900
5100
6300
7500

BRIDGE 6

TIME PERIOD: 1 DATE: 7 - 13 - 65 N=432

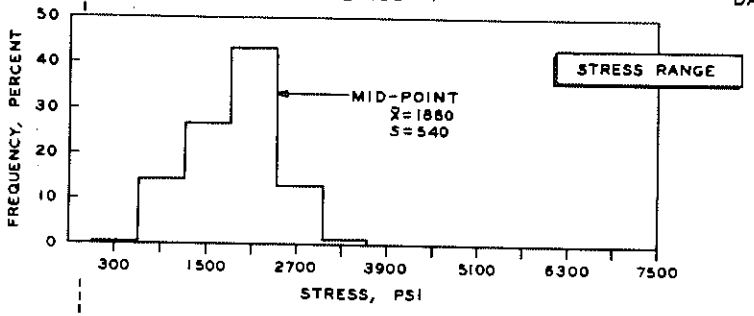

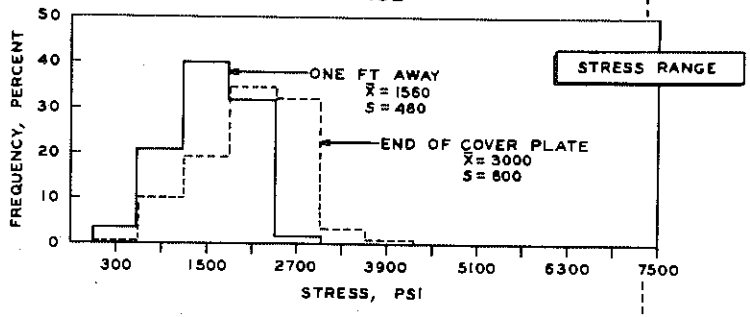

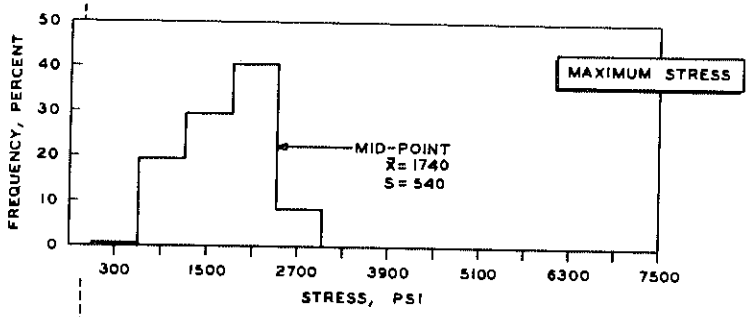

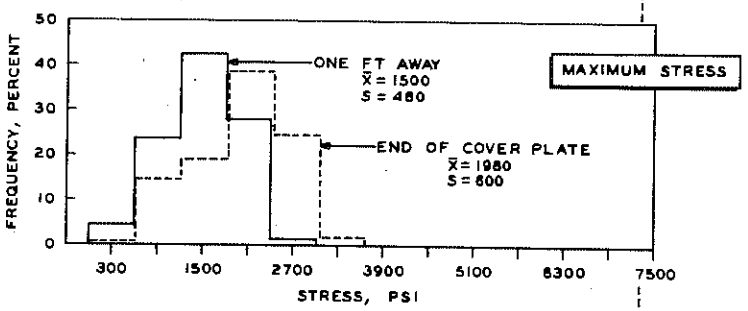

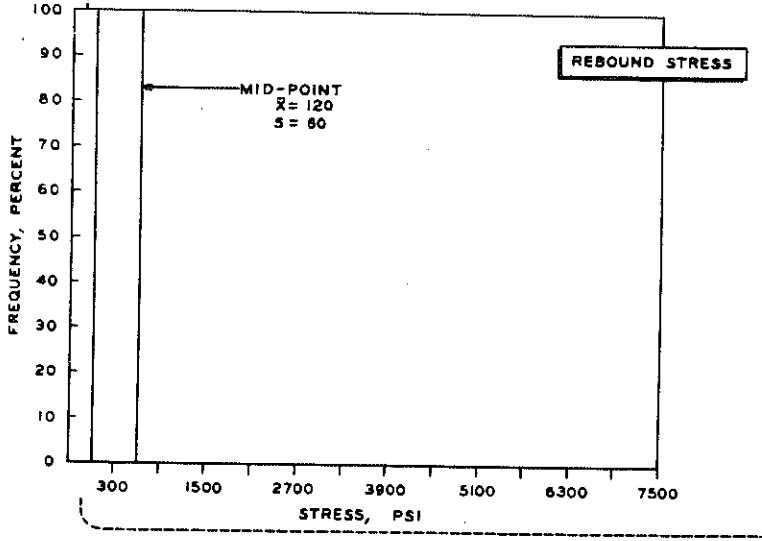

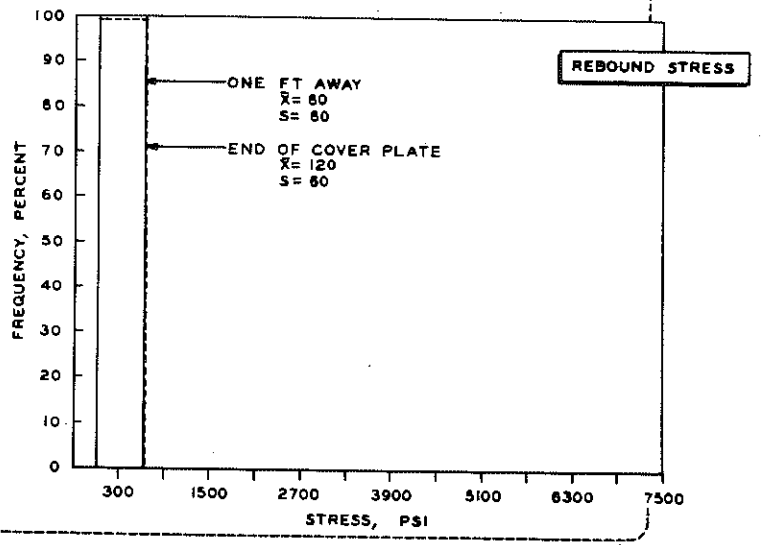

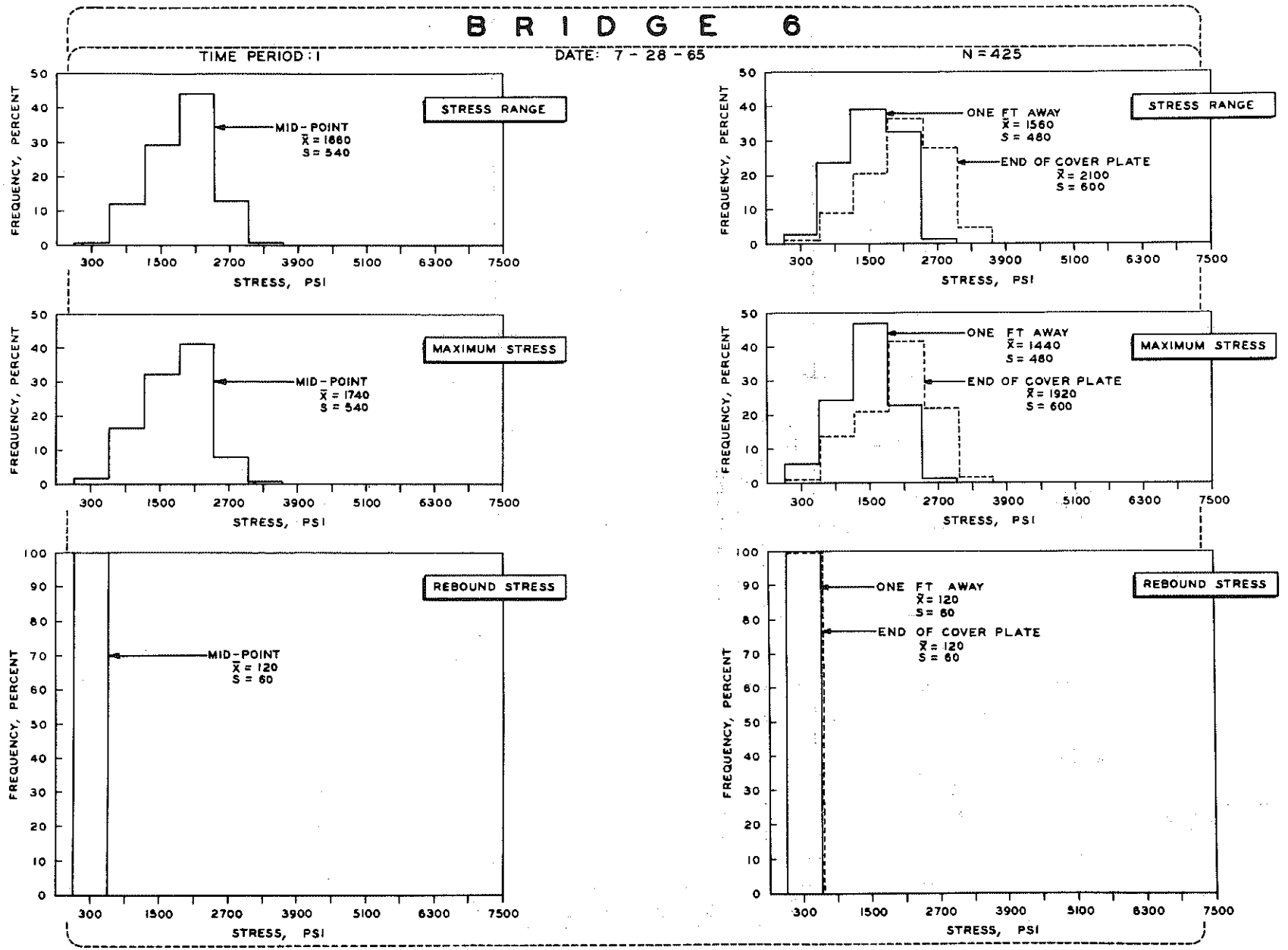
BRIDGE 6
TIME PERIOD: I
DATE: 7 - 28 - 65
N = 425
STRESS RANGE
MID-POINT
X̄ = 1860
S = 540
ONE FT AWAY
X̄ = 1560
S = 480
END OF COVER PLATE
X̄ = 2100
S = 600
MAXIMUM STRESS
MID-POINT
X̄ = 1740
S = 540
ONE FT AWAY
X̄ = 1440
S = 480
END OF COVER PLATE
X̄ = 1920
S = 600
REBOUND STRESS
MID-POINT
X̄ = 120
S = 60
ONE FT AWAY
X̄ = 120
S = 60
END OF COVER PLATE
X̄ = 120
S = 60
FREQUENCY, PERCENT
STRESS, PSI
300
1500
2700
3900
5100
6300
7500

BRIDGE 6

TIME PERIOD: 2 DATE: 7-7-65 N=462

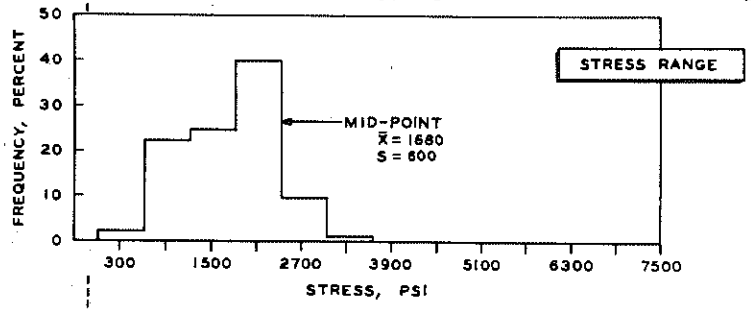

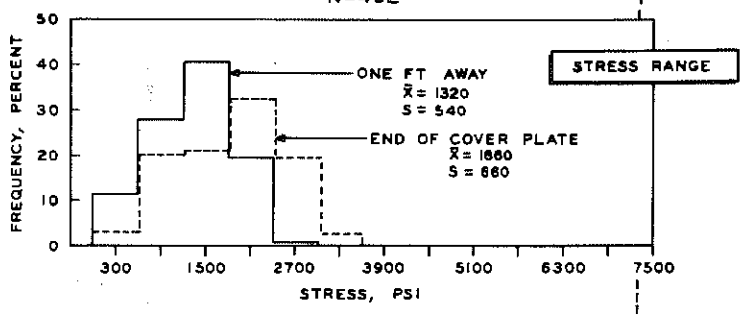

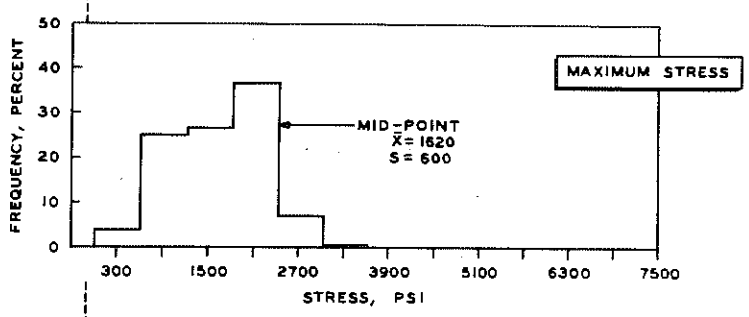

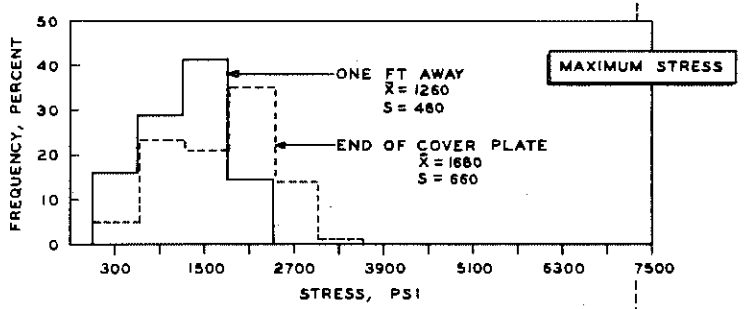

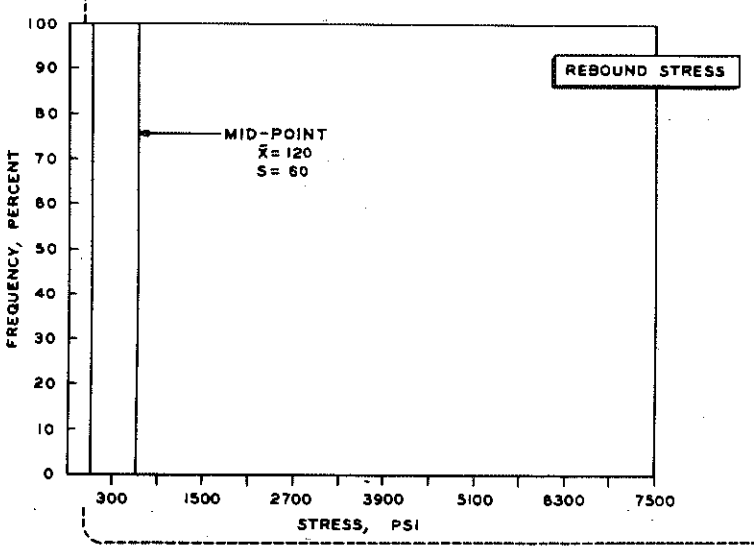

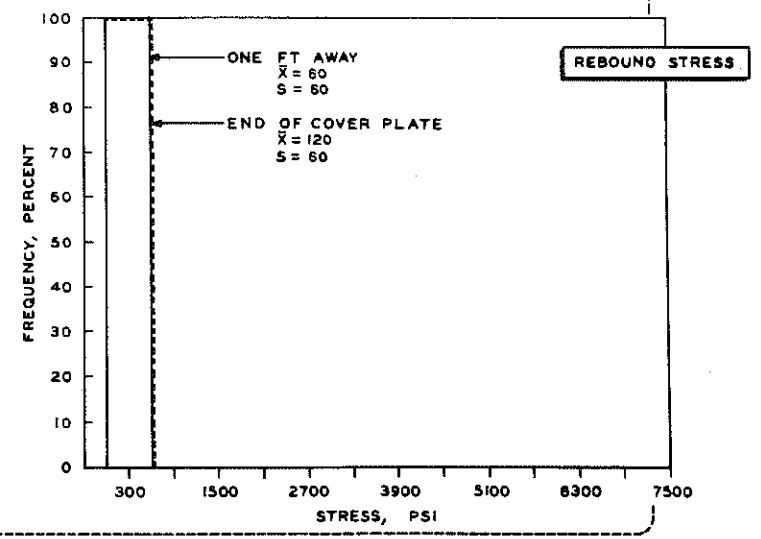

BRIDGE 6

TIME PERIOD: 2 DATE: 8 - 5 - 65 N = 417

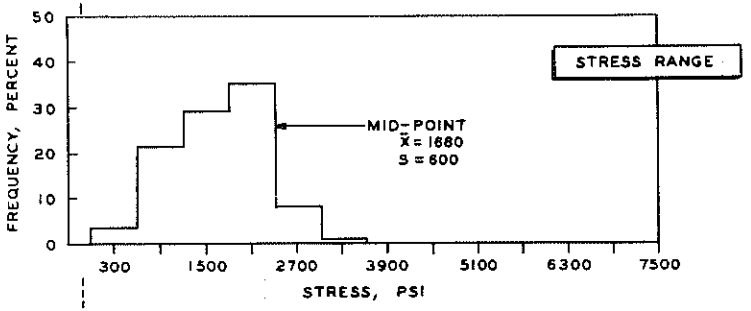

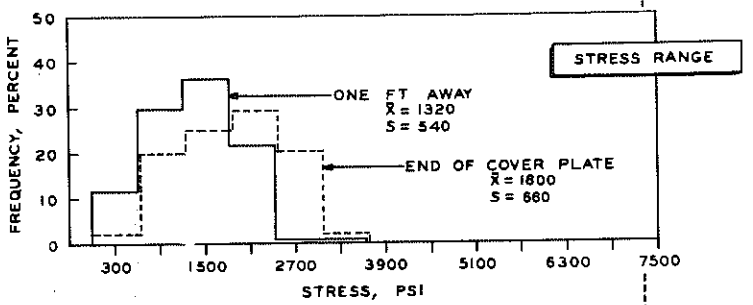

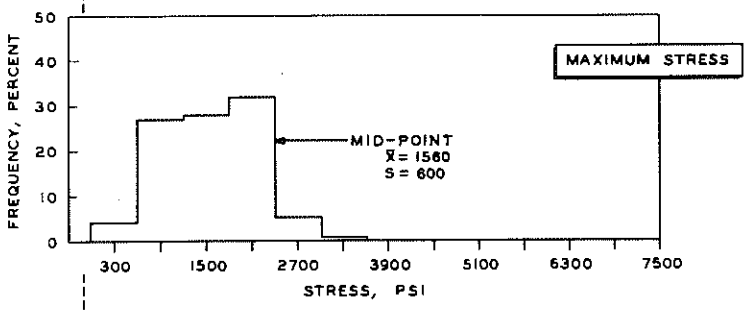

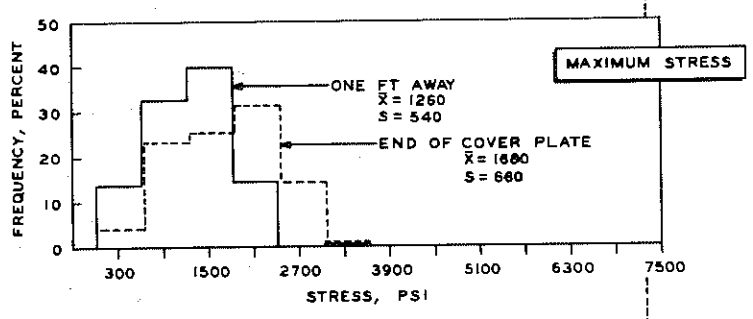

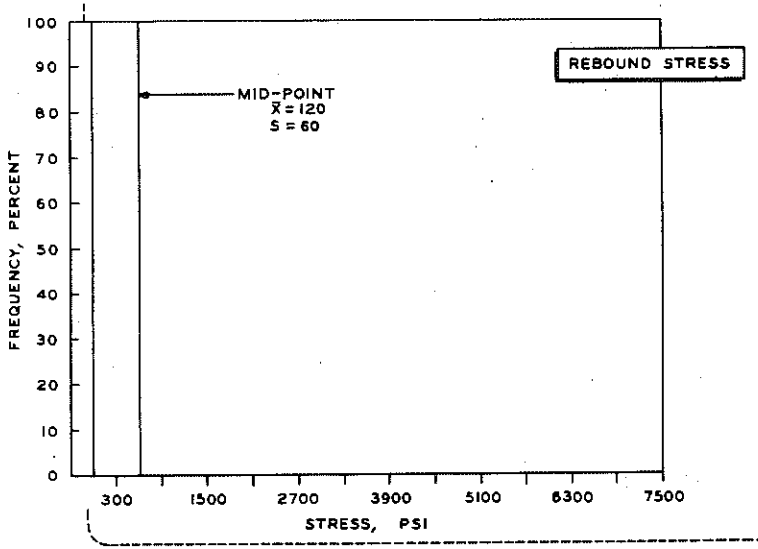

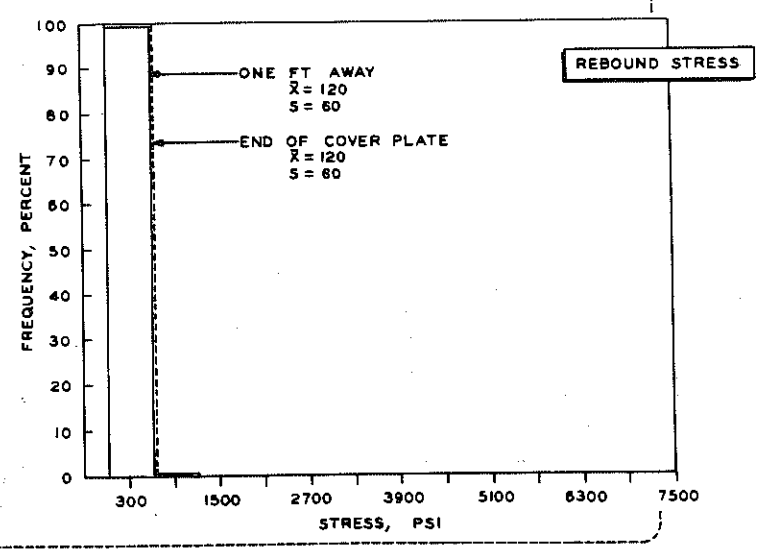

BRIDGE 6

TIME PERIOD : 3 DATE: 7 - 1 - 65 N = 325

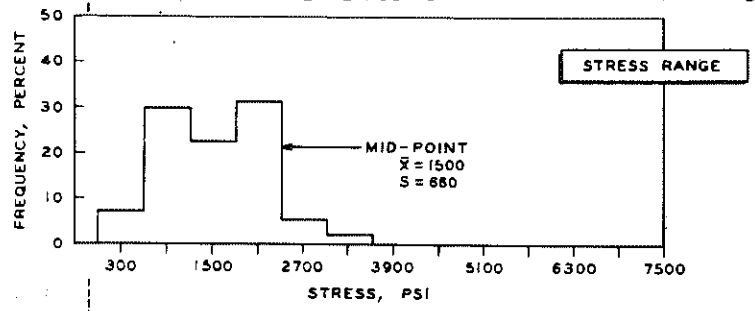

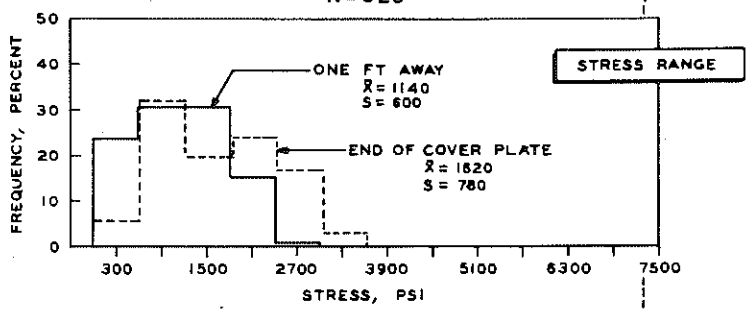

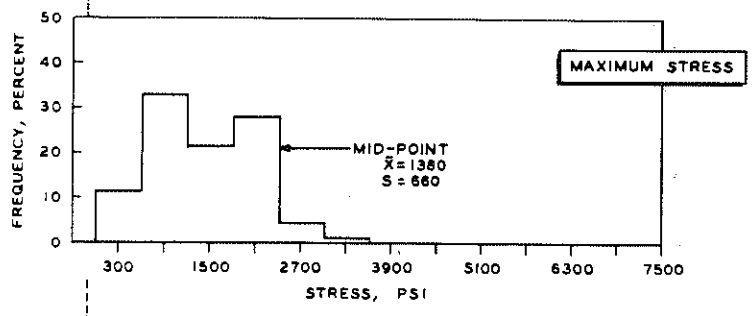

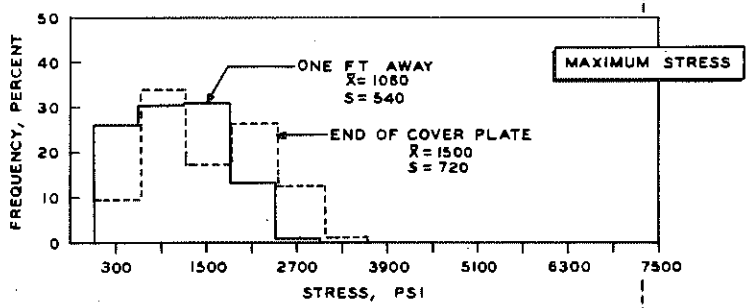

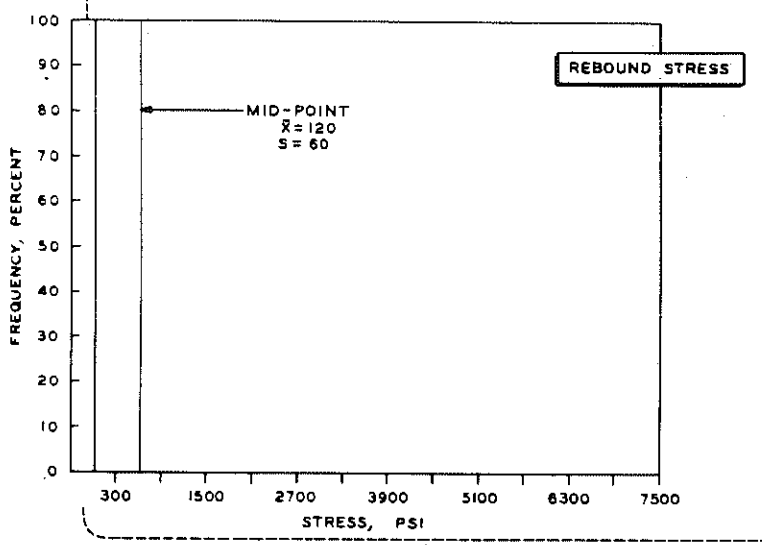

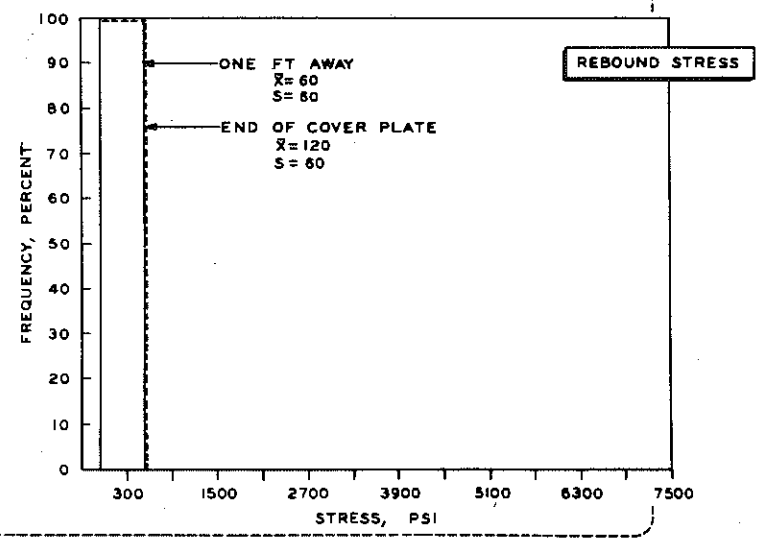

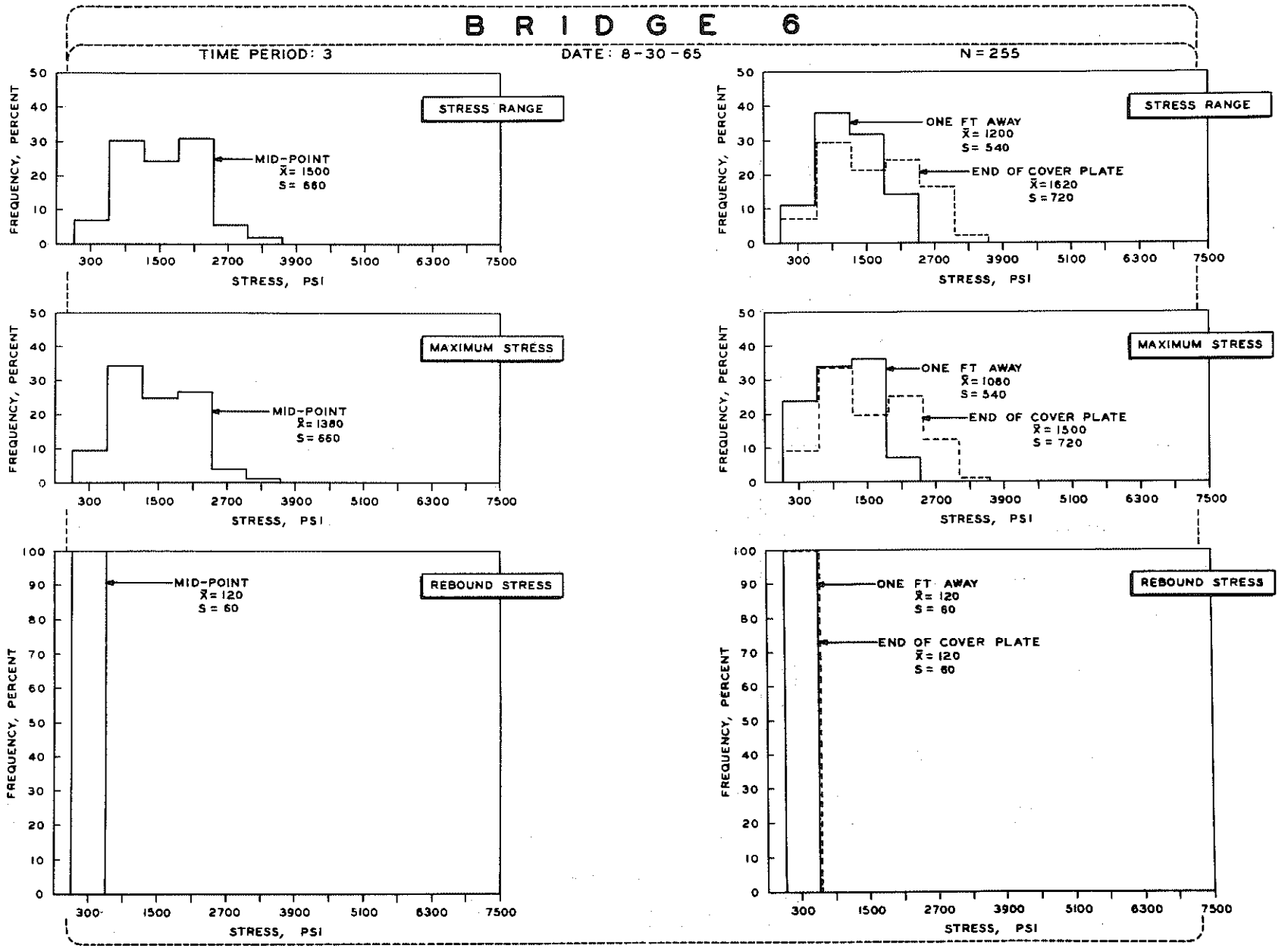
BRIDGE 6
TIME PERIOD: 3
DATE: 8-30-65
N = 255
STRESS RANGE
MID-POINT
X̄ = 1500
S = 660
ONE FT AWAY
X̄ = 1200
S = 540
END OF COVER PLATE
X̄ = 1620
S = 720
MAXIMUM STRESS
MID-POINT
X̄ = 1380
S = 660
ONE FT AWAY
X̄ = 1080
S = 540
END OF COVER PLATE
X̄ = 1500
S = 720
REBOUND STRESS
MID-POINT
X̄ = 120
S = 60
ONE FT AWAY
X̄ = 120
S = 60
END OF COVER PLATE
X̄ = 120
S = 60
FREQUENCY, PERCENT
STRESS, PSI
300
1500
2700
3900
5100
6300
7500

BRIDGE 6

TIME PERIOD: 4 DATE: 6-22-65 N = 284

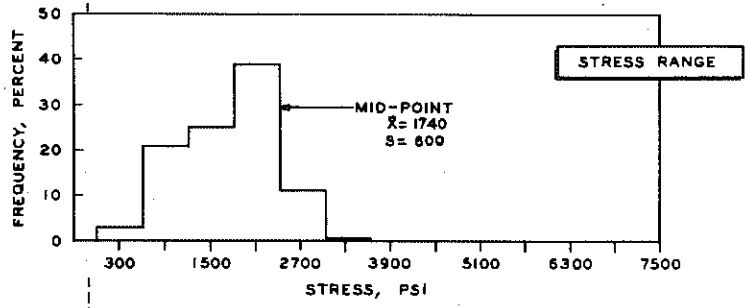

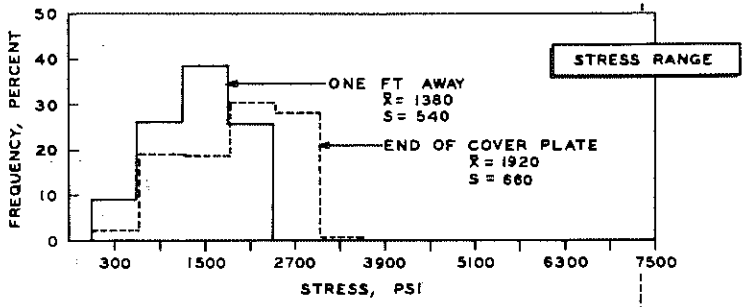

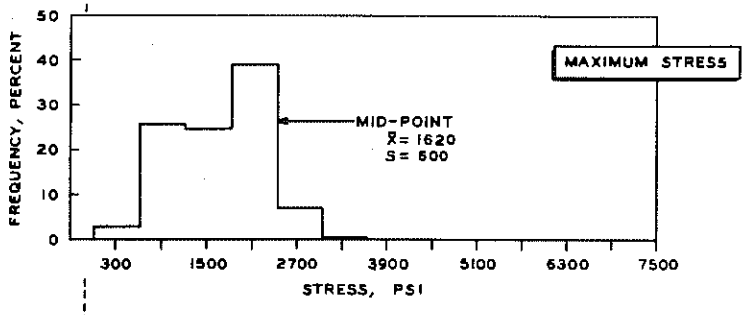

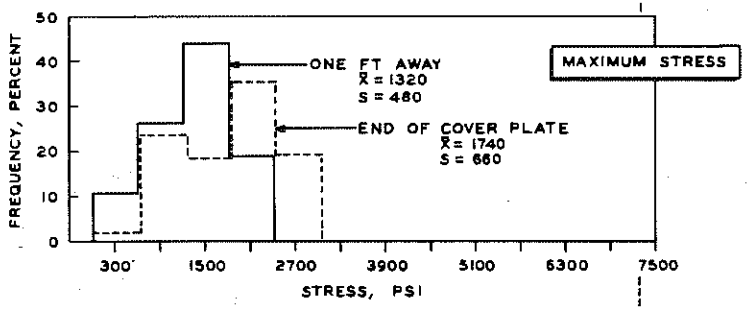

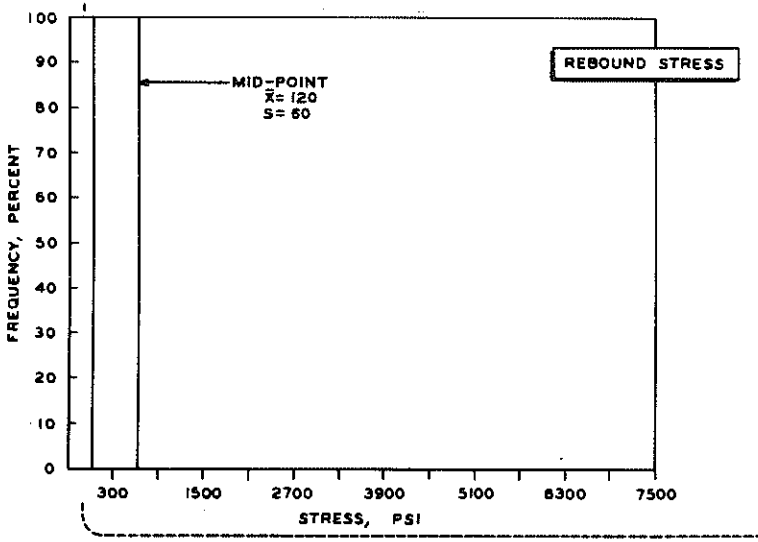

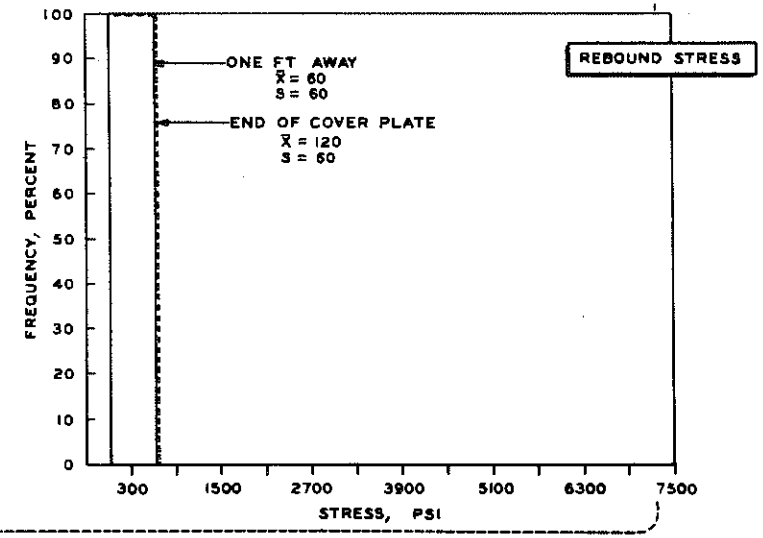

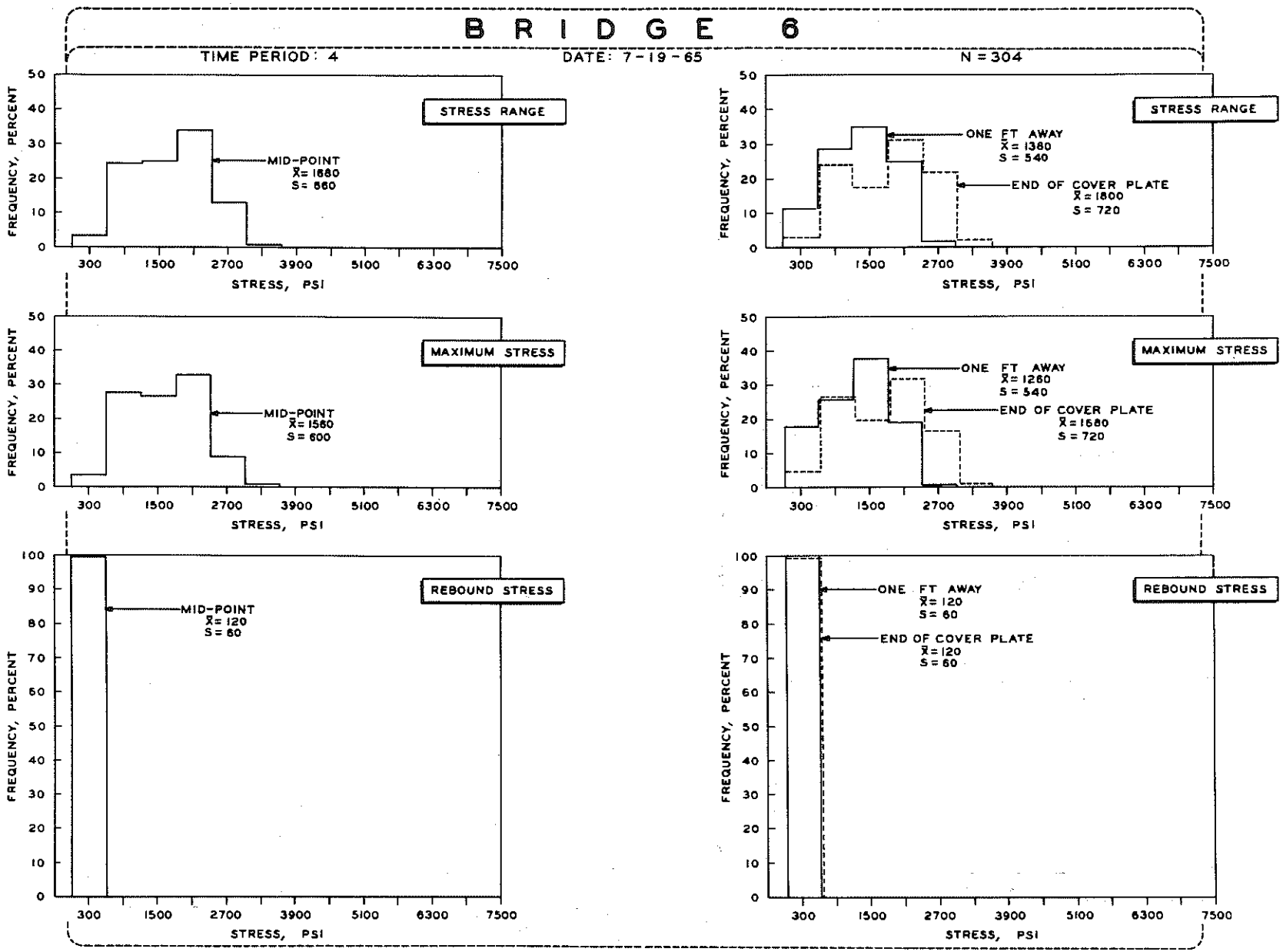
BRIDGE 6
TIME PERIOD: 4
DATE: 7-19-65
N = 304
STRESS RANGE
MID-POINT
X̄ = 1680
S = 660
ONE FT AWAY
X̄ = 1380
S = 540
END OF COVER PLATE
X̄ = 1800
S = 720
MAXIMUM STRESS
MID-POINT
X̄ = 1560
S = 600
ONE FT AWAY
X̄ = 1260
S = 540
END OF COVER PLATE
X̄ = 1680
S = 720
REBOUND STRESS
MID-POINT
X̄ = 120
S = 60
ONE FT AWAY
X̄ = 120
S = 60
END OF COVER PLATE
X̄ = 120
S = 60
FREQUENCY, PERCENT
STRESS, PSI
300
1500
2700
3900
5100
6300
7500

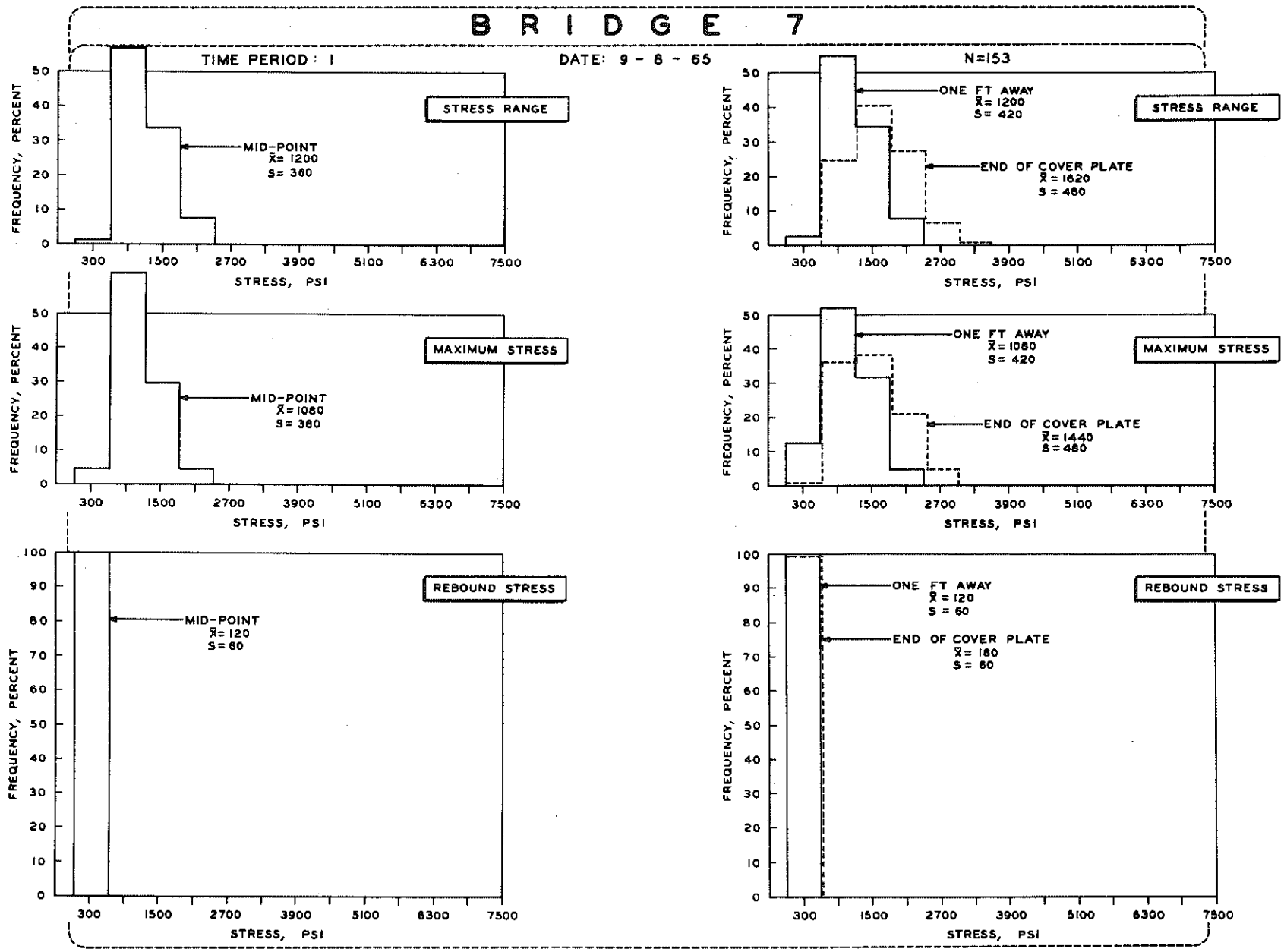
BRIDGE 7
TIME PERIOD : 1
DATE: 9 - 8 - 65
N=153
STRESS RANGE
MID-POINT
X̄= 1200
S= 360
ONE FT AWAY
X̄= 1200
S= 420
END OF COVER PLATE
X̄= 1620
S= 480
MAXIMUM STRESS
MID-POINT
X̄= 1080
S= 360
ONE FT AWAY
X̄= 1080
S= 420
END OF COVER PLATE
X̄= 1440
S= 480
REBOUND STRESS
MID-POINT
X̄= 120
S= 60
ONE FT AWAY
X̄= 120
S= 60
END OF COVER PLATE
X̄= 180
S= 60
FREQUENCY, PERCENT
STRESS, PSI
300
1500
2700
3900
5100
6300
7500

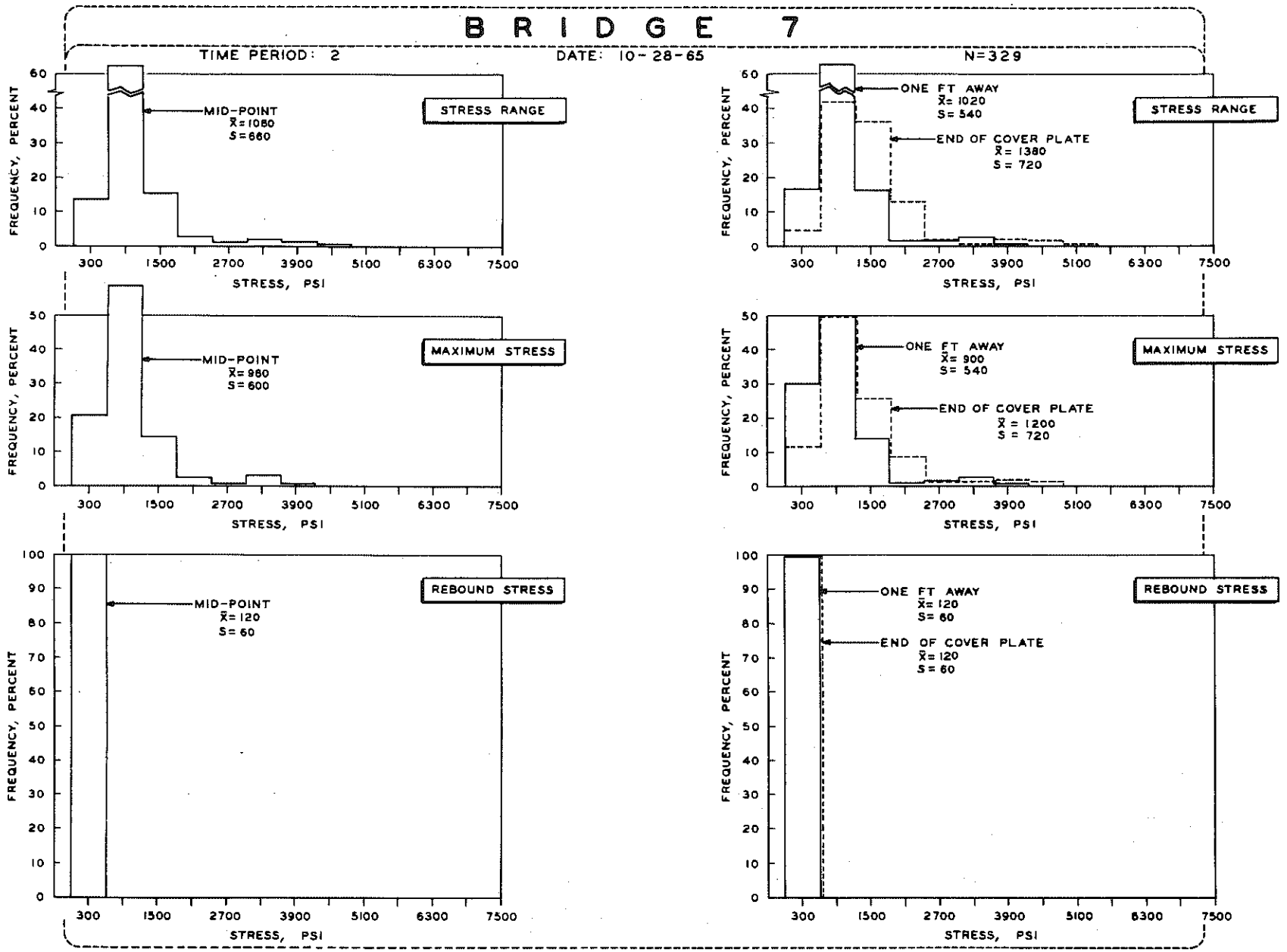
BRIDGE 7
TIME PERIOD: 2
DATE: 10-28-65
N=329
STRESS RANGE
MID-POINT
X̄=1080
S=660
ONE FT AWAY
X̄=1020
S=540
END OF COVER PLATE
X̄=1380
S=720
MAXIMUM STRESS
MID-POINT
X̄=980
S=600
ONE FT AWAY
X̄=900
S=540
END OF COVER PLATE
X̄=1200
S=720
REBOUND STRESS
MID-POINT
X̄=120
S=60
ONE FT AWAY
X̄=120
S=60
END OF COVER PLATE
X̄=120
S=60
FREQUENCY, PERCENT
STRESS, PSI
300
1500
2700
3900
5100
6300
7500

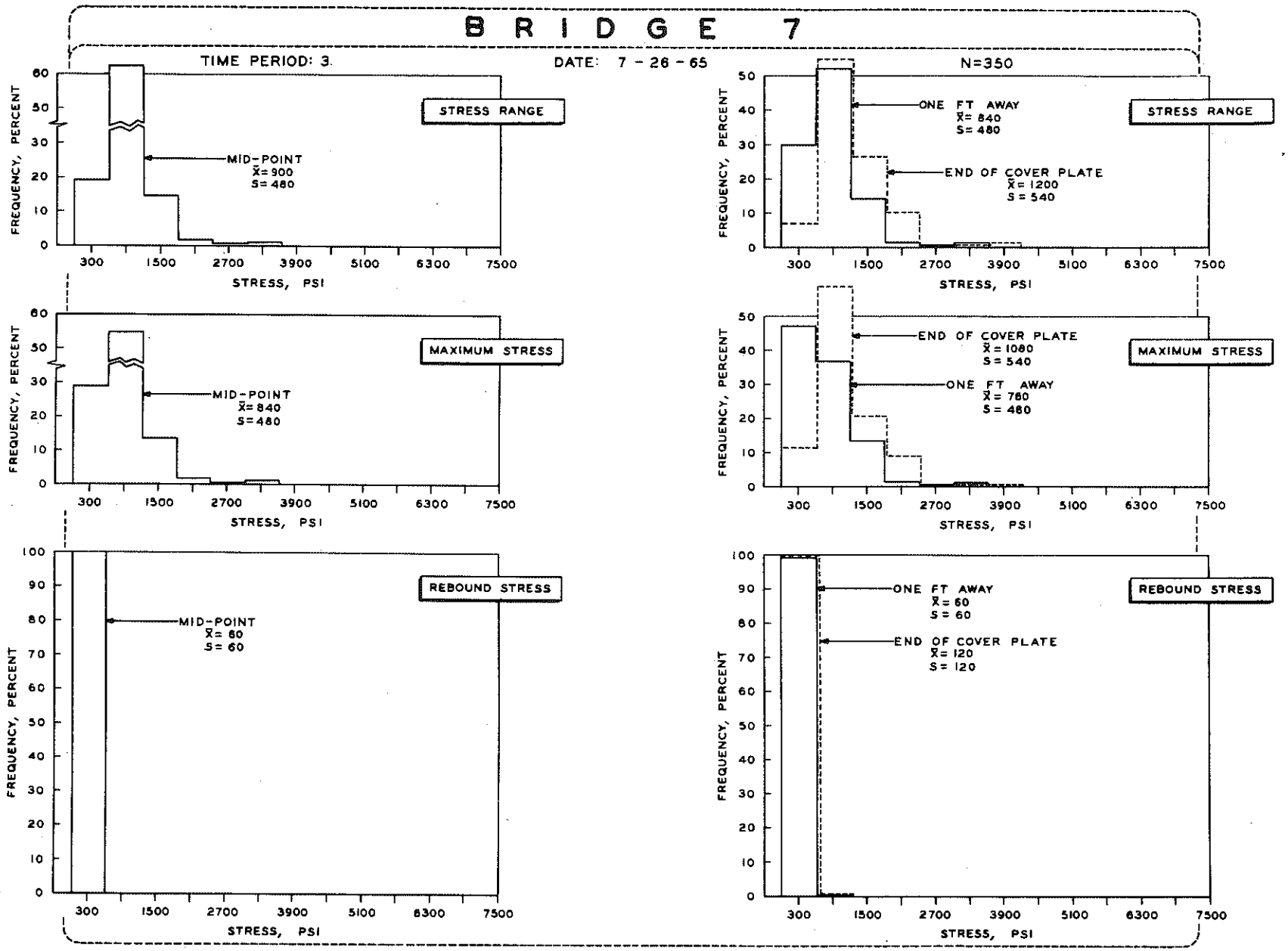
BRIDGE 7
TIME PERIOD: 3.
DATE: 7 - 26 - 65
N=350
STRESS RANGE
MID-POINT
X̄= 900
S= 480
ONE FT AWAY
X̄= 840
S= 480
END OF COVER PLATE
X̄= 1200
S = 540
MAXIMUM STRESS
MID-POINT
X̄= 840
S= 480
END OF COVER PLATE
X̄= 1080
S = 540
ONE FT AWAY
X̄= 780
S = 480
REBOUND STRESS
MID-POINT
X̄= 60
S= 60
ONE FT AWAY
X̄= 60
S = 60
END OF COVER PLATE
X̄= 120
S = 120
FREQUENCY, PERCENT
STRESS, PSI
300
1500
2700
3900
5100
6300
7500

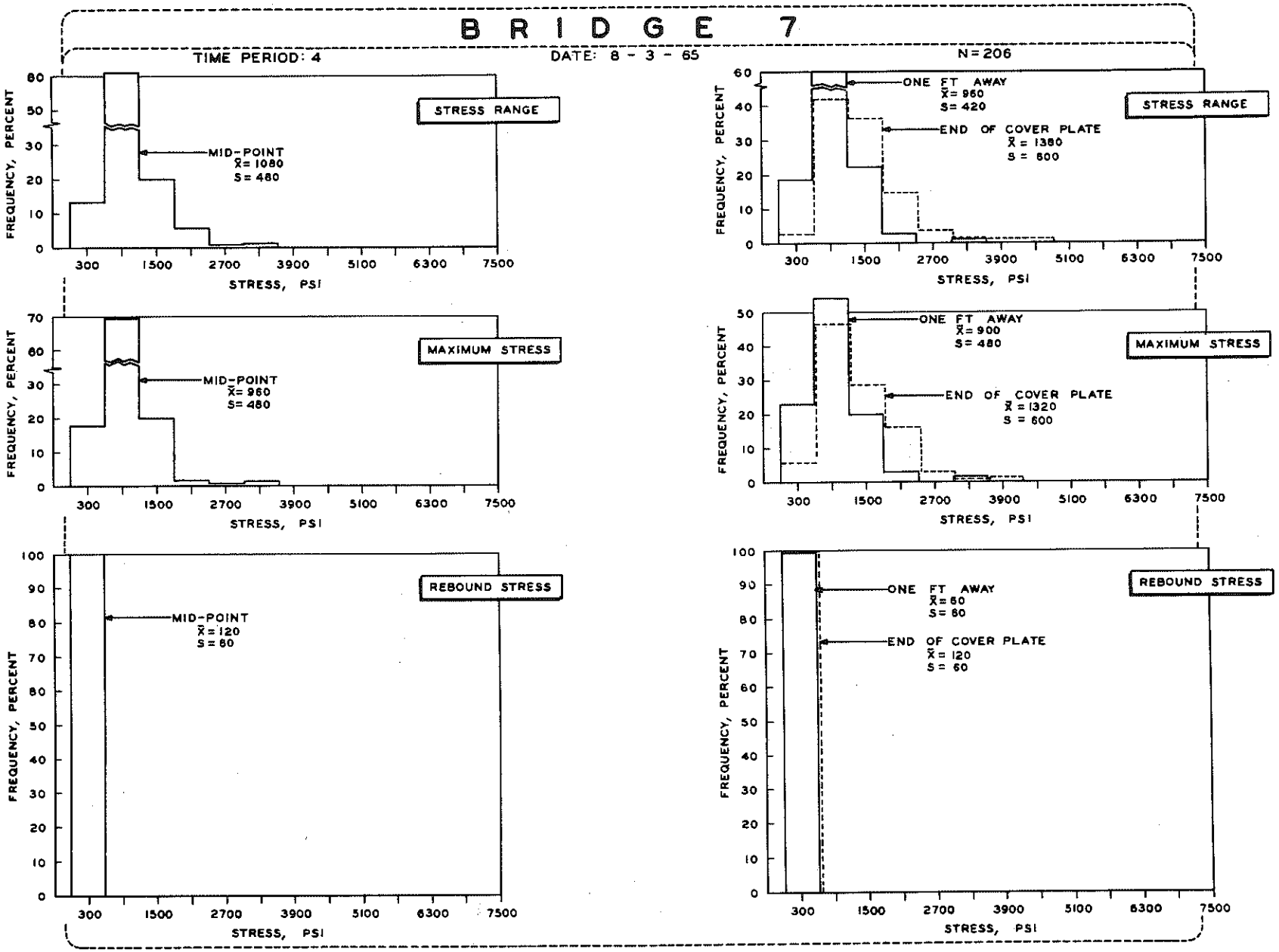
BRIDGE 7
TIME PERIOD: 4
DATE: 8 - 3 - 65
N=206
STRESS RANGE
MID-POINT
X̄= 1080
S= 480
ONE FT AWAY
X̄= 960
S= 420
END OF COVER PLATE
X̄ = 1380
S = 600
MAXIMUM STRESS
MID-POINT
X̄= 960
S= 480
ONE FT AWAY
X̄= 900
S= 480
END OF COVER PLATE
X̄ = 1320
S = 600
REBOUND STRESS
MID-POINT
X̄= 120
S= 60
ONE FT AWAY
X̄= 60
S= 60
END OF COVER PLATE
X̄= 120
S= 60
FREQUENCY, PERCENT
STRESS, PSI
300
1500
2700
3900
5100
6300
7500

B R I D G E 8

TIME PERIOD: 1 DATE: 8 - 13 - 65 N = 215

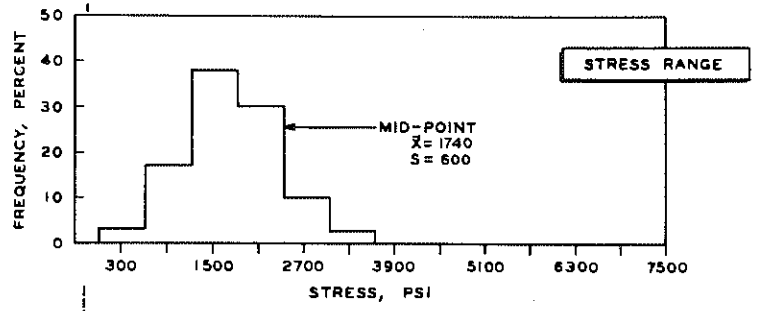

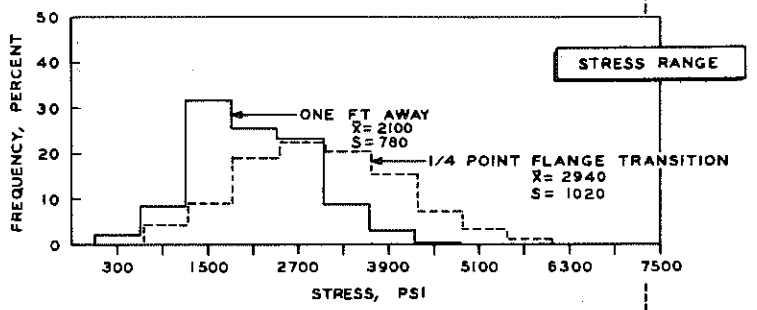

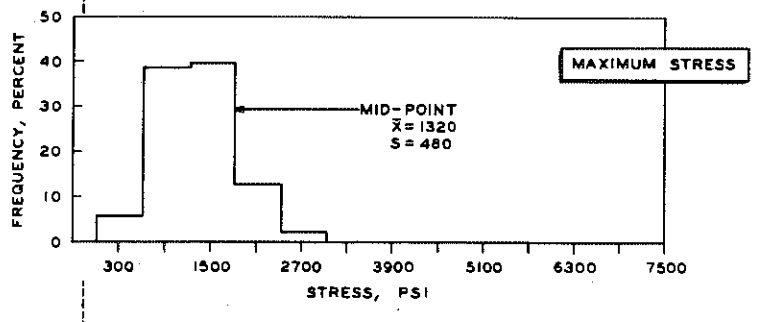

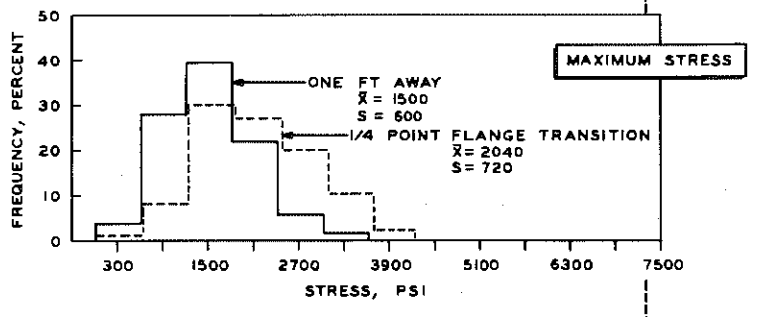

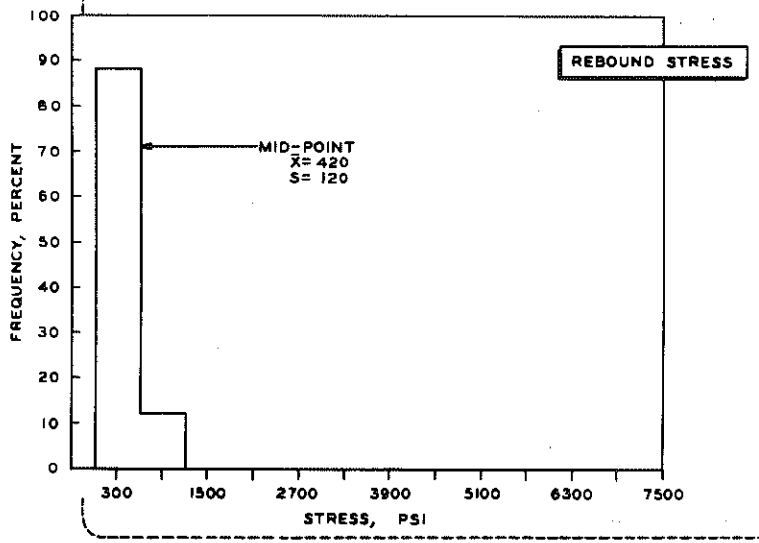

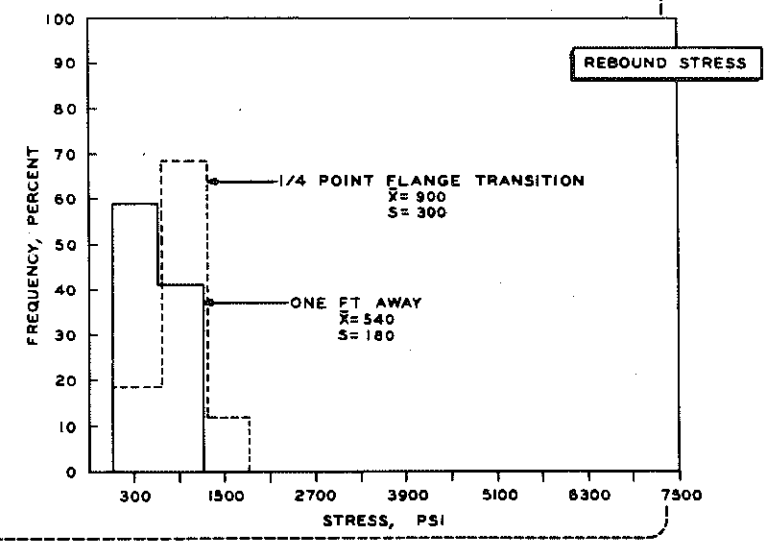

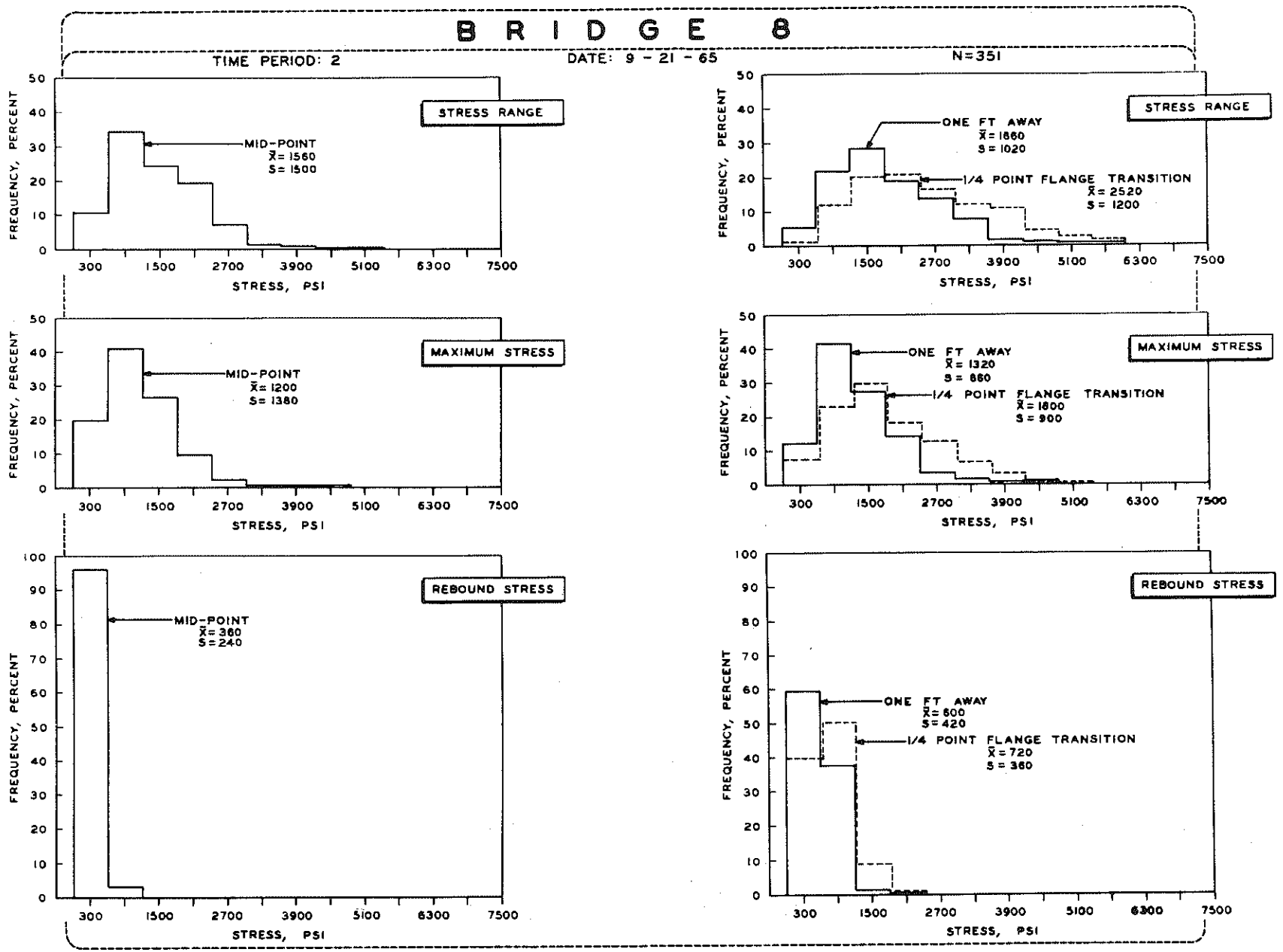
BRIDGE 8
TIME PERIOD: 2
DATE: 9 - 21 - 65
N=351
STRESS RANGE
MID-POINT
X̄= 1560
S= 1500
ONE FT AWAY
X̄= 1860
S= 1020
1/4 POINT FLANGE TRANSITION
X̄= 2520
S= 1200
MAXIMUM STRESS
MID-POINT
X̄= 1200
S= 1380
ONE FT AWAY
X̄= 1320
S= 860
1/4 POINT FLANGE TRANSITION
X̄= 1800
S= 900
REBOUND STRESS
MID-POINT
X̄= 360
S= 240
ONE FT AWAY
X̄= 600
S= 420
1/4 POINT FLANGE TRANSITION
X̄= 720
S= 360
FREQUENCY, PERCENT
STRESS, PSI
300
1500
2700
3900
5100
6300
7500

BRIDGE 8

TIME PERIOD : 3 DATE: 10 - 27 - 65 N=294

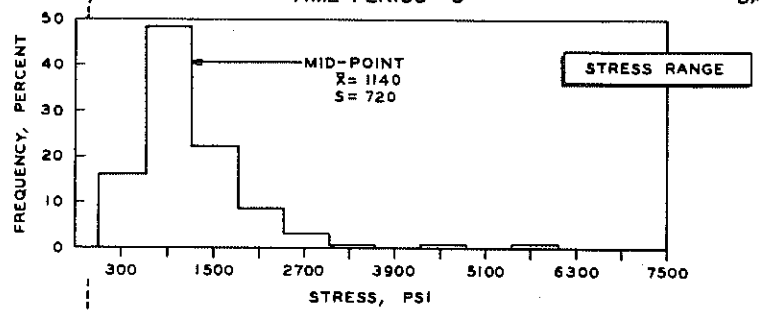

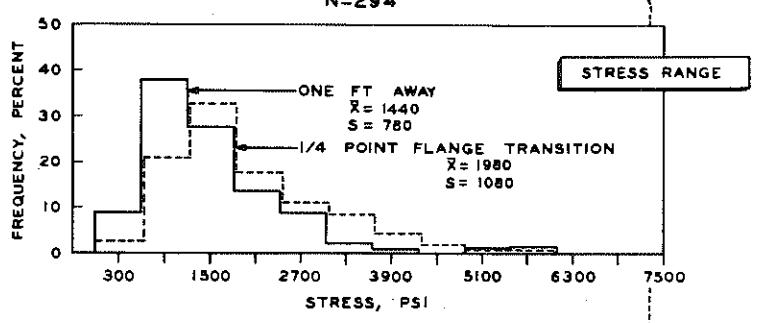

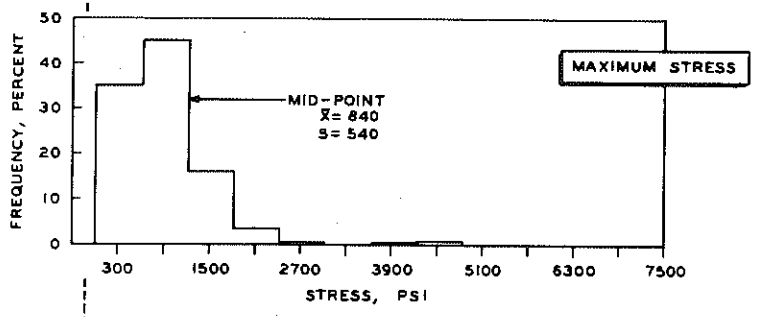

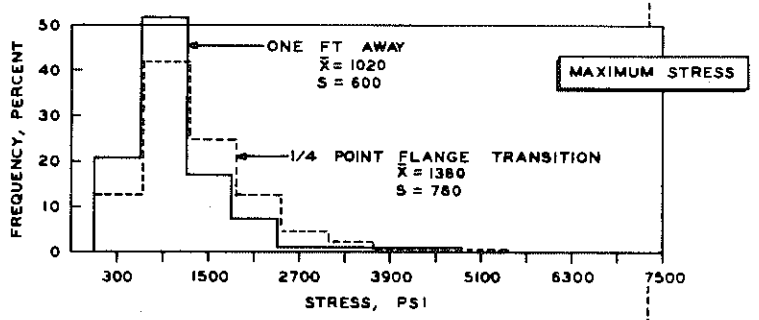

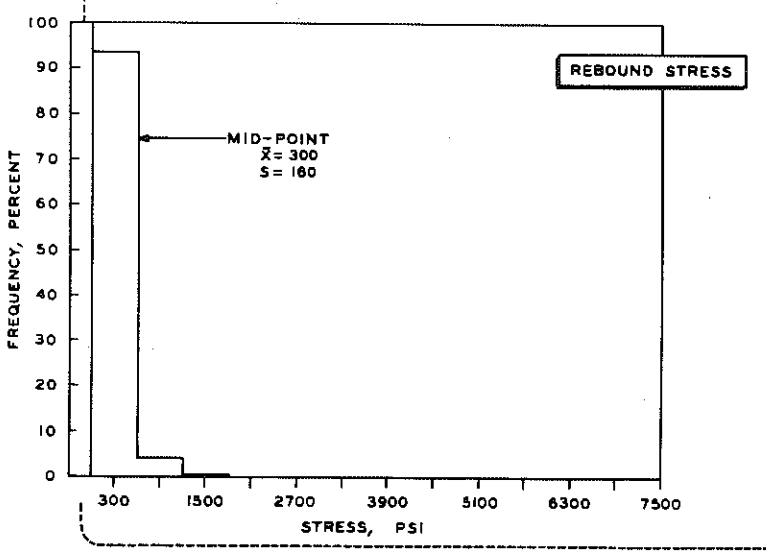

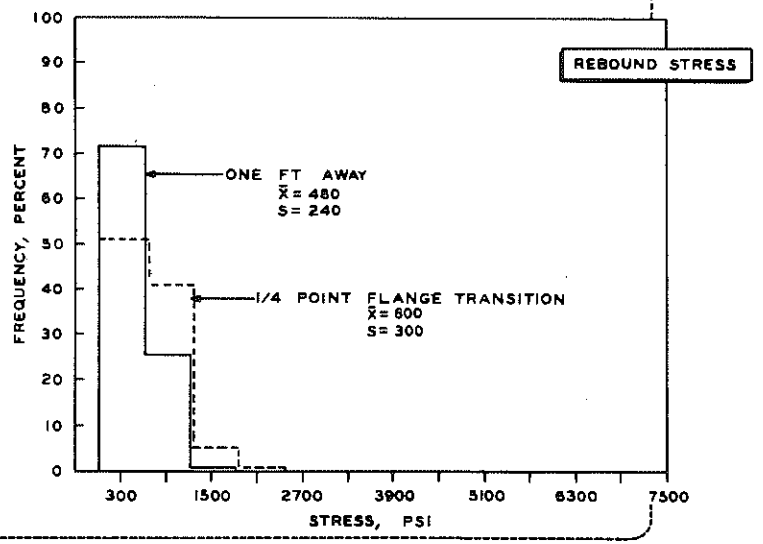

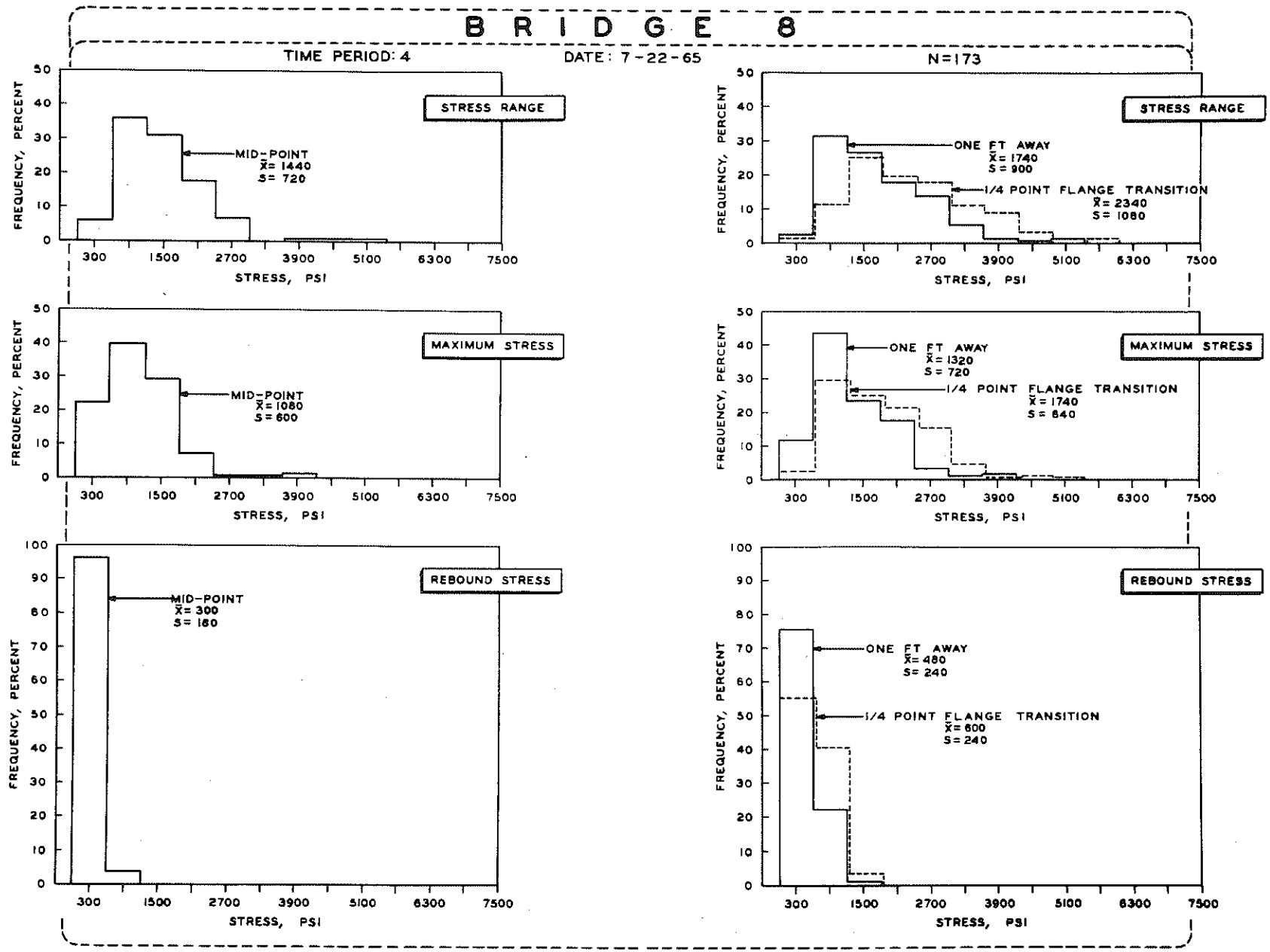
BRIDGE 8
TIME PERIOD: 4
DATE: 7-22-65
N=173
STRESS RANGE
MID-POINT
X̄= 1440
S= 720
ONE FT AWAY
X̄= 1740
S= 900
1/4 POINT FLANGE TRANSITION
X̄= 2340
S= 1080
MAXIMUM STRESS
MID-POINT
X̄= 1080
S= 600
ONE FT AWAY
X̄= 1320
S= 720
1/4 POINT FLANGE TRANSITION
X̄= 1740
S= 840
REBOUND STRESS
MID-POINT
X̄= 300
S= 160
ONE FT AWAY
X̄= 480
S= 240
1/4 POINT FLANGE TRANSITION
X̄= 600
S= 240
FREQUENCY, PERCENT
STRESS, PSI
300
1500
2700
3900
5100
6300
7500

APPENDIX B

Frequency Distributions of the Eleven Most Common Truck Types for Individual Test Bridges and Sample Periods

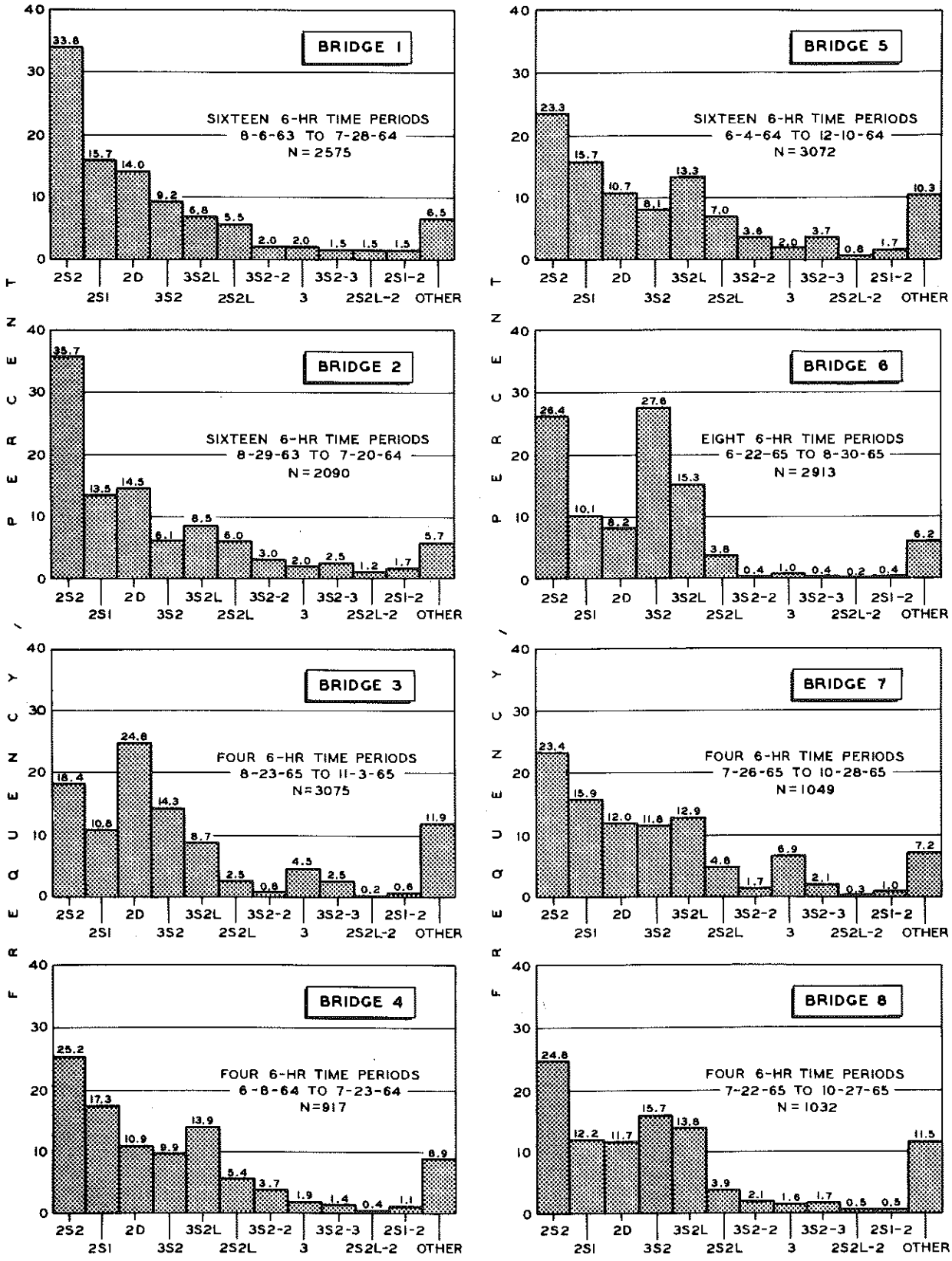
BRIDGE 1
SIXTEEN 6-HR TIME PERIODS
8-6-63 TO 7-28-64
N = 2575
33.8
15.7
14.0
9.2
6.8
5.5
2.0
2.0
1.5
1.5
1.5
6.5
BRIDGE 5
SIXTEEN 6-HR TIME PERIODS
6-4-64 TO 12-10-64
N = 3072
23.3
15.7
10.7
8.1
13.3
7.0
3.6
2.0
3.7
0.8
1.7
10.3
BRIDGE 2
SIXTEEN 6-HR TIME PERIODS
8-29-63 TO 7-20-64
N = 2090
35.7
13.5
14.5
6.1
8.5
6.0
3.0
2.0
2.5
1.2
1.7
5.7
BRIDGE 6
EIGHT 6-HR TIME PERIODS
6-22-65 TO 8-30-65
N = 2913
26.4
10.1
8.2
27.6
15.3
3.8
0.4
1.0
0.4
0.2
0.4
6.2
BRIDGE 3
FOUR 6-HR TIME PERIODS
8-23-65 TO 11-3-65
N=3075
18.4
10.8
24.8
14.3
8.7
2.5
0.8
4.5
2.5
0.2
0.6
11.9
BRIDGE 7
FOUR 6-HR TIME PERIODS
7-26-65 TO 10-28-65
N=1049
23.4
15.9
12.0
11.8
12.9
4.8
1.7
6.9
2.1
0.3
1.0
7.2
BRIDGE 4
FOUR 6-HR TIME PERIODS
6-8-64 TO 7-23-64
N=917
25.2
17.3
10.9
9.9
13.9
5.4
3.7
1.9
1.4
0.4
1.1
8.9
BRIDGE 8
FOUR 6-HR TIME PERIODS
7-22-65 TO 10-27-65
N = 1032
24.8
12.2
11.7
15.7
13.8
3.9
2.1
1.6
1.7
0.5
0.5
11.5
PERCENT
FREQUENCY
0
10
20
30
40
2S2
2S1
2D
3S2
3S2L
2S2L
3S2-2
3
3S2-3
2S2L-2
2S1-2
OTHER

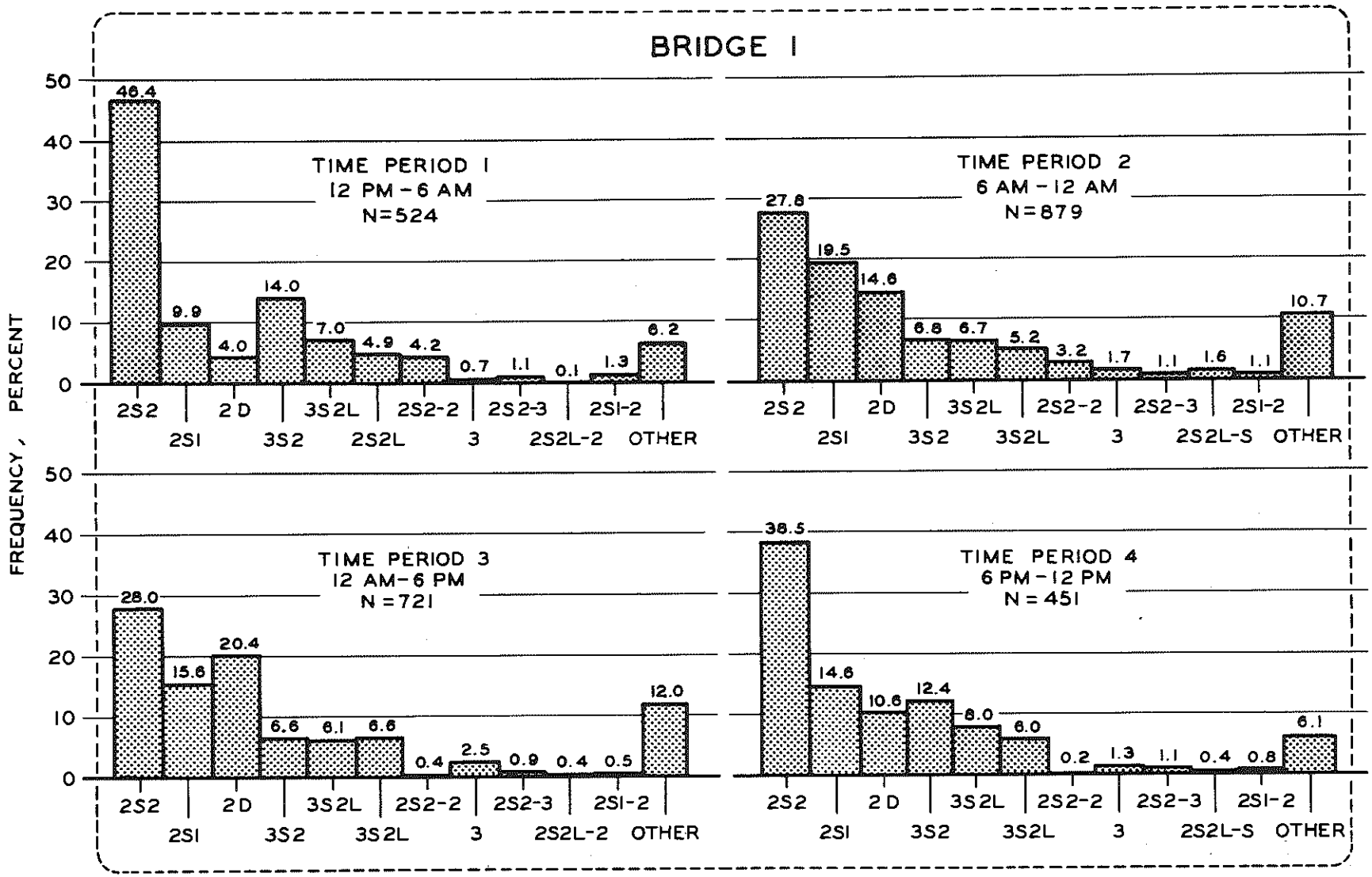
BRIDGE 1
FREQUENCY, PERCENT
TIME PERIOD 1
12 PM - 6 AM
N=524
46.4
9.9
4.0
14.0
7.0
4.9
4.2
0.7
1.1
0.1
1.3
6.2
2S2
2D
3S2L
2S2-2
2S2-3
2SI-2
2SI
3S2
2S2L
3
2S2L-2
OTHER
TIME PERIOD 2
6 AM - 12 AM
N=879
27.8
19.5
14.6
6.8
6.7
5.2
3.2
1.7
1.1
1.6
1.1
10.7
2S2
2D
3S2L
2S2-2
2S2-3
2SI-2
2SI
3S2
3S2L
3
2S2L-S
OTHER
TIME PERIOD 3
12 AM - 6 PM
N = 721
28.0
15.6
20.4
6.6
6.1
6.6
0.4
2.5
0.9
0.4
0.5
12.0
2S2
2D
3S2L
2S2-2
2S2-3
2SI-2
2SI
3S2
3S2L
3
2S2L-2
OTHER
TIME PERIOD 4
6 PM - 12 PM
N = 451
38.5
14.6
10.6
12.4
8.0
6.0
0.2
1.3
1.1
0.4
0.8
6.1
2S2
2D
3S2L
2S2-2
2S2-3
2SI-2
2SI
3S2
3S2L
3
2S2L-S
OTHER

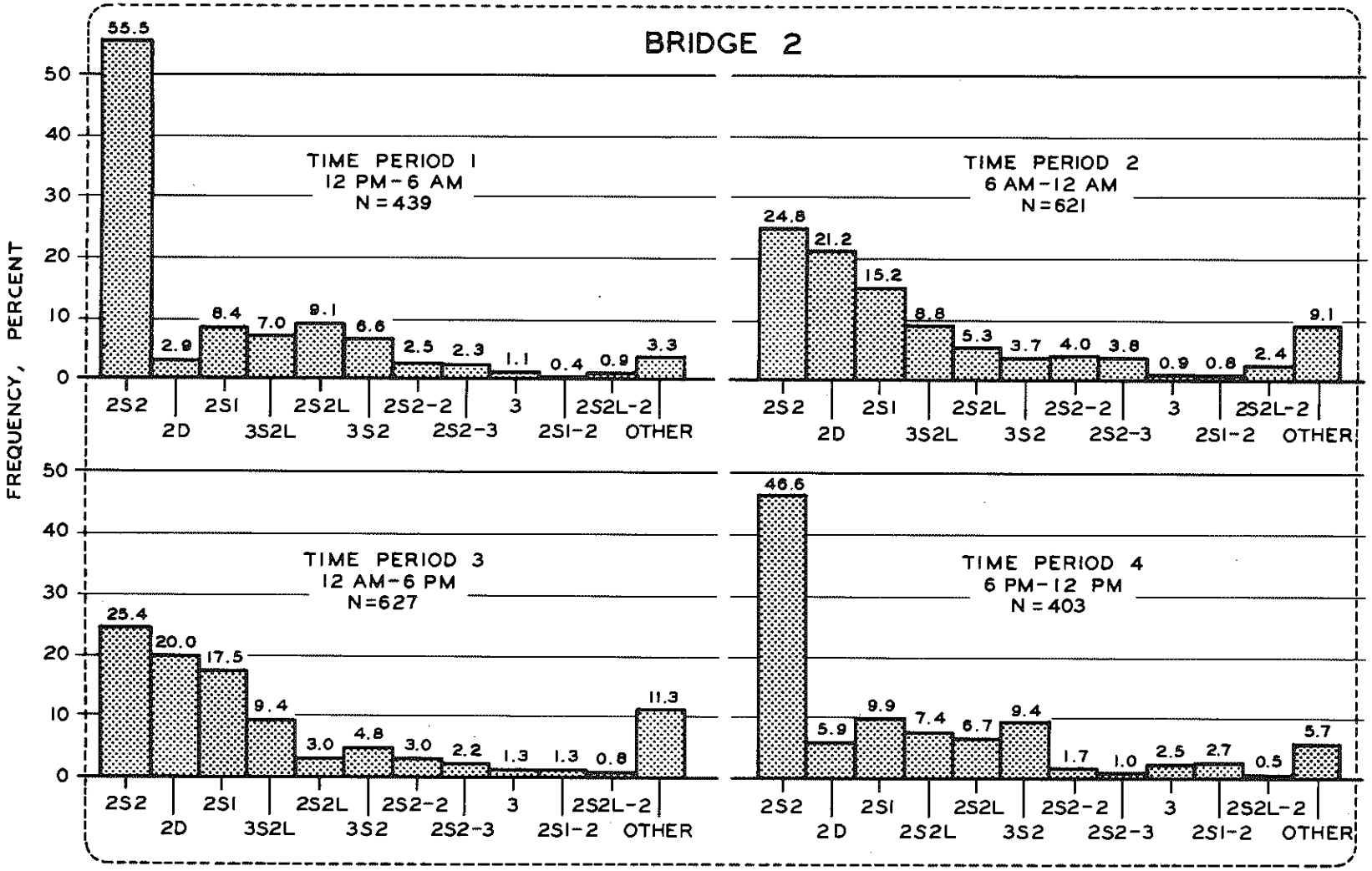
BRIDGE 2
FREQUENCY, PERCENT
TIME PERIOD 1
12 PM-6 AM
N=439
55.5
2.9
8.4
7.0
9.1
6.6
2.5
2.3
1.1
0.4
0.9
3.3
TIME PERIOD 2
6 AM-12 AM
N=621
24.8
21.2
15.2
8.8
5.3
3.7
4.0
3.8
0.9
0.8
2.4
9.1
TIME PERIOD 3
12 AM-6 PM
N=627
25.4
20.0
17.5
9.4
3.0
4.8
3.0
2.2
1.3
1.3
0.8
11.3
TIME PERIOD 4
6 PM-12 PM
N=403
46.6
5.9
9.9
7.4
6.7
9.4
1.7
1.0
2.5
2.7
0.5
5.7
0
10
20
30
40
50
2S2
2D
2S1
3S2L
2S2L
3S2
2S2-2
2S2-3
3
2S1-2
2S2L-2
OTHER

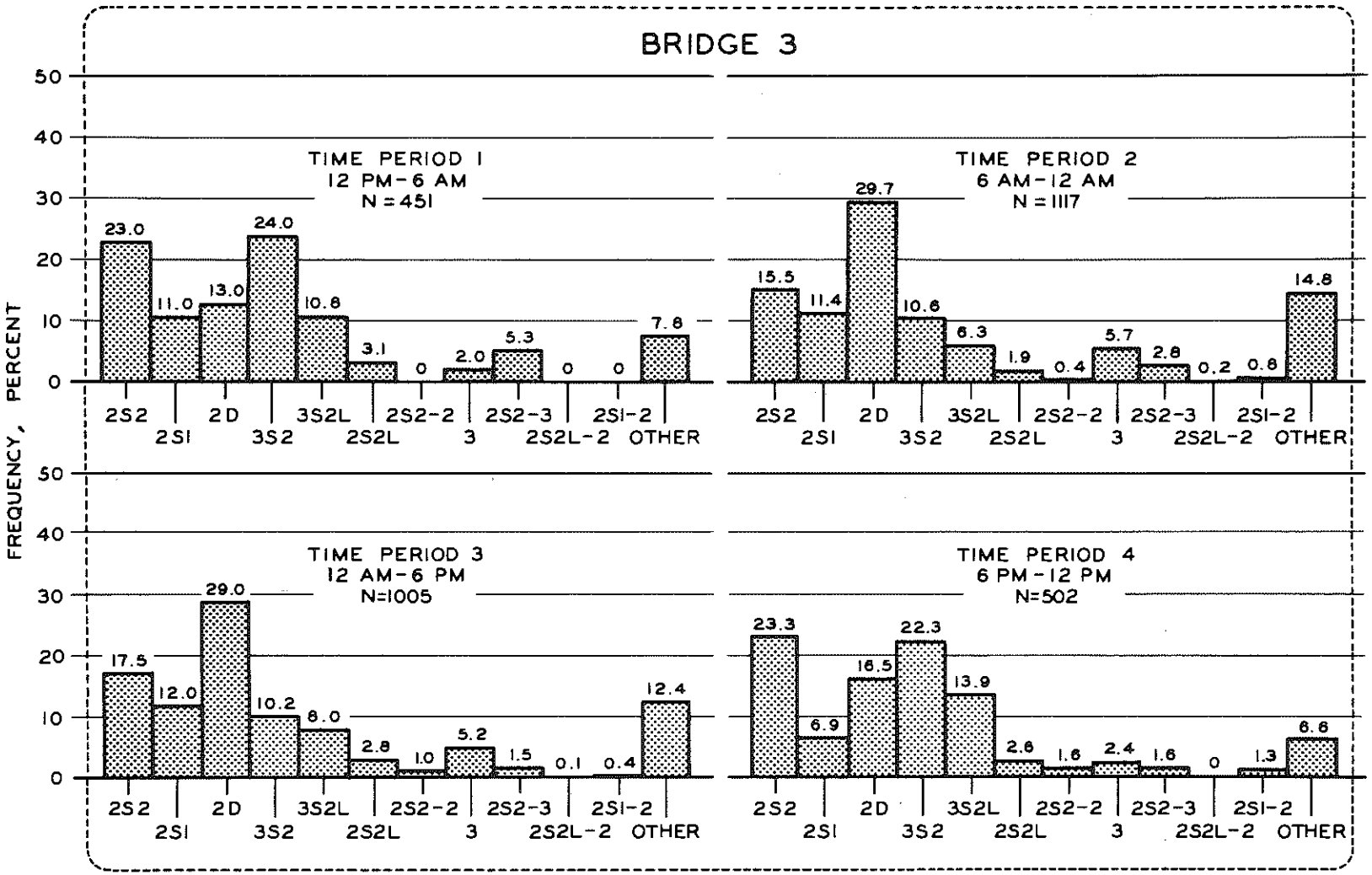
BRIDGE 3
FREQUENCY, PERCENT
TIME PERIOD 1
12 PM-6 AM
N=451
23.0
11.0
13.0
24.0
10.6
3.1
0
2.0
5.3
0
0
7.8
TIME PERIOD 2
6 AM-12 AM
N=1117
15.5
11.4
29.7
10.6
6.3
1.9
0.4
5.7
2.8
0.2
0.8
14.8
TIME PERIOD 3
12 AM-6 PM
N=1005
17.5
12.0
29.0
10.2
8.0
2.8
1.0
5.2
1.5
0.1
0.4
12.4
TIME PERIOD 4
6 PM-12 PM
N=502
23.3
6.9
16.5
22.3
13.9
2.6
1.6
2.4
1.6
0
1.3
6.6
2S2
2S1
2D
3S2
3S2L
2S2L
2S2-2
3
2S2-3
2S2L-2
2S1-2
OTHER

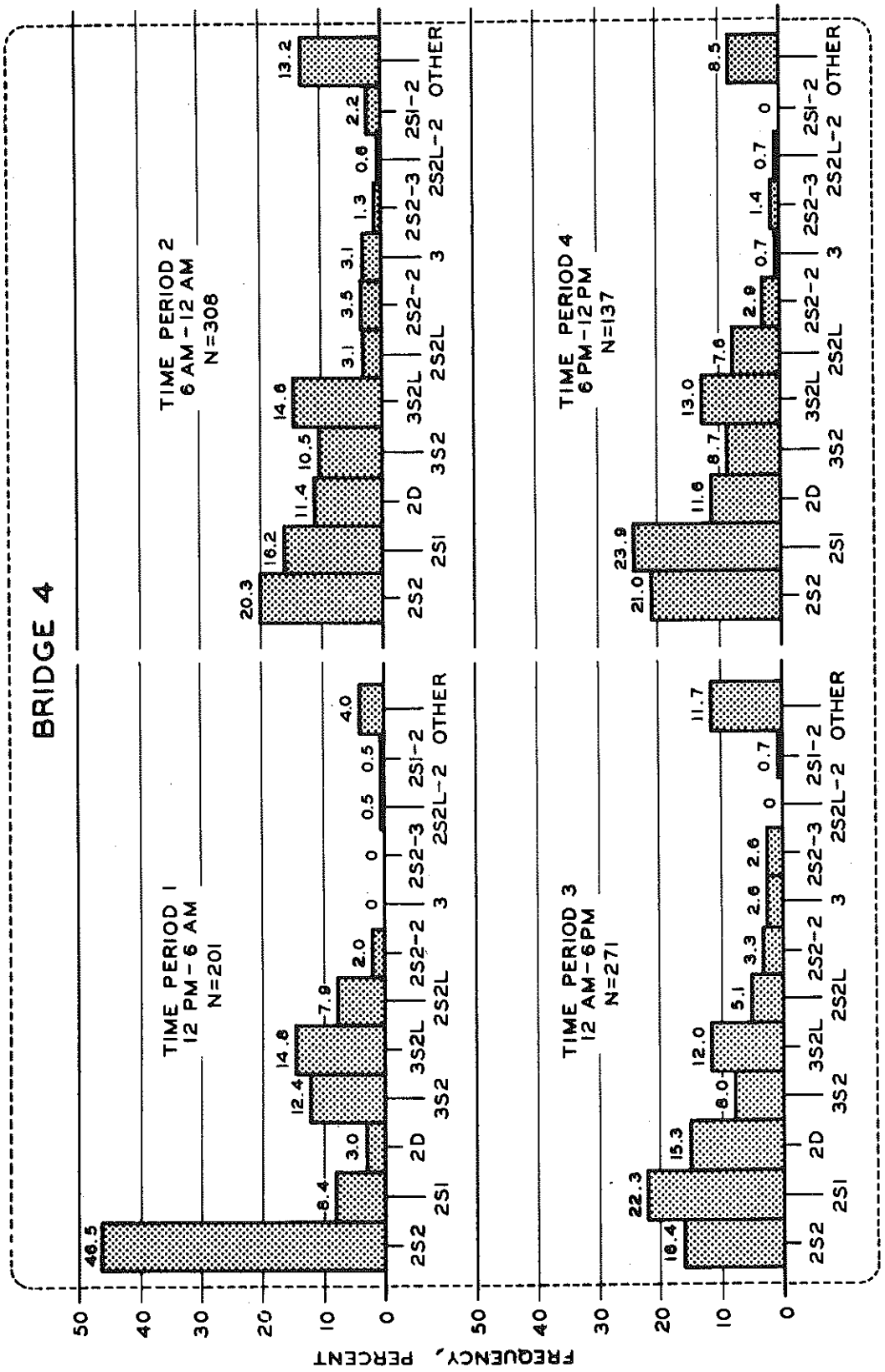
BRIDGE 4
TIME PERIOD 1
12 PM - 6 AM
N=201
TIME PERIOD 2
6 AM - 12 AM
N=308
TIME PERIOD 3
12 AM - 6PM
N=271
TIME PERIOD 4
6PM - 12 PM
N=137
FREQUENCY, PERCENT
0
10
20
30
40
50
2S2
2SI
2D
3S2
3S2L
2S2L
2S2-2
3
2S2-3
2S2L-2
2SI-2
OTHER

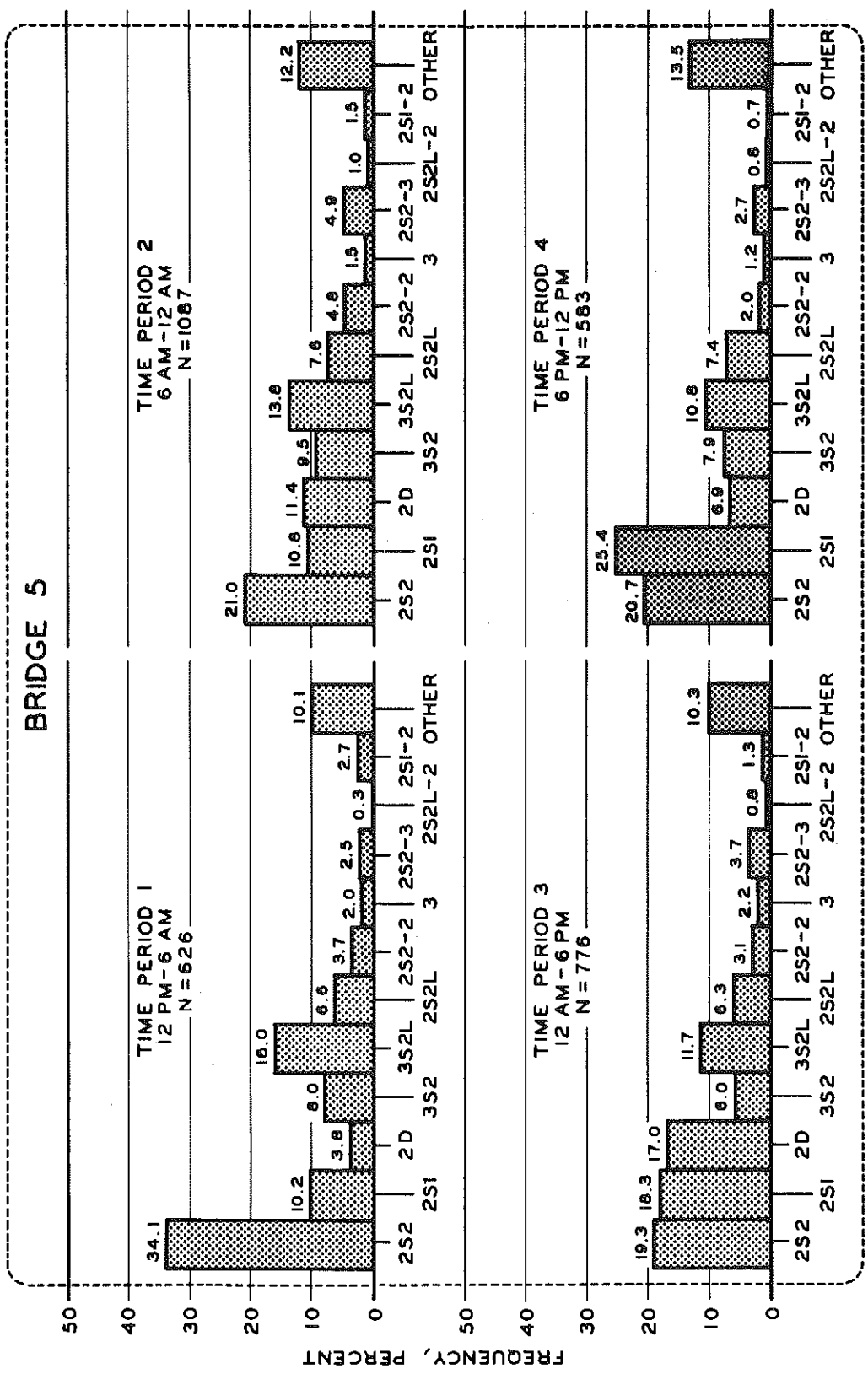
BRIDGE 5
TIME PERIOD 1
12 PM-6 AM
N=626
TIME PERIOD 2
6 AM-12 AM
N=1087
TIME PERIOD 3
12 AM-6 PM
N=776
TIME PERIOD 4
6 PM-12 PM
N=583
FREQUENCY, PERCENT
0
10
20
30
40
50
2S2
2S1
2D
3S2
3S2L
2S2L
2S2-2
3
2S2-3
2S2L-2
2SI-2
OTHER
34.1
10.2
3.8
8.0
16.0
6.6
3.7
2.0
2.5
0.3
2.7
10.1
21.0
10.8
11.4
9.5
13.0
7.6
4.8
1.5
4.9
1.0
1.5
12.2
19.3
18.3
17.0
6.0
11.7
6.3
3.1
2.2
3.7
0.8
1.3
10.3
20.7
25.4
6.9
7.9
10.8
7.4
2.0
1.2
2.7
0.8
0.7
13.5

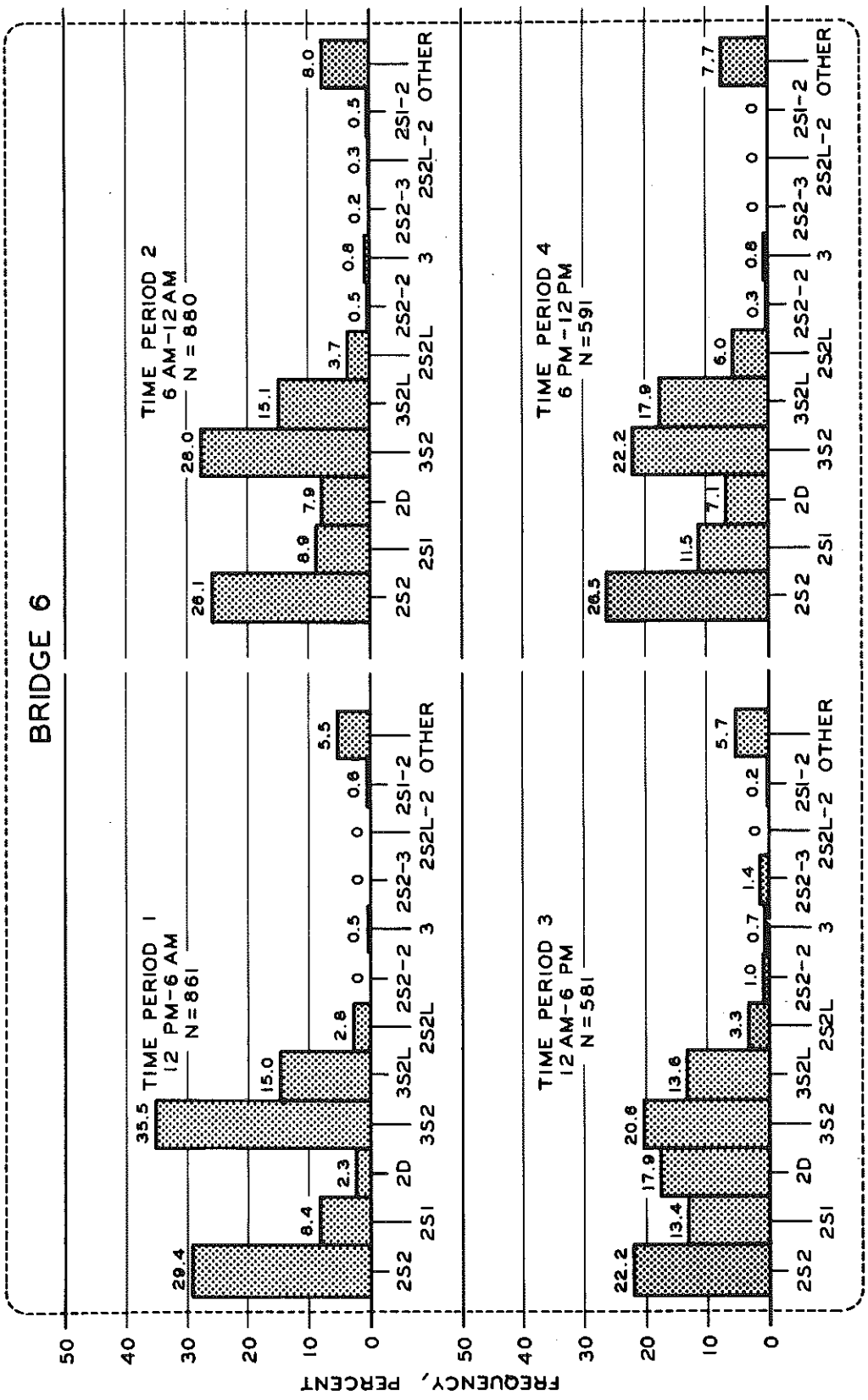
BRIDGE 6
TIME PERIOD 1
12 PM-6 AM
N=861
TIME PERIOD 2
6 AM-12 AM
N=880
TIME PERIOD 3
12 AM-6 PM
N=581
TIME PERIOD 4
6 PM-12 PM
N=591
FREQUENCY, PERCENT
0
10
20
30
40
50
2S2
2S1
2D
3S2
3S2L
2S2-2
2S2L
3
2S2-3
2S2L-2
2SI-2
OTHER

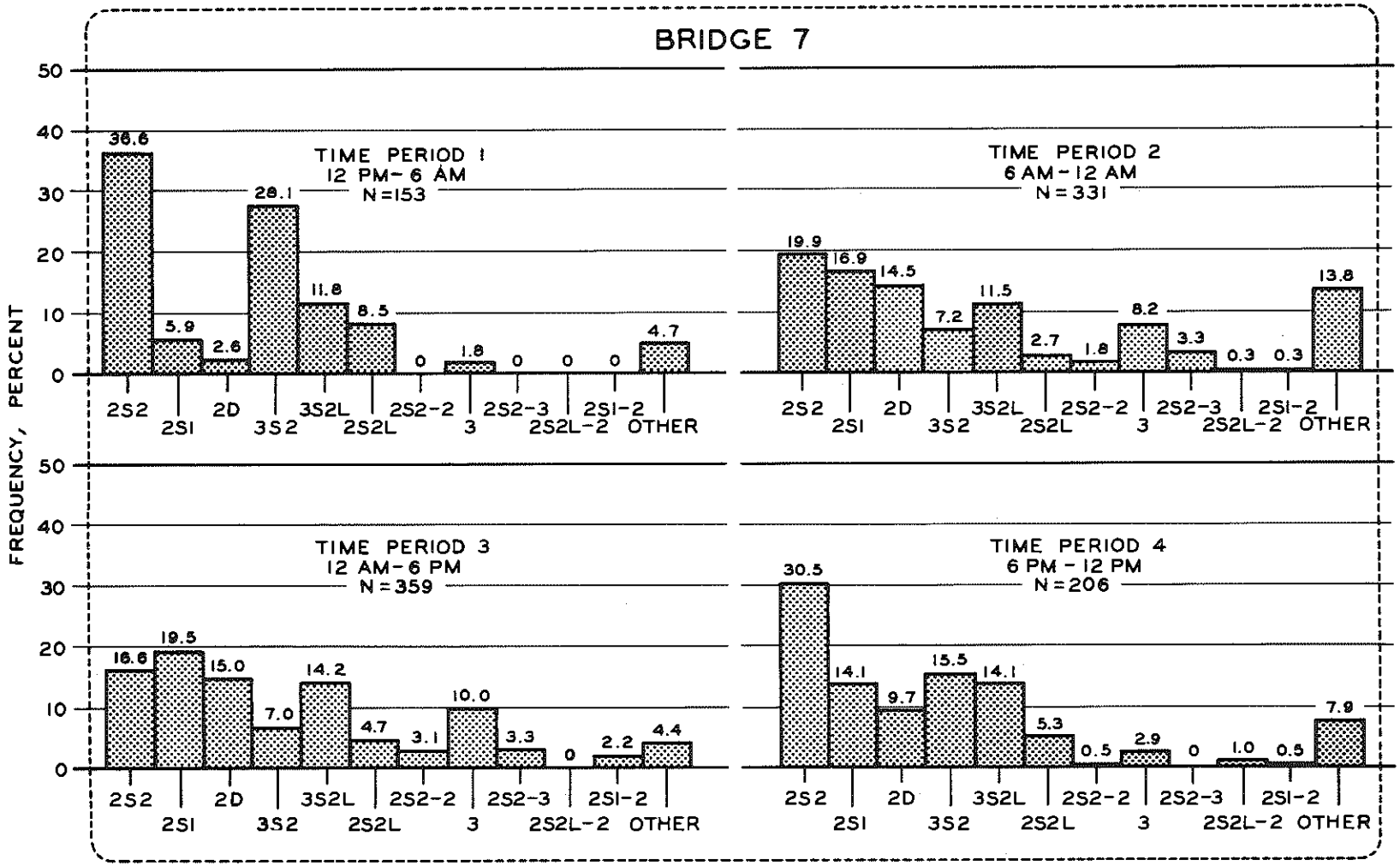
BRIDGE 7
FREQUENCY, PERCENT
TIME PERIOD 1
12 PM - 6 AM
N = 153
36.6
5.9
2.6
28.1
11.8
8.5
0
1.8
0
0
0
4.7
TIME PERIOD 2
6 AM - 12 AM
N = 331
19.9
16.9
14.5
7.2
11.5
2.7
1.8
8.2
3.3
0.3
0.3
13.8
TIME PERIOD 3
12 AM - 6 PM
N = 359
16.6
19.5
15.0
7.0
14.2
4.7
3.1
10.0
3.3
0
2.2
4.4
TIME PERIOD 4
6 PM - 12 PM
N = 206
30.5
14.1
9.7
15.5
14.1
5.3
0.5
2.9
0
1.0
0.5
7.9
2S2
2S1
2D
3S2
3S2L
2S2L
2S2-2
3
2S2-3
2S2L-2
2S1-2
OTHER

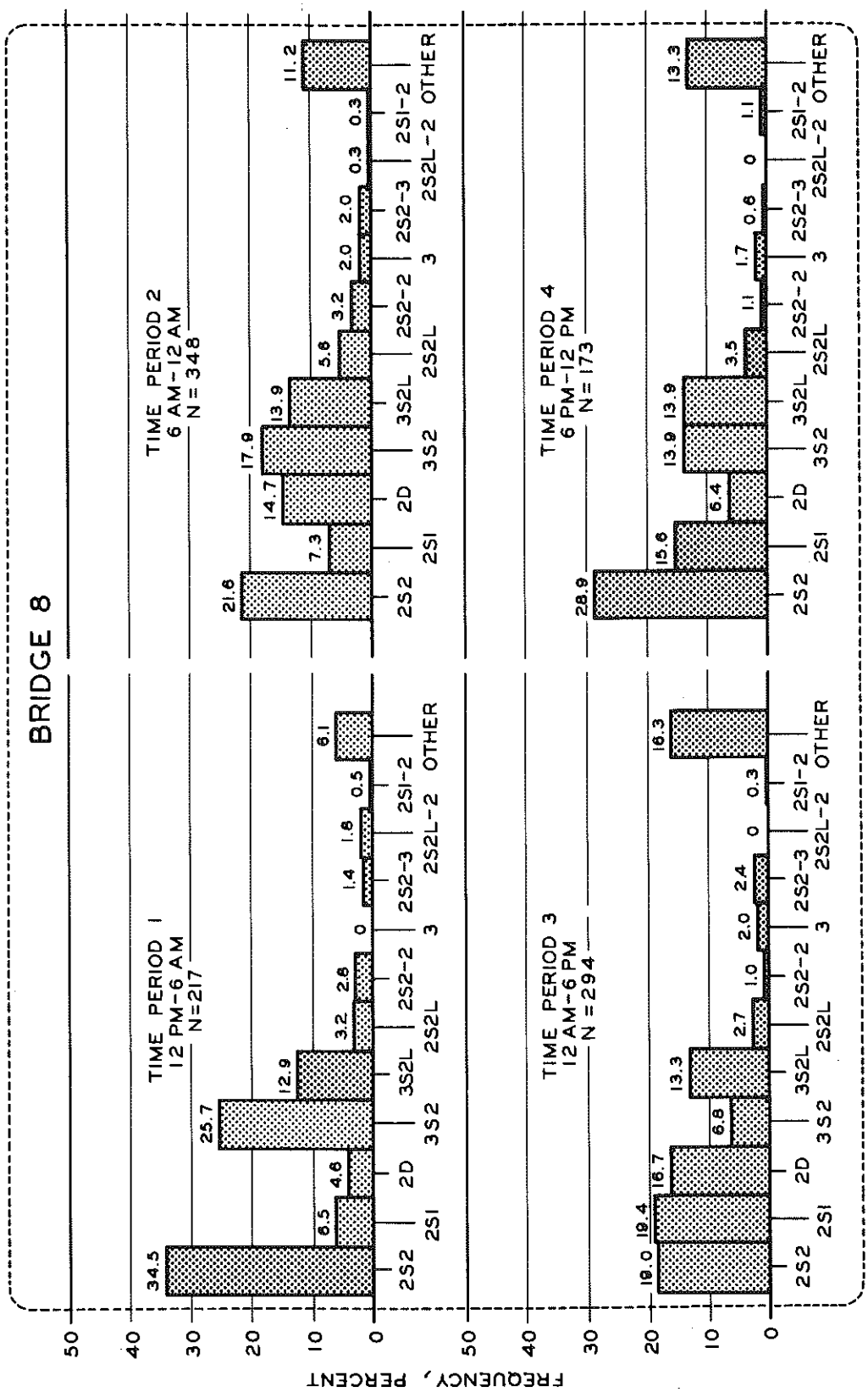
BRIDGE 8
TIME PERIOD 1
12 PM-6 AM
N=217
TIME PERIOD 2
6 AM-12 AM
N = 348
TIME PERIOD 3
12 AM-6 PM
N = 294
TIME PERIOD 4
6 PM-12 PM
N = 173
FREQUENCY, PERCENT
0
10
20
30
40
50
2S2
2D
3S2L
2S2-3
2SI-2
2SI
3S2
2S2L
2S2-2
3
2S2L-2
OTHER